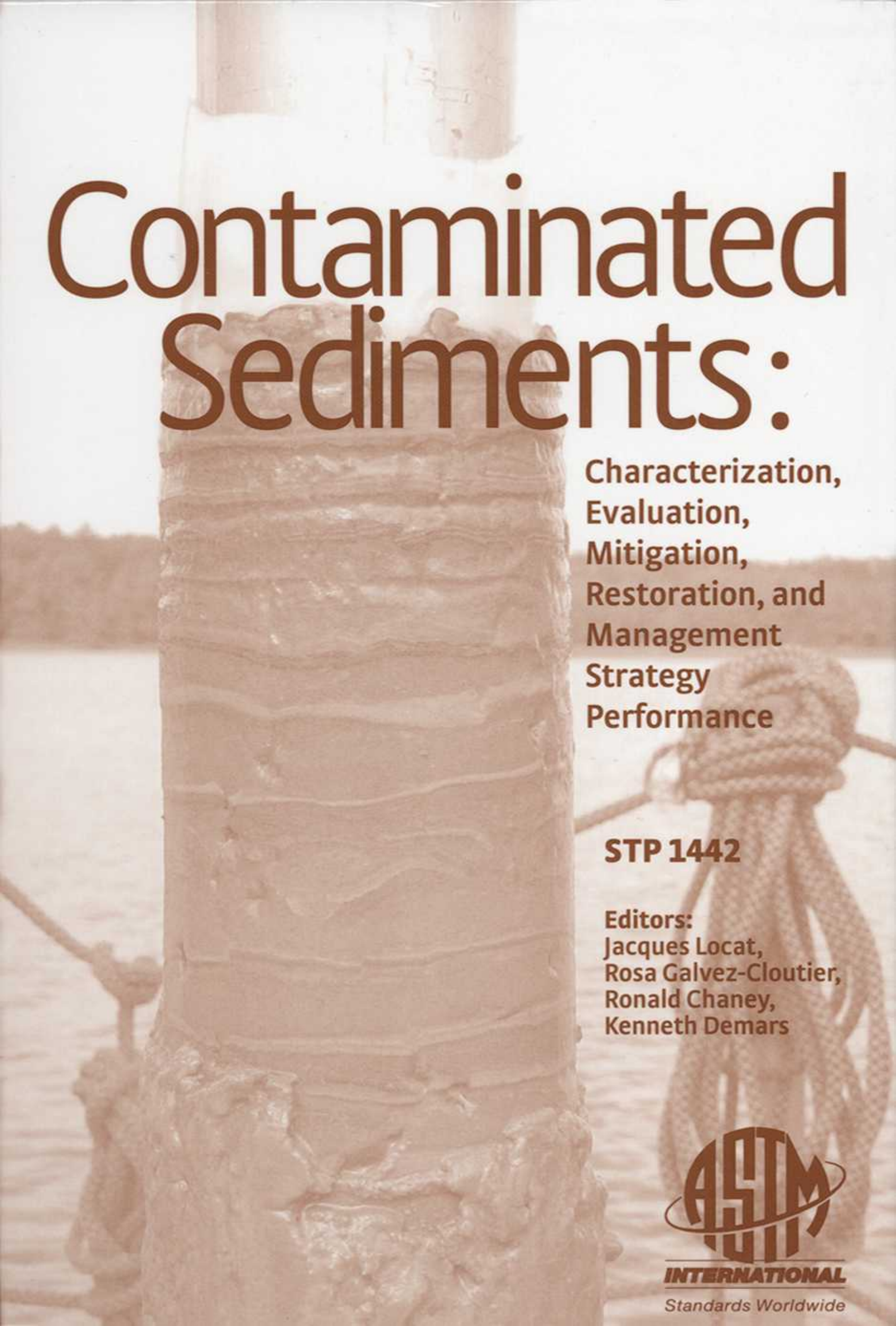

Contaminated Sediments:

Characterization, Evaluation, Mitigation, Restoration, and Management Strategy Performance

STP 1442

Editors:
Jacques Locat,
Rosa Galvez-Cloutier,
Ronald Chaney,
Kenneth Demars

ASTM INTERNATIONAL
Standards Worldwide

STP 1442

Contaminated Sediments: Characterization, Evaluation, Mitigation/Restoration, and Management Strategy Performance

Jacques Locat, Rosa Galvez Cloutier, Ronald Chaney,
and Kenneth Demars, editors

ASTM Stock Number: STP1442

ASTM International
100 Barr Harbor Drive
PO Box C700
West Conshohocken, PA 19428-2959

Printed in the U.S.A.

Library of Congress Cataloging-in-Publication Data
ISBN: 0-8031-3466-5

Contaminated sediments : characterization, evaluation,
mitigation/restoration, and management strategy performance / Jacques
Locat...[et al.].
p. cm. — (STP ; 1442)
"ASTM stock number: STP 1442."
"Second International Symposium on Contaminated Sediments ... in Quebec
City, Canada on May 26-28 May 2003"—Foreword.
Includes bibliographical references and index.
ISBN 0-8031-3466-5
1. Contaminated sediments-Management-Congresses.2. Soil
remediation–Congresses. I. Locat, Jacques. II. International
Symposium on Contaminated Sediments (2nd : 2003 : Quebec, Quebec) III. Series:
ASTM special technical publication ; 1442.

TD878.C663 2003
628.5'5–dc21

2003049606

Photocopy Rights

Peer Review Policy

Each paper published in this volume was evaluated by two peer reviewers and at least one editor. The authors addressed all of the reviewers' comments to the satisfaction of both the technical editor(s) and the ASTM International Committee on Publications.

To make technical information available as quickly as possible, the peer-reviewed papers in this publication were prepared "camera-ready" as submitted by the authors.

The quality of the papers in this publication reflects not only the obvious efforts of the authors and the technical editor(s), but also the work of the peer reviewers. In keeping with long-standing publication practices, ASTM International maintains the anonymity of the peer reviewers. The ASTM International Committee on Publications acknowledges with appreciation their dedication and contribution of time and effort on behalf of ASTM International.

Printed in Ann Arbor, MI
2003

Foreword

The Second International Symposium on Contaminated Sediments: Characterization, Evaluation, Mitigation/Restoration, and Management Strategy Performance in Quebec City, Canada on 26-28 May 2003 is sponsored by ASTM International Committee D18 on Soil and Rock. The symposium chairs and co-chairs of this publication are Jacques Locat, Laval University (CGS) and Rosa Galvez-Cloutier, Laval University (CSCE, ASTM); and Ronald C. Chaney, Humboldt State University (ASTM) and Kenneth Demars, University of Connecticut (ASTM).

Contents

SECTION I: SEDIMENT CHARACTERIZATION

SECTION II: MITIGATION AND RESTORATION METHODS

SECTION III: MONITORING AND PERFORMANCE

Overview

Recent advances in our understanding of contaminated sediments have been assembled in this Special Technical Publication, which is one of the major scientific contributions to the Second International Symposium on Contaminated Sediments held in Québec City from May 26 to 28, 2003. This volume is part of the overall technical program of ASTM Committee D18 on soil and rocks.

For many decades, waterways have been exposed to a wide variety of contaminants. Even if regulations and a better control of contaminants have been established to reduce their emission, many contaminants are still present in bottom sediments. In fact, some of them are persistent and continue to pose a potential risk to the environment with direct and cumulative toxic impacts on aquatic life, organisms, and eventually on human health.

In recent years, major advances have been made in the study and understanding of contaminated sediments, particularly via major projects in areas such as Los Angeles, California, Saguenay Fjord in Québec, and Singapore.

The symposium covers the areas of sediment characterization, contaminant evaluation, mitigation/restoration methods, and management strategy performance from the geological, geotechnical, biological, and geophysical perspectives. It reviews recent advances in contaminated sediments-management-related research and focuses on engineering aspects of contaminant transport, erosion, stability, monitoring, and modeling. The main goal of the symposium is to identify both established and innovative physico-chemical and biological tests and methods used to characterize and evaluate properties and behavior of contaminated sediments, as well as the potential for contaminant transfer.

The papers gathered in this publication cover the primary goal of the symposium and reflect research activities in many parts of the world. Keynote papers, selected for this volume, reflect recent work carried out on large coastal investigations (e.g., in the Los Angeles area), and on natural and artificial capping of contaminated sediments. Other papers in this volume have been assembled into three groups: (1) sediment characterization, (2) mitigation and restoration methods, and (3) monitoring and performance. Each of these sections begins with the corresponding keynote paper.

Sediment characterization of contaminated sediments has become more and more complex. It involves *ex situ* techniques from standard tests (e.g., physical properties) to biological analyses in addition to all the chemical analyses, but also *in situ* ones like erodability tests. Mitigation and restoration methods assembled herein are diversified and touch on many different environments from river sediments and harbor lagoons to land reclamation. It involves techniques ranging from the use of geotextiles and geocomposites to selective sequential extraction methods. The monitoring and performance aspects of contaminated sediments are largely supported by extensive site investigations, like the Southern California project, but also by the development of modeling tools.

A few papers included in this volume summarize a five-year research effort aimed at evaluating the performance of a catastrophic capping layer resulting from the major 1996 Saguenay flood disaster that proved to be very beneficial to the Saguenay Fjord environment and ecosystem by covering most of the ancient contaminated sediments!

Finally, the editors would like to thank all contributing authors for their effort and timely response. This book represents the achievements of a process strongly supported by various learning societies or agencies, including ASTM International (Committee D-18), the Canadian Geotechnical Society,

the Canadian Society of Civil Engineering, the Society for Environmental Toxicology and Chemistry (St. Lawrence Chapter), and the National Science and Engineering Research Council of Canada. The Editors are very grateful to Mrs. Hélène Tremblay, Secretary of the Symposium, and to Mrs. Crystal Kemp for their dedication towards ensuring the completion of this Special Technical Publication.

Jacques Locat
Laval University (CGS)

Rosa Galvez-Cloutier
Laval University (CSCE, ASTM)

Section I: Sediment Characterization

Emilien Pelletier,[1] Gaston Desrosiers,[1] Jacques Locat,[2] Alfonso Mucci,[3] and Hélène Tremblay[2]

The Origin and Behavior of a Flood Capping Layer Deposited on Contaminated Sediments of the Saguenay Fjord (Quebec)

Reference: Pelletier, E., Desrosiers, G., Locat, J., Mucci, A., and Tremblay, H., "**The Origin and Behavior of a Flood Capping Layer Deposited on Contaminated Sediments of the Saguenay Fjord (Quebec),**" *Contaminated Sediments: Characterization, Evaluation, Mitigation/Restoration, and Management Strategy Performance, ASTM STP 1442*, J. Locat, R. Galvez-Cloutier, R. C. Chaney, and K. R. Demars, Eds., ASTM International, West Conshohocken, PA, 2003.

Abstract: The upper section of the Saguenay Fjord was impacted by a catastrophic flood in July 1996. Contaminated sediments were capped by a layer of clean silty post-glacial sediments with background levels of trace metals and polycyclic aromatic hydrocarbons (PAHs). The capping layer was characterized by geotechnical and geochemical methods and its biological recolonization was monitored by annual sampling of the macrofauna. The strong dominance of surface deposit feeders Cirratulidae and Ampharetidae was observed at most stations in the first 2-3 years followed by carnivorous annelids such as Lumbrineridae and Nephtidae species indicating a well recolonized benthic habitat in the Baie des Ha!Ha!. The presence of benthic fauna was a major factor in modifying the density of sediments by physical mixing and irrigation, and in changing the surface roughness. The slope stability of the capping layer is considered as very good except in limited deltaic sectors at the head of the Baie des Ha!Ha! The new layer showed a good efficiency to isolate contaminated sediments from the sediment/water interface. Although manganese and iron were remobilized as the new layer became anoxic, mercury, arsenic and PAHs showed a very limited mobility through the flood layer which allowed geochemists to calculate the present fluxes of toxicants to the Baie des Ha!Ha! without interferences from older contaminated sediments trapped below the flood layer. The present flux of PAHs to bay (0.9 $ng.cm^{-2}.g^{-1}$) is about 300 times lower than the 1974 flux and 8 times lower than the 1986 flux.

Keywords: Saguenay Fjord, flood layer, contaminated sediments, extreme meteorological event, biogeochemical barrier, metal remobilization, bioturbation, layer instability

---

[1] Professors, Institut des sciences de la mer (ISMER), Université du Québec à Rimouski, 310 allée des Ursulines, Rimouski (Que) Canada G5L 3A1.

[2] Professor and post-doctoral fellow, respectively, Département de géologie et génie géologique, Université Laval, Québec (Que), Canada G1K 7P4.

[3] Professor, Department of Earth & Planetary Sciences, McGill University, 3450,University St., Montreal (Que) Canada H3A 2A7.

Introduction

The Saguenay Fjord is the largest fjord in eastern Canada. Its long, narrow glacially-scoured submerged valley joins the St. Lawrence Estuary at Tadoussac, about 200 km downstream of Quebec city. Typical of classical fjords, it has a U-shaped cross-section and two shallow sills that subdivide it into two distinct basins. The upstream basin reaches a maximum depth of 280 m near Baie Eternité. Intrusions of cold and dense seawater from the intermediate layer of the St. Lawrence Estuary are responsible for the periodical renewal of the fjord deep waters (Seibert et al. 1979). The upper section of the fjord opens in two branches, giving birth to the North Arm toward the Saguenay River and the Baie des Ha!Ha!. The Saguenay River is the main freshwater tributary of the fjord with an average annual flow rate of 1600 m^3s^{-1} and spring flood flow rates rarely exceed 3000 m^3s^{-1} due to the presence of a number of dams and dikes regulating the outflow of the Saguenay drainage basin.

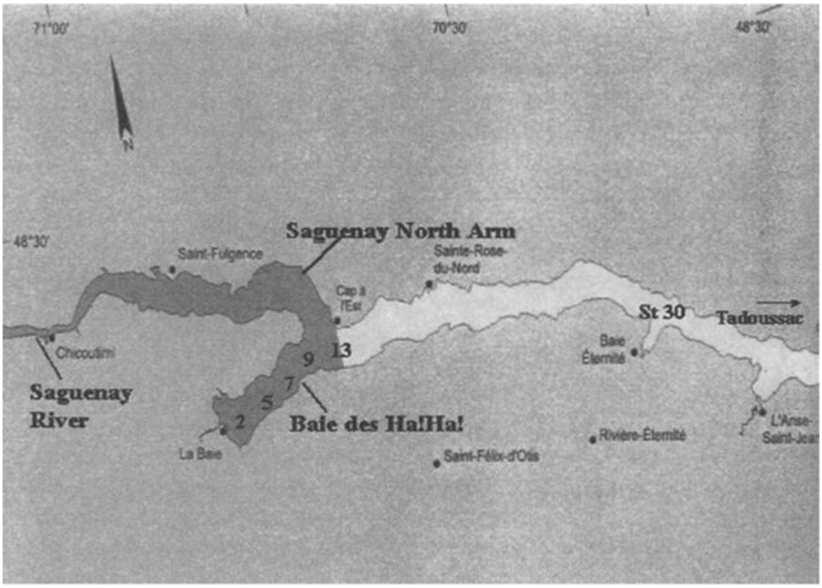

Figure 1 – *Map of the Upstream Section of the Saguenay Fjord Showing in Dark Gray the Benthic Area Directly Affected by the 1996 Flood.*

On July 18th , 1996, heavy rain started in the Saguenay region and continued for 3 more days, resulting in precipitation of about 200 mm with peaks at 280 mm in some areas (Nicolet et al 1997). Because of a wet early summer and high moisture conditions, this precipitation event caused widespread flooding in the steep catchments along the Saguenay River and Fjord. The resulting floods caused over $1 billion in damages as the Chicoutimi and Ha! Ha! rivers made their way through the city of Chicoutimi and the industrial town and port terminal of Ville La Baie. The incision of new river channels and widening of existing channels through late-glacial deltaic fill sediments and the transport of an estimated 15 million m^3 of solids to the Saguenay Fjord resulted in a massive sedimentation event in the North Arm of the Fjord and the Baie des Ha!Ha!. Shortly after this catastrophic event, a multidisciplinary team of marine scientists (physical oceanographers, geological engineers, geochemists, chemists and biologists) from universities and governmental agencies was assembled to study the effects and behavior of the capping layer deposited on contaminated sediments of the Saguenay Fjord. This huge research effort mainly supported by NSERC (Natural Sciences and Engineering Research Council of Canada) and ALCAN International Limitée was motivated by the uniqueness of the event and the challenge of integrating the knowledge from many disciples into a conceptual model which could serve as a unique source of information for those involved in the management of further catastrophic events occurring in coastal environments.

The objective of this paper is to provide a first summary of the main findings on the performance of the capping layer either for geological, geotechnical and geochemical parameters, and chemical and biological indicators.

Sediment Deposition and Capping Process

Water samples collected in the Baie des Ha!Ha! on September 1996 have clearly shown the influence of the flood on the abundance, distribution and chemical composition of suspended particle matter (SPM). The abundance of SPM in surface water (0-5 m) was still 2-3 times higher than values recorded before 1990 (Pelletier et al 1999a). The deep water layer of the Baie des Ha!Ha! was still loaded with about 5 mg.L^{-1} of terregeneous particles (low organic carbon content), a concentration about 15 to 20 times higher than values recorded 20 years before the flood (Sundby and Loring 1978).

Sediment box cores, collected in the North Arm and the Baie des Ha!Ha! three weeks after the flood revealed that 10 to 50 cm of a fluidic sediment (with a shear strength <0.5 kPa) were deposited in both sections of the Fjord (Fig. 1). The flood deposit was still clearly visible in cores collected in Baie des Ha!Ha! in 1998 and years after as a lighter brown-gray layer on the gray-black indigenous sediment. Grain size analysis of 13 samples of surface sediment (0-5 mm) collected in September 1996 in the Baie des Ha!Ha! showed a constant composition of the surface layer with an average high water content of 57 % in weight, and a composition of 18% clay, 72% silt and 10% sand (Pelletier et al 1999b). Chemical analysis revealed a relatively high contain in inorganic carbon content (up to 0.5%) but very low concentrations in mercury, lead, and arsenic. Higher levels of inorganic carbon were attributed to detrital, calcareous materials from the post-Winsconsin marine clays transported by the flood event.

Subaqueous capping is known as an efficient means for isolating contaminated sediments and residues from the aquatic environment (Zeman 1994). The natural capping process which occurred in the Baie des Ha!Ha! and North Arm in July 1996 covered an area of about 60 km^2 at water depth varying from 50 to 180 m. The thickness of the new sediment layer, as estimated a few weeks after the flood and before the consolidation process, ranged from about 60 cm at station 2 near the delta of the small Rivière des Ha!Ha! close to the city of La Baie to a few mm in the deepest basin of the fjord near Baie Eternité (Fig. 1). The North Arm also received a large volume of post-glacial sediments and the capping layer was estimated to 40 cm near Saint-Fulgence to 5-10 cm at the junction with the Baie des Ha!Ha!

During the flood, the sediments were most probably transported into the Fjord by hyperpycnal flow meaning that the mass of sediments was heavy enough to sink to the seafloor, increasing the turbidity, current regime, and erosion of the seafloor. The modification of the current regime has resulted in the formation of many dunes on the main flowing channels, typical of strong currents (Tremblay et al. 2001). The bed-material load was principally transported by traction and suspension and by turbidity currents (Cremer et al. 2002; Tremblay et al. 2003). The coarser particles were transported by a traction process and were mostly accumulated at the river deltas. The finer particles were held temporarily in suspension by fluid turbulence and were deposited gradually in a fining downstream sequence. Following the quick accumulation and progradation of the deltaic structures, gravitational movements on the unstable delta front created successive sequences of deposition in the basin (Crémer et al. 2002). Each episodic deposition was constituted of fine sandy laminations at its base, topped with clayey silt.

To evaluate the extent of the flood layer and its morphology, a series of box core samples, geophysical and multibeam sonar surveys (SIMRAD EM1000) were carried out and compared with pre-flood surveys. The extent of the covered area is shown on backscatter images (Fig. 2).

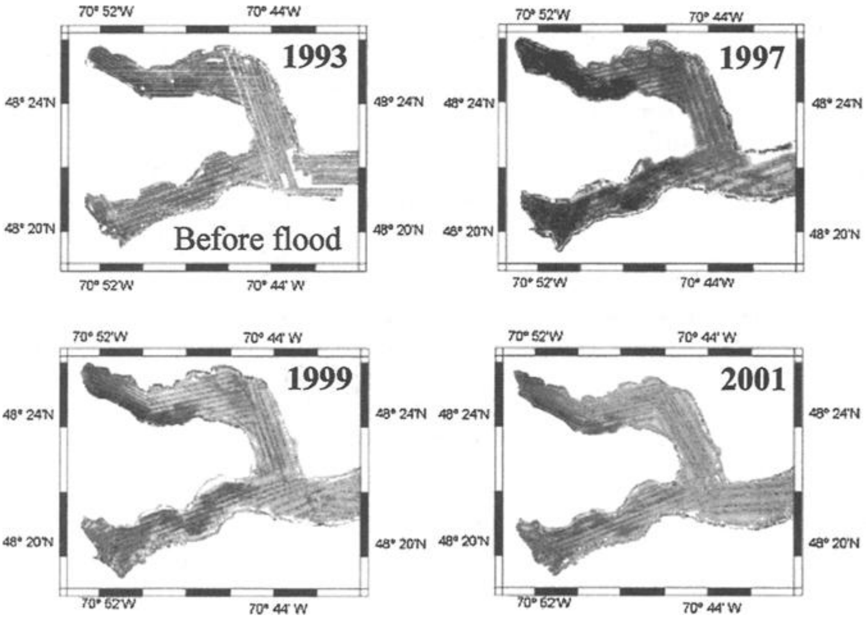

Figure 2 – *Temporal Evolution of the Backscatter Data Over Multibeam Sonar Surveys (modified from Urgeles et al. 2002)*

On these images, a difference in backscatter of sediments before (in 1993) and after the flood (in 1997) can be observed. The darker zones in 1997 correspond to the limits of the capping layer that seems to end just downstream to the confluence of the Baie des Ha!Ha! and the North Arm (Urgeles et al. 2002). Box cores revealed a thickness varying from almost nothing to 60 cm in most of the covered area, generally decreasing in the downstream direction. The accumulation of sediment reached 7 m at the river mouths of the Baie des Ha!Ha! (Kammerer et al. 1998).

Anthropogenic Contamination of the Fjord

The rapid expansion of the metallurgic industry and urbanization in the Saguenay – Lac Saint-Jean region in years 1940-1970 contributed to the degradation of the aquatic environment, and particularly the Saguenay Fjord. The presence of high concentrations of mercury (Hg) in the sediments of the Fjord was first pointed out by Loring (1975) who observed concentrations reaching 6 to 12 mg.kg^{-1} in the North Arm and 3 to 6 mg.kg^{-1} in the Baie des Ha!Ha! for sediment sampled in 1964. The flux of Hg to sediments to the fjord reached 60 000 ng.cm^{-2}.yr^{-1} in early 1970s and then was progressively reduced with the cutbacks of liquid effluents from a chlor-alkali plant in 1970-1974 (Smith and Loring 1981). An estimated 60 tons of mercury still reside in the sediments at sediment depths varying between 15 cm and over one meter. In addition to Hg, other trace metals such as cadmium (Cd), chromium (Cr), copper (Cu), lead (Pb), and zinc (Zn) have been found in elevated concentrations in the sediments of the fjord, and their presence has been attributed to the industrial and urban activities of Chicoutimi and other upstream human communities (Gagnon et al. 1993).

The flux of polycyclic aromatic hydrocarbons (PAHs) to the fjord has been estimated at 11 000 ng.cm^{-2}.yr^{-1} in 1966 in the North Arm (Martel et al. 1987). This flux was reduced by one order of magnitude between 1970 and 1981 with the enforcement of new environmental regulations in Canada.

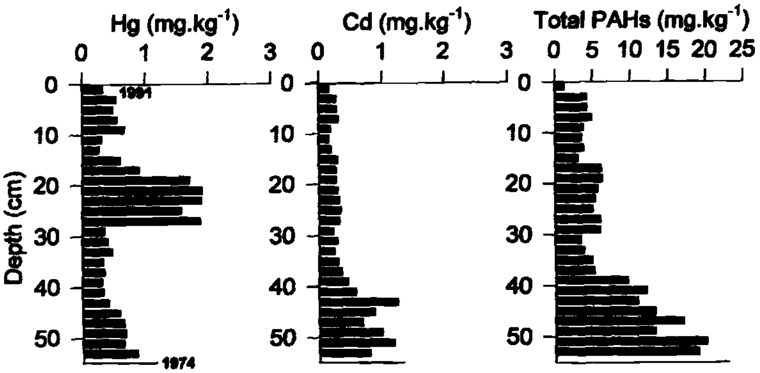

Figure 3: *Hg, Cd and Total PAHs Profiles From a Core Sampled in 1991 in the North Arm near St. Fulgence. The Local Sedimentation Rate is Approximately 3 cm.yr^{-1}.*

Changes in Hg, Cd and PAHs concentrations in a sediment core collected in the North Arm in 1991 are shown in Fig. 3. Total PAHs decreased from about 20 mg.kg^{-1} to less than 5 mg.kg^{-1} within 17 years whereas Cd concentrations also decreased by a factor of 4-5 during the same period. The behavior of mercury was more puzzling as the concentration in the core seems to increase in the early1980s and then decreased again in the early 1990s to a value of 0.4 mg.kg^{-1} (two times the pre-industrial background level) The presence of PAHs in the Baie des Ha!Ha! and elsewhere in the Fjord was first reported by Martel et al. (1987) who found total PAHs concentrations reaching 3.5 mg.kg^{-1} at a sediment depth corresponding to the early 1970s. The flux of PAHs to the bay was estimated to be 279 ng.cm^{-2}.yr^{-1} in 1974, a value about 25 times lower than the flux to North Arm at the same period. The explanation for such a difference hold in the fact that most of the PAH-loaded sediments came from the Saguenay River, and the Baie des Ha!Ha! was only indirectly touched by the contamination. A new core was sampled in the bay in 1988 and PAHs were analyzed (Ouellet 1990). The top 40 mm of the core showed an average total PAHs concentration of 1.83 mg.kg^{-1} confirming the important reduction already observed in the North Arm although the sedimentation rate in the bay was <0.3 cm.yr^{-1}.

In the last few years, a new environmental problem surfaced with the use of antifouling paints on large commercial and navy ships. The powerful biocide tributyltin (TBT) contained in these paints is released into the water column on the passage of the vessels and accumulated in suspended particulate matter and sediments along waterways and near important harbors. The Saguenay Fjord acts as a sink for TBT because of the slow renewal process of its deep water mass. Concentrations over 100 ng.g^{-1} of total organotins (expressed as Sn) have been observed in sediments and organisms collected in the Baie des Ha!Ha! and elsewhere in the Fjord from 1999 to 2001.

The Performance of the Capping Layer

Geotechnical Results

The flood layer is a turbidite, except at the river mouths, usually characterized by a thin sandy layer at the bottom. The grain size distribution varies from sand to clay. Near the river mouths, the sediments were coarser and mainly constituted of sand and gravel. Compared to sediments existing before the flood, they have higher water content, a lower consistency and a lower plasticity index (Maurice et al. 2000). In the North Arm, the new layer is harder to identify because the sandy layer at its base is very thin or absent, and an important bioturbation process has quickly erased the signature of the turbidite through mixing of sediments.

The temporal evolution of some sediment properties was monitored using backscatter data (Fig. 2). The intensity of the backscattering depends on the water content of the sediment, its density and surface roughness (Urgeles et al. 2002). Sediment with a low water content shows high backscattering which increases with the increasing density. On the 2001 image the extent of the dark zones is quite similar to the 1993 image, meaning that the properties of the flood layer have returned to the pre-flood conditions.

In their recent work, Maurice et al. (2000) estimated that the consolidation of the layer was completed within 3 months after the flood. Authors also noted that bioturbation, easily observed in cores, clearly influenced the consolidation process of the newly deposited sediments. On the non bioturbated profile (Fig. 4a) one can easily determine the thickness of the flood layer by quick changes of the water content, intact (C_u) and remolded (C_{ur}) undrained shear strength and liquidity index (I_L). In the flood layer, the water content (w %) decreases regularly with depth and the shear strength increases following the consolidation process. The peaks between 25-30 cm correspond to the sandy layer. The liquidity index is high, around 4, meaning that the consistency is very low, like sludge. For samples where bioturbation is well established (Fig. 4b), an reverse situation is observed. Water content increases with depth, the resistance decreases and the sediment is more consistent. These changes are directly attributed to the action of organisms that drain and mix the sediment, causing a decrease in the water content and an accelerated densification. Without bioturbation, the value of I_L is around 4 at the sediment surface with a slight decrease with depth, whereas it rapidly decreases to a value of 2 when bioturbation is present.

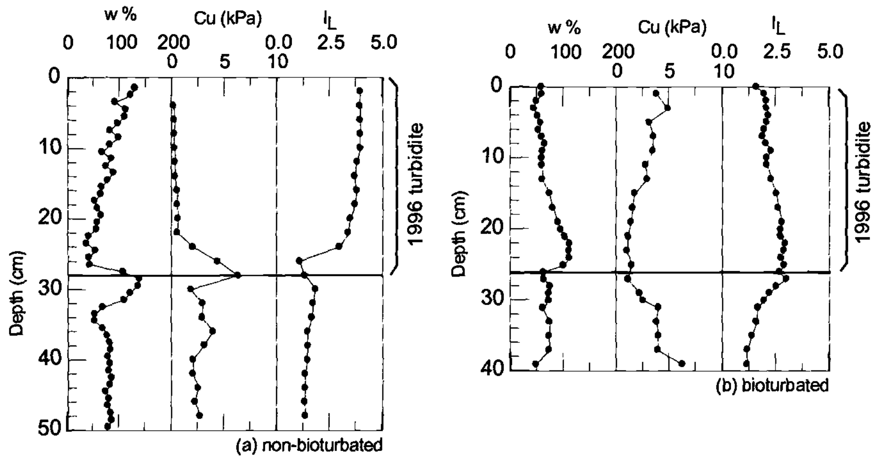

Figure 4 – *Geotechnical Profiles of the 1996 Turbidite*
a) Non Bioturbated Sample Taken in the Baie des Ha! Ha! in 1997 and b) Bioturbated Sample Taken in the North Arm in 1998 (Modified from Maurice et al, 2000)

The profile in Fig. 4b shows that the organism activities contribute to an increase in the shear strength of sediments at the surface. For bioturbated sediments, C_u is around 5 kPa while it is less than 1 kPa for non-bioturbated sediments. Consequently, this increase in C_u at the sediment surface contributes to increase the resistance to erosion. To evaluate if the bottom current in the Fjord could erode the sediment surface, a study on the erodability has been conducted by measuring the *in situ* critical shear stress and erosion rates using a circular benthic flume (Miniflume) (Moreau et al. 2003). The results reflect the spatial variability of sediment properties observed for the bioturbated flood layer (Tremblay et al. 2003), with critical shear stress (τ_c) varying between 0.06 and 0.44 Pa (corresponding to current velocity of 5.4 and 14.7 cm.s^{-1}), and the mean erosion rate for total erosion phase (E_{mean}) between 3.42 x10^{-4} and 1.25 x10^{-5} kg.m^{-2}.s^{-1}. These results reveal that the surface layer could be resuspended even by low currents.

Geochemical Results

The distribution of four metals (Fe, Mn, Hg, and As) was monitored in the sediments and their response to diagenetic processes following the deposition of the flood material. The geochemical cycles of iron and manganese in sediments dictate the diagenetic behavior of many elements since their oxides are strong adsorbents and play a pivotal role in determining the distribution and partitioning of other elements in the sedimentary column (Gagnon et al. 1997; Mucci et al. 2000)

Under stead-state conditions, such as those encountered at the deep inner basin near Baie Éternité (Fig. 1, St 30), which received only an ineffectual, discontinuous, thin film of the flood material, reactive Fe and Mn (i.e., soluble in a 1M HCl solution) are concentrated in the oxic sediments (Fig. 5). The concentration of the reactive Fe and Mn oxides near the sediment-water interface results from the reductive dissolution of authigenic and detrital oxides as they are buried below the oxygen penetration depth (~5mm) and dissolved Fe(II) and Mn(II) diffuse back to the oxic layer where they are oxidized and precipitated (Mucci and Edenborn 1992). The highest arsenic concentrations were also found near the sediment/water interface where this element is actively concentrated by adsorption onto the iron oxides (Fig. 5). The distribution of Hg in these sediments reflects, mostly, the history of metal discharge to the Fjord. Similar metal accumulation profiles in the sediments were observed in 1991 in the North Arm (Fig. 1). Sulfate reducing conditions are encountered within the first two cm below the sediment/water interface as evidenced by the porewater sulfate depletion and/or the appearance of acid volatile sulfides (AVS) in the solid sediments (Fig. 6; Gagnon et al. 1995; Mucci et al. 2000a).

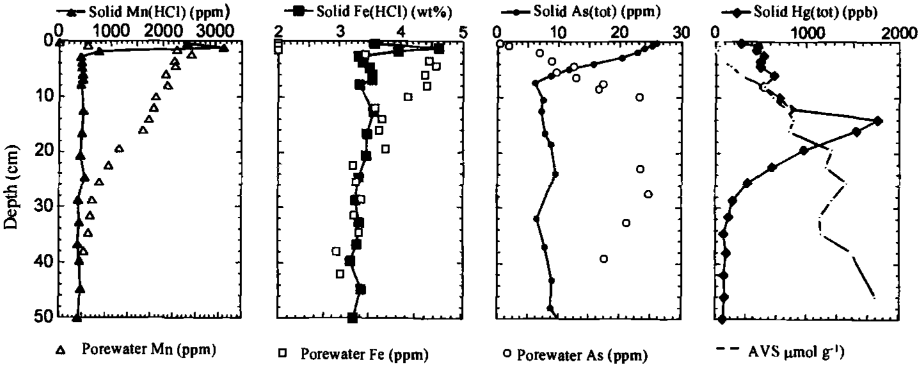

Figure 5 – *Steady State Diagenetic Conditions in the Fjord as Represented by the Geochemistry of Sediments at Station 30, a Site Unaffected by the Flood Deposit.*

Manganese remobilization occurred almost unimpeded following the emplacement of the flood deposit. As indicated in the abridged time-series from station 9 in the Baie des Ha! Ha! (Fig. 6 a and b), authigenic manganese oxides (i.e., Mn_{HCl}) present at the original sediment-water interface and delivered with the flood material were reduced and most of the Mn(II) diffused freely to the newly established interface where it was oxidized and re-precipitated. Dissolved Mn (II) profiles show that it originates both from the former sediment-water interface and the dissolution of detrital oxides delivered with the flood material (Fig. 6 a and b). The shape of the dissolved manganese profiles is dictated by the strength of the sources (i.e., reactivity of reducible phases at the former sediment/water interface and within the flood deposit) and sinks (i.e, precipitation of authigenic oxides close to the new sediment/water interface, the formation of a mixed carbonate and adsorption to AVS at depth (Mucci and Edenborn 1992; Saulnier and Mucci 2000).

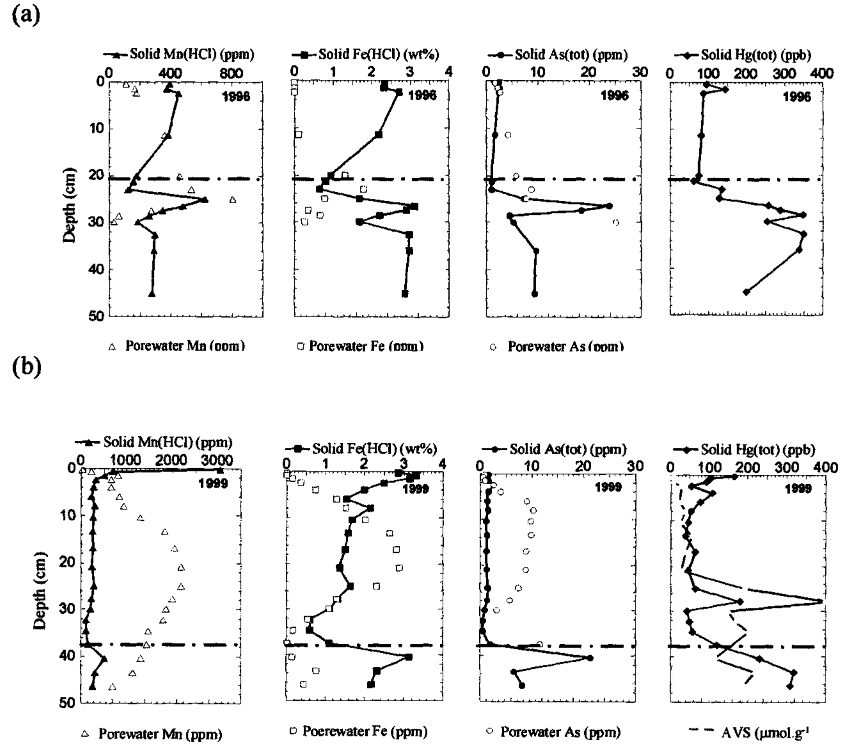

Figure 6 – *Evolution of Sediment and Porewater Geochemistry at Station 9 in the Baie des Ha!Ha!: (a) Less than one Month after the Flood and (b) Nearly Three Years after the Flood Event. The Dashed Line Marks the Lower Boundary of the Flood Layer.*

In contrast to Mn, reactive iron associated with the authigenic oxides at the original interface displayed limited mobility. Following the reductive dissolution of these oxides, Fe(II) was trapped as sulfides (i.e., mostly AVS with minor authigenic pyrite) under the sulfate-reducing conditions that were rapidly established. At station 9, the sulfides (see

AVS profile in Fig. 6b) are found immediately above and below the solid, Fe(HCl) peak and the lower boundary of the flood deposit whereas a single and broader sulfide peak is only observed below the former sediment-water interface at station 5 (data not shown). The difference between the two behaviors may be explained by the higher sedimentation rate ($<0.2 cm.yr^{-1}$ in the Baie des Ha!Ha! vs $\sim 1 cm.yr^{-1}$ in the North Arm) and a greater reduction potential of the indigenous sediments in the North Arm. Mucci and Edenborn (1992) proposed a conceptual model to explain the different, diagenetic behaviour of iron and manganese in the Saguenay Fjord sediments following the Saint Jean Vianney landslide of May 1971. A revision of this model as well as a numerical model describing the remobilization of reactive manganese can be found in Mucci et al. (2003).

Arsenic is reduced from As(V) to As(III) under suboxic conditions and forms a stable sulfide mineral under sulfidic conditions. In marine sediments, however, it usually co-precipitates with authigenic iron sulfides (Belzile and Lebel 1986). Likewise, we observe that most of the arsenic, which was also concentrated at the original interface by adsorption to the authigenic iron oxides (Fig. 5) appears to be trapped by co-precipitation with the iron sulfides (i.e., AVS; Fig. 6b), thus limiting its diffusion through the flood deposit. The porewater arsenic profile (Fig. 6b) attests to its limited mobility through the flood layer.

Very little mercury was delivered to the fjord with the flood material (Fig 6a). The vertical distributions of Hg in the sediments recovered since the flood event indicate that most of the Hg is still found within the indigenous, contaminated sediments buried under the flood deposit but a fraction was remobilized and is associated with the AVS within the deposit (Fig. 6b). Based on the time-series data, the peak concentration at the new sediment-water interface would originate from inputs of Hg-laden particles under the normal sedimentation regime (Fig. 6b).

Recolonization of the New Layer in the Baie des Ha!Ha!

The benthic recolonization process of the new sediment layer deposited in the Baie des Ha!Ha! was monitored by a series of stations located on the longitudinal axis of the bay (Fig. 1). Five stations were sampled annually using a Van Veen grab of $1/8 m^2$. A particular attention was given to stations 2 and 13 which were located at the head of the bay near La Baie and at the junction between the North Arm and the Baie des Ha!Ha!, respectively. For station 2, no macrobenthic organisms were found in fall 1996, but the recolonisation process started quickly after our sampling and the average density peaked in 1999 with $3101 \pm 868 ind.m^{-2}$ (Fig. 7). This average density suddenly dropped to $802 \pm 269 ind.m^{-2}$ in 2000, and then returned to values previously observed in 2001 with $3133 \pm 314 ind.m^{-2}$. Station 13 showed an increasing average density of organisms from 1996 to 1998 ($421 \pm 82 ind.m^{-2}$), but again an unexpected progressive reduction of the biota was observed until 2001 ($128 \pm 11 ind.m^{-2}$). For stations 5, 7, 9 located a few km away from direct sources of sediment, the densities were higher in 1996 than those observed for the same year at stations 2 and 13. Their average density seems to strongly decrease in 1997 and dominate in 1998 for these three stations. We again observed a decrease in the following years at these stations, except for station 9 in 2001($176 \pm 8 ind.m^{-2}$) (Fig. 7). The Kruskal-Wallis nonparametric test showed significant differences between the five annually sampled stations from 1996 to 2001 (Chi-square = 16,66, df = 4, $p = 0.22$).

The strong predominance of the polychaete annelids was observed for all stations in the first year. In this particular zoological group, the dominant species responsible for the recolonization process at station 2 is the surface deposit feeders *Chaetozone setosa* and *Ampharete cf arctica*, and the subsurface deposit feeder *Cossura longocirrata*. In the following years, even if the deposit feeders are still well represented, carnivorous polychaetes became dominant with the strong presence of the *Lumbrineris fragilis* species and Nephtydae *Aglaophamus neotenus* for the other stations.

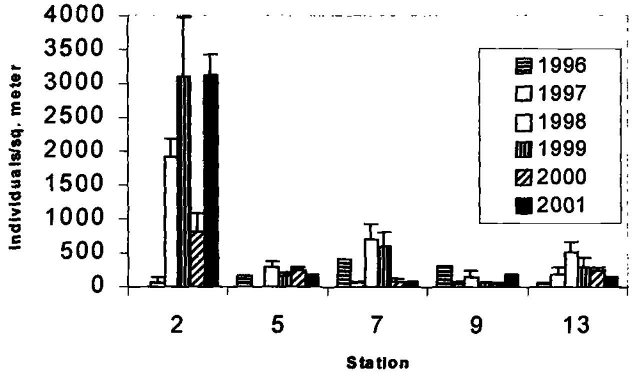

Figure 7- *Distribution of Macrobenthic Organisms Found in Sediments of Five Stations of the Baie des Ha!Ha! from 1996 to 2001.*

Station 2 was catastrophically affected by the 1996 flood as no benthic organisms were found at this station in September 1996 (Pelletier et al. 1999b). The Spionidae group was supplanted in 1997 by Lumbrineridae (*Lumbrinereis fragilis*) and Cirratulidae (*Chaetozone setosa*) in most stations. For example, station 13 was occupied by Spionidae only in 1996, and we found at this same station in 1997 a much higher diversity with six annelid families among which Ampharetidae (*Ampharete cf arctica*) and Capitellidae (*Capitella capitata*) were present. In all stations after the flood, the polychaete annelids represented the dominant benthic fauna by their density and diversity, thus indicating a rapid recolonisation process of this new sediment layer with the presence of pioneer species such as Spionidae (Pearson and Rosenberg 1978). From 1997, Spionidae were gradually replaced by species being more characteristic of deep muddy circalittoral biotopes and species indicating possible organic contamination (Pearson and Rosenberg 1978; Pelletier et al. 1999b). While polychaetes were recolonizing this new sedimentary layer they created a network of tubes and burrows down to the ancient layer. This new bioturbation of the top layer of sediment has been directly observed by axial tomodensitometry (de Montety et al. 2000). The high mean density observed at station 2 is due to the high abundance of surface deposit feeders, particularly Cirratulidae (*Chaetozone setosa*) and Ampharetidae (*Ampharete cf arctica*). Other stations showed a lower mean density and a gradual reduction of deposit feeders compared to carnivores like *Lumbrinereis fragilis* of the family of Lumbrineridae and Nephtydae (*Aglaophamus neotenus*). Station 2 received terrigenous sediment with a relatively high organic content when compared to the other stations along the bay.

However, the recolonization process which quickly started at station 2 was unstable in time and clearly related to the capping instability in that area. Indeed, the significant fall of average densities observed at this station in 2000 was caused by the local erosion of the sedimentary surface layer in 2000 (Michaud et al. 2001, 2002).

Occurrence of PAHs in the New Layer

In sediment sampled in the Baie des Ha!Ha! in 1988 and analyzed by Ouellet (1990) the concentration of a major PAH contributor, benzo(a)pyrene (BaP), was about 0.25 mg.kg^{-1} in the top 10 mm and increased with depth to a maximum of 1.963 mg.kg^{-1} in the 10-12 cm layer. Since 1998, we analyzed each year the evolution of the distribution profile of high molecular weight PAHs in the flood deposit layer at station 9 in the Baie des Ha!Ha!. The post-glacial sediments eroded by the flood and transported to the bay were very poor in PAHs with a total concentration of about 0.1-0.2 mg.kg^{-1} which is well below the background level (0.5 mg.kg^{-1}) found by Martel *et al* (1987) in the pre-industrial sediment layers of the Saguenay Fjord. The lowest concentration of BaP (0.003 mg.kg^{-1}) was measured at 4-12 cm depth in a core collected in 1998. Interestingly, the top 2 cm layer of the same core showed BaP concentrations ranging from 0.02 to 0.035 mg.kg^{-1}. This thin enriched surface layer is attributed to the late deposition (within the year after the flood) of very fine clay and black carbon particles which were enriched in hydrophobic high molecular weight PAHs. These particles were mixed with underlying sediments in the following years by the bioturbation of macrobenthic organisms recolonizing the area. The BaP profile in 2001 was characterized by a maximum value of 0.047 mg.kg^{-1} in the 5-6 cm layer with a steady decrease toward the surface reaching 0.021 mg.kg^{-1} in the top 0-1 cm layer. The lower values appearing near the surface seem to indicate a very low input of new PAHs from the natural sedimentation process of the bay in the last three years. Using the average concentration of BaP in the top 5 cm (0.03 mg.kg^{-1}) and a sedimentation rate of 30 mg.cm^{-2}.yr^{-1} (Leclerc et al. 1986) the present flux of BaP in the Baie des Ha!Ha! can be estimated to be about 0.9 ng.cm^{-2}.yr^{-1}. This value is about 300 times lower than the 1974 flux (Martel et al. 1987) and 8 times lower than the 1988 flux (Ouellet 1990).

Slope Stability Analysis

The nature of the capping layer in the Baie des Ha!Ha! and the North Arm varies greatly near major slopes found along active deltas. The capping layer in nearshore areas consists mostly of sand and gravel which have been rapidly deposited over pre-existing organic rich fine-grained sediments. The multibeam image of the upper part of the Baie des Ha!Ha! showed that the rapid loading of the underlaying sediments has produced some failures visible as submarine slides (Tremblay et al. 2001). No measurements of pore pressures are available in these sectors but as time goes on, excess pore pressure related to the rapid loading process shall vanish. Elsewhere, Maurice et al. (2000) have shown that all excess pore pressures due to rapid sedimentation and consolidation have been dissipated so that for most of the area covered by the capping layer, the stability analysis can be carried out assuming hydrostatic conditions.

The analysis of the stability of the capping layer included considerations for both drained and undrained conditions and also seismic acceleration. On such low angle slopes with such a thin layer (assume here at an average of 0.5 m) we can use infinite slope stability for evaluating the factor of safety against failure. In such a situation, it was hypothesized that the failure could take place under undrained conditions. The following equation for the infinite slope stability (Lee et al. 2000) was used:

$$FS = \left[\frac{k\gamma' z \cos\beta}{\gamma' z \cos\beta \sin\beta + a_h \gamma z \sin\beta} \right] \qquad [1]$$

where k is the strength ratio (C_u/σ'_{vo} ,where C_u is the undrained shear strength and σ'_{vo} the effective stress at a given depth), z is the depth to the failure plane, γ and γ' the total and buoyant unit weight, respectively, σ the slope angle and a_h the equivalent seismic acceleration. From the geotechnical investigation carried by Maurice et al. (2000) the value of k varies around 0.5, which is often the case for recently deposited sediments of the Saguenay Fjord (Perret et al. 1995). Using Eq. [1], the parametric analysis has indicated that in absence of an earthquake, slopes as high as 10 degrees are stable, even with a k value of 0.2. Considering a seismic event similar to the one which occurred in 1988, a slope at 6 degrees is stable for an acceleration of 0.3. Even with a k value at 0.5 and the same seismic loading, slopes at 10 degrees are still stable. Therefore, it appears that under seismic loading conditions, only limited sectors would be affected near actual deltas of the Baie des Ha! Ha!. The actual slope stability of these sectors could also be very dependent on remaining high pore pressures resulting from the rapid loading generated by the capping layer. More work remains to be done in these areas to ascertain actual stability conditions.

Conclusion

In summary, the flood capping layer was clearly identified and characterized in the Baie des Ha!Ha! using geotechnical and geochemical tools. The presence of benthic fauna was monitored over 5 years and was a major factor in modifying the density of sediments by physical mixing and irrigation, and in changing the surface roughness. In all stations after the flood, the polychaete annelids represented the dominant benthic fauna by their density and diversity indicating a rapid recolonization process with the presence of pioneer species such as Spionidae. Then, Spionidae were rapidly replaced by carnivorous species of the family of Lumbrineridae and Nephtydae. The slope stability of the capping layer is considered as very good, except in some limited deltaic sectors at the head of the Baie des Ha!Ha! Although manganese and iron were remobilized as the new layer became anoxic, mercury, arsenic and PAHs showed a very limited mobility through the flood layer. The impermeability of the flood layer trapped the old aromatic hydrocarbons far below the sediment surface and allowed the geochemists to calculate the present flux of PAH to the sediment floor of the Baie des Ha!Ha! The multidisciplinary approach, adopted from the beginning, was proved to be an efficient and high productive path to reach a clear understanding of a very complex geological, chemical and biological process. Team leaders and students are grateful to NSERC, ALCAN International Ltée, FCAR (Québec), and Parc Marin Saguenay-Saint-Laurent for financial support.

References

Crémer, J.-F., Long, B., Desrosiers, G., de Montety, L., and Locat, J., 2002, "Application de la scanographie à l'étude de la densité des sédiments et à la caractérisation des structures sédimentaires: exemple des sédiments déposés dans la rivière Saguenay (Québec, Canada) après la crue de juillet 1996", *Canadian Geotechnical Journal*, Vol. 39, pp. 440-450.

de Montety, L., Long, B., Desrosiers, G., Crémer, J.-F., and Locat, J., 2000, "Quantification des structures biogènes en fonction d'un gradient de perturbation dans la baie des Ha! Ha! à l'aide de la tomodensitométrie axiale", *Proceedings of the 53rd Canadian Geotechnical Conference, Montreal*, pp. 131-135.

Gagnon, C., Pelletier, E., and Maheu, S., 1993, "Distribution of Trace Metals and some Major Constituents in Sediments of the Saguenay Fjord, Canada," *Marine Pollution Bulletin*, Vol. 26, pp.107-110.

Gagnon C., Pelletier E., and Mucci A., 1997, "Behaviour of Anthropogenic Mercury in Coastal Marine Sediments", *Marine Chemistry*, No 59, pp. 159-176.

Kammerer, E., Hughes Clarke, J.E., Locat, J., Doucet, N. and Godin, A., 1998, "Monitoring Temporal Changes in Seabed Morphology and Composition using multibeam Sonars: A Case Study of the 1996 Saguenay River Flood", *Proceedings of the Canadian Hydrographic Conference*, Victoria, Canada, pp. 450-461.

Leclerc, A., Gagnon, M.J., Côté, R., and Rami, A., 1986, "Compaction and Movement of Intertidal Water in Bottom Sediments of the Saguenay Fjord, Quebec, Canada ", *Sedimentary Geology*, Vol. 46, pp. 213-230.

Lee, H.J., Locat, J., Dartnell, P., Minasian, D., and Wong, F., 2000, "A GIS-Based Regional Analysis of the Potential for Shallow-Seated Submarine Slope Failures" In *Proceedings of the 8th International Symposium on Landslides*, Cardiff, U.K., pp. 917-922

Loring, D.H., 1975, "Mercury in the Sediments of the Gulf of St Lawrence", *Canadian Journal of Earth Sciences*, Vol. 12, pp. 1219-1225.

Martel, L., Gagnon, M., Massé, R and Leclerc A., 1987, "The Spatio-temporal Variations and Fluxes of Polycyclic Aromatic Hydrocarbons in the Sediments of the Saguenay Fjord, Québec, Canada", *Water Research*, Vol. 21, pp. 699-707.

Maurice, F., Locat, J., and Leroueil, S., 2000, "Caractéristiques géotechniques et évolution de la couche de sédiment déposée lors du déluge de 1996 dans la Baie des Ha! Ha! (Fjord du Saguenay, Québec)". *Proceedings of the 53rd Canadian Geotechnical Conference*, Montreal, pp. 123-130.

Michaud, E., Long, B., Crémer, J. F., Desrosiers, G., and de Montety, L., 2001, "Les phases de construction deltaïques, influence d'un apport catastrophique ", *Proceedings of the Canadian Coastal Conference, Québec,* pp. 533-547.

Michaud, E., Desrosiers, G., Long, B., de Montety, L., Crémer, J.-F., Pelletier, E., Locat, J., Gilbert, F., and Stora, G., 2002, "Use of axial tomography to follow temporal changes of benthic communities in an unstable sedimentary environment : (Ha! Ha! Bay, Saguenay Fjord), *Journal of Experimental Marine Biology and Ecology,* Vol. 4060, pp. 1-8.

Moreau, A-L., Locat, J., Long, B., Hill P., and Ouellet Y., 2003, "*In situ* Flume Measurements of Sediment Erodability in Saguenay Fjord (Quebec, Canada)" *Contaminated Sediments: Characterization, Evaluation, Mitigation/Restoration, and Management Strategy Performance, ASTM STP 1442,* J. Locat, R. Galvez-Cloutier, R.C. Chaney, and K. Demars, Eds., ASTM International, West Conshohocken, PA.

Mucci A. and Edenborn H. M., 1992, "Influence of an organic-Poor Landslide Deposit on the Early Diagenesis of Iron and Manganese in a Coastal Marine Sediment", *Geochimica. Cosmochimica. Acta,* Vol 56, pp. 3909-3921

Mucci A., Richard L.-F., and Lucotte M., 2000, "The Differential Geochemical Behavior of Arsenic and Phosphorus in the Water Column and Sediments of the Saguenay Fjord Estuary, Canada", *Aquatic Geochemistry,* No 6, pp. 293-324.

Mucci A., Boudreau B. and Guignard C., 2003, "Diagenetic Mobility of Trace Elements in Sediments Covered by a Flash Flood Deposit: Mn, Fe and As", *Applied Geochemistry,* (in press)

Nicolet, R., Roy, L., Arès, R, Dufour, J., Marinier, G., and Morin, G., 1997, "Rapport de la Commission scientifique et technique sur la gestion des barrages ", *Bibliothèque nationale du Québec,* Québec, Canada.

Ouellet, S., 1990, "Etude des hydrocarbures aliphatiques et aromatiques polycycliques (HAP) dans les sédiments du Fjord du Saguenay", MSc thesis, Université du Québec à Rimouski, 148 pp.

Pearson, T. H. and Rosenberg, R., 1978, "Macrobenthic Succession in Relation to Organic Enrichment and Pollution in Marine Environment", *Oceanography Marine Annual Review,* No 16, pp 229-311.

Pelletier, E., Mostajir, B., Roy, S., Gosselin, M., Gratton, Y., Chanut, J.-P., Belzile, C., Demers, S., and Thibault, D., 1999a, "Crue éclair de juillet 1996 dans la région du Saguenay (Québec). 1. Impacts sur la colonne d'eau de la baie des Ha!Ha! et du fjord du Saguenay", *Canadian Journal of Fisheries and Aquatic Sciences,* No 56, pp. 2120-2135.

Pelletier, E., Deflandre, B., Nozais, C., Tita, G., Desrosiers, G., Gagné, J.-P., and Mucci, A., 1999b, "Crue éclair de juillet 1996 dans la région du Saguenay (Québec). 2. Impacts sur les sédiments et le biote de la baie des Ha! Ha! Et du Fjord du Saguenay", *Canadian Journal of Aquatic Sciences*, No 56, pp 2136-2147.

Perret, D., Locat, J., and Leroueil, S., 1995, "Strength Development with Burial in Fine-Grained Sediments from the Saguenay Fjord, Quebec", *Canadian Geotechnical Journal*, Vol. 32, No. 2, pp. 247-262.

Saulnier I., and Mucci A., 2000, "Trace Metal Remobilization Following the Resuspension of Estuarine Sediments: Saguenay Fjord, Canada", *Applied Geochemistry,* No 15, pp. 203-222.

Seibert, G.H., Trites, R.W., and Reid, J., 1979, "Deepwater Exchange Processes in the Saguenay Fjord", *Journal of Fisheries Research Board of Canada*, No 36, pp. 42-53.

Smith, J.N. and Loring, D.H., 1981, "Geochronology of Mercury Pollution in the Sediments of the Saguenay Fjord, Quebec", *Environmental Science & Technology*, Vol. 15, pp. 944-951.

Sundby, B. and Loring, D.H., 1978, "Geochemistry of Suspended Particulate Matter in the Saguenay Fjord", *Canadian Journal of Earth Sciences*, Vol. 15, pp., 1002-1011.

Tremblay, H., Locat, J. and Urgeles, R., 2001, "Géodynamique littorale de la couche diluvienne de 1996, Baie des Ha!Ha!, Fjord du Saguenay, Québec, Canada", *Proceedings. of the 2001 Canadian Coastal Conference*, Québec. pp. 507-522.

Tremblay, H., Desrosiers, G., Locat, J., Mucci, A., and Pelletier, É., 2003, "Characterization of a Catastrophic Sediment Layer : Geological, Geotechnical, Biological and Geochemical Signatures", *Contaminated Sediments: Characterization, Evaluation, Mitigation/Restoration, and Management Strategy Performance, ASTM STP 1442*, J. Locat, R. Glavez-Cloutier, R.C. Chaney, and K. Demars, Eds. ASTM International, West Conshohocken, PA.

Urgeles, R., Locat, J., Schmitt, T. and Hughes Clarke J., 2002, "The July 1996 Flood Deposit in the Saguenay Fjord, Québec, Canada: Implications for Source of Spatial and Temporal Backscatter Variations", *Marine Geology*, No 184, pp. 41-60.

Zeman, A. J., 1994, "Subaqueous Capping of Very Soft Contaminated Sediments", *Canadian Geotechnical Journal,* Vol. 31, pp. 570-577.

Michael Schubert[1], Peter Morgenstern[1], Rainer Wennrich[1], Klaus Freyer[1], Albrecht Paschke[1], and Holger Weiss[1]

The Weathering Behaviour of Contaminated Industrial Sediments After Their Exposure to Atmospheric Oxygen

Reference: Schubert, M., Morgenstern, P., Wennrich, R., Freyer, K., Paschke, A., and Weiss, H., **"The Weathering Behaviour of Contaminated Industrial Sediments After Their Exposure to Atmospheric Oxygen,"** *Contaminated Sediments: Characterization, Evaluation, Mitigation/Restoration, and Management Strategy Performance, ASTM STP 1442,* J. Locat, R. Galvez-Cloutier, R. C. Chaney, and K. R. Demars, Eds., ASTM International, West Conshohocken, PA, 2003.

Abstract: Mining and ore processing of "copper shale" in the Mansfeld region, Germany, were stopped in 1990 as a consequence of the obsolete level of the applied technology. One of the residues of the former pyrometallurgical activities is a flue dust, which was scrubbed out of the process gases. The scrubbing resulted in an extremely fine-grained sludge, which was stored in "ponds" where it settled down as sediment. The need to assess the risk of heavy metal emissions posed by such sludge deposits when they dry up and become exposed to weathering prompted the question over the depth to which heavy metals can possibly be mobilized. A drill hole was bored into the dried-up sediment of such a "pond" and the sediment material was analysed. The results show a substantial influence of weathering in the upper 0.5 m of the material. In particular the oxidation of the heavy metal sulphides abundant in the sediment and the subsequent dissolution of the sulphates is nowadays a major problem for the quality of the nearby ground- and surface waters.

Keywords: heavy metals, sediments, weathering, mobilization

Introduction

For more than 800 years the Mansfeld region of Saxony-Anhalt / Germany was known for the mining of a low-grade metalliferrous Permian black shale - the Kupferschiefer or "copper shale." However, for economical and ecological reasons mining and ore processing stopped in 1990. Whereas the shutdown of the works had an immediate effect on the local air quality the ground- and the surface waters even now, about twelve years later, still suffer a continuing contamination closely linked to the former mining activities. Now that the actual smelters are closed and demolished the sources of that contamination are the various by-products left behind by the former mining and ore processing.

---

[1] Research scientist, Centre for Environmental Research Leipzig-Halle, Permoserstrasse 15, D-04318 Leipzig, Germany, schubert@ana.ufz.de

Two major by-products can still be found abundantly in the area. These two major by-products are waste rocks and slag, which were piled up in huge heaps during the last century. These dumps are today a characteristic feature of the local landscape (Wege et al. 2000). However, a third by-product with a less striking impact on the topography but with a noticeable negative effect on the local ground- and surface water quality is a flue dust, which has been scrubbed out of the process gases which left the blast-furnaces at temperatures of about 400°C. The scrubbing was basically done by spraying a veil of water into the gas stream and thereby binding the dust particles in a slurry of about 3 g /l of solids. The slurry was transferred into conic tanks where the solids were allowed to bed down. The excess water was finally decanted and the water content of the remaining sludge could be reduced to about 30% w/w.

The scrubbing of the process gasses, that went on for almost a century until 1990 consequently resulted in an accumulation of several hundred thousands of tons of the sludge. By the end of the pyrometallurgical activities in 1990 a total of about 225 000 tons of sludge had been piled up. Aside from its still substantial water content the main components of the sludge (by dry weight) were Zn (~ 20%), Pb (~ 13%), SiO_2 (~ 18%), S_{total} (~ 18%) and C_{total} (~ 13%).

Due to its high heavy metal concentrations the sludge had to be considered as an industrial waste product and to be put in safekeeping. For that purpose it was washed into huge "ponds" that sat atop of the slag and waste rock heaps. To enable a further dewatering of the material the basis of these ponds had not been sealed. As a consequence the water and considerable amounts of the extremely fine grained sludge oozed away into the slag and waste rock heaps. Finally the ponds dried up and the sediment became exposed to the atmospheric oxygen. The weathering of these dried up sediments are nowadays one of the main sources for the inorganic and organic contaminants that are found in the groundwater and the surface waters of the region.

As it could be shown by other authors who work on sites comparable to the sediment deposit described in this paper, a detailed mineralogical analysis of tailings solids conducted in combination with adequate pore water and pore gas analysis can provide a comprehensive insight into the future geochemical evolution of the materials (Blowes et al. 1990). However, the dense, clay-like, and virtually dry tailings material we focus on here does neither allow a pore gas nor a promising pore water analysis. Due to the extremely fine grained particles (about 1 μm) a mineralogical analysis of the material has its limitations, too. Weiss et al. (1997) who carried out a mineralogical analysis of the unweathered sludge pointed out that all inorganic compounds of the sludge should be referred to as "chemical compounds" rather than "minerals" because they formed rapidly in the smelting process and not in a "natural" manner. Apart from this limitation the predominant crystalline phases in the unaltered sludge have been identified as wurzite / sphalerite (ZnS, 37%), galena (PbS, 6.9%), anglesite ($PbSO_4$, 6.3%), and quartz (SiO_2, 2.5%). Traces of pyrite / marcasite (FeS_2) have also been detected. However, about 38% of the inorganic material was found to be amorphous. For a more detailed discussion of the physical and chemical properties of the sediment see Weiss et al. (1997) and Morency et al. (1998).

The major local disposal site today is the so called "Pond 10," which sits in a basin atop of a waste rock heap. Pond 10 contains about 225 000 m^3 of the described industrial sediment. Most of the sludge has been brought to this pond between 1982 and 1990 coming directly from the production site, i.e. from the scrubbers. It was washed into the basin using huge amounts of water (1000 - 1200 m³/d). During these years the sediment in the pond was permanently covered with water and thus virtually sealed from the atmospheric oxygen. After the close down of the copper works in 1990 Pond 10 dried up and remained untouched until midsummer 1993 when a transfer of some additional 10 000 tons of flue dust and alike materials to this site began. These additional materials, which had before been stored at other less suitable sites, cover the whole 25 000 m² site with a layer of about 0.5 m in thickness.

Today a central problem for the quality of the groundwater and surface waters in the vicinity of Pond 10 is the weathering of the dried-up sediment. Especially the oxidation of heavy metal sulphides, which are abundant in the sediment and the subsequent dissolving and leaching of the sulphates gives rise to considerable heavy metal emissions out of the sediment disposal site into the surrounding environment.

A theoretical prediction of these leaching processes is difficult due to the many different potential effects, such as the complexation and co-precipitation of heavy metals and their adsorption onto the solid matrix particles such as organic components or iron / manganese oxy-hydroxides. With the aim to assess the leaching behaviour of the material some basic information on the leachability of the heavy metals in the unaltered sludge have been obtained previously to the experiments discussed in this paper (Paschke et al. 2001). Besides a standardized leaching test which aimed to investigate the initial contact of the material with distilled water over a 24 hours period (German Standard Methods for the Examination of Water, Waste Water, and Sludge; DIN 38 414-S4), a five-step shaking cascade test was performed. In each step of the cascade test 200 g solids and 1000 ml water were shaken in an overhead shaker for 24 h. After each step the leached material was removed by centrifugation and the eluate was shaken again with a fresh solid sample at the same liquid/solid ratio. As a third test Paschke et al. (2001) applied the standardized pH_{stat} shaking test developed by Obermann and Cremer (1992). For the test the solid sample was eluted with an aqueous solution over periods of 24 h and 336 h, while the pH was constantly maintained at 4 (at a liquid/solid ratio of 1:10).

Table 1 - *Leachate pH-Value and Heavy Metal Concentration of Leaching Tests [mg/l]; Element Concentrations in the Unaltered Sludge by dry weight (EC_{Sludge}) [g/kg]*

	pH	Pb	Cu	Zn	Cd
DIN S4 (24h)	6.8	4.03	0.025	639	0.29
pH_{stat} (24h)	4.0	30.43	0.028	2056	1.02
pH_{stat} (336h)	4.0	23.40	0.056	2710	3.92
Cascade (step 1)	6.7	3.78	0.028	1206	0.44
Cascade (step 5)	6.5	8.89	0.127	4923	1.68
EC_{Sludge}	--	130.6	15.9	208.8	0.54

Some of the results achieved by Paschke et al. (2001) which are relevant for the presented paper are compared to the respective element concentrations in the unaltered sludge in Table 1 (for the element concentrations see also Table 2). The results show that the pH_{stat} test (pH 4) resulted in much higher eluate concentrations than the DIN S4 (pH 6.8) for most of the investigated elements. The shaking cascade concentrations successively approached or even exceeded the pH_{stat} test results.

The comparison of the amounts of heavy metals eluted from the unaltered sediment shows clearly the difference in the behaviour between the easily mobilisable elements Cd and Zn on the one hand, and Cu and Pb on the other.

With the aim to assess the risk potential of the sediment deposited in Pond 10 the question was raised down to which depth the dried up sediment can be chemically altered by weathering. Since the sediment is a very dense, dry, and clay-like material it was expected that oxidation and solution processes do only occur within a relatively thin top layer. Provided that a significant chemical alteration of the sediment in this layer does take place, the question which metals are mainly mobilized by oxidation and solution processes becomes the problem of central interest.

Experimental

The goal of the experiments was to investigate the weathering behaviour of the dried-up sediment in-situ under the given conditions. Due to the history of the site the following facts could be presupposed.

- The industrial sediment stored in Pond 10 has a thickness of about 9 m. It consists virtually entirely of dried-up, clay-like flue dust.
- The sludge that has been washed into Pond 10 continuously between 1982 and summer 1990 was brought here directly from the production site and can thus be considered as "fresh" flue dust. In this period the sediment body was permanently covered with water.
- Following September 1990 the pond remained practically untouched for about three years. During that time it dried up and the surface of the sediment became exposed to atmospheric oxygen.
- Starting in summer 1993 additional materials have been brought to Pond 10 from other sites less suitable for the storage. That material represents the top 0.5 m of the sediment body and can not be considered as "fresh" sludge. The conditions under which the material had been stored before being transferred to Pond 10 are not reproducible.

With the aim to investigate the influence of oxidation and weathering on the chemical composition of the sediment and to examine its chemical alteration as a function of depth a drill hole was bored at the centre of Pond 10. The hole penetrated the whole 9 m of the sediment body and reached the basis of the pond. Thus the drill core material represents the sludge that has been dumped in the basin from the very beginning in 1982 to the last deposits washed into the basin in 2001.

The core material was stored under cool and damp conditions. Initially the drill core was examined visually for inhomogeneities in its physical characteristics such as grain size distribution, colour and moisture content. Subsequently the core material was investigated for alterations in its chemical composition using XRF-analysis.

The samples for the XRF-analysis were taken from the axis of the core which had a diameter of 15 cm. Thus they can be expected to be representative for the sediment under the actual conditions on site. For the quantitative analysis of heavy metal concentrations that are out of the range of the heavy metal concentrations in available reference materials, the original material was diluted with SiO_2 powder (Riedel-de-Haen). Dilution factors of 5 - 10 reduced the concentrations of the elements of interest to the desired level and yielded sample compositions, which matched the working range of calibrations performed by the EDXRF spectrometer (XLAB 2000, Spectro A.I.). The determination of the matrix constituents Al_2O_3 and SiO_2 was provided by wavelength dispersive X-ray fluorescence-measurements of the undiluted material (SRS-3000, Siemens AG). In any case the prepared sample material was mixed with wax, 20% w/w, (Hoechst wax for XRF-analysis) as a binder and compacted in a hydraulic press at a pressure of 100 MPa.

Results and Discussion

The visual examination of the drill core material confirmed the expected physical homogeneity of the sediment body. Virtually the whole drill core could be described as a clay-like, black, slightly moist material.

Figures 1 and 2 illustrate concentration profiles determined in the drill core material. The concentrations of the samples taken from a depth of < 50 cm have not been referred to since that layer of material was, as mentioned previously, added to the original "fresh" sediment after 1993.

To enable better comparability the concentrations of the elements discussed here were normalized to a mean composition of the fresh, i.e. unaltered sediment. That mean composition was derived from the analytical results of the samples taken from the drill core section between 2.5 and 9.0 m which is assumed to be not affected by weathering and should therefore represent the chemical composition of the sludge as it came from the scrubbers. The mean composition was defined as summarized in Table 2.

Table 2 - *Mean Element Concentrations (MC) in the Sediment and the Relative Standard Deviations (RSD) for the Discussed Elements (n = 8)*

	Si	Al	Fe	Zn	Pb	Mn	Cu	Cd
MC [g/kg]	85.3	15.3	24.1	208.8	130.6	0.78	15.9	0.54
RSD [%]	4.5	10.4	12.9	9.9	15.9	12.50	15.5	8.10

Figure 1 shows the normalized concentrations of silica, aluminium, and iron in the drill core samples. As it can be seen the concentrations of these elements vary in a range of less than ± 20%.

Figure 2 shows the normalized concentrations of the heavy metals of concern. It can be seen that the heavy metal concentrations do also vary within a ± 20% range of the mean concentrations in the zone below 2.5 m. That implies the chemically homogeneous composition of the fresh sludge. However, the samples taken in 50, 75 and 100 cm show that in these upper layers the concentrations of cadmium, manganese and zinc are significantly lower than the respective mean concentrations. In contrast to this the concentrations of lead and copper remain within the ± 20% range.

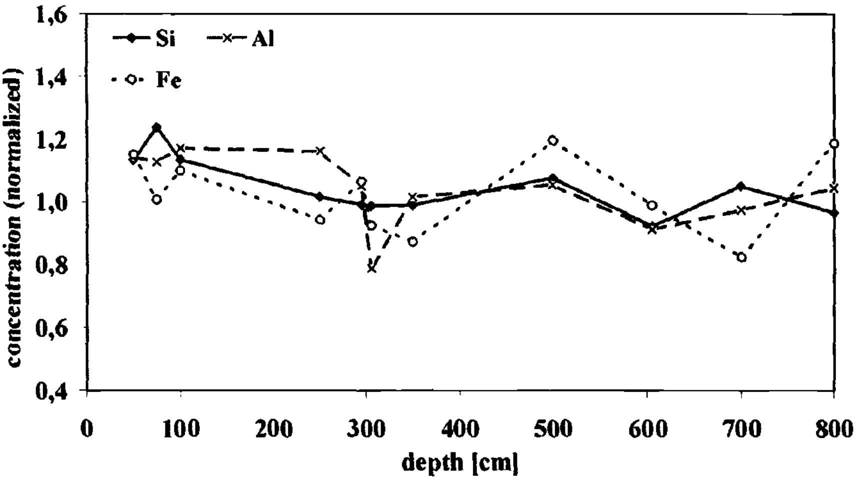

Figure 1 - *Normalized Concentrations of Si, Al, and Fe vs. Depth in the Sediment*

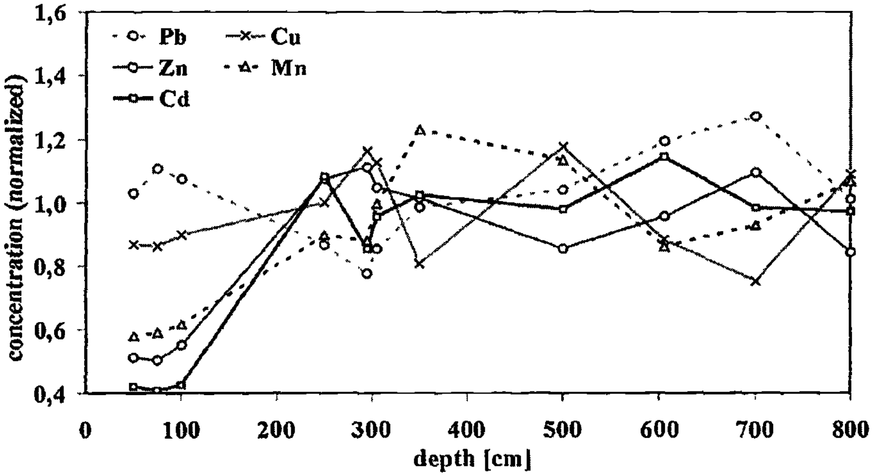

Figure 2 - *Normalized Concentrations of Heavy Metals vs. Depth in the Sediment*

The obtained chemical data indicate that the fresh sludge was chemically fairly homogeneous. The concentrations of silicon, aluminium, and iron change in a range of only about ± 20%. Silicon, which appears as SiO_2 in the whole sludge body is not considerably affected by solution processes. Aluminium appears as Al_2O_3 which also shows a very poor solubility and is thus not leached out of the material. Iron has been identified as FeS in the unaltered sediment. Since the sulphide is not stable in the upper, oxidized layers it is subject to alteration. However, FeO(OH) and $FeSO_4$ show only poor solubilities too and are for that reason not leached out of the sediment. Consequently the iron concentration in the altered zone does not change significantly and stays in the mentioned 20% range.

In the lower part of the depth profile the heavy metal concentrations do also stay in a range of just about ± 20%. However, in the upper 50 cm of the discussed section the concentrations of zinc, manganese and cadmium are considerably lower than in the mean unaltered sediment. The cadmium concentration determined in the most upper sample is only about 40% of the cadmium concentration in the unaltered sludge. Zinc and manganese show concentrations of about 50 and 60%, respectively, compared to the unaltered sludge. On the other hand it can be seen that the concentrations of lead and copper do not show such a general decrease in the upper section. The concentrations remain in the ± 20% range.

The mobilization of zinc, manganese and cadmium and the more or less stable behaviour of lead and copper can be explained with the solubility of the respective sulphates. In the fresh sludge the discussed metals appear mainly as metal-II-sulphides. The respective solubility data are summarized in Table 3. As it can be seen the sulphides of the discussed metals are virtually insoluble.

As long as the sediment was covered with water the reducing conditions in the actual sludge body were stable. After the pond had dried up oxidation processes started at the surface of the sediment and the sulphides were transformed into sulphates. That oxidation front penetrated into the sludge deposit. However, due to the clay-like structure of the material, the hydraulic conductivity of the tailings material is $< 10^{-9}$ m/s, most of the rain water runs off the sediment surface towards the surrounding coarse grained waste rock dams where it oozes away immediately.

Since the sediment was exposed to rainfall the sulphates that show high solubilities were mobilized much more easily than the sulphates that show only poor solubilities. As can be seen in Table 3 the solubilities of the discussed sulphates decrease in the order $ZnSO_4 > CdSO_4 > MnSO_4 > CuSO_4 > FeSO_4 > PbSO_4$. That is in good correspondence with the data illustrated in the Figures 1 and 2. The concentrations of Zn, Cd, and Mn, i.e., of the metals that have easily soluble sulphates, are considerably lower in the upper sludge layer due to oxidation and mobilization. On the other hand the concentrations of the metals that have sulphates with only low or very low solubilities (Fe, Cu, and Pb) do exhibit more or less stable concentrations even in the top layer of the sediment.

Table 3 - *Solubilities of the Sulphides and Sulphates [g/l] of the Discussed Metals in "Cold Water" (Lide 1993); s = Highly Soluble, sl s = Slightly Soluble, * = $FeSO_4 \times H_2O$*

	Zn	Cd	Mn	Cu	Fe	Pb
M-II-Sulphate	s	755	520	143	sl s *	0.0425
M-II-Sulphide	0.00067	0.0013	0.0047	0.00033	0.0062	0.00086

Besides $FeSO_4$ iron is, to a certain degree, likely to be bound in oxy-hydroxides, which are also poorly soluble. An adsorption of heavy metals onto these oxy-hydroxides is a possible way of heavy metal fixation, too, but due to the low iron concentrations in the sediment, compared to the extreme heavy metal concentrations even in the altered zone, that mechanism does not play an important role in the case discussed here.

Besides the different solubilities of the sulphates and oxides of the discussed metals their different affinity to organic matter might be another effect responsible for the observed weathering behaviour. Copper shows a much higher tendency to form metal-organic complexes than zinc, manganese, cadmium and lead (Hornburg et al. 1993, Asche and Beese 1986, Gruhn et al. 1985). That means that in the presence of organic matter copper becomes adsorbed or chemically bound and thus fixed in complex insoluble metal-organic structures, whereas zinc, manganese and cadmium are much more mobile. Since the sludge consists of up to 20% of organic compounds, such as PAHs, the formation of metal-organic complexes is likely to be of some importance for the fixation of copper in the oxidized zone of the sediment.

Conclusions

The weathering of the dried-up sediment, i.e. the oxidation of heavy metal sulphides and the subsequent dissolution of the sulphate salts, gives rise to considerable heavy metal emissions in the local ground- and surface waters.

The elements Si, Al, Fe, Pb, and Cu show concentration changes versus depth in a range of only about ± 20% of the respective mean concentrations of the "fresh" sludge. On the other hand the concentrations of Cd, Mn, and Zn display considerably lower concentrations in the upper 50 cm of the original sediment body.

After the sediment had dried up an oxidation process started at the surface and transformed the sulphides into sulphates and oxides. That gave rise to a mobilization of Zn, Mn and Cd whereas Fe, Pb, and Cu show more or less stable behaviour due to the poor solubilities of their sulphates or oxides/hydroxides. Another reason for the different weathering behaviour of the metals might be their dissimilar affinity to organic matter.

References

Asche, N. and Beese, F., 1986, "Untersuchungen zur Schwermetalladsorption in einem sauren Waldboden," *Zeitschrift fuer Pflanzenernaehrung und Bodenkunde*, Vol.149, pp.172-180.

Blowes, D. W. and Jambor, J. L., 1990, "The Pore Water Geochemistry and the Mineralogy of the Vadose Zone of Sulphide Tailings, Waite Amulet, Quebec, Canada," *Applied Geochemistry*, Vol. 5, pp. 327-346.

Gruhn, A., Matthess, G., Pekdeger, A., and Scholtis, A., 1985, "Die Rolle der geloesten organischen Substanz beim Transport von Schwermetallen in der ungesaettigten Bodenzone," *Zeitschrift der deutschen geologischen Gesellschaft*, Vol.136, pp. 417-427.

Hornburg, V. and Bruemmer, G., 1993, "Verhalten von Schwermetallen in Boeden - Untersuchungen zur Schwermetallmobilitaet," *Zeitschrift fuer Pflanzenernährung und Bodenkunde*, Vol. 156, pp. 467-477.

Lide, D.R., 1993, *CRC Handbook of Chemistry and Physics*, 73 ed., CRC Press, Boca Raton, USA.

Morency, M., Weiss, H., Freyer, K., Bourne, J., Fontaine, D., Mineau, R., Moeder, M., Morgenstern, P., Popp, P., Preda, M., Treutler, H.-C., and Wennrich, R., 1998, "Oxidation treatment of a sulphide-bearing scrubber dust from the Mansfeld Region – Germany," *Science of Total Environment*, Vol. 223, No. 2-3, pp. 87-97.

Obermann, P., Cremer, S., 1992, „Mobilisierung von Schwermetallen in Porenwässern von belasteten Böden und Deponien," in *Materialien zur Ermittlung und Sanierung von Altlasten, Vol. 6,* Landesamt für Wasser und Abfall Nordrhein-Westfalen, Germany.

Paschke, A., Freyer, K., Treutler, H. C., Wennrich, R., Popp, P., Moeder, M., Weiss, H., and Schueuermann, G., 2001, "Assessment of Theisenschlamm Leaching Behaviour", in *Fine-rained residues from copper smelting and their environmental impacts, A case study from the Mansfeld District, Germany, UFZ-Report Nr. 22/2001,* UFZ Verlag, Leipzig, Germany, pp. 71-82.

Wege, F.-W., 2000, "Das Haldenkonzept der Landkreise Mansfelder Land und Sangerhausen," in: *Bergbau- und Rueckstandshalden des Mansfelder Kupferschieferbergbaus, Schriftenreihe des Mansfeld-Museums, Neue Reihe, 5* - Eigenverlag des Foerdervereins Mansfeld-Museum und des Mansfeld-Museums, Hettstedt, Germany, pp. 2-13.

Weiss, H., Morency, M., Freyer, K., Bourne, J., Fontaine, D., Ghaleb, B., Mineau, R., Moeder, M., Morgenstern, P., Popp, P., Preda, M., Treutler, H.-C., and Wennrich R., 1997, "Physical and chemical characterization of a complexly contaminated scrubber dust - a by-product of copper smelting in Sachsen-Anhalt, Germany," *Science of Total Environment*, Vol. 203, No. 1, pp. 65-78.

Mathias Ricking, [1] and Tobias Schulze [1]

Deep-Freeze Sampling Methods for Soft Sediments

Reference: Ricking, M., and Schulze, T., "**Deep-Freeze Sampling Methods for Soft Sediments**", *Contaminated Sediments: Characterization, Evaluation, Mitigation/Restoration, and Management Strategy Performance, ASTM STP 1442*, J. Locat, R. Galvez-Cloutier, R. C. Chaney, and K. R. Demars, Eds., ASTM International, West Conshohocken, PA, 2003.

Abstract: Freeze coring systems were applied for sampling high-water-content sediments or very coarse sediments for a couple of years. At the Free University within the last 20 years different systems were developed and applied for sampling the upper 1.5–2.5 m in an undisturbed stratified way. The difficulty in controlling the depth penetration has been overcome by applying a small echo sounding system onboard. The LINDE-LANCE device runs on liquid nitrogen pressurized through a copper pipe, where the sediment freezes in concentric layers onto the lance at -193°C. A low weight system with a closed aluminium lance (CO_2-LANCE) running on a eutectic mixture of dry ice and alcohol that freezes the concentric sediment layers onto the lance at -90°C was developed for a much easier sampling by means of a Zodiac. Advantages and limits are addressed.

Keywords: freeze-core techniques, sediment, high-resolution analysis, environmental chemistry

---

[1] Free University of Berlin, Department of Earth Sciences, Environmental Geochemistry and Hydrogeology, Malteserstr. 74-100, House B, 12249 Berlin (Germany); e-mail: ricking@zedat.fu-berlin.de.

Introduction

Freeze coring systems were applied for sampling high-water-content sediments (Renberg and Hansson 1993, Lotter et al. 1997 Anderson et al. 2000, Quinlan et al. 2002) or very coarse sediments (Hill 1999) for a couple of year

The main scientific interest in freeze coring systems is the high resolution analysis of the sediment record in paleoecological studies (GFZ-Potsdam-UWITEC corer; Quinlan et al. 2002), and pigment and other chemical analysis in high-water-content surface sediments if a fine resolution is required (Lotter et al. 1997; Anderson et al. 2000). In very coarse systems only the few top layers are sampled for biofilm analysis (Hill 1999).

Within the urban area of Berlin the eutrophic to hypertrophic riverine system of the Havel and Spree Rivers is enlarged by several canals, connecting the Havel and Spree River upstream of their confluence, and numerous lake-like broadenings, with very slow flowing conditions. In these regions the sedimentation rates are very high, up to 3 cm/year.

The muds are characterized by high water contents of more than 90% in the upper decimetres, accompanied by total organic carbon (TOC) contents up to 15%. In highly organic sediments methane ebullition often occurs when the core is ascended to the water phase. Such gas ebullition may destroy or homogenize the laminations.

Therefore, freeze coring systems were developed and optimized for a high-resolution analysis of heavy metals and organic compounds within the top sediment layers (e.g., Koch et al. 1999, Schwarzbauer et al. 2001).

At the Free University (Department of Earth Sciences) within the last 20 years 3 different systems were applied and developed for sampling the upper 1.5–2.5 m in an undisturbed stratified way. These layers represent an accumulation time from 1960 to now, as determined by gamma spectrometric measurements of Pb-210 and Cs-137 of sediment core slices. The difficulty in controlling the depth penetration has been overcome by applying a small echo sounding system onboard.

Methods

The first system developed was a hollow core system, later on published by Pachur et al. (1984), which was used for a few cores only (Ballschmiter et al. 1980). The core length is restricted to 1 m. The main disadvantage was that it was too laborious and could be applied only by means of a drilling platform. Based on the experiences with the hollow core sediment coring system, during the mid to late 1980s a system used for the subway construction was adapted to obtain aquatic sediments in the (West-) Berlin area.

The LINDE-LANCE system runs on liquid nitrogen pressurized through a copper pipe, where the sediment freezes in concentric layers onto the lance at -193°C. The system is 2.50 m in length and has a diameter of 10 cm.

During the early 1990s a low weight system with a closed aluminum lance (CO_2-LANCE) running on an eutectic mixture of dry ice and alcohol, which freezes the concentric sediment layers onto the lance at -90°C, was developed for a much easier sampling by means of a Zodiac. The system is 1.78 m in length and has a diameter of 7 cm.

The LINDE-LANCE system is used from a drilling platform where the system is lowered very slowly down to the sediment surface by means of a wire to the pre-selected depth via an echo sounding system (Figure 1). To protect the lance from penetrating water an Armaflex® tape was used, characterized by a watertight protection at very low temperatures. Through a copper lance the liquid nitrogen is pressed out of the DEWAR container by applying a nitrogen gas pressure of 0.5–0.8 MPa.

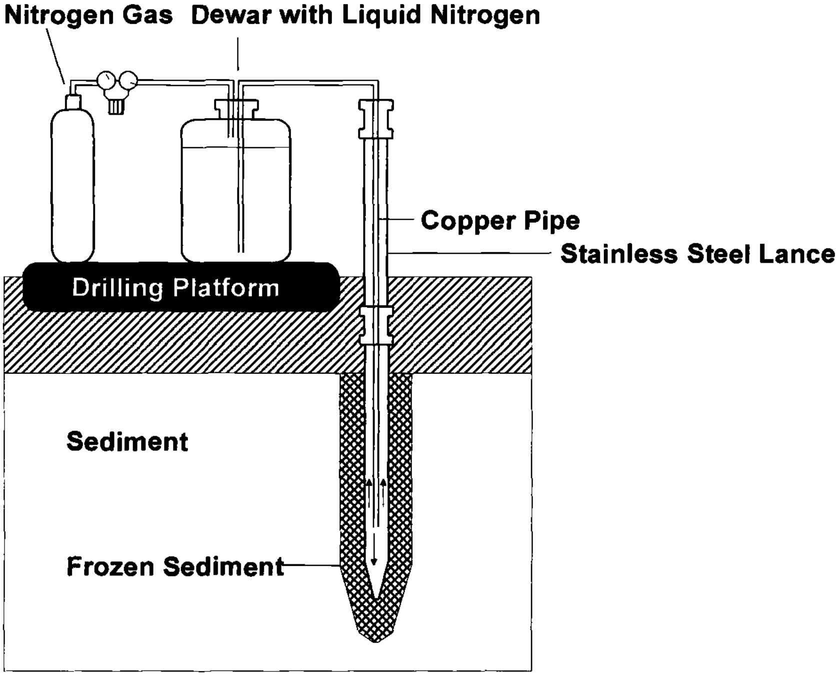

Figure 1: *The liquid nitrogen system (LINDE-LANCE)*

Liquid nitrogen volatilises in the lance and the sediment freezes onto the lance due to the cold advection nitrogen gas. About 100 L liquid nitrogen are required for each core. The copper pipe was adjusted at different depths to sample especially the sediment/water-interface. The maximum core length is in the range of 2.5 m with a diameter of 15–30 cm.

It takes at least 2–2.5 hours to obtain one core. The application is limited to a water depth of 10 m. After the lance has warmed to ambient temperature, it is filled with hot water and the frozen sediment crust is detached. The core is cut onboard into pieces of 50 cm by means of a stainless steel saw or can be obtained as one piece. To remove contamination the non-frozen sediment is washed away by pure water, surfaces are cleaned with a metal scraper and the pieces are wrapped in pre-cleaned aluminium foil.

The sediment core is transported on dry ice to the laboratory, where it is stored at -20°C in the dark. The core is subsampled into slices using a glowing silver wire, heated by using a current of 12 V, or using a stainless steel saw under a laminar flow bank. The freeze-dried samples can be used for geochemical, isotopical, and biostratigraphical analyses.

The CO_2-LANCE (Figure 2) is applied from a ship/zodiac by use of an anchor rope or a thin coring linkage. Ten kg crushed dry ice and 0.3 L alcohol are filled into the lance where an eutectic mixture develops

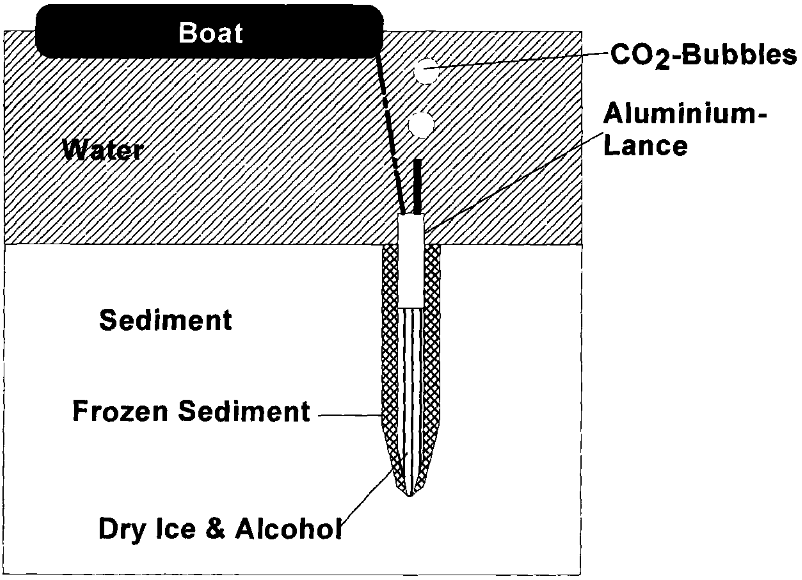

Figure 2: *The dry-ice system* (CO_2*-LANCE)*

The closed lance is lowered down to the pre-selected depth immediately. The sediment freezes undisturbed in layers of up to 20–25 cm thickness on the outside of the lance. The sampling takes at least 20–30 minutes and is finished when no gas bubbles are appearing on the water surface. Then the sediment core is lifted to the surface, the lance is filled with hot water, the core is detached, and the contamination of the sediment core is washed away by pure water. The sediment pieces or the whole core is wrapped in aluminium foil and transported on dry ice to the laboratory, where the storage was realized at -20°C in the dark. The preparation for analysis was realized under the same conditions as for the LINDE-LANCE.

Discussion

Besides a small smearing of the inner few mm, which are withdrawn, preliminary results indicate no modification of the samples and compounds, as deduced by microscopic analysis of laminated sediments.

Using now a stainless steel lance eliminates problems with heavy metals like Zn by applying the zinced LINDE-LANCE. Earlier experiments revealed no contamination via Zn (78% of the outer LINDE-LANCE mantle). Tests by members of the working group in 1991, where 6 lance parallel sections were analysed in 1 cm intervals revealed no contamination by the steel lance at a concentration level of ≥ 500 µg/g Zn. Pre-industrial sediments in Lake Bogen (Brandenburg, Germany) or Lake Nikolas (Berlin, Germany) displayed no contamination via the lance at a concentration level of 15–70 µg/g Zn.

There are no pore-water processes registered during the freezing-process, as the sediment freezes immediately, revealed by the water content analysis with a measured uncertainty area of 1.1% for the water content analysis.

The main advantages for these methods are the definitive control on the depth of penetration, also controllable by video systems, no hydraulic systems, the easier handling, and the gaining of more sediment material and the relatively low costs per core.

Limiting factors for the LINDE-LANCE are the necessity to protect the lance from penetration of water by sealing de connections between the stainless steel parts with a special tape for refrigerator techniques.

Limiting factors for the CO_2-LANCE are water depths of maximum 40 m, in maximum 4 cores per day and less sediment material than with the LINDE-LANCE method.

Both methods will be used for sampling surface sediments and sediment cores for the German Environmental Specimen Bank (ESB). Warved sediments of Lake Belau (Northern Germany) with high water contents illustrate the feasibility of the freeze coring system (Figure 3).

First results relating to possible modifications during the sampling and storage will be presented at the symposia, initial test revealed no modification.

Conclusions

Both methods are suitable for sampling high-water-content sediments without disturbing the stratigraphy. The LINDE-LANCE system gains more material, but is limited to water depths of less than 10 m. The CO_2-LANCE provides less material but is applicable to water depths of up to 40 m. The frozen sediment cores have to be prepared for transport within 30 min after archiving them.

Figure 3: *CO_2-LANCE sediment core of Lake Belau (Northern Germany)*

REFERENCES

Anderson, N. J., Clarke, A., Juhler, R. K., McGowan, S., and Renberg, I., 2000, "Coring of laminated lake sediments for pigment and mineral magnetic analyses, Søndre Strømfjord, southern West Greenland", *Geology of Greenland Survey Bulletin* Vol. 186, pp. 83-87.

Hill, M. T. R. 1999, "A freeze-corer for simultaneous sampling of benthic macroinvertebrates and bed sediment from shallow streams", *Hydrobiologia* Vol. 412, No. 10, pp. 213-215.

Koch, M., Ricking, M., Rotard, W., Mailahn, W., Knoth, W., Pribyll, J., and Pachur, H.-J., 1999, "PCDD/Fs, PCBs and PAHs in sediments of North-East Germany and their source identification", Posterpresentation on Dioxin '99 in Venice, *Organohalogen Compounds*, Vol. 43, pp. 359-363.

Pachur, H.-J., Denner, H. D., and Walther, M., 1984, "A freezing device for sampling the sediment-water interface in lakes", *Catena*, Vol. 11, pp. 65-70.

Quinlan, R., Leavitt, P. R., Dixit, A. S., Hall, R. I., and Smol, J. P., 2002, "Landscape effects of climate, agriculture, and urbanization on benthic invertebrate communities of Canadian prairie lakes", *Limnology and Oceanography*, Vol. 47, No. 2, pp. 378-391.

Schwarzbauer, J., Ricking, M., Franke, S., and Francke, W., 2001, "Organic pollutants in sediments of Havel and Spree River. Part 5: Halogenated compounds", *Environmental Science and Technology*, Vol. 35, No. 2, pp. 4015-4025.

Rosa Galvez-Cloutier[1], Marie-Eve Brin[2], Gerardo Dominguez[3], Serge Leroueil[4] and Sylvain Arsenault[5].

Quality Evaluation of Eutrophic Sediments at St. Augustin Lake, Quebec, Canada

---

Reference: Galvez-Cloutier, R., Brin, M.E., Dominguez, G., Leroueil, S. and Arsenault, S., "**Quality Evaluation of Eutrophic Sediments at St. Augustin Lake, Quebec, Canada,**" *Contaminated Sediments: Characterization, Evaluation, Mitigation/Restoration, and Management Strategy Performance, ASTM STP 1442*, J. Locat, R. Galvez-Cloutier, R. C. Chaney, and K. R. Demars, Eds., ASTM International, West Conshohocken, PA, 2003.

Abstract: St. Augustin Lake is located 20 kilometers west from Quebec City in the territory of Quebec's Provincial Capital. The whole basin land is largely urbanized with some agricultural and wetland zones, some forest spots and surrounded by an important network of highways. The lake neighbors an industrial park that includes airport installations and storage facilities for chemical products. In 1993, a first quality study revealed the presence of some toxic metals in lake sediments. Although, lower levels were found, these analyses were performed at a time where neither standards methods nor quality guidelines were available in Canada. Recently launched, a major City project aims to open the lake to public recreational activities and involves the cleaning of water. St. Augustin Lake is in a eutrophic state most of the year, and all usages have been limited. However, a recent paleo-limnologic study showed that the lake used to be in the past (60 years ago) rather mesotrophic. The water clean-up program cannot succeed without the evaluation and restoration (if needed) of the bottom sediments. Indeed, bottom sediments may constitute important reservoirs for contaminants such as phosphorus, nitrogen, heavy metals and hydrocarbons. These contaminants may be strongly attached to organic colloids, clay and carbonates that are usually present in sediments. This study shows metal profiles and their distribution and correlations between metals and some sediment constituents.

Keywords: sediment, heavy metals, eutrophication, nutrients.

---

[1] Associate Professor, Department of Civil Engineering, Faculty of Science and Engineering, Laval University, Quebec, Quebec G1K 7P4.

[2, 3] Graduate students, Department of Civil Engineering, Faculty of Sciences and Engineering, Laval University, Quebec, Quebec G1K 7P4.

[4] Professor, Department of Civil Engineering, Faculty of Science and Engineering,Laval University, Quebec, Quebec G1K 7P4.

[5] Biologist, EXXEP consultants, 3470 Chemin de Quatre Bourgeois, Ste. Foy, Quebec, Canada, G1W 2K4.

1.0 Introduction

This study is included in the project "*La grande Corvé*'" launched by the ancient city council of St. Augustin City whose final objective is the opening of the lake to its citizens for recreational activities that aim to include bathing and fishing. However, the Saint-Augustin Lake is in a eutrophic state almost all year round, and all usages have been limited. The water clean-up program cannot succeed without the evaluation and restoration (if needed) of bottom sediments. Indeed, bottom sediments may represent important reservoirs for nutrients and contaminants such as phosphorus, nitrogen, heavy metals and hydrocarbons. These contaminants may be attached to organic colloids, clay, carbonates or be co-precipited with iron and manganese in hydroxides present in the sediments constituents. The objective of the present study was to firstly characterize physically and chemically the sediments and secondly to evaluate environmental quality of the sediments.

2.0 Study Area and Sampling Schedule

2.1 Description

St. Augustin Lake is located 20 kilometers west from Quebec City on the territory of Quebec's National Capital between latitudes N 46° 42' and N 48°41' and longitudes W 71°22 and W 71°36'. The Lake is 2225 m long and 380 m width. Its whole basin has been largely urbanized but still presents agricultural zones, wetlands, and forest spots all surrounded by an important network of highways. It also includes hydroplanes port installations. The lake neighbors an industrial park and landfill. In Figure 1, a general diagram shows a summary of the main limnological and geochemical characteristics of the St. Augustin Lake. As it can be seen, St. Augustin Lake is a shallow lake with the maximum depth of 6 m. The sediment occurs in a 30 cm - 1m thick layer above the bedrock. The average annual precipitation around the area is 800mm, apart form the precipitation, the lake is fed with groundwater and it counts with one tributary and one discharge. In 1993, a first quality study (Landry 1993) revealed the presence of toxic metals in the sediments. Although, low levels were found: cadmium (0.5 – 1 ppm), chrome (15 – 28 ppm), copper (10 – 25 ppm), nickel (20 – 30 ppm), lead (25 – 30 ppm) and arsenic (1 – 4 ppm), these analyses were performed at a time where no standard methods, no quality guidelines were available in Canada. Despite the fact that the Lake can reach extremes eutrophic conditions, a recent paleo-limnologic study (Roberge et *al.* 2002) has shown that the lake used to be mesotrophic about 60 years ago. The method alpha was employed using the Pb ^{210} datation. The constant rate of supply (CRS) has been used in the Roberge et *al.*,'s study to change the data for a period of time.

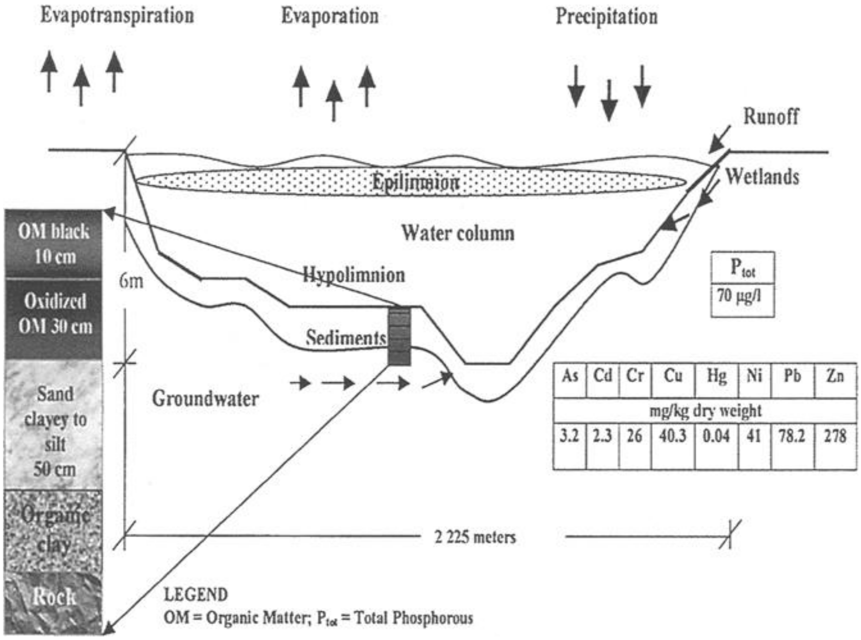

Figure 1 -*Schematic Conception of the Actual situation at St. Augustin Lake*

2.2 Sampling Schedule

During fall 2001, a systematic sampling program used a stochastic approach (Baudo 1990) in order to obtain 42 sediment samples shown in Figure 2that were representative of the sediments at the bottom of the Lake. The sampling used 8 transepts that defined triangular areas from which samples were obtained, covering the whole lake surface. The coordinates at each sampling station were recorder by using a Global positioning system (GPS) equipment. In addition, 5 extra samples were taken at hot spot areas such as the discharging points of: surface runoff from the highway system, agricultural runoff, hydroplane port, Keno Camping Station. As shown in Figure 3, the sediment samples were taken with an Ekman grab containing a volume of 5.3 L and with the following dimensions 150 X 150 X 225mm. The grab took this volume of the surface sediments to different depths inside the water column varying between 1 to 6 m. At each site, pH, redox, temperature and conductivity were measured *in-situ* using a WTW TETRA COM 325 multimeter. The sediments were stored in a cold room (4° C) in polypropylene containers.

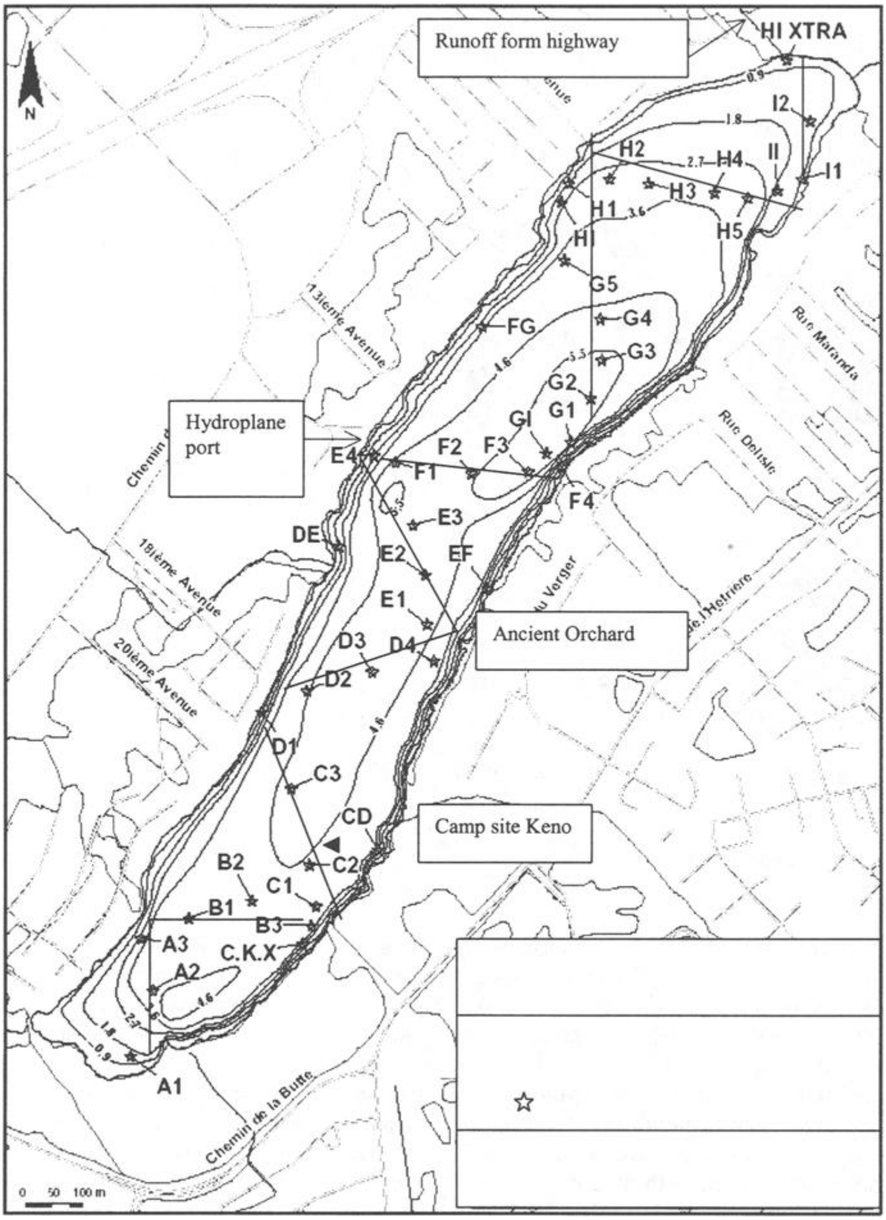

Figure 2- *The Samples Site and the Transects at the St. Augustin Lake*

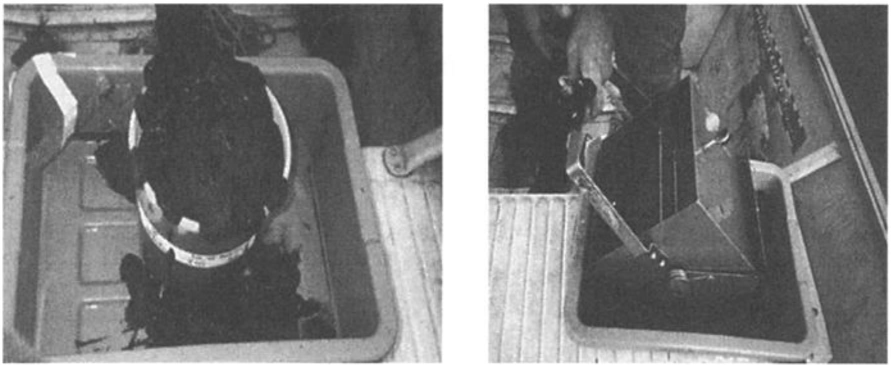

Figure 3 - *Typical Sediments (left) and Ekman Grab (right)*

2.3 Sediments characteristics

Sediments presented high organic matter and in some instances strong sulphur and decomposition odours. The characterization program covered two aspects: 1) mineralogy, and grain size evaluation and, 2) Contamination: concentration of priority contaminants such as heavy metals (Cd, Cr, Ni, Pb, Hg etc.), metalloids (As), anions (CO_3, NO_3, PO_4 and SO_4), organochlorinated pesticides known to be used in the area and polycycling aromatics hydrocarbons (PAHs).

3.0 Experimental methods

3.1 Grain size analysis and mineralogy

After destruction of organic matter with oxygen peroxide, grain size analysis was run separately on fine and coarse fractions. Fine grain size analysis was done using a laser counter (Mastersizer of Malvern Instuments). This equipment measures sizes from 0,05 µm to 556 µm. Results are summarized by a representative graphic (Figure 4). The fine fraction consisted mainly of silty loam and sand. Coarse grain size (sieve # 30 > 600 µm) was done gravimetrically using sieve analysis according to BNQ 2560-040 (BNQ 1982). Two methods of classification are shown for the coarse fraction. The first one cames from the Unified Soil Classification System (ASTM D2487) and the second one from the United State Department of Agriculture. Only seven samples required this method. Mineralogy was performed using X-ray diffraction and scanning electron microscopy. X-ray diffraction was run on a D 5000 Siemens instrument. Operating conditions were the following: 40 kv and 30 ma, Cu lamp and angle span from 10° to 70° and shooting speed of 1°/minute and aperture of 0.02° / 1.2 seconds. Samples were

1 cm x 2 cm. Scanning Electron Microscopy was performed in a JEOL 840A instrument using a retrodiffusion method of radiation that allows for the study of both morphology and elemental analysis. For X-ray diffraction and SEM analysis, samples F2 and H2 were chosen due to their high content on Pb and Zn.

3.2 Anions and metals analysis

The interstitial water was taken as the supernatant of a sediment sample after 10 minutes of centrifugation. The filtration of the supernatant and the dilution were required for measuring the ions concentration with an ion chromatograph (Dionex). Heavy metals were measured by AAS following the procedure described by the Saint. Lawrence Centre (SLC 1993). Sediments were digested using 5ml HNO_3 and 2 ml of peroxide (30 %) for 1 gram (dry weight). Then, the mix was heating until the volume reached 1 at 2 ml. After, 10 ml of regal water (HNO_3 20% and HCl 5%) was adding in the solution, during 60 minutes the heating continued. Mercury and arsenic were measure out by and external certified laboratory (Bodycote). Quality control included the usage of reference materials like the PACS-2 from the National Research Council of Canada

3.3 *Organic compounds analyses*

Pesticides were measured on HPLC and PAHs by GC-MS according to EPA standard methods by an external certified laboratory (Bodycote).

4.0 Results

4.1 Geochemistry of water and sediments

The summary of in-situ results is presented in Table 1. The pH and conductivity values of water present in the grab were homogeneous and stable for most of the stations. On the contrary, redox values presented a large variability from 174 mV to -114 mV. Among the 42 samples, 13 stations (about the third) presented negative value of redox potential. Otherwise, there is no correlation between the pE and the depth of the sample (R^2= 0.02). It seems that the depth of water does not have an influence on the potential redox. In eutrophic lakes dissolved oxygen can rapidly be consumed due to oxidation process. At this point anaerobic conditions may reach various stratification layers (Wetzel 1983).

Table 1 - *In-situ Characteristics*

Parameters	Average and Standard Deviation
pH	7.70
Conductivity (µS)	796.63 ± 12.44
Temperature (°C)	8.71 ± 0.60
pE (mV)	36.98 ± 68.96
Alkalinity (mg/L $CaCO_3$)	118.14 ± 4.48
Water content (%)	347.30 ± 115.44

Organic matter (measured according to Centre d'Expertise en Analyse *Environnementale du Québec, 2001, M.A. 100-S.T. 10,*) ranged from 6 to 19%, with the average value of 11%. In fact, two kinds of organic layers were visually detectable as shown in the scheme of Figure 1.

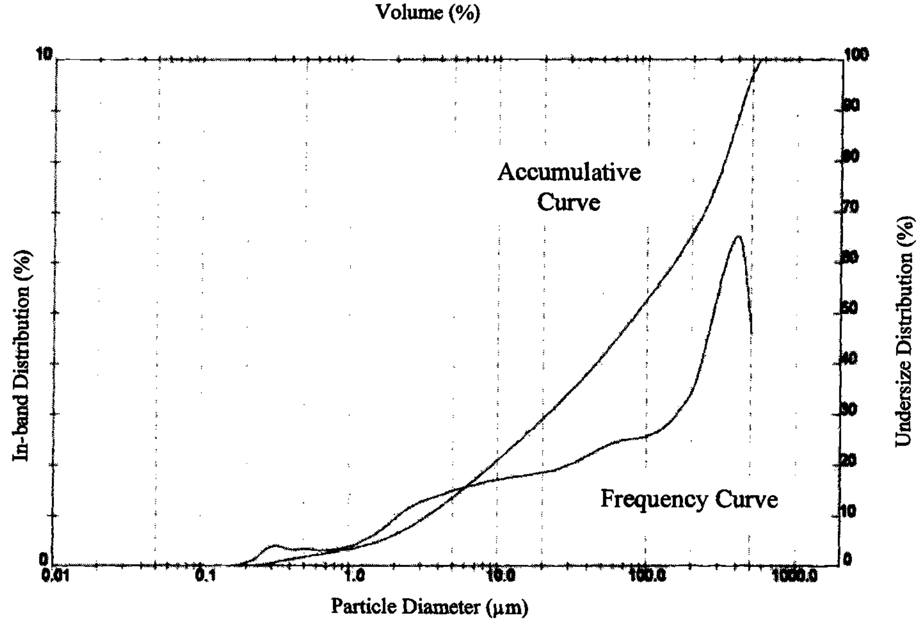

Figure 4 - *Grain Size Distribution of the Representative Sample F2.*

From the result of grain size analysis a general pattern arises. This typical pattern is represented in a Figure 4. This one illustrates the general distribution of the fine grain size. The coarse grain results are shown in Table 2

Table 2- *Grain Size Analysis of Coarse Samples*

Sample	Composition (%)	(W_L)[1] (%)	Classification	
			USCS	USDA
HI	Sand : 50 Clay : 5 Silt : 40 Fragments : 5	38.8	Silty sand (SM)	Sandy loam
CD	Sand : 30 Clay : <1 Silt : 60 Fragments : 9	58.8	Organic silt (OH)	Silty loam
F4	Sand : 40 Clay : 5 Silt : 53 Fragments : 2	58.8	Organic silt (OH)	Silty loam
D1	Sand : 45 Clay : 2 Silt : 53 Fragments : <1	58.8	Organic silt (OH)	Silty loam
HI extra	Sand : 45 Clay : 0 Silt : 25 Fragments : 30	38.8	Silty sand (SM)	Loamy sand
EF	Sand : 42 Clay : 5 Silt : 53 Fragments : <1	58.8	Organic silt (OH)	Silty loam
II	Sand : 92 Clay : 0 Silt : 8 Fragments : <1	N/A	Sand (SP)	Sand

[1] Water limit

Theses results confirm the similarity between both classifications. The sediments were characterized by a grain size sample S curve and can be classified as silty loam. The diffraction results show the strong presence of quartz, feldspars (albite) and mica (biotite) as primary minerals. As secondary minerals, calcite, and dolomite were found in trace concentrations, few clays (mostly illite and chlorite) were also found in low concentrations. Figure 5 shows various grains of sediments. In particular, sphalerite indicated as zinc sulphate was identified. In the same figure, the second structure at the left is a grain of clay characterized by its multiple lattice structure. Organic matter was identified abundantly in all samples. In Figure 6 from sample F2, white spots can be seen, which were identified as pyrite (FeS_2).

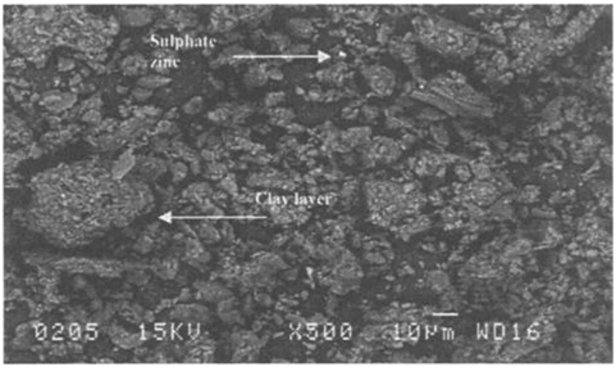

Figure 5 - *SEM Photography of sample H2.*

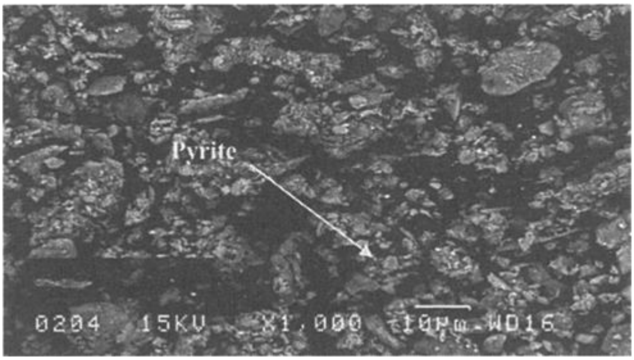

Figure 6 -*SEM Photography of sample F2*

4.2 Contamination

St. Augustin Lake is also reservoir of highway runoffs. These highways are maintained in winter by de-icing products. For this reasons chloride and sulphate were measured in interstitial water sediments. As an example, the longitudinal profile of Cl concentrations is shown in Figure 7. Chloride concentrations were generally high compared to other lakes in Quebec. In particular, site D2 and H3 reached 200 ppm. Site H3 is closer to the discharging point of highway runoff. Sulphate was also high, concentrations ranged from 100 to 350 ppm with a strong peak at the Keno Camping site of almost 500 ppm. Unfortunately, in Quebec there are no quality guidelines for Cl or SO_4. It seems that anions phosphorus and nitrogen were not present in soluble state (ortho-phosphates and nitrates) in the interstitial water. Further investigations must be done to quantify the concentration of these anions responsible of eutrophisation

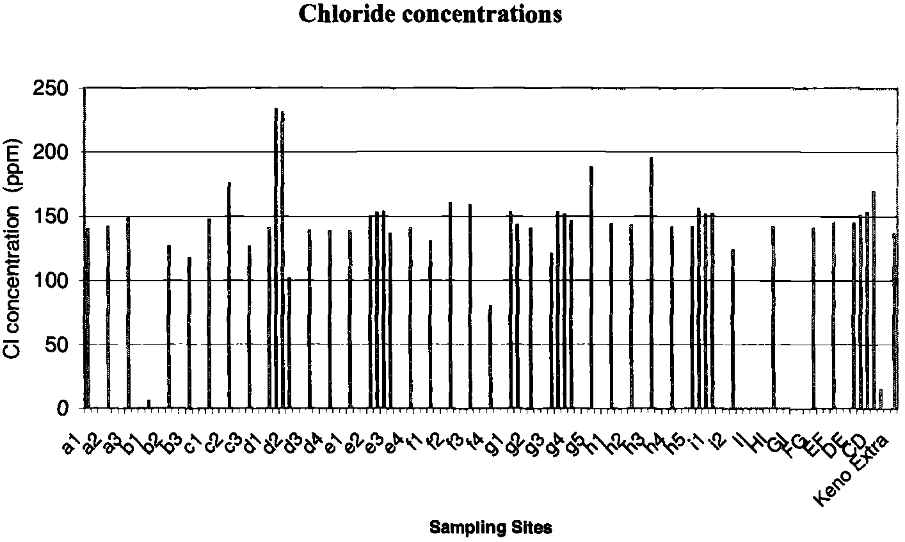

Figure 7- *Chloride Concentrations on Interstitial Water Samples of the Sediments of St. Augustin lake*

The evaluation of contaminants included the concentrations of heavy metals (Cu, Cd, Cr, Ni, Zn, Pb and Hg), transition metal (As), organochlorinated pesticides and PAHs. Heavy metals were dosed in the 42 samples while Hg, As, pesticides and PAHs were measured on 5 samples representatives of each transect (A3, D3, F1, G3, H2).

Presently, quality criteria in Canada are mostly based on the comparison of total concentrations against guidelines that defines levels of toxicity (Galvez-Cloutier et al. 1995). In Canada three guidelines are frequently used: that one of the St. Lawrence Centre (1996), that one of the Ontario's Ministry of Environment and that one of the Canadian Council of Ministries of Environment (OME 1990, EC 1992, CCEM 1999, SCL 1996). The table in Figure 1 shows the average values of contaminants found in the sediments, all metals were found in various concentrations being Zn the most abundant. Concentrations were higher than those reported in the Landry (1993) study. Table 3 summarizes the results of the heavy metal analysis. The second column shows the average concentration in 2001. These results could be compared with the results from 1993 (third columns) and the background values (fourth column). At the fifth column the SEM (minor effect level) values of the EC (1992) guidelines are shown. The order of decreasing concentration was Zn > Pb > Cu > Cr > Ni > As > Hg. Cadmium, zinc and lead profiles are shown, respectively, in figures 8-10. The majority of the results obtained in 2002 exceed the background value and the SEM criteria. Moreover, the present results are higher than those obtained in 1993.

Table 3 -*Summary of Metals Concentrations*

Metals and Metalloids	St. Augustin Sediments Concentration (mg/kg)	Landry Data (1993) (mg/kg)	Background values From (CCEM)[1] (mg/kg)	SEM Criteria SLAP[2] (mg/kg)
Arsenic (As)	6.68 ± 1.13	3.20 ±0.78	2.5	7
Cadmium (Cd)	2.38 ± 0.65	0.63 ± 0.10	0.32	0.9
Chrome (Cr)	25.87 ± 7.24	22.72 ± 4.36	47	55
Copper (Cu)	40.87 ± 9.47	18.38 ± 4.00	31	28
Lead (Pb)	77.82 ± 26.47	24.27 ± 4.50	6	42
Mercury (Hg)	0.12 ± 0.02	0.05 ±0.01	0.074	0.2
Nickel (Ni)	42.18 ± 9.54	28.77 ± 5.27	n/a	35
Zinc (Zn)	280.83 ± 74.91	121.33 ± 27.22	104	150

[1] Canadian Council of Environment Ministers; [2] St-Lawrence Action Plan

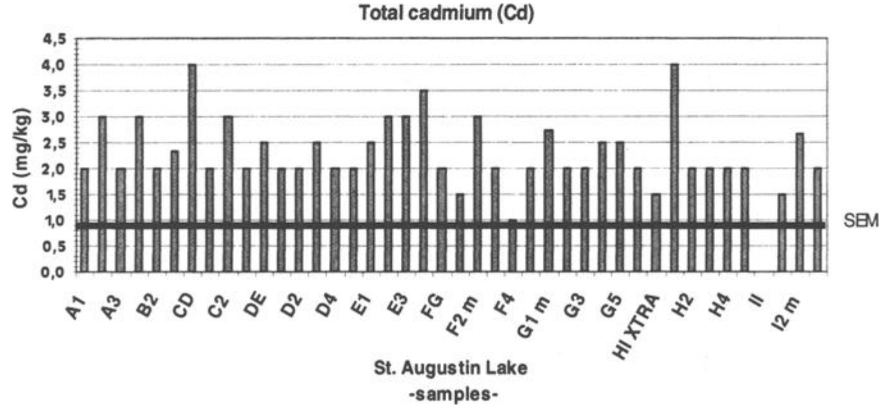

Figure 8 - *Concentration Profile of Cadmium at St. Augustin Lake*

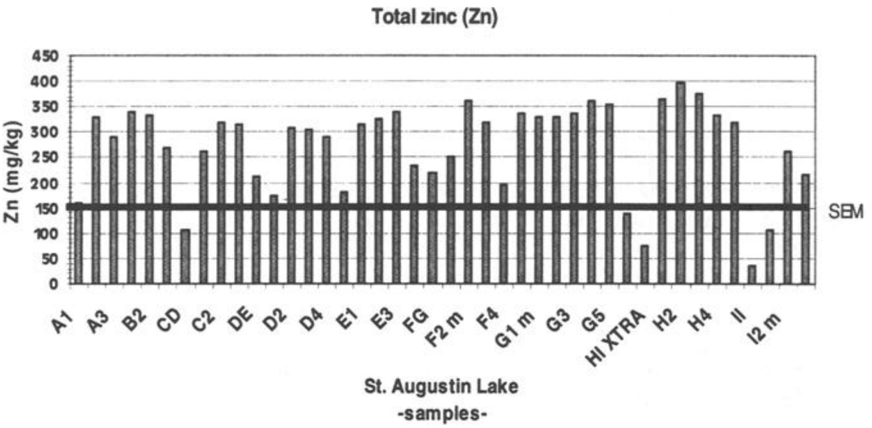

Figure 9 - *Concentration Profile of Zinc at St. Augustin Lake*

As it can be seen from Table 3 and Figures 8, 9 and 10, most heavy metals exceeded the SEM level of toxicity. In the case of Cd and Zn, over 90% of samples exceeded the SEM level. Zinc is an essential element vital for growth while cadmium may be highly toxic.

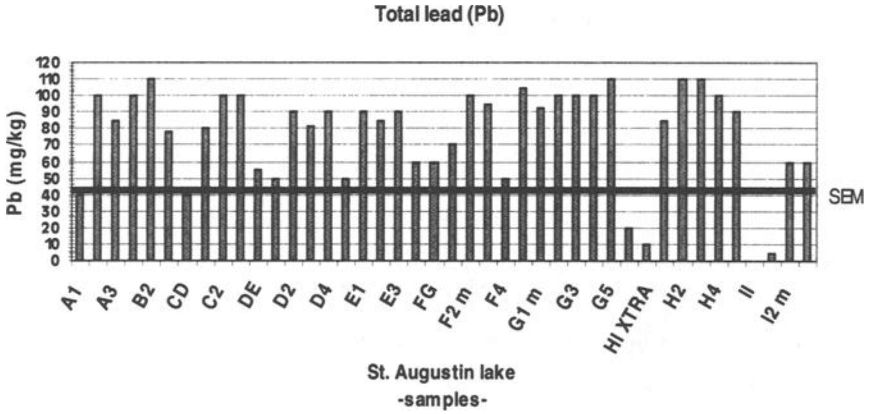

Figure 10- *Concentration Profile of Lead at St. Augustin Lake*

Compared to geogenic background values (approximately 100 ppm for Zn, 20 ppm for Pb, 30 ppm for Cr and 0.2 ppm for Cd) and compared to SEM criteria it is evident that sediments at the St. Augustin lake have been contaminated most probably by the anthropogenic activities that had taken place in the past. Comparing values from the

Landry study (1993) concentrations have increased for all metals measured. Spatially, contamination was not homogenous. For instance, figure 11 shows the spatial distribution of Cd at the sediment's surface. Samples from the darker area exceeded 3 ppm of Cd. As it can be seen, the central-north and extremes zones of the lake were the most contaminated.

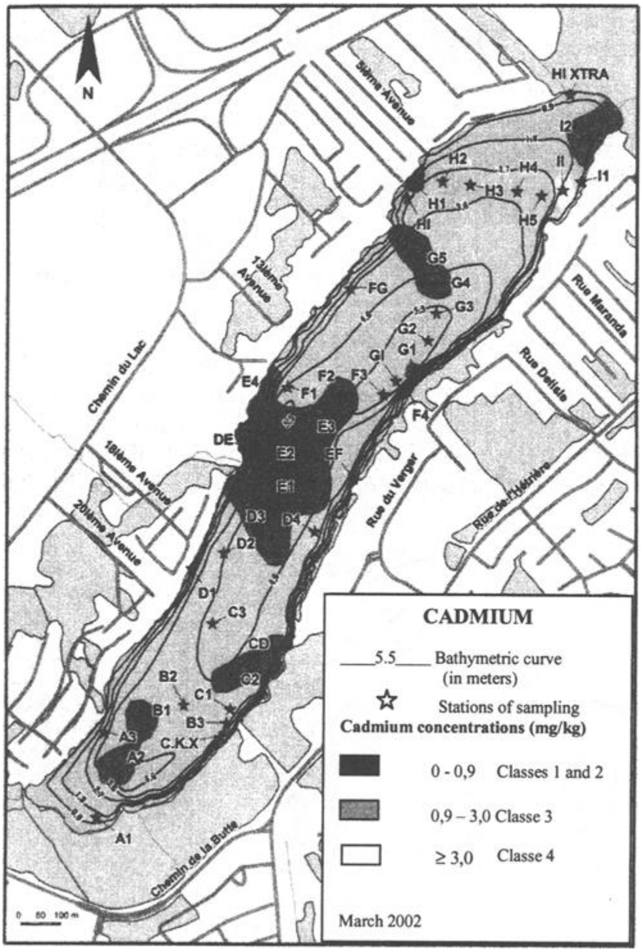

Figure 11 - *Spatial Distribution of Cd.*

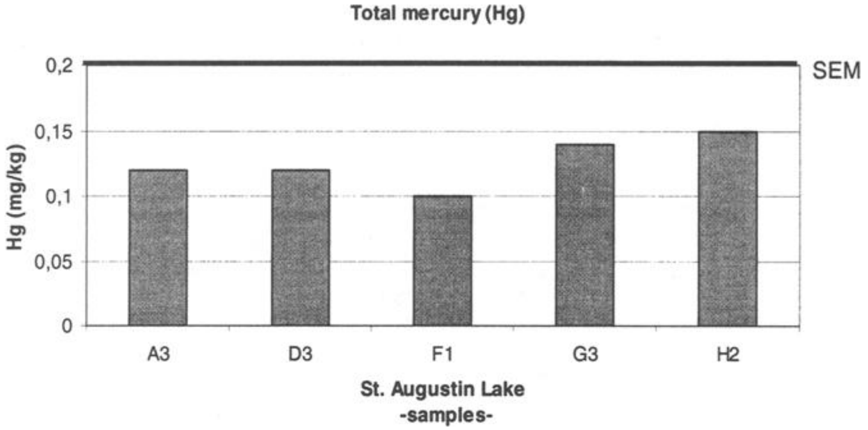

Figure12 –*Concentration of the Mercury of 5 Samples of the St. Augustin lake.*

Results for Mercury and Arsenic are presented in Figures 12 and 13. While Hg values did not exceed SEM criteria, arsenic was found in greater concentrations. Higher concentrations of Arsenic were obtained also at the longitudinal extremes of the lake. The CCEM (1999) has indicated a background value for As of 2.5 ppm. Due to the high toxicity of arsenic it has to be considered for further evaluation.

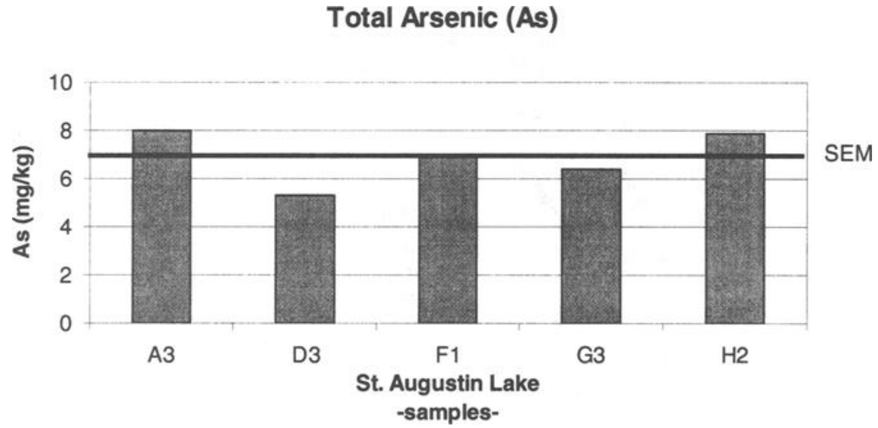

Figure13 - *Arsenic Concentrations of five Samples of the St-Augustin lake*

Organochlorinated pesticides and PAH were not found in any of the 5 samples analyzed. Results fall under the detection limits, for pesticides from 0.02 to 0.10 ppm and for PAH 0.25 ppm.

5.0 Discussion

5.1 The clay and the organic matter content

Sediments at the St. Augustin Lake consist of silt and sand with very high concentrations of organic matter (OM). By colour, this organic matter can be divided in two layers of about 30 cm each one. One highly oxidized and deeper and one superficial and less oxidized. Together with organic matter, clay and carbonates are other adsorbing materials with affinities for heavy metals. Correlation analysis was performed for all heavy metals against 3 reactive materials: organic matter, clay content and carbonates. As an example, Figure 14 shows the positive correlations between Zinc concentration and OM and clay. Indeed, to sites presenting higher contents on OM or Clay corresponded higher concentrations of Zn. The relationship was positive with OM (logarithmic relation) and less pronounced with clay (linear relationship). These results confirm the affinity of heavy metals for OM and clay colloids.

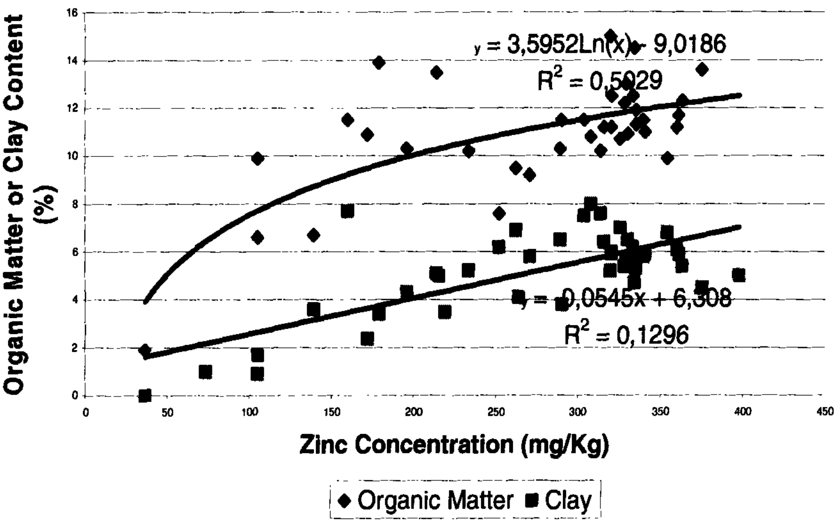

Figure 14 - *Correlation between Zn Concentration and Clay and Organic Matter*

5.2 Eutrophication

The high organic matter found in the sediments is a result of the eutrophication status of the lake. The analyses of nitrate and phosphate did not reveal the presence of these anions in the interstitial water. Further investigations will determine the forms of phosphorus in the sediments and their implication in eutrophisation. Otherwise, the water contains phosphorus at an average concentration of 70 µg/L. This level of P may characterize hypereutrophic lakes according to Ryding and Rast (1994). According to the Landry (1993) study, nutrients were already present in high concentrations in the water column. Given the fact that most nutrients inputs (domestic effluents, agricultural farm discharges) have been closed or reduced, results seem to indicate that these nutrients, particularly phosphorus, may come from what was accumulated at the bottom sediments over the last 20 years. The second assumption is that the P and N are transported by groundwater coming, for example, from the agricultural subsoil basements.

5.3 The second part

A second phase will study these two possibilities. In addition, phosphorus speciation into organic and inorganic forms will be determined in order to complete a global mass balance for nutrients. Although some correlations can be drawn between contaminants and sediments components, toxicity, mobility or availability of heavy metals are not evaluated by the method of total concentrations, speciation and distribution information is essential to evaluate final fate of contaminants or clean-up alternatives. The second phase of this study will carry heavy metal speciation and bioassays for further evaluation of toxicity. These analyses will complete the evaluation and determination of the role of sediments in the process of retention and leaching of heavy metals. The fact is that heavy metals and arsenic could become available for organisms when a change of conditions like pH, redox potential, oxygen concentration or bioturbation occurs.

6.0 Conclusions

From the above results and discussions, it is concluded that St. Augustin Lake presents with respect to sediments two geoenvironmental problems: 1) contamination by metals and 2) contamination by nutrients. Indeed, the five heavy metals and a metalloid measured were found in concentrations exceeding the background values found in the literature. In the case of Cd, Pb and in a lesser extent Cr, concentrations exceeded, for over 50% of the samples, the level of minimum toxicity. These metals were not distributed homogenously along the surface of the lake; on the contrary, concentrations were higher at the central north zone and longitudinal extremes of the lake, sometimes corresponding to points close to the remaining discharges (e.g. highway runoff, recreational activities centre). Total concentrations do not give insight with respect to toxicity, thus further metal analysis needs to include metal speciation and bioassays. A high concentration of phosphorus has been found in the water column. The sediments displayed a high content of organic matter. This is the cause of the eutrophic state of the lake. Further studies need to be carried in order to identify the sources of P and N and its distribution in water and sediment components. Finally, the problems at St. Augustin Lake are representative of a more global and widely spread environmental problem not only particular to Quebec or the rest of Canada but all over the world. Any attempt to clean up the water can be jeopardized by the presence of remaining contaminants hold within the sediments. Thus, this aspect needs to be settled before. Today it exist several methods for capping, isolating or treating sediments; these alternatives need to be explored for the sediments in St. Augustin Lake.

Acknowledgments

The authors wish to thank EXXEP Consultants and the FCAR funds for making this study possible.

References

American Public Health Association, American Water Work Association, WaterPollution Control Federation (APHA, AWWA, WPCF), 1989, *Standards Methods for the Examination of Water and Wastewater*, Port City press, Baltimore.

Baudo, R., 1990, *.Sediment Sampling, Mapping and Data Analysis, In: Sediments Chemistry and Toxicity of in Place Pollutants*, Edited by Baudi, R., Giesy, J.P., and Muntau, H., Lewis Publishers, pp.15-50.

Bureau de Normalisation du Québec., 1982, *Granulats-Analyse Granulométrique par Tamisage*, Ministère de l'Industrie, du Commerce et du Tourisme, BNQ 260-040-1982-08-11.

Centre d'Expertise en Analyse Environnementale du Québec, 2001, *Méthode d'Analyse M.A. 100-S.T. 10, Détermination des Solides Totaux et des Solides Totaux Volatils; Méthode Gravimétrique.*

Conseil Canadien des Ministres de l'Environnement (CCEM), 1999, *Recommandations Canadiennes pour la Qualité des Sédiments: Protection de la Vie Aquatique,* Winnipeg.

Environment Canada (EC), 1992, *Review and Recommendations for Canadian Interim Environmental Quality Criteria for Contaminated Sites*, Inland Water Directorate, Water Quality Branch, Scientific Series No 197.

Ministry of Environment Ontario (MOE), 1990, *Provincial Sediment Quality Guidelines* (draft project),. p. 21.

Landry, P., 1993, *Expertise et Aménagements Réalisés au lac St. Augustin et à l'Intérieur de son Bassin de Drainage*, 48 p.

Galvez-Cloutier, R., Yong, R.N., Chan, J., and Bahout, E., 1995, *Critical Analysis on Sediment Quality Criteria and Hazard-Risk Assessment Tools*, . Dredging, Remediation and Containment Contaminated Sediments ASTM STP No 1293, pp. 306-318.

Roberge, K., Pienitz, R., and Arsenault, S., 2002, *Eutrophisation Rapide du lac Saint-Augustin, Québec,: Étude Paléolimnologique pour une Reconstitution de la Qualité de l'Eau*, Le Naturaliste Canadien, Vol 126, No 2, pp68-82. .

Ryding, S.O., and Rast, W., 1994, *Le Contrôle de l'Eutrophisation desLacs et des Réservoirs*, Masson, Unesco, 294p.

St. Lawrence Centre (SLC), 1993, *Methods Manual for Sediments Characterization*, Action Plan St.Lawrence.

St. Lawrence Centre (SCL), 1996, *Rapport Synthèse sur l'État du St-Laurent. Volume 1 :L'Écosystème du St-Laurent*, Environnement Canada- Région du Québec, Conservation de l'Environnement et Éditions MultiMondes, Montréal.

Yong, R.N., 1995, *The Fate of Toxic Pollutants in Contaminated Sediments*. Dredging, Remediation and Containment Contaminated Sediments ASTM STP No 1293, pp. 306-318.

Wetzel, R.G., 1983, *Limnology*, 2nd edition, Saunders College Publishing, 767 p.

Thresiamma Joseph,[1] K. K. Balachandran,[1] Maheswari Nair,[1] V. Kesavadas,[1] K. K. C. Nair,[1] and Joseph Sebastian Paimpillil[2]

Trace Metal Levels in Nearshore Sediments Close to Industrial Discharges off Cuddalore (Bay of Bengal)

Reference: Joseph, T., Balachandran, K. K., Nair, M., Kesavadas, V., Nair, K. K. C., and Paimpillil., J. S., "**Trace Metal Levels in Nearshore Sediments Close to Industrial Discharges off Cuddalore (Bay of Bengal),**" *Contaminated Sediments: Characterization, Evaluation, Mitigation/Restoration, and Management Strategy Performance, ASTM STP 1442,* J. Locat, R. Galvez-Cloutier, R. C. Chaney, and K. R. Demars, Eds., ASTM International, West Conshohocken, PA, 2003.

Abstract: Trace metals in the sediment and in the overlying water column along with texture characteristics in the vicinity of industrial discharges at Cuddallore were analyzed, covering the seasonal changes to identify probable anthropogenic influence on this coast. During monsoon, cadmium and zinc had insignificant correlation with other trace metals. Other metals, except Mn, had a positive significant correlation. The spatial distribution of metals and the correlation were drastically changed during post-monsoon, loosing significant correlation for Pb, Ni, and Mn with other metals and the observed correlations being mostly negative. Cobalt and copper had strong positive correlation with all metals. Among the trace metals in water column Cu and Ni had strong positive correlation (0.88). Most of the correlation was positive except for Fe and Ni. During post-monsoon, levels of Cd, Co, Cu, Pb, Zn, and Mn had dropped down to 33-94%. The maximum amount of lowering was noticed for Pb and Cu. Ni (148%) and iron (110%) levels had an increasing trend. The trace metals in the water column had a similar decreasing trend (41-76%) for Cu, Ni, Fe and Zn. Cluster analysis had shown three distinct clusters of sampling points and was classified as least (4 stations), moderate (5 stations) and high (5 stations) trace metal contaminated regions. The least contaminated stations were all in the offshore area. Wilks lambda (0.027) denoted the good discriminatory power of the current model with the three groups. Partial lambdas indicated that Cr contributed the most, Cd the second most, Ni the third most and Mn contributed the least for the overall discrimination. The other trace metals also contribute to this function, but with negative sign. The forcing mechanisms behind the rapid changes in trace metal levels; their spatial distribution patterns and correlation strengths were indicated.

Keywords: Trace metals, anthropogenic influence, discriminatory power, monsoon effect

---

[1] Scientist, Regional Center, National Institute of Oceanography, Cochin, India.

[2] Director, Enviro Solutions, Ferric Lane, Aluva, Kerala, India.

Introduction

Marine sediments fringing the west coast of India exhibit well-defined patterns in their texture, chemical and mineral composition (Murthy et al.1981). Present knowledge of the distribution patterns of heavy metals in shelf sediments off the west coast of India is based on the studies of Murthy et al.(1981) and Balachandran (2001). On the east coast of India, the available information on the concentration of heavy metals in the sediments are limited to the work of Padma and Periakali (1999) and Senthilnathan and Balasubramanin (1999) and seriously lack a geochemical data from Cuddallore region.

The Cuddalore Power Company (CPC) situated in the city of Chennai, had set up a thermal power plant south of Cuddalore Port (South India) with two units with 660 MW capacities. The site of the plant is about 5 km from Cuddalore Port and 15 km south of Cuddalore Town. On the eastern side of the plant site is the Bay of Bengal and the Uppanar estuary borders the western side. The SIPCOT industrial area (mainly chemical industries) is situated on the western shore of the Uppanar estuary (Fig.1). The cooling water is taken from the sea and the heated cooling water is discharged into sea. In addition to this plant a desalination plant and a demineralization plant were also set up in the vicinity. The quantity of cooling water intake was of the order of 302, 400 m^3/hr. A portion (950 m^3/hr) of this water is required for the desalination plant and the desalinated water output is 328 m^3/hr. The remaining water is discharged at the rate of 622 m^3/hr. This is mixed with the heated cooling water and is discharged (302, 000 m^3/hr) into the sea.

The rivers that drain into Bay of Bengal in this region are the Pannaiyar River, Gadilam River and Uppanar River in the south near Cuddalore Port and Vellar River in the south near Portonovo. Uppanar River runs somewhat parallel to the coast in this area and drains into the sea at Cuddalore Port. The Gadilam River also joins the sea at Cuddalore and a narrow canal connects the estuarine portion of these two rivers.

The continental shelf in this region is narrow (20 km), taking the 50 m depth as the edge of the shelf. Near the shore up to 10 m depth, the slope of the sea bottom is greater and beyond the 50-m the slope is very steep. The slop between 10 and 20 m contours appears to be gentle. The 20-m-depth contour is at a distance of 9-10 km from the shore. The nearshore bathymetry in this area appears to undergo seasonal changes. The coastal region from Nellore to Cuddalore is reported to be strong upwelling zone during southwest monsoon. As information on geochemistry associated with textural characteristics of this coastal region can throw some light on the processes by which they have been incorporated in the sediments, the present studies have been carried out in this direction.

Materials and Methods

The shelf-sediment samples were taken from 24 stations with three transects perpendicular to the coast covering the anticipated discharge point. The first sampling was during the end of southwest monsoon season and the second one was during the middle of the post-monsoon season (1997-98), thus enabling to decipher the seasonal

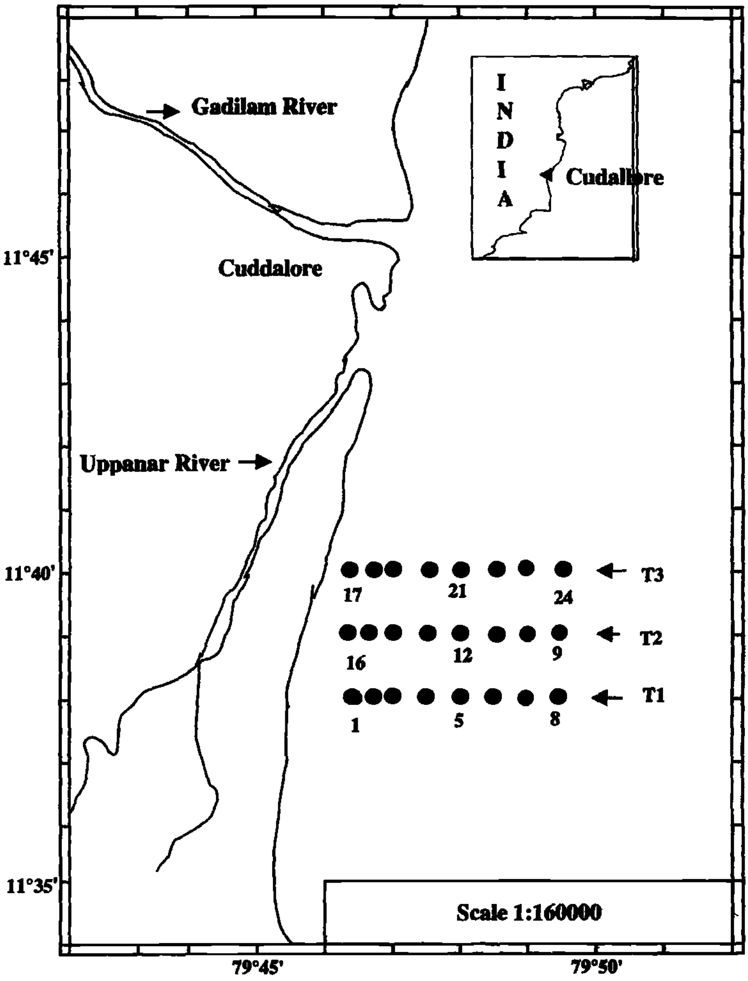

Figure 1 - *Sampling locations off Cudallore*

changes in sediment geochemistry. The sampling stations are shown in Fig.1 and the sediment sampling technique is discussed in Anon (1998). Water samples were collected using *Hydrobios-Niskin* samplers and sediments using a Van Veen grab. Water samples were filtered through 0.45 µm Miillipore filter papers and the filtrate acidified to pH 4.5 for extraction. The analytical method used for the extraction of dissolved heavy metals was chelation with ammonium pyrrollidine dithiocarbamate (APDC) and extraction with methyl isobutyl ketone (MIBK). The organic layer was then stripped off the metals with concentrated nitric acid and the aqueous extract analyzed in an air-acetylene flame of AAS (*PE AAanalyst 100*). Textural characteristics were determined following pipette analysis (Krumbein and Petijohn. 1938) and organic carbon using wet digestion followed by back titration with ferrous ammonium sulphate (El Wakeel and Riley. 1957). Sediments, dried and finely powdered, were digested in Teflon^{TM} (trifluoroethylene) bomb using aquaregia-hydrofluric acid mixture at 90°C for 2 hours, cooled and made up to 50 mL in a boric acid medium (Loring and Rantala. 1992). Analytical accuracy was checked by running a procedural and a standard reference material (BCSS-1) as a control and the precision was found to be better than 15%.

Results and Discussion

The sediments in the nearshore area move along the coast due to the action of waves, which generate longshore currents and cause sediment transport. The littoral transport in the region appears to be northerly from April to October and southerly from November to March. The annual net transport is northerly between Pondichery and Allur. The longshore transport in the Cuddalore area is about 6.98 x 10^2 m^3/yr when the direction is northerly (Anon.1998). In general, the annual net transport in this region appears to be low as compared to other places. The net direction of transport is towards southwesterly as compared to other places.

Many trace metals such as copper, chromium, zinc and lead get rapidly fixed to particulate matter and carried to the bottom because of which the sediments are considered to provide reliable estimate of metal pollution levels. It was seen that all the trace elements were more enriched in the nearshore sediments as compared to offshore region. The variation in the levels were in narrow range and comparable to the reported values for the East Coast of India. Organic carbon in these sediments were very low (Tables 1 and 2) and hence, these concentrations could be taken as lithogenic in origin.

The highest heavy metal concentrations in the shelf sediments (Muraleedharan Nair et al. 1992) at the southern tip of West Coast of India were of the order of Cr 250, Cu 38, Ni 80, Pb 37 and Zn 11 ppm. The concentrations of copper during the study period had ranged from 0.77 ppm to 16 ppm (Table. 3a, 3b). The mean concentration of nickel was comparable to that reported for unpolluted areas. The high values for certain trace metals may be due to the domestic and industrial pollutants. The concentrations of various trace elements follow closely the texture of sediments (Table. 2). Higher concentrations of elements are associated with the silt-clay fractions of sediments. In Table 4, the concentrations of heavy metals reported from some of the unpolluted coastal regions are given. A perusal of these values with the average values for Cuddalore shelf sediments revealed that the sediments of the coastal region do not

Table 1 – *Sediment characteristics off Cuddallore*

Stations	Sand %	Clay %	Silt %	Organic Carbon (mg/g)
1	54.32	8.00	37.68	14.27
2	93.21	2.95	3.84	3.57
4	92.53	6.90	0.57	3.57
5	94.45	4.15	1.40	2.98
6	95.80	0.30	3.90	1.19
7	95.61	4.30	0.09	5.95
8	98.73	0.35	0.02	6.55
10	98.00	1.50	0.50	9.52
11	97.15	2.25	0.60	2.98
12	97.07	2.50	0.43	8.33
13	94.96	3.70	1.34	5.95
14	91.06	8.50	0.44	3.57
15	16.66	30.45	52.89	11.90
16	95.50	2.35	2.15	0.60
17	92.99	4.50	2.51	12.50
18	32.07	39.55	28.38	9.52
19	19.99	43.80	36.21	0.60
20	90.94	9.00	0.06	3.57
21	85.87	13.55	0.58	5.36
22	52.97	33.55	13.48	4.76
23	94.87	4.35	0.78	0.60
24	97.23	2.75	0.02	0.60

Table 2 – *Sediment Characteristics along different transects (Ranges and Averages)*

Transect	Sand %	Clay %	Silt %	Organic carbon (mg/g)
T1	54.32-98.73	0.30- 8.00	0.02-37.68	2.58-14.27
	(89.24)	(3.85)	(6.90)	(5.44)
T2	16.66-98.00	1.50-30.45	0.43-52.89	0.60-11.90
	(84.34)	(7.32)	(8.34)	(6.12)
T3	19.99-97.23	2.75-43.80	0.02-36.21	0.60-12.50
	(70.87)	(18.88)	(10.25)	(4.68)

( ) Values in paranthesis are the mean for each transect.

Table 3a – *Heavy Metals in Sediments**, *September, 1997*

Stn.	Cd	Co	Cr	Cu	Fe	Mn	Ni	Pb	Zn
1	2.1	25.1	59.2	13.5	5.5	212	33.0	55.4	30.5
2	2.5	24.5	45.3	10.6	14.8	388	27.1	37.9	111.0
4	1.9	16.1	29.9	4.4	10.1	306	17.3	25.6	14.0
6	1.5	9.4	29.1	4.5	6.7	330	8.2	25.8	9.7
7	1.6	14.7	36.9	5.4	8.7	577	17.2	36.1	12.5
8	2.4	15.7	36.3	6.1	9.2	523	14.9	35.6	16.6
10	1.2	22.9	37.0	8.0	10.2	286	23.4	46.6	25.5
11	1.7	16.5	33.7	6.4	10.0	525	20.0	28.1	20.5
13	1.9	15.3	84.8	5.2	9.4	332	16.5	34.6	15.8
15	2.4	30.6	82.9	16.3	21.3	460	41.9	63.0	50.7
16	2.1	28.2	83.6	7.3	14.8	386	27.0	47.2	34.1
17	1.6	26.8	79.2	5.3	16.0	320	25.6	35.8	32.4
18	1.6	24.7	65.7	11.7	17.6	372	29.3	63.6	47.9
20	2.1	25.1	77.4	15.1	17.1	377	34.1	64.5	42.0
22	1.2	10.6	38.8	3.7	9.7	354	14.4	25.9	15.4
23	0.8	11.3	35.5	4.0	7.7	424	15.4	27.7	13.1
24	1.2	16.1	46.6	7.8	12.1	535	22.8	27.3	39.8

* concentration in ppm dry weight except for Fe, mg/g

Table 3b – *Heavy Metals in Sediments**, *January, 1998*

Stn.	Cd	Co	Cu	Fe	Mn	Ni	Pb	Zn
1	1.7	24.5	8.9	21.4	454	30.8	20.9	34.6
3	1.2	13.5	0.8	5.4	360	15.4	9.8	16.1
5	1.7	19.6	3.6	9.4	143	25.2	21.4	16.4
6	0.4	12.2	0.9	7.5	497	12.5	10.6	8.6
7	0.7	12.5	0.7	7.7	363	14.2	9.1	6.6
13	1.3	21.4	3.5	11.6	380	22.4	10.4	16.3
14	1.7	29.5	10.0	21.8	357	31.5	21.4	48.5
15	0.9	26.8	3.6	17.4	425	29.1	10.6	33.0
17	1.7	26.6	8.1	21.0	562	26.9	21.0	35.9
18	2.1	23.6	6.1	19.2	445	28.2	10.3	30.5
19	1.3	9.7	0.9	6.7	423	29.0	21.1	11.8
20	1.7	21.7	6.3	17.7	105	39.2	21.0	27.4
21	1.7	19.2	4.4	15.3	383	26.6	0.0	13.3
22	0.4	11.5	0.9	9.5	402	55.1	10.0	8.8
23	0.4	10.9	0.8	7.3	285	104.0	9.5	6.9
24	1.7	17.0	0.9	8.9	424	35.3	10.6	9.5

* concentration in ppm dry weight except for Fe, mg/g

Table 4 – *Average concentration of heavy metals in coastal sediments in the study area and for other regions (cited from Balachandran, 2001)*

No.	Region	Fe %	Zn	Mn	Ni	Co	Cu	Cd
1.	Present study	8.9	35	385	27	19	6	--
2.	SW Coast of							
3.	India (Cochin)	3.3	99	171	72	22	32	--
4.	Cochin estuary, India	5.5	1266	337	67	25	53	--
5.	Pulikkat estuary (east coast of India)	2.8	--	495	--	--	--	8.6
6.	Pondicherry harbour (east coast of India)	--	--	--	--	--	42	2.5
7.	Mumbai, India	--	138	1059	89	51	105	-
8.	Thana creek, Mumbai	--	206	980	132	50	132	-

*concentration in ppm dry weight except for Fe, mg/g

Table 5 – *Trace metal concentration in sediment and water column during Southwest monsoon and post-monsoon period.*

	Cu	Pb	Cd	Co	Ni	Zn	Fe	Mn
Water								
SW Monsoon	0.7	--	--	--	1.2	3.0	31	--
Post-monsoon	1.0	--	--	--	1.6	7.2	67	--
Ratio	1.4	--	--	--	1.4	2.4	2.1	--
Sediment								
SW Monsoon	8.0	40.1	1.7	19.6	22.8	31.3	11.6	395
Post-monsoon	3.4	13.5	1.2	18.6	33.7	19.3	12.8	343
Ratio	0.4	0.3	0.7	0.9	1.5	0.3	1.1	0.9

*concentration in ppm dry weight except for Fe, mg/g

indicate any sign of pollution. The effects of nearshore circulation in the trace metal levels in coastal sediments was clear during the period of study with the high concentration levels during the withdrawal of southwest monsoon season. Enrichment during the post-monsoon period was noticed only for nickel and the levels of iron remained the same. The significant reduction in concentration levels was noticed for copper and lead. During the same period, the overlying water column had experienced enrichment in heavy metals as shown in Table 5.

A cluster analysis using the heavy metal concentrations had shown two cluster formations. The stations on the northern transect and nearshore stations in middle transect formed the first cluster. The offshore stations in all the three transect form the next cluster. Most of the heavy metals had very high levels at stations in cluster one.

This indicates that the sources of trace metals are coastal points north of transect one and it hints towards the estuarine and industrial contributions.

The trace metals cadmium and zinc had no significant correlation with other metals. Other metals had a positive significant correlation except for Mn. After a time gap of six months, the correlation had changed drastically with lack of significant correlation for Pb, Ni and Mn with other metals and with negative correlation. Cobalt and copper had strong positive (> 0.70) correlation with other metals. Cadmium and zinc had strong positive correlation with Cu, Co and Fe. Among the trace metals in water column Cu and Ni had strong positive correlation (0.88). Most of the correlation was positive except for Fe and Ni. After a six-month gap, no correlation among the metals was statistically significant and most of them were negative.

The spatial distribution of copper in the coastal sediments had shown similar patterns during the two seasons with the maximum concentration centered at coastal stations of transect 2. There was a noticeable reduction (42%) in copper concentration at the coastal stations during the post-monsoon season. The cadmium distribution was not having a well-defined spatial pattern and with no nearshore enrichment. During the post-monsoon season, a slight increase in cadmium levels was noticed at coastal stations in the northern transect. The distribution pattern of lead remained to be similar to the copper distribution with the coastal stations at mid transect showing the maximum levels and with an offshore decrease of concentration. During the post-monsoon season, the lead concentration had reduced by 50% and the well-marked high levels at mid transect had disappeared with almost same concentration at coastal stations. The pattern of cobalt distribution remained nearly the same during the two seasons with a pronounced peak at coastal station in mid transect. There was no significant reduction in concentration levels of cobalt during the two seasons. The spatial distribution pattern for zinc had shown a pocket with very high zinc levels (>100 ppm) in the coastal waters on the southern transect at the end of the monsoon season. During the post-monsoon sampling period, the zinc levels in coastal sediments had reduced by one third of its monsoon level. This spatial distribution patterns indicated a flux of zinc in the northward direction or a local enriching contribution from a land based source.

In a canonical correlation analysis using trace metals in the three transect, the main root had accounted for 92% of the variability of the canonical variate. The main contributions to the canonical root were from Cd, Cu, Ni and Co in the order of magnitude. The sampling stations were grouped into a contaminated coastal (station no.1,15,16,17,18), moderately contaminated nearshore (st.nos. 2,3,13,14,19) and an uncontaminated offshore (st.nos. 8,9,10,24) zones, based on the distance from shore line. A discriminant analysis was conducted to see which trace metal discriminate between the three groups. Wilks lambda (0.27) denoted the good discriminatory power of the current model with the three groups. Partial lambdas for overall discrimination showed the magnitude of contribution in the order Cr > Cd > Ni > Mn. The first root accounts for 81% of the explained variance, inferring that a single function could explain 81% discriminatory power, thus establishing the role of Cr, Cd and Ni in classifying the contamination levels of sediment. The other trace metals also contribute to this function, however with negative sign.

Conclusion

The industrial development along the coastline had shown some impact on the environment of the shelf region. Heavy metal distribution in the coastal region showed an alongshelf pattern. Metal distribution in this shelf is controlled by the fine sediment dynamics which are mainly regulated by the low-energy alongshore currents. As the shelf currents do not effectively disperse the anthropogenic discharges, the metal enrichment is restricted to the sediments of shallower regions only. The present study, in general, indicates that trace metals do not seem to constitute a potential threat to marine environment of this region and the release of metals into the coastal zone through anthropogenic activities are adequately dealt with by the dominant coastal processes of this region resulting in minimal biological impact. Taking the data presented here as the baseline, it may be worthwhile to resurvey the area to understand the impact of the recent developmental activities and to what level the area has been polluted.

Reference

Anon, 1998. Rapid environmental impact assessment of proposed jetty, cooling water intake and disposal of heated cooling water off Cuddalore coast for CPC thermal power plant. *Technical report of National Institute of Oceanography*, Goa, India. pp.93.

Balachandran, K.K, 2001. "Chemical oceanographic studies of the coastal waters of Cochin", *Ph.D Thesis*, Cochin University of Science and Technology, Cochin, pp.148.

El Wakeel, S.K. and Riley, J.P., 1957. "The determination of organic carbon in marine muds". *Journal of Du. Conseil International Pour. Explor. Mer.*, Vol.22, pp.180.

Krumbein, W.C. and Pettijohn, F.J., 1938. "Manual of sedimentary petrography". *Appletion Century Crofts Inc.*, New York, pp.549.

Loring, D.H. and Rantala, R.T.T., 1992. "Manual for Geochemical Analsis", *Earth Science Reviews*, Vol.32, pp.235-283.

Muraleedharan Nair, M.N. and Ouseph, P.P., 1992. "Elemental distribution in the nearshore sediments along the Kerala Coast". *Proceedings, Fourth Kerala Science Congress*, pp.37-38.

Murthy, P.S.N. and Veerayya, M., 1981. "Studies on the sediments of Vembanad Lake, Kerala State: Part IV- Distribution of trace elements", *Indian Journal of Marine Science*, Vol.10, pp.165-172.

Padma, S. and Periakali, P., 1999. "Physico-chemical and geochemical studies in Pulikkat Lake, east coast of India", *Indian Journal of Marine Science*, Vol.28, pp.434-437.

Senthilnathan, S. and Balasubramanian, T., 1999. "Heavy metal distribution in Pondicherry Harbour, southeast coast of India", *Indian Journal of Marine Science*, Vol.28, pp.380-382.

Maria Lucia K. Rodrigues,[1] Maria Teresa Raya-Rodríguez, [2] and Valério D. Pillar [2]

Randomization Tests: A Statistical Tool to Assess Heavy Metal Pollution in Caí River Basin Sediments (RS, Brazil)

Reference: Rodrigues, M. L. K., Raya-Rodríguez, M. T., and Pillar, V. D., "**Randomization Tests: A Statistical Tool to Assess Heavy Metal Pollution in Caí River Basin Sediments (RS, Brazil),**" *Contaminated Sediments: Characterization, Evaluation, Mitigation/Restoration, and Management Strategy Performance, ASTM STP 1442*, J. Locat, R. Galvez-Cloutier, R. C. Chaney, and K. R. Demars. Eds., ASTM International, West Conshohocken, PA, 2003.

Abstract: This study evaluated the use of statistical randomization tests in data analysis regarding heavy metals content in sediments from the Caí River basin (Brazil). During one year, four samplings took place at eleven sites in the Caí River and tributaries. The results showed significant differences between some locations, enabling spatial segregation of sites affected by natural and anthropic sources. Considering a significance level (α) of 5%, the control station, above polluted areas, showed the best quality; Caí River station after the mouth of Pinhal/Belo stream indicated influence from the industrial complex of Caxias do Sul region, as well as copper compounds use in vineyards; and the Cadeia and Forromeco streams showed effects of natural contribution from basalts and surface runoff on naked soils. For α=10%, it was possible to identify chromium pollution by tanneries in the Cadeia stream. Long-term studies should be performed, since understanding temporal aspects such as alteration processes in sediments involves a much longer time scale.

Keywords: randomization tests, multivariate statistics, sediment, heavy metals

---

[1] Chemical Engineer, Divisão de Química, FEPAM, Rua Aurélio Porto 45, 90620-010 Porto Alegre, RS, Brazil.

[2] Professor, Departamento de Ecologia, UFRGS, Av. Bento Gonçalves 9500, 91540-000 Porto Alegre, RS, Brazil.

Introduction

Rivers act as carriers of dissolved heavy metals or those associated with suspended solid particles. They are also potential reservoirs of these elements, by deposition in the bottom sediment and assimilation by the biota. In aquatic ecosystems, sediment is the main compartment of accumulation, reprocessing and transference of heavy metals (Förstner and Wittman 1981). The potentially mobile metallic elements, with greater bioavailability, can be released from sediments by microbial activity and changes in the various physicochemical factors that characterize the aquatic environment.

In order to analyze data resulting from monitoring multiple variables in environmental samples, statistical methodologies must be sought in order to show the significance of differences, both spatial and temporal, and enable the preparation of consistent diagnoses.

Among the techniques that involve multivariate statistics, randomization tests have demonstrated their usefulness in comparing groups of sampling units described by a given number of variables (Pillar and Orlóci 1996). The groups of sampling units may be defined by one or more external factors, such as location, time of data collection, or experimental treatments, arranged in different designs. The advantage of these tests is that they do not require the assumptions involved when classic statistical tests are used (Manly 1991). A randomization test generates a probability P which is used to judge whether the groups differ significantly. P is generated under the null hypothesis (H_0) that the difference between groups, measured by an appropriate test criterion, is the result of chance alone. In other words, under H_0 the observations for the variables in a given sampling unit are independent from the group to which the sampling unit belongs. If P is sufficiently low, compared to a defined level of significance α, it is rare to find by chance a difference between groups as large as the observed one. Therefore, the null hypothesis is rejected. On the contrary, if P is larger than α, H_0 is accepted, and it is concluded that there is no significant difference between the groups.

In classic statistics, P is obtained assuming that the distribution of the test criterion (e.g., F, t) agrees with the theoretical distribution, usually the normal one. In randomization tests, P is generated from the data themselves, considering the conditions established in H_0. The observed set of data is viewed as one of the many possible outcomes were H_0 true. That is, under H_0 any permutation of the data vectors among the groups is equally possible. A data vector contains observations on one or more variables describing a sampling unit. Based on this, an iterative algorithm is used for the random generation of permutations. Sampling units may be stratified in blocks, in which case random permutations are restricted to within blocks. The method described in Pillar and Orlóci (1996) uses as test criterion a sum of squares between groups (Q_b) defined as

$$Q_b = Q_t - Q_w \tag{1}$$

where

$$Q_t = \frac{1}{n}\sum_{h=1}^{n-1}\sum_{i=h+1}^{n} d_{hi}^2 \tag{2}$$

is the total sum of squares involving $n(n\text{-}1)/2$ pair-wise squared distances (d^2_{hi}) between n sampling units and

$$Q_W = \sum_{c=1}^{k} Q_{wc} \tag{3}$$

is the sum of squares within k groups, such that

$$Q_{WC} = \frac{1}{n_c} \sum_{h=1}^{n-1} \sum_{i=h+1}^{n} d^2_{hi|c} \tag{4}$$

is the sum of squares involving $n_c(n_c\text{-}1)/2$ pair-wise squared distances between n_c sampling units belonging to group c. At each iteration a new Q_{b0} is computed and compared to the Q_b observed in the data. After many iterations, usually not less than 1000, the proportion of iterations in which $Q_{b0} \geq Q_b$ is taken as the probability $P(Q_{b0} \geq Q_b)$ sought by the test. By convention, the observed data set is taken as the first iteration and thus the minimum value for P is

$$P = (1 \ / \ \text{total number of iterations}) \tag{5}$$

The greater the number of iterations, the more reliable will be the test result, since the value of P will be closer to that which would be obtained if we had worked with all the possible permutations.

In this paper we evaluate the usefulness of a randomization test to analyze the association of heavy metals content in sediments with location and time of sample collection, in the Caí River basin, south Brazil.

Methodology

Study Area

The Caí Basin, located in the state of Rio Grande do Sul in the extreme south of Brazil, has a surface of 5000 km^2 (Figure 1). The Caí River is a tributary of Guaíba Lake and extends about 260 km from the headwaters in the Plateau (1000 m altitude) until the mouth almost at the sea level. On the banks of the Caí River significant urban and industrial concentrations occur, especially from petrochemical, metallurgical, tannery, food and textile branches, that are potential sources of heavy metals. The region also has concentrated agricultural activities, such as viticulture, vegetable and fruit production, in which fungicides and inputs containing these elements are applied. The local geology consists mainly of Serra Geral Formation rocks, in which basalts that are naturally rich in metallic elements predominate (FEPAM/GTZ 1997).

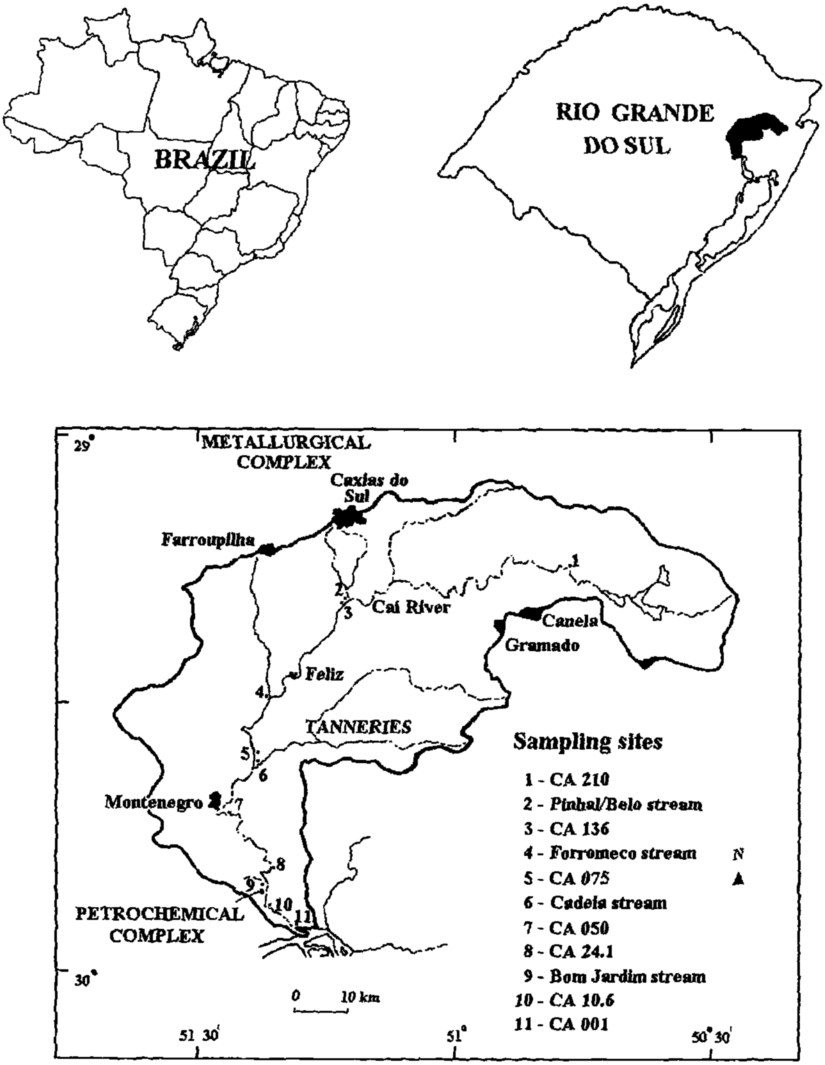

Figure 1 - *Location of Sampling Stations in the Caí River Basin, Rio Grande do Sul State (RS), Brazil*

Sampling and Analysis of Sediment Samples

As described by Rodrigues (1997), from July 1994 to July 1995 two sampling expeditions were performed during the flood season and two during the dry season, at seven stations along the Caí River. In addition, four stations near the mouths of some important tributaries were also sampled. Sampling stations located in the Caí River were identified by the letters CA followed by the distance in kilometers from the mouth (Figure 1). As a control point, sediment was collected in the Caí River, at a site located above the areas impacted by domestic and industrial discharges.

The elements cadmium (Cd), copper (Cu), lead (Pb), nickel (Ni), chromium (Cr), vanadium (V), zinc (Zn), aluminum (Al), iron (Fe), manganese (Mn) and titanium (Ti) were analyzed in the silt-clay fraction (dry weight), by inductively coupled plasma optical emission spectrometry (ICP/OES). In the extraction of total metals content, 0.25000 g of sediment samples were digested with 2 mL of hydrofluoric acid (HF) and 3 mL of nitric acid (HNO_3) in PTFE closed vessels, heated in an oven at 150°C for 4 hours. In order to eliminate HF residues, the extracts were dried on a hot plate and then diluted to an appropriate volume. For potentially mobile metals, a partial determination (Malo 1977) was used, involving digestion with hydrogen peroxide (H_2O_2) and hot extraction with 0.3 M hydrochloric acid (HCl).

Grade p.a. reagents that had previously been tested as to metal content and ultra-purified water were used to process the samples duplicates. The certified reference material CANMET STSD-4 was analyzed at the same time in order to assess the accuracy of results for total metals content. The mean recovery was between 95 and 105%, except for Cr (75%) and for Al (35%), which was further analyzed by X-ray fluorescence.

Additionally, organic matter was determined by calcinating the samples at 450°C until constant weight. Grain size analysis was performed using sieving and sedimentation techniques.

Statistical Analysis of the Data Using Randomization Tests

The initial analysis aimed at assessing whether the sampling sites differed significantly in terms of metal concentration in the sediments by following the randomization test described by Pillar and Orlóci (1996). In data processing, the sampling dates were fixed as blocks in order to evaluate the existence of a significant difference between the sampling sites. The null hypothesis in this case was that the metal content in the sediments was independent from the sampling site. In a second analysis the sampling locations were taken as blocks to test whether the sampling dates differed. In this case the null hypothesis was that the metal content in the sediments was independent from the sampling date.

The database, with 22 columns corresponding to the variables, and 44 rows designating the sample units, was processed via the MULTIV computer program (Pillar 2000). Total Al, analyzed only in the third sampling campaign (n=11), was ignored, in order to avoid gaps in the data matrix. The data set was submitted to standardization by centering and normalization within variables. The test criterion Q_b was computed from pair-wise Euclidean distances between sampling units. The probability $P(Q_{bo} \geq Q_b)$ was obtained by 1 000 iterations of random permutation. Specific contrasts between groups, pair-wise or multiple, were also evaluated, for which probabilities $P(Q_{b0} \geq Q_b)$ were generated and interpreted in a way similar to a Scheffé test (Pillar and Orlóci 1996).

A significance level $\alpha = 0.05$ was used to interpret the results, which means that the probability of error in rejecting H_0 is 0.05. Comparing the probability P obtained in the randomization test to the chosen level of significance, the null hypothesis established for each case was rejected or not. In the final assessment, in order to provide a better demonstration of the existence of tendencies, the results were also discussed as regards an $\alpha = 0.10$, since a strict criterion often do not apply to environmental studies involving extremely complex phenomena, with a high degree of uncertainty.

Results and Discussion

The analytical results of the sediment samples are summarized in Table 1. In the first statistical analysis of data, comparing the different sampling locations, the use of randomization test generated a probability P=0.001, which indicated the sites differed significantly. Table 2 displays the results of the contrasts between sites, which enabled the following observations.

Table 1- *Heavy Metals and Organic Matter Contents (Dry Weight, Fraction < 63 μm) in the Sediments from Caí River Basin (RS, Brazil), Average of 11 Sampling Locations in the Period from July 1994 to July 1995*

Variable	*n*	Mean	P/T (%)	Minimum	Maximum	Standard deviation
Cd T (mg/kg)	44	1.10	44.3	0.445	1.73	0.293
Cd P (mg/kg)	44	0.487		< 0.220	0.811	0.145
Cu T (mg/kg)	44	102	47.3	48.1	158	24.8
Cu P (mg/kg)	44	48.2		16.0	82.5	15.5
Pb T (mg/kg)	44	34.8	58.3	21.2	49.2	7.81
Pb P (mg/kg)	44	20.3		11.9	36.0	5.25
Fe T (mg/kg)	44	53 457	30.6	24 659	72 276	10 101
Fe P (mg/kg)	44	16 333		9 946	23 355	3 368
Ni T (mg/kg)	44	50.2	27.3	7.68	71.2	14.9
Ni P (mg/kg)	44	13.7		1.28	26.8	5.79
Zn T (mg/kg)	44	136	61.5	67.4	352	57.4
Zn P (mg/kg)	44	83.7		24.2	321	54.1
Mn T (mg/kg)	44	1 080	88.0	432	1 704	299
Mn P (mg/kg)	44	950		389	1 479	297
Cr T (mg/kg)	44	117	46.8	14.1	305	56.7
Cr P (mg/kg)	44	54.8		2,31	223	50.5
Al T (mg/kg)	11	89 155	8.3	84 300	106 800	7 508
Al P (mg/kg)	44	7 415		4 966	9 633	1 277
Ti T (mg/kg)	44	10 429	0.8	8 196	14 071	1 501
Ti P (mg/kg)	44	78.9		32.1	142	23.6
V T (mg/kg)	44	230	21.6	101	356	54.3
V P (mg/kg)	44	49.6		19.2	78.9	15.0
Organic Matter (%)	44	14.8		10.7	18.5	1.47

Note: T = total content; P = potentially mobile content

Table 2 – *Results of Randomization Tests by Analyzing Contrasts Between Sediment Sampling Stations in the Caí River Basin (RS, Brazil), from July 1994 to July 1995*

Contrasts	Sites	P	Decision about H_0 (α=0.05)	Decision
1 -1 0 0 0 0 0 0 0 0 0	CA 210 – Pinhal/Belo	0.001	Rejected	Different
1 0 -1 0 0 0 0 0 0 0 0	CA 210 – CA 136	0.001	Rejected	Different
1 0 0 -1 0 0 0 0 0 0 0	CA 210 – Forromeco	0.001	Rejected	Different
1 0 0 0 -1 0 0 0 0 0 0	CA 210 – Cadeia	0.001	Rejected	Different
1 0 0 0 0 -1 0 0 0 0 0	CA 210 – CA 075	0.001	Rejected	Different
1 0 0 0 0 0 -1 0 0 0 0	CA 210 – CA 050	0.002	Rejected	Different
1 0 0 0 0 0 0 -1 0 0 0	CA 210 – CA 24,1	0.002	Rejected	Different
1 0 0 0 0 0 0 0 -1 0 0	CA 210 – Bom Jardim	0.003	Rejected	Different
1 0 0 0 0 0 0 0 0 -1 0	CA 210 – CA 10,6	0.001	Rejected	Different
1 0 0 0 0 0 0 0 0 0 -1	CA 210 – CA 001	0.004	Rejected	Different
0 1 -1 0 0 0 0 0 0 0 0	Pinhal/Belo - CA 136	0.455	Accepted	Not different
0 1 0 -1 0 0 0 0 0 0 0	Pinhal/Belo – Forromeco	0.016	Rejected	Different
0 1 0 0 -1 0 0 0 0 0 0	Pinhal/Belo – Cadeia	0.001	Rejected	Different
0 1 0 0 0 -1 0 0 0 0 0	Pinhal/Belo - CA075	0.308	Accepted	Not different
0 1 0 0 0 0 -1 0 0 0 0	Pinhal/Belo - CA 050	0.309	Accepted	Not different
0 1 0 0 0 0 0 -1 0 0 0	Pinhal/Belo - CA 24,1	0.408	Accepted	Not different
0 1 0 0 0 0 0 0 -1 0 0	Pinhal/Belo - Bom Jardim	0.232	Accepted	Not different
0 1 0 0 0 0 0 0 0 -1 0	Pinhal/Belo - CA 10,6	0.245	Accepted	Not different
0 1 0 0 0 0 0 0 0 0 -1	Pinhal/Belo - CA 001	0.174	Accepted	Not different
0 0 1 -1 0 0 0 0 0 0 0	CA 136 – Forromeco	0.001	Rejected	Different
0 0 1 0 -1 0 0 0 0 0 0	CA 136 – Cadeia	0.001	Rejected	Different
0 0 1 0 0 -1 0 0 0 0 0	CA 136 – CA075	0.018	Rejected	Different
0 0 1 0 0 0 -1 0 0 0 0	CA 136 – CA 050	0.016	Rejected	Different
0 0 1 0 0 0 0 -1 0 0 0	CA 136 – CA 24,1	0.027	Rejected	Different
0 0 1 0 0 0 0 0 -1 0 0	CA 136 – Bom Jardim	0.012	Rejected	Different
0 0 1 0 0 0 0 0 0 -1 0	CA 136 – CA 10,6	0.013	Rejected	Different
0 0 1 0 0 0 0 0 0 0 -1	CA 136 – CA 001	0.007	Rejected	Different
0 0 0 1 -1 0 0 0 0 0 0	Forromeco – Cadeia	0.074	Accepted	Not different
0 0 0 1 0 -1 0 0 0 0 0	Forromeco - CA075	0.523	Accepted	Not different
0 0 0 1 0 0 -1 0 0 0 0	Forromeco - CA 050	0.473	Accepted	Not different
0 0 0 1 0 0 0 -1 0 0 0	Forromeco - CA 24,1	0.133	Accepted	Not different
0 0 0 1 0 0 0 0 -1 0 0	Forromeco - Bom Jardim	0.054	Accepted	Not different
0 0 0 1 0 0 0 0 0 -1 0	Forromeco - CA 10,6	0.165	Accepted	Not different
0 0 0 1 0 0 0 0 0 0 -1	Forromeco - CA 001	0.153	Accepted	Not different
0 0 0 0 1 -1 0 0 0 0 0	Cadeia – CA 075	0.021	Rejected	Different
0 0 0 0 1 0 -1 0 0 0 0	Cadeia – CA 050	0.063	Accepted	Not different
0 0 0 0 1 0 0 -1 0 0 0	Cadeia – CA 24,1	0.010	Rejected	Different
0 0 0 0 1 0 0 0 -1 0 0	Cadeia – Bom Jardim	0.006	Rejected	Different
0 0 0 0 1 0 0 0 0 -1 0	Cadeia – CA 10,6	0.024	Rejected	Different
0 0 0 0 1 0 0 0 0 0 -1	Cadeia – CA 001	0.026	Rejected	Different
0 0 0 0 0 1 -1 0 0 0 0	CA075 - CA 050	0.917	Accepted	Not different
0 0 0 0 0 1 0 -1 0 0 0	CA075 – CA 24,1	0.726	Accepted	Not different
0 0 0 0 0 1 0 0 -1 0 0	CA075 - Bom Jardim	0.138	Accepted	Not different
0 0 0 0 0 1 0 0 0 -1 0	CA075 – CA 10,6	0.477	Accepted	Not different
0 0 0 0 0 1 0 0 0 0 -1	CA075 – CA 001	0.448	Accepted	Not different
0 0 0 0 0 0 1 -1 0 0 0	CA 050 – CA 24,1	0.932	Accepted	Not different
0 0 0 0 0 0 1 0 -1 0 0	CA 050 – Bom Jardim	0.361	Accepted	Not different
0 0 0 0 0 0 1 0 0 -1 0	CA 050 – CA 10,6	0.969	Accepted	Not different
0 0 0 0 0 0 1 0 0 0 -1	CA 050 – CA 24,1	0.983	Accepted	Not different
0 0 0 0 0 0 0 1 -1 0 0	CA 24,1 – Bom Jardim	0.391	Accepted	Not different
0 0 0 0 0 0 0 1 0 -1 0	CA 24,1 – CA 10,6	0.931	Accepted	Not different
0 0 0 0 0 0 0 1 0 0 -1	CA 24,1 – CA 001	0.889	Accepted	Not different
0 0 0 0 0 0 0 0 1 -1 0	Bom Jardim - CA 10,6	0.291	Accepted	Not different
0 0 0 0 0 0 0 0 1 0 -1	Bom Jardim - CA 001	0.227	Accepted	Not different
0 0 0 0 0 0 0 0 0 1 -1	CA 10,6 - CA 001	0.981	Accepted	Not different

The control point (CA 210), which presented the lowest concentrations of the evaluated elements and consequently the best environmental quality, differed significantly from all the other sampling sites at a 5% level of significance (α).

For $\alpha = 0.05$, the sampling site CA 136 was only similar to the Pinhal/Belo stream station, that receives part of industrial and domestic runoff waters from Caxias do Sul city. When compared to the control point, these two locations (especially CA136) showed increased concentrations of the trace-elements Cd, Cu, Cr, Pb, Ni and Zn, which could be associated to metallurgical, electroplating and textile industries concentrated in this region. The results also suggested the influence of the use of copper-based fungicides in viticulture.

Considering $\alpha = 0.05$, the Cadeia stream was different from the other stations, except for point CA 050 in the Caí River, which suffers its direct influence, and for Forromeco stream that equally drains major agricultural areas in the basin, and is also subject to erosion. In the sediment of these streams, comparatively high contents of Fe, Ti, Mn, Al, and V were observed. The relief of these regions, located on steep slopes with a predominance of basalts, together with the action of rainfall on naked soils, could favor the bank erosion and the entrainment of material to the stream beds.

If an $\alpha = 0.10$ were chosen, all the sampling points would be considered significantly different in relation to the Cadeia stream. For $\alpha = 0.05$ the power of the test was not sufficient to segregate the Forromeco and Cadeia streams, but it is known that a large input of pollution by chromium has an impact on the latter due to the contribution of tannery effluents (FEPAM/GTZ, 1997).

In the final stretch of the Caí River, under influence of a petrochemical complex, all the sampling stations were similar for $\alpha = 0.05$, including the upstream points CA 050 and CA 24.1. Therefore, in this study, no influence of the petrochemical complex was detected on the contents of the elements analyzed in the sediment samples. However, the grain size distribution in the sediments showed it is a preferential site for fine particles settlement and may represent a reservoir for trace elements. Due to possible changes in aquatic environmental properties and dredging activities, which can modify redox conditions, this would be a potentially fragile site concerning trace elements remobilization to the water column.

Table 3 - *Results of Randomization Tests by Analyzing Contrasts Between Sediment Sampling Dates in the Caí River Basin (RS), from July 1994 to July 1995*

Contrasts	Dates	*P*	Decision about H_0 (α=0.05)	Decision
1 -1 0 0	July/94 - November/94	0.251	Accepted	Not different
1 0 -1 0	July/94 - March/95	0.031	Rejected	Different
1 0 0 -1	July/94 - July/95	0.016	Rejected	Different
0 1 -1 0	November/94 - March/95	0.337	Accepted	Not different
0 1 0 -1	November/94 - July/95	0.082	Accepted	Not different
0 0 1 -1	March/95 - July/95	0.203	Accepted	Not different

In the second statistical analysis, related to the temporal aspect, the randomization test indicated that the sampling dates differed significantly (P=0.025). Table 3 contains the results obtained in the contrasts, showing similar tendencies between the subsequent collection dates, to a 5 % level of significance. For intercalated collection dates, there was a significant difference when one considered $\alpha = 0.05$, except for the pair of dates of November/94-July/95, where the difference was significant with $\alpha = 0.10$.

Summary and Conclusions

The randomization tests proved to be an appropriate tool for the spatial assessment of the proposed database, showing consistency in the segregation of areas that suffer the impact of different sources of heavy metals contribution.

Considering α =0.05, the results showed a better environmental quality for the control point and contamination of the area affected by the proximity of Caxias do Sul industrial complex with metals Cd, Cu, Pb, Ni and Zn. Forromeco and Cadeia streams, with comparatively high contents of Al, Fe, Mn, Ti and V, did not differ significantly, showing the effect of natural contribution by basaltic rocks, associated with surface runoff through naked soils on steep slopes. Considering α =0.10, Cadeia stream showed a tendency to differ from all other sampling units, indicating the influence of Cr emission by tanneries. In the stretch located between the Caí River mouth and kilometer 50, including the Bom Jardim stream that drains a petrochemical complex area, all collection stations did not differ significantly, with $\alpha = 0.05$. These results indicated that, during the monitoring period, no detectable influence of the petrochemical complex on the contents of the elements analyzed in the sediment was observed. However, the final stretch of the Caí River, under influence of the complex, is a preferential site for fine particles settlement and may represent a reservoir for trace elements, which can be subjected to remobilization to the water column. Therefore, this section of the river also deserves great attention in terms of monitoring and preservation of environmental quality.

As to the temporal aspect, the randomization tests showed similarity between the subsequent collection dates, to a 5% level of significance. Meanwhile, long-term studies should be performed, since understanding processes of change in the sediments involves a larger time scale.

Be that as it may, the possibility of applying this statistical tool, to data interpretation and to preparing spatial and temporal environmental diagnoses, was clearly demonstrated.

References

1.FEPAM-GTZ, 1997, "Levantamento dos Principais Usos do Solo e da Água na Bacia Hidrográfica do Rio Caí," Vol.1, Projeto de Cooperação Técnica Brasil / Alemanha, Porto Alegre, Brasil, 138 p.

2.Förstner, U., Wittman, G.T.W., 1981, "Metal Pollution in the Aquatic Environment," Springer-Verlag, Berlin, 486 p.

3.Malo, B.A., 1977, "Partial Extration of Metals from Aquatic Sediments," *Environmental Science & Technology*, Vol. 11, pp. 277-282.

4.Manly, B. F. J., 1991, "Randomization and Monte Carlo Methods in Biology," Chapman and Hall, London, 281 p.

5.Pillar, V.D.P., Orlóci, L., 1996, "On Randomization Testing in Phytocoenology: Multifactor Comparisons of Relevé Groups," *Journal of Vegetation Science*, Vol. 7, pp. 585-592.

6.Pillar, V.D.P., 2000, "MULTIV. Software para Análise Multivariada e Testes de Aleatorização," Departamento de Botânica da Universidade Federal do Rio Grande do Sul, Porto Alegre, Brasil.

7.Rodrigues, M.L.K., 1997, "Diagnóstico da Poluição por Elementos-Traço no Sedimento da Bacia Hidrográfica do Rio Caí, RS," dissertation, Instituto de Biociências da Universidade Federal do Rio Grande do Sul, Porto Alegre, Brasil, 124 p.

Elba C. Teixeira,[1] Maria Lucia K. Rodrigues,[2] Marta F. C. Alves,[1] and Jane R. Barbosa[2]

Study of the Geochemical Distribution of Heavy Metals in Sediments in Areas Impacted by Coal Mining

Reference: Teixeira, E. C., Rodrigues, M. L. K., Alves, M. F. C., and Barbosa, J. R., **"Study of the Geochemical Distribution of Heavy Metals in Sediments in Areas Impacted by Coal Mining,"** *Contaminated Sediments: Characterization, Evaluation, Mitigation/Restoration, and Management Strategy Performance, ASTM STP 1442,* J. Locat, R. Galvez-Cloutier, R. C. Chaney, and K. R. Demars, Eds., ASTM International, West Conshohocken, PA, 2003.

Abstract: This study evaluated the geochemical distribution and potential mobility of heavy metals in sediments impacted by coal extraction in the Candiota Region of Brazil. Sampling was performed in Candiota stream and tributaries, at eleven sites, in February and June 2000. The silt/clay fraction of sediments was analyzed by total and sequential extraction schemes established by the EPA and European Commission, respectively. The results indicated higher mobility for manganese, intermediary for nickel, zinc, copper, and lower for iron, chromium, and aluminum. The mouth of Poacá Stream, most affected by mining activities, presented an increase of iron in the oxidizable fraction, as well as zinc, nickel, and copper, suggesting association with sulfides and presence of pyrite in the sediments. The same behavior was observed in the Candiota Stream, after the entrance of the Poacá. Due to a lower pH (4.3) caused by mining acid drainage, at the mouth of Poacá Stream, manganese content decreased in sediments and increased ten times in the water column.

Keywords: sequential extraction, geochemical distribution, sediments, heavy metals, coal

---

[1] Research Scientist and Chemist, respectively, Programa de Pesquisas, FEPAM, Rua Carlos Chagas, 55, 90030-020 Porto Alegre, RS, Brazil.

[2] Research Scientist and Chemist, respectively, Divisão de Química, FEPAM, Rua Aurélio Porto 45, 90620-010 Porto Alegre, RS, Brazil.

Introduction

The load of heavy metals discharged into aquatic systems is probably reflected by their accumulation in the sediments. These pollutants are preferentially adsorbed on the finest particles and in different phases of the sediments, becoming available to the biota through physicochemical changes of the system. Therefore, it is important to estimate which fraction of the metallic elements could be potentially released into the water column or directly transferred to the biota, leading to the knowledge of the different types and degrees of pollution in the sediments.

Among the techniques used to identify anthropogenic contributions, several authors have mentioned the sequential extraction as an appropriate method to determine the chemical distribution of heavy metals in contaminated sediments (Kersten and Forstner 1995). Many of the proposed sequential schemes were derived from the work of Tessier et al. (1979). However, the majority of the employed techniques presented significant differences, impairing the comparison of the results and the evaluation of heavy metals mobility. Although the recommended extractants were selective, few of them were specific enough to isolate well defined fractions. Aiming at the standardisation of procedures, the European Community (Ure et al. 1993, Fiedler et al. 1994, Quevauviller et al. 1994) proposed a Certified Reference Material (CRM) - BCR 601 for sequential schemes, involving a three-step extraction (Lopez-Sanchez et al. 1998).

Concerning the geochemical distribution of heavy metals in aquatic sediments, in Rio Grande Sul, Brazil, some studies are available, which applied sequential extraction procedures in regions contaminated by coal mining (Teixeira et al. 1997, Teixeira et al. 1994). In the southwest of the State, in the Candiota Region, is located the biggest Brazilian coal reserve (Great Candiota Deposit), estimated 12 billion tons and accounting for 38% of the coal reserves of Brazil (Neves and Chaves 2000). The total production of coal in Rio Grande do Sul State is approximately 3 000 000 t/year, representing about 60% of the nation's overall production, which is mainly used to generate electrical power. The main economic activities in this region are: coal and limestone mining, coal power plant, cement industries, agriculture and cattle-raising. Such activities are favored by the easy access to the site, the topography, geology and availability of water resources. All these activities are located inside the limits of the Candiota Stream Basin, approximately 1430 km^2. Regarding the anthropogenic input, the most affected tributaries of Candiota Stream are the small-sized watercourses Poacá and Candiotinha.

The purpose of this work was to study the geochemical distribution of the metallic elements copper (Cu), nickel (Ni), zinc (Zn), chromium (Cr), aluminum (Al), iron (Fe), and manganese (Mn) in the stream sediments impacted by coal mining along the Candiota Stream Basin, Rio Grande do Sul State, Brazil, in order to assess their potential mobility and bioavailability in the aquatic environment.

Study Area

The Candiota Stream Basin (Figure 1) is included in the basin of the upper course of Jaguarão River, the main tributary of the Mirim Lagoon. This river delimits the border between Brazil and Uruguay in the Southeast of Rio Grande do Sul State.

The climate of this region is classified as Cfa (subtropical climate, according to Von Koepen classification system), with well-distributed precipitation during all the year. The minimum temperatures occur in winter (June and July) and the maximum ones in summer (January and February), and the annual average temperature is approximately 18°C (DNM 1992).

The geological structure of the Candiota Region is formed mainly by the rocks of the Paraná Basin, which are characterized regionally as an extensive deposition depression located in the Center-East part of the South American Continent (Schneider et al. 1974). The Pre-Cambrian basement of Candiota Region is represented, in the Northeast part of the area, by metamorphic rocks of the Porongos Group and early Palaeozoic sedimentary units of the Bom Jardim Group (Arroio dos Nobres Formation) and Camaquã (Guaritas Formation). The crystalline basement occurs in the far Northwest and Southeast parts of the region and is represented, respectively, by gneiss of the Cambaí Complex and granite rocks of the associations CGgPM (Pinheiro Machado Granite-Gnaiss Complex) and CGDF (Dom Feliciano Granite Complex). The other litho-stratigraphic units observed at Candiota Region belong to the Permian age sedimentary packages of the Paraná Basin.

The lithology of the region is constituted by fine whitish-gray sandstone, locally coarse, intercalated with dark-gray silt, carbon silt and coal layers.

Experimental Method

Sediments samples were collected at eleven sites along the Candiota Stream Basin, in February and June 2000, taking into consideration the proximity of potential pollutant sources and the access to sampling spots (Figure 2). Three sites were considered as backgrounds, due to the absence of any human activity. According to their geological diversity they were classified as follows: CA01 - background site of Candiota Stream, with soils formed over the arenite rocks of the top of Rio Bonito Formation; PO01 - site located over sedimentary rocks of Rio Bonito Formation, which is under the natural influence of the coal layers that emerge along the river bed in the headwaters of Poacá Stream; and CC01 - site situated over schists intercalated with marbles of Porongos Group.

Corers were used in the sample collection, avoiding disturbance of fine sediments. In order to obtain representative samples and enough material for analysis, at each sampling station, at least four plastic pipes were employed. In this study, only the first 5-cm layer was taken for the sample composition, which corresponded to a recent deposition. The samples were transported to the laboratory, under refrigeration at 4°C, and wet-screened through a 63 μm nylon mesh, to obtain the silt/clay fraction (Salomons and Förstner 1980). The fraction < 63 μm was oven dried at a temperature < 40°C and disaggregated in an agate mortar for chemical analyses.

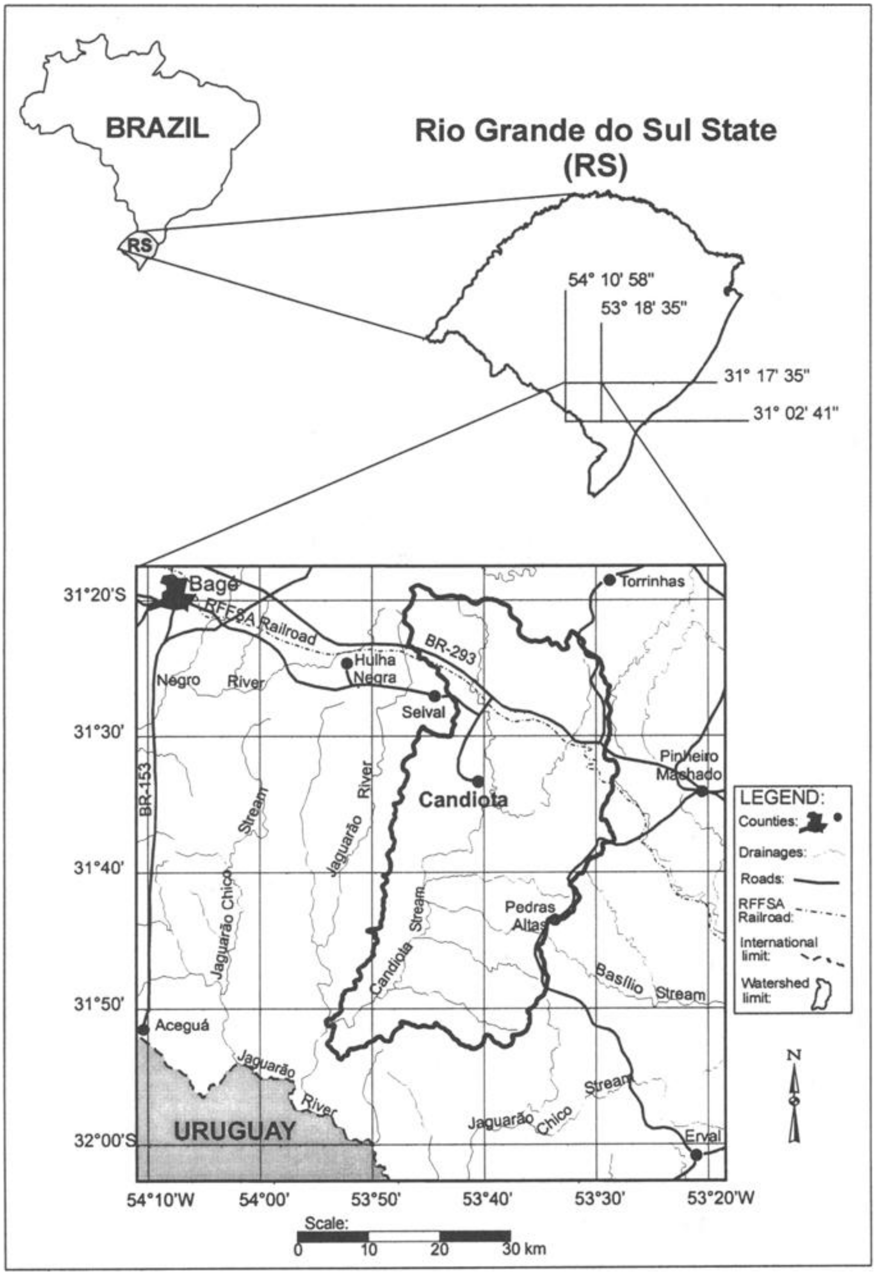

Figure 1 – *Location Map of Candiota Region*

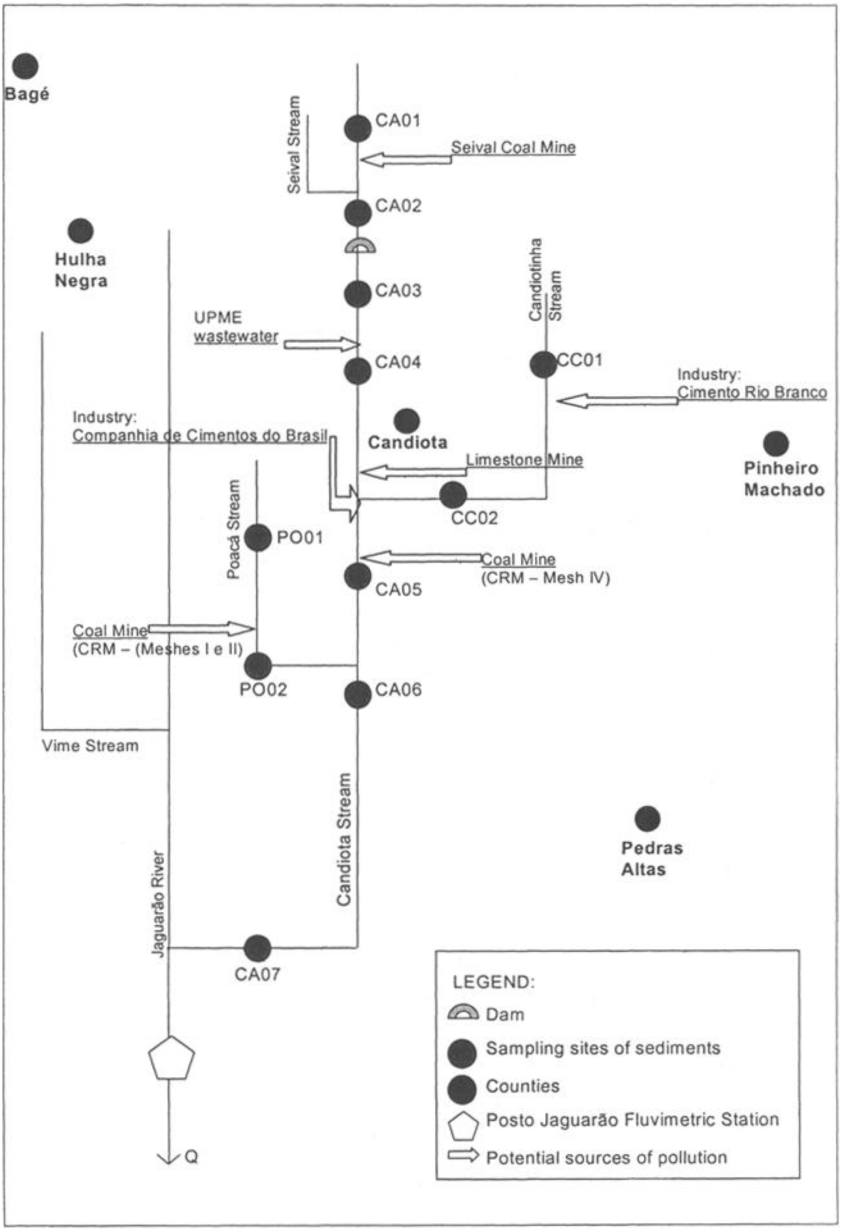

Figure 2 - *Schematic Drawing of Candiota Stream Basin, RS*

The sequential extraction scheme, applied to the samples and simultaneously to the CRM BCR-601 comprised three phases: carbonatic (first step), reducible (second step) and oxidizable (third step) (Lopez-Sanchez et al. 1998). In the present study, a fourth step was added – residual fraction, to obtain a mass balance for each studied element. Since the BCR-601 certification was given only for certain metals (Ni and Cd for the three phases, Cr for the first phase, and Zn for the first two phases), it was necessary to determine the analytical accuracy for the other investigated elements (Mn, Cu, Fe, Cr, and Al) by comparing the sum of concentrations obtained in the four steps of the sequential extraction to the total metallic content.

The total metals and the fourth phase extractions were conducted in accordance with USEPA analytical method for Microwave Assisted Acid Digestion of Siliceous and Organically Based Matrices (EPA 3052), with addition of fluoric, nitric and hydrochloric acids. Boric acid was employed to eliminate fluoric acid residues. The metal determinations in all the extracts was accomplished by inductively coupled plasma optical emission spectrometry (ICP/OES). In the quality control of total content determinations, the CRM CANMET STSD-3 was also analyzed. Total sulfur (St) determination followed the procedures of Test Method for Sulfur in the Analysis Sample of Coal and Coke Using High Temperature Tube Furnace Combustion Methods (D-4239), and the analysis of organic carbon (OC) content was performed through the method proposed by Walkley-Black (1965).

Grade p.a. reagents that had previously been tested with respect to metal content and ultra-purified water were used to process the sample duplicates and CRM triplicates.

Statistical Analysis of the Data Base

Initially, for each metallic element, linear regression and Student's *t* test were applied to verify the existence of significant differences between the sampling dates. In the latter test, the concentration differences between dates were previously checked as to normal distribution. Considering a 5% confidence level, the results showed similar contents for the investigated elements in the two sampling dates, except for Mn, that did not show a recognizable pattern of variability. Meanwhile, concerning the whole data set, the dates did not differ significantly, allowing the presentation of the average values calculated for February and June 2000.

In an attempt to synthesize all the information obtained in the sequential extraction scheme and to recognize patterns of distribution for the metallic elements in the different phases, a metric ordination of the sampling units (spatial and temporal measures resulting from data collection), by principal components analysis, was additionally performed. This multivariate statistical procedure was carried out with the software *Statistica for Windows 4.3TM*, and also included the variables St and OC.

Results and Discussion

Certified Reference Materials

Table 1 displays the results obtained for the sequential extraction scheme and for the total extraction applied to the CRM BCR-601, as well as the relative recovery between the two procedures.

For the elements that presented certification, the accuracy of the sequential extraction scheme was satisfactory, except for the element Ni in the reducible fraction, where an overestimation (approx. 80%) has been verified. This fact is probably explained by a partial attack of oxidizable and/or residual phases. Further significant differences were observed in the second phase especially for Cu and Cr concentrations (Table 1), when compared with corresponding indicative values mentioned by Rauret et al. (1999) for the BCR-601. A considerable error for Ni in the reducible fraction was also reported by the European Commission (Ure et al. 1999). In order to reduce uncertainties, Lopez-Sanchez et al. (1998) recommended modifications of the BCR sequential extraction scheme, among them the increase in the extractant concentration and a better control of the final pH in the second phase.

Table 1 - *Sequential Extraction Applied to the Certified Reference Material (CRM) - BCR 601*

	Ni µg/g	Ni µg/g	Zn µg/g	Zn µg/g	Cr µg/g	Cr µg/g	Cu µg/g	Mn mg/g	Fe mg/g	Al mg/g
First step	7.44	8.01[1]	215	264[1]	0.3	0.36[1]	11.4	0.255	0.041	0.093
Second step	10.9	6.05[1]	202	182[1]	7.5	1.43[2]	47.2	0.161	3.05	2.95
Third step	6.96	8.55[1]	120	137[2]	24.2	18.3[2]	99.6	0.064	2.92	1.58
Four step	57.8	---	195	---	102	---	56.1	0.644	41.6	59.7
Σ	83.1	---	733	---	134	---	215	1.12	47.6	64.3
Total extraction	71.1	---	785	---	139	---	210	1.13	49.9	66.4
Recovery, %	116	---	93.3	---	96.4	---	101	99.8	95.3	96.8

[1] BCR–601 certified concentration

[2] BCR–601 indicative value

Concerning the accuracy of total metals determination, evaluated in this work by the analysis of the CRM CANMET STSD-3, the mean recovery for the studied elements was between 95 and 100%, except for Cr (78%).

The reproducibility of the analyses was largely satisfactory, with a coefficient of variation lower than 2% for all the determinations, including samples.

Total and Sequential Extraction of the Samples

As mentioned before, with the application of linear regression and Student's *t* test, no significant difference was observed, at a 5% confidence level, between the data sets obtained for February and June 2000. Among the metallic elements, Mn was an exception, but no distribution pattern was identified. Therefore, in an attempt to facilitate the data interpretation and the disclosure of results, the average geochemical distribution of the studied elements was determined. The same procedure was adopted for total contents of metals, sulfur and organic carbon. The mean values are presented in Table 2, including a mass balance for each studied element, which evaluated the efficiency of the extractions by comparing the sum of the four phases and the concentration obtained in the total extraction.

Although total extraction enables the quantification of metallic elements in sediments, it didn't allow a quantitative assessment of the anthropogenic contribution and the potential risk of an element release. Generally, the results of total metal contents in the sediments of Candiota, Candiotinha and Poacá streams, when compared to the corresponding background sites, did not show a recognisable trend. On the other hand, the sequential extraction scheme results pointed out the phases in which the elements occurred in the sediments, thus allowing the evaluation of their mobility and availability to the aquatic environment.

The results of geochemical distribution obtained with the sequential extraction scheme are illustrated in Figures 3 to 5. The potential mobility of the metallic elements in the Candiota region, indicated by the sum of the first three extraction phases, was higher for Mn. For Fe, Cr and Al, between 70 and 90% of the total concentration was found in the residual fraction, indicating a lower mobility for these elements.

Cu presented a higher percentage of extraction in the oxidizable fraction of Candiota stream (CA03 and CA06) and Poacá Stream (PO02), in relation to the points considered as backgrounds (CA01 and PO01, respectively). These results, especially for PO02, can be related to the contents of St and OC (Table 2), indicating some contamination of sediments by coal. The preferential association of Cu with the oxidizable fraction has been verified in some works, that pointed out this metal correlation to organic matter (Salomons, 1995) and to sulfides in sediments (Teixeira et al. 2001, Teixeira et al. 1997).

Although more than 70% of Fe concentration was found in the residual fraction, this element also appeared associated to the oxidizable fraction in sites CA06 and PO02. The presence of Fe in the oxidizable fraction (PO02), associated with the higher S content in the sediment, also indicates the presence of sulfide in the sediments.

Zn showed association with the carbonatic fraction for site CA04 (30%), in response to the sediments contamination by waste coal combustion (Figure 2). This association could be attributed to the substitution of calcium (Ca) by Zn in calcite (Davidson and Clarke 1996). Otherwise, in sites CA06 and PO02, Zn presented preferential association to the oxidizable fraction, with percentage contents varying between 25 and 31%, what could be attributed to an association with sulfides, probably spharelite (Finkelman 1995, Davidson and Clarke 1996). Accordingly, in this study, the highest concentration of St was found at the sampling station PO02. The presence of Zn in the sediments was more evident at sites contaminated by coal (Figure 3). The contribution of Zn to CA06 sampling point showed influence of coal mining drainage from Seival Mine, CRM-Mesh IV, and inputs from the basin of the Poacá Stream.

As to the Ni results, a high percentage in the oxidizable fraction was found at the sites CA04, CA06 and PO02 (between 37 and 49%), in response to local anthropogenic sources (coal mining and ashes). The association of this metal to sulfides in sediments and coal has been reported in several works (Teixeira et al.1994, Pires et al. 1997, Finkelman 1995).

Table 2 - *Sequential and Total Extraction Applied to Sediment Samples from the Candiota Region, RS, Brazil*

		CA01	CA02	CA03	CA04	CA05	CA06	CA07	CC01	CC02	PO01	PO02
	First step	0.25	0.60	0.85	0.20	0.45	0.30	0.29	0.50	0.25	0.45	0.08
	Second step	2.15	2.25	2.83	2.10	2.35	0.173	1.55	2.38	2.10	2.05	1.45
Cu	Third step	1.95	1.80	4.05	3.05	1.55	3.20	0.81	2.15	1.53	2.48	3.33
μg/g	Four step	9.50	7.75	14.9	13.8	11.4	13.4	12.3	11.4	7.92	8.75	9.16
	Σ	13.8	12.4	22.6	19.1	15.7	17.0	15.0	16.4	11.8	13.7	14.0
	Total extr.	14.0	11.4	21.2	18.6	13.8	16.0	16.2	17.4	12.6	13.9	14.3
	Recov., %	98.6	109	107	103	114	106	92.6	94.2	93.6	98.6	98.0
	First step	10.8	10.0	19.5	54.8	7.36	11.1	5.70	5.80	2.95	7.33	2.92
	Second step	12.3	10.4	18.5	18.0	9.65	11.5	11.0	9.50	9.20	4.70	1.20
Zn	Third step	8.55	6.8	11.7	13.4	7.85	19.9	3.80	6.50	6.4	5.36	8.56
μg/g	Four step	42.3	31.0	59.6	56.4	45.7	36.5	61.8	47.8	57.9	34.5	16.4
	Σ	73.8	58.1	109	143	70.5	78.9	82.3	69.6	76.4	51.9	29.1
	Total extr.	79.6	56.9	100	163	64.5	75.1	80.8	73.3	72.5	56.4	33.2
	Recov., %	93	102	109	87	109	105	102	95	105	92	88
	First step	2.15	1.93	1.59	3.10	1.65	3.00	1.40	5.05	0.700	1.79	1.39
	Second step	2.35	1.90	1.80	3.45	2.30	2.60	1.95	3.91	1.55	1.40	1.10
Ni	Third step	3.30	3.40	3.02	4.70	4.06	10.1	1.95	6.60	1.94	1.47	2.91
μg/g	Four step	7.67	5.61	11.3	11.8	5.65	6.30	12.3	42.4	9.20	6.70	3.02
	Σ	15.5	12.8	17.7	23.0	13.7	22.0	17.6	58.0	13.4	11.4	8.4
	Total extr.	13.7	15.0	19.4	19.2	15.3	22.5	17.9	52.8	11.8	10.8	7.2
	Recov., %	113	86	91	120	90	98	99	110	113	105	117
	First step	0.049	0.035	0.075	0.106	0.041	0.065	0.055	0.150	0.048	0.070	0.046
	Second step	0.496	0.330	0.836	0.604	0.313	0.098	0.200	0.780	0.413	1.30	1.00
Cr	Third step	4.64	3.24	7.41	5.93	4.59	6.95	2.35	16.5	4.78	4.19	5.56
μg/g	Four step	29.9	30.7	42.5	36.4	38.7	36.5	36.2	76.2	33.8	37.7	32.0
	Σ	35.0	34.3	50.8	43.0	43.6	43.6	38.8	93.5	39.0	43.3	38.6
	Total extr.	38.3	32.1	46.7	42.8	37.3	39.2	38.4	81.2	34.2	35.9	43.4
	Recov., %	91.5	107	109	101	117	111	101	115	114	121	89
	First step	0.761	0.539	0.220	0.375	0.348	0.368	0.362	0.540	0.701	0.031	0.029
	Second step	0.357	0.200	0.102	0.136	0.192	0.097	0.323	0.195	0.372	0.099	0.012
Mn	Third step	0.110	0.035	0.263	0.906	0.40	0.061	0.063	0.040	0.072	0.038	0.013
mg/g	Four step	0.105	0.055	0.118	0.136	0.089	0.054	0.186	0.111	0.162	0.083	0.027
	Σ	1.33	0.828	0.466	0.738	0.668	0.580	0.934	0.884	1.31	0.535	0.082
	Total extr.	1.26	0.750	0.416	0.745	0.655	0.577	0.981	0.930	1.34	0.533	0.093
	Recov., %	106	110	112	99	102	101	95	95	98	100	88
	First step	0.077	0.188	0.321	0.070	0.159	0.122	0.039	0.149	0.736	0.122	0.040
	Second step	6.32	4.90	5.26	2.62	2..99	2.47	2.08	4.43	6.16	6.20	1.41
Fe	Third step	2.52	1.44	2.67	1.36	1.34	5.08	1.08	2.07	1.70	1.71	5.37
mg/g	Four step	24.9	22.2	23.7	30.0	21.1	19.7	29.9	18.2	33.6	33.0	17.0
	Σ	33.8	28.7	31.9	34.0	25.6	27.3	33.1	24.8	41.6	41.0	23.8
	Total extr.	31.5	28.5	36.6	35.5	27.1	28.7	32.9	26.5	38.7	31.7	28.2
	Recov., %	107	100	87	96	94	95	100	94	107	129	84
	First step	0.062	0.062	0.048	0.186	0.035	0.194	0.044	0.038	0.038	0.052	0.091
	Second step	0.888	0.805	1.01	1.23	0.577	0.758	0.875	0.552	1.22	0.644	0.671
Al	Third step	2.01	1.69	2.00	1.91	1.98	1.39	2.62	2.13	2.08	1.34	0.151
mg/g	Four step	76.5	76.0	73.9	6.82	80.2	75.7	67.0	55.9	78.6	78.3	69.6
	Σ	79.5	78.6	76.9	71.6	82.8	78.0	70.6	58.7	81.9	80.3	71.8
	Total extr.	88.1	81.9	81.9	84.8	79.2	83.7	71.8	59.3	67.6	57.3	82.2
	Recov., %	90	96	94	84	105	93	98	99	121	140	87
St %		0.08	0.06	0.11	0.22	0.08	0.15	0.07	0.06	0.05	0.10	0.37
OC %		3.39	3.06	3.7	3.04	3.71	2.76	1.79	3.34	2.00	2.44	7.02

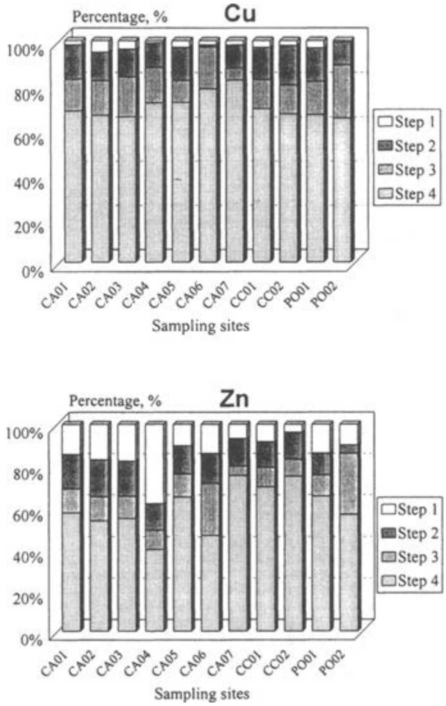

Figure 3 – *Geochemical Distribution of Copper and Zinc in Sediments from Candiota Region, RS, Brazil*

High percentages of Al and Cr were found in the residual fraction of the sediment samples (Figures 4 and 5). In other sequential extraction studies, the labile Cr has been shown to be associated to clay minerals (Teixeira et al 2001, Teixeira *et al* 1997).

The increased content of Mn in the available fractions and specially in the carbonatic phase (Figure 4), confirmed its high potential mobility, as mentioned above. The geochemical distribution of this element, concentrated on the carbonatic phase, followed by the reducible one, has been verified in other studies where the sequential extractions in sediments was applied (Teixeira et al. 1997, Kersten and Förstner 1995).

However in the Poacá Stream, in comparison to the site PO01, the sampling station PO02 showed a decrease in Mn mobility and, consequently, an increase in the residual fraction. This fact was due to a lower pH (4.3) caused by mining acid drainage that brought about an increase of the metal availability (Streck 2001) and a reduction in its mobile fraction in sediments.

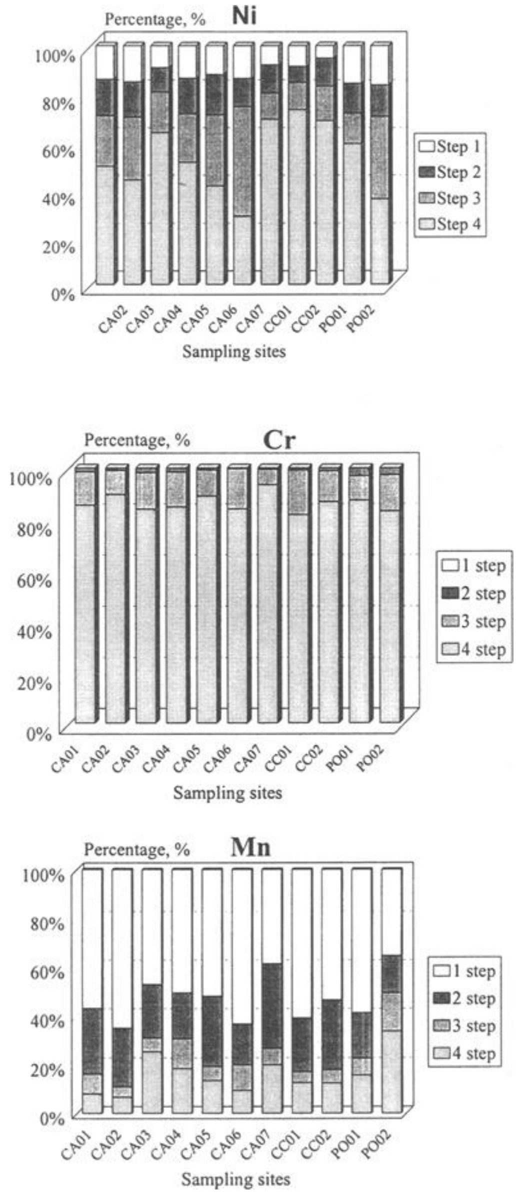

Figure 4 - *Geochemical Distribution of Nickel, Chromium and Manganese in Sediments from Candiota Region, RS, Brazil*

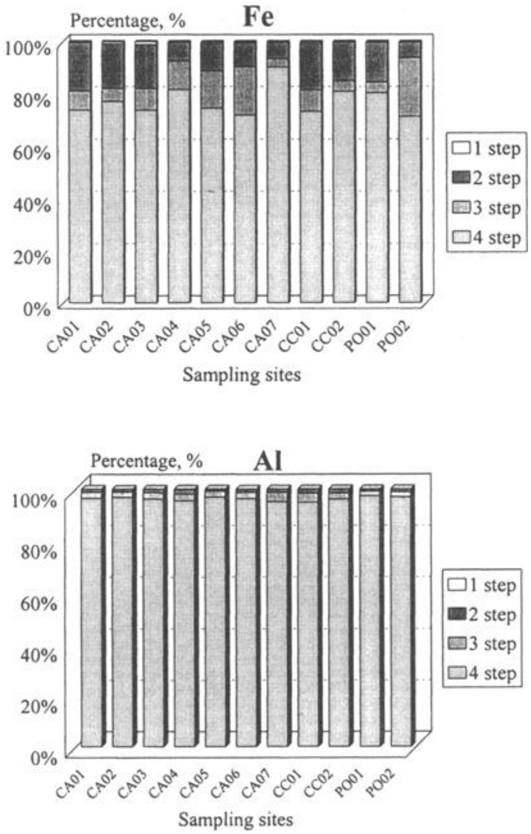

Figure 5 - *Geochemical Distribution of Iron and Aluminum in Sediments from Candiota Region, RS, Brazil*

Principal Components Analysis

Following this method, the data base was synthesized by a set of orthogonal axes. The first, considered the best summary of the relationship exhibited by the data, and accounting for 21.9% of the variance, was retained for interpretation. Attempting to a better visualization of tendencies, the second axis (18.9% of the data variability) was also used to prepare a diagram (Figure 6), representing the dispersion of sampling units.

In the first component, the most relevant variables, with positive correlations were: Fe (0.73), Cu (0.67), Ni (0.57) and Zn (0.57), all in the oxidizable phase; St (0.68); and OC (0.67). The good correlation between these parameters in the oxidizable fraction suggested the presence of pyrite in the sediments collected in sites CA06 and, mainly, PO02. The results were in agreement with those presented above about the geochemical distribution, that indicated contamination in these sediments by coal and ashes, originating from coal mining.

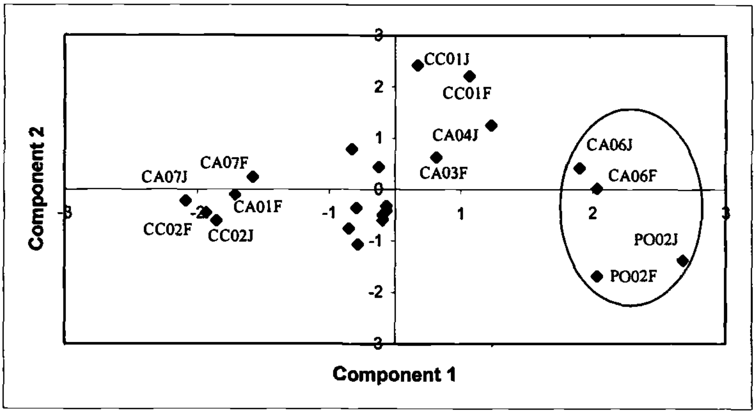

Figure 6 - *Dispersion of the Sampling Units, According to Ordination Scores in Principal Components 1 and 2 (F=February, J=June)*

Conclusions

The results obtained with total metal extractions in sediment samples from the Candiota Region didn't allow a quantitative assessment of the anthropogenic contribution. On the other hand, the application of sequential extraction displayed the phases in which the elements occurred, allowing the prediction of their potential mobility.

The results indicated higher potential of release from sediments for manganese, intermediary for nickel, zinc, copper, and lower for iron, chromium, and aluminum.

Metal geochemical distributions showed that sediment contamination occurred particularly in sites CA06 and PO02, which represented the area strongly affected by coal mining activities. This contamination was demonstrated by the higher percentages of Fe, Cu, Zn, and Ni in the oxidizable phase, and by the significant sulfur content in sediments, notably in PO02. These results revealed the sulfide contamination of sediments produced by coal mining.

In the Poacá Stream sediments, due to a lower water pH (4.3) caused by mining acid drainage, the site PO02 presented a decrease in Mn concentration in the three mobile phases and an increase in the residual fraction content, in comparison to the control station PO01. At the same time, an increase of the Mn availability was observed in the water column, where the concentration was ten times higher in comparison with the control site. Eventhough, the Mn potential mobility at the site PO02, represented by the sum of the three mobile phases, was still superior to the other metals.

Applying the metric ordination by principal components analysis, it was possible to identify associations between variables in the different phases of the sequential extraction scheme. Additionally, it allowed evaluation of the degree of relevance of each variable in the diagnosis of the area, and detection of trends over space or time. The first component summarized the most relevant information, showing the good correlation between St, OC and the metals Fe, Cu, Ni, and Zn present in the third phase. The association between these variables in the oxidizable fraction confirmed the presence of pyrite in the sediments at site CA06 and especially PO02. The results were in agreement with those presented above about the geochemical distribution that indicated contamination in these sediments by coal and ashes originating from coal processing activities. As concluded by linear regression and Student's *t* test application, no relevant temporal trend was detected for the whole data set with this statistical tool.

Aknowledgements

Acknowledgements to PADCT/CIAMB, FAPERGS, and CNPq for the financial support; and to Cledion Peixoto - technician of FEPAM, for the accomplishment of the sampling.

References

ASTM, 1995, "Standard Test Methods for Sulfur in the Analysis Sample of Coal and Coke Using High Temperature Tube Furnace Combustion Methods," ASTM-D 4239-94. 5 (5): 363-375.

Davidson, R.M., Clarke, L.B., 1996, "Trace Elements in Coal," United Kingdom, IEA Coal Research, London, IEAPER/21.

DNM, Departamento Nacional de Meteorologia (Brasil), 1992, "Normas Climatológicas (1961-1990)," Brasília.

EPA,1996, "Microwave Assisted Acid Digestion of Siliceous and Organically Based Matrices," Method 3052, pp 1-20.

Fiedler, H.D., López-Sânchez, J.F., Rubio, R., Rauret, G., Quevauviller, Ph.,Ure, A.M. and Muntau, H., 1994, "Study of the Stability of Extractable Trace Metal Contents in a River Sediment Using Sequential Extraction,"*Analyst*, Vol. 119, pp. 1109-1114.

Finkelman, R.B., 1995, "Modes of Occurrence of Environmentally-Sensitive Trace Elements in Coal." *In*: Swaine, D.J. and Goodarzi, F., *Environmental Aspects of Trace Elements in Coal,* Kluwer Academic Publishers, Netherlands, pp. 24-50.

Kersten, M., Förstner, U., 1995, "Speciation of Trace Metals in Sediments and Combustion Waste," *In*: A.M. Ure and C.M. Davidson, *Chemical Speciation in the Environment*, pp. 234-275.

Lopez-Sanchez, J. F., Sahuquillo, A., Fiedler, H.D., Rubio, R., Rauret, G., Munteau, H. and Quevauviller, P., 1998, "CRM 601, a Stable Material for its Extractable Content of Heavy Metals," *Analyst*, Vol.123, pp. 1675-1677.

Neves, G. R., Chaves, S. H. A., 2000, "A Região Carbonífera "Tradicional" do Rio Grande do Sul," *Carvão e Meio Ambiente*, Centro de Ecologia /UFRGS, Porto Alegre, RS, pp. 108-129.

Pires, M., Fiedler, H., Teixeira, E.C., 1997, "Geochemical Distribution of Trace Elements in Coal: Modelling and Environmental Aspects," *Fuel*, Vol. 76, No. 14/15, pp. 1425-1437.

Quevauviller, Ph., Rauret, G., Muntau, H., Ure, A. M., Rubio, R., Lopez-Sanchez, J.F., Fiedler, H.D., Griepink , B., 1994, "Evaluation of a Sequential Extraction Procedure for the Determination of Extractable Trace Metal Contents in Sediments," *Fresenius Journal of Analytical Chemistry*, Vol. 349, pp. 808-814.

Salomons, W., 1995, "Environmental Impact of Metals Derived from Mining Activities: Processes, Predictions, Prevention," *Journal of Geochemical Exploration*, Vol. 52, pp. 5-23.

Salomons, W., Förstner, U., 1980, "Trace Metal Analysis on Polluted Sediments, Part I: Assessment of Sources and Intensities," *Environmental Technology Letters*, Vol. 1, pp. 494-505.

Schneider, R. L., Mühlmann, H., Tommasi, E., Medeiros, R. A., Daemon, R. F. and Nogueira, A. A., 1974. *Proceeding* ... XXVIII Congresso Brasileiro de Geologia, 1974, Porto Alegre, pp. 41-67.

Streck, C., 2001, "Estudo da Qualidade das Águas Superficiais e Estimativa dos Fluxos de Elementos-Traço na Região de Candiota-RS," M.Sc. Dissertation, PPGEE/PUCRS, 159 p.

Teixeira, E.C., Ortiz, L.S., Sanchez, J.C.D., Alves, M.F.C.C., 2001, "Distribution of Selected Heavy Metals in Fluvial Sediments of the Coal Mining Region of Baixo Jacui, RS, Brasil," *Environmental Geology*, Vol. 41, pp. 128-144.

Teixeira, E.C., Sanchez, J.D., Fernandes, I., Formoso, M.L., Pegorini, J., Pestana, M.H.D., 1997, "A Preliminary Study of Metals in Sediments from Areas Influenced by Coal Processing and Steel Industry Activities in Baixo Jacuí Region, RS-Brazil," *Environmental Technology*, Vol. 18, pp. 581-592.

Teixeira, E.C., Pestana, M.H.D., Sanchez, J.D., Fernandes, I., 1994, "Geochemical Distribution of Metallic Elements in the Mineral Matter of Brazilian Coals," *Environmental Technology*, No. 15, pp. 989-996.

Tessier, A., Campbell, P.G.C., Bisson, M., 1979, "Sequential Extraction Procedure for the Speciation of Particulate Trace Metals," *Analytical Chemistry*, Vol. 51, No. 7, pp. 844-851.

Ure, A., Quevauviller, Ph., Muntau, H., Griepink, B., 1993, "Improvements in the Determination of Extractable Contents of Trace Metals in Soil and Sediment Prior to Certification, BCR Information-Chemical Analysis," Brussels-Luxembourg: ECSC-EEC-EAEC, 85 p.

Walkley-Black, C.A, 1965, "Chemical and Microbiological Properties," *Methods of Soil Analysis*, Madison, Wisc : Soil Science Society of America, Vol. 2, pp. 1372-1378 (Agronomy, n.9).

Hélène Tremblay,[1] Gaston Desrosiers,[2] Jacques Locat,[3] Alfonso Mucci,[4] and Émilien Pelletier[2]

Characterization of a Catastrophic Flood Sediment Layer: Geological, Geotechnical, Biological, and Geochemical Signatures

Reference: Tremblay, H., Desrosiers, G., Locat, J., Mucci, A., and Pelletier, É. **"Characterization of a Catastrophic Flood Sediment Layer: Geological, Geotechnical, Biological, and Geochemical Signatures,"** *Contaminated Sediments: Characterization, Evaluation, Mitigation/Restoration, and Management Strategy Performance, ASTM STP 1442*, J. Locat, R. Galvez-Cloutier, R. C. Chaney, and K. R. Demars, Eds., ASTM International, West Conshohocken, PA, 2003.

Abstract: In 1996, an important rainstorm took place in the Saguenay region, Canada, that caused severe flooding and erosion of a large amount of post-glacial sedimentary material. Consequently, about 20 million tons of sediment were deposited in the upstream part of the Saguenay Fjord, covering the recent, contaminated sediments with a 10 to 60 cm thick layer of relatively clean material. This flood layer was distinguished from the pre-flood sediments by various properties: low consistency and low resistance, high water content, the absence of benthic organisms, or the presence of inherited geochemical components. In this study, we evaluated the criteria used by the various investigators to identify the 1996 flood deposit, then finally compared its signature. Subsequently, we assessed the spatial variability of the deposit and its effect on the interpretation of temporal studies.

Keywords: sediments, flood layer, geological signature, geotechnical signature, biological signature, geochemical signature, spatial variability

---

[1] Postdoctorate Fellow, Dept. of Geology and Engineering Geology, Laval University, Quebec, Quebec, Canada, G1K 7P4.

[2] Professor, Institut des Sciences de la Mer de Rimouski (ISMER), 310 allée des Ursulines, Rimouski, Quebec, Canada, G5L 3A1.

[3] Professor, Department of Geology and Engineering Geology, Laval University, Quebec, Quebec, Canada G1K 7P4.

[4] Professor, Department of Earth and Planetary Sciences, McGill University, 3450 University St., Montreal, Quebec, Canada, H3A 2A7.

Introduction

Background on Signature of Catastrophic Sediment Layer

Sediments can record different events through time, such as earthquakes, tsunamis, floods, forest fires, and sea-level fluctuations. These events are often used as absolute markers when the event date is known. The signature of these events is also used to determine the extent of the affected area. The main problem is to be able to identify and recognize the layer corresponding to one particular event.

Studies on sediments from a recent flood event (in 1995) have been conducted on the Northern California shelf, U.S. (Drake 1999, Leithold and Hope 1999). The authors indicate that the flood layer is easily recognized by its lighter color, higher water content, the high content of fine particles, a sharp basal contact and common occurrences of "fresh" terrigenous plant material.

In the Saguenay Fjord, Canada, many large slides have occurred on land and under water. These disasters were identified in cores and distinguished from the "normal" sediments by a lighter color, the absence of bioturbation, a higher water content, a coarsening with depth within the layer, and a higher inorganic carbon content (Perret et al. 1995, St-Onge et al. 1999, St-Onge and Hillaire-Marcel 2000). In their study, Schafer et al. (1983) identified different events in the sedimentary history of the Saguenay Fjord such as floods and landslides. The landslides, especially the 1971 St-Jean-Vianney landslide, which occurred in the marine clay from the Laflamme post-glacial sea, are distinguished from recent sediments by the presence of marine clay pellets. St-Onge and Hillaire-Marcel (2000) identified up to 10 accidental sediment layers in a 37.6 m long piston core taken in 1999 in the inner basin, including a 15m thick deposit triggered by an estimated magnitude 7 earthquake in 1663. The other nine are older than the 1663 event.

Saguenay Fjord Context

Saguenay Fjord characteristics – The Saguenay Fjord is located in the Province of Quebec, Canada, about 200 km northeast from Quebec City. It is a long (93 km) and narrow (1 to 6 km) glacial valley that joins the St. Lawrence estuary (Fig. 1). It is composed of 3 main basins from west to east, 275, 180 and 250 m deep, respectively that are separated by shallow sills 130, 65 and 20 m deep, in the same order (Schafer et al. 1990). The geological, geotechnical, hydrographic and biological characteristics of the fjord are described by Schafer et al. (1990), Perret et al. (1995), and Bossé et al. (1996). Recent sediment accumulation rates vary from 7 cm/yr. at the head of the fjord (in the Bras Nord) to less than 0.1 cm/yr in the deepest basin (Smith and Walton 1980).

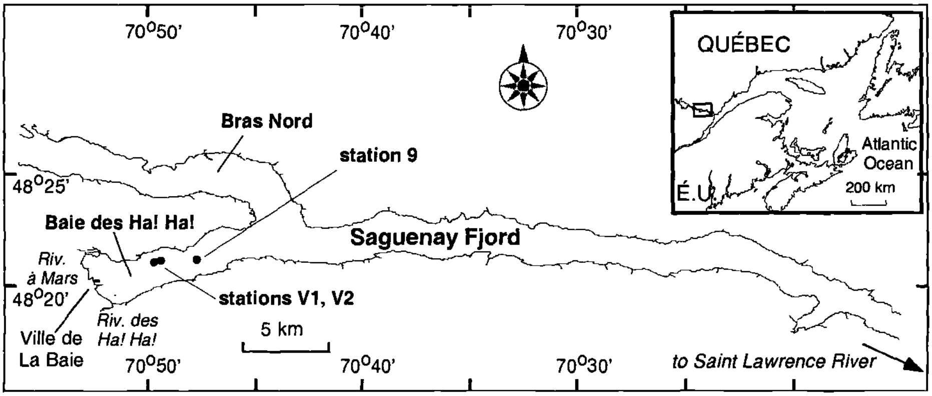

Figure 1 - *Location map.*

The 1996 flood layer – The most recent catastrophic input of sediment in the Saguenay Fjord resulted from the 1996 flood. From July 18th to 20th, 1996, exceptional rainfalls occurred in the upper part of the fjord, mainly in the Bras Nord and the Baie des Ha! Ha! (Fig. 1) (Yu et al. 1997). This extreme precipitation event caused flooding of the main tributary rivers, where about 15 to 20 million tons of post-glacial sediments were eroded and transported down to the fjord. The sediments were deposited as deltaic deposits close to river mouths, and, in much of the covered area, as turbidites, i.e with a sharp basal contact and normally graded beds. This catastrophic sediment deposit covered the pre-existing contaminated sediments in this part of the fjord, with a clean layer of sediment of about 10 to 60 cm thick in most of the covered area. The newly deposited sediments act as a natural capping layer.

The 1996 event has created a major perturbation on the seafloor of the fjord. During the first investigation, barely 3 weeks after the flood, the benthic community had almost been eliminated. The biodiversity decreased from 40 to 4 species and the density of the most abundant species, nematodes, was reduced by ten-fold (Pelletier et al. 1999). The new deposit has also modified the geochemical steady state at the sediment-water interface, causing the upward migration of the redox limit and the remobilization of some metals such as iron and manganese (Mucci et al. 2000a).

This catastrophic flood event has been studied by many researchers who have worked in the Saguenay Fjord environment in the past two decades. Their interests are varied, and combine in one project different disciplines such as, geology, geotechnics, geochemistry, biology and hydraulics. Although they work on different aspects of the project, they have two common needs: the identification of the flood layer and the evaluation of the spatial variability of its thickness for temporal evolution of given parameters. As the investigators used different parameters to evaluate the thickness of the 1996 layer, it is of interest to compare the way each discipline defines the new layer. The next sections will present the different signatures of the flood layer and a study on the variability of its thickness. One station was selected for the comparative study, station 9 in the Baie des Ha! Ha!, where the 1996 layer is easily recognizable (Fig. 1), and stations V1 and V2 for the variability study.

Methodology

To evaluate the extent and thickness of the flood layer as well as the evolution of its properties with time, a large number of cores were taken using a 0.06 m² (22 x 30 cm) Ocean Instruments Mark II box corer to a maximum sub-bottom depth of 60 cm. Up to 4 sub-samples were taken in each box with 10.16 cm diameter PVC tube with a beveled end to facilitate its penetration and a fixed piston at the top to avoid sediment compaction. Samples were extruded, on board whenever possible, or in the laboratory a few days following the end of cruises. A visual description was noted and a variety of properties were measured. The results were compiled as a function of depth and the position of the interface between the pre-flood and the 1996 flood sediments was noted. Positioning of sampling stations was provided by the ship's differential GPS and, in some cases, by a relative positioning system, the Track Point II, that gives the relative position of the sampler with respect to the ship.

The measured physical properties were: water content, grain size distribution, density, magnetic susceptibility, and P-wave velocity. The water content is given as the ratio between the wet and dry weights of sediment samples and the grain size distribution was obtained on bulk sediments using a laser sediment analyzer. The density, magnetic susceptibility, and P-wave velocity were determined using a GEOTEK™ multi-sensor track instrument (MST). A Computerized Axial Tomography Scanner (CAT-scan) was also used to evaluate the density (Holler and Kögler 1990, Boespflug et al. 1995, Crémer et al. 2002).

For the purpose of this study, the following geotechnical properties were measured: intact and remolded undrained shear strength (C_u and C_{ur}) using the Swedish fall cone, and liquidity index as a function of both the water content and the C_{ur}. The liquidity index is a measure of the sediment consistency. Details of the measurement protocols are given by Maurice et al. (2000).

A study of the distribution of the organisms within the flood layer was conducted to characterize its biological signature. As the abundance and diversity of benthic organisms were modified by the flood event, the trace of their activity (i.e. bioturbation) in the surface and sub-surface sediment layer should be visible in the sediment column. De Montety et al. (2000) evaluated the quantity of biogenic structures, *i.e.* burrows and tunnels in sub-surface sediments using CAT-scan images.

The geochemical and isotopic parameters used to identify the catastrophic layer of 1996 were the organic and inorganic carbon content, and the ^{210}Pb and ^{137}Cs activity. The analytical methods to measure the carbon and nitrogen contents are described by St-Onge et al. (1999). Data reported herein are expressed in percent of the total dry weight of sediments. The ^{210}Pb and ^{137}Cs activity measurements are described by Savard (2000).

A major problem occurring in the present study, especially for temporal evolution of certain properties is the variability of the 1996 flood layer thickness. To evaluate it, a spatial variability study was conducted on 29 box cores taken on two square areas of 90 m x 90 m each, which were close to each other. The sites selected for this study are located at station V1 and V2 (Fig. 1). They have been selected because at these locations, the flood layer is easily recognizable by visual observation due to a well-defined sandy layer at its base.

Signature of the 1996 Layer

The mean thickness of the flood layer in the investigated area varies from 10 to 60 cm (Maurice et al. 2000). In the first year following the flood, the 1996 flood layer was easily differentiated from pre-flood deposits by its light color, its low consistency, and the absence of bioturbation.

Physical and Geological Signature

The 1996 flood layer is characterized by a normally graded bed with a sandy layer at its base. The thickness of the sandy layer varies from zero to a few centimeters. In the 1996 sandy layer, 75% of particles are distributed between 36 and 120 µm with a mean size of 58 µm. In the layer deposited by the flood, the mean size of particles is 21 µm and 75% of the particles have a diameter >16 µm indicating a broad spectrum of particles.

Some physical measurements on a core taken in 1997 close to station 9 are presented in Figure 2. The lower contact between the underlying sediments and the 1996 layer is characterized by discontinuities in density, magnetic susceptibility and P-wave velocity. The high values correspond to the sandy layer found at 20 to 27 cm depth.

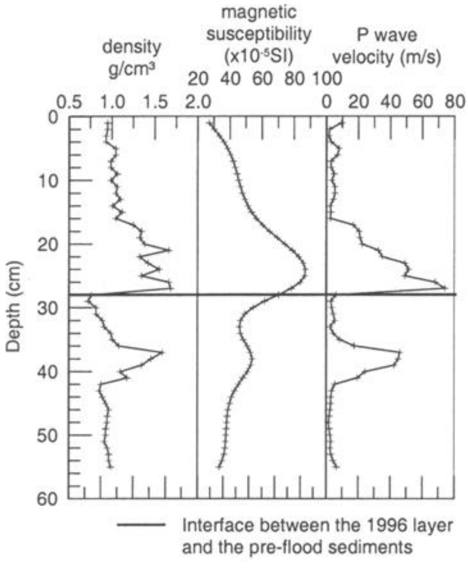

Figure 2 - *Profiles of some physical properties of a sample taken near station 9 in 1997 (from Savard 2000).*

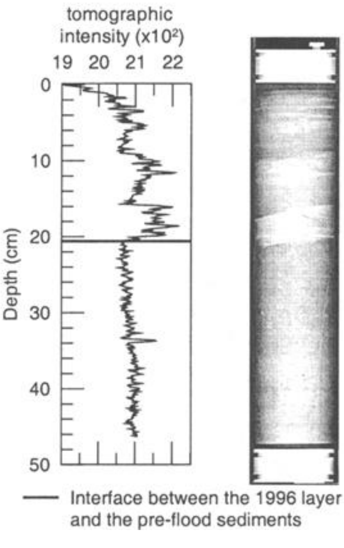

Figure 3 - *Tomographic intensity profile of a core taken near station 9 in 1997 (from Crémer et al. 2002).*

Figure 3 shows a profile of a sample taken near station 9 in 1997 (Crémer et al. 2002). The tomographic intensity (TI) profile (left) reveals a discontinuity of the sedimentation regime marked by a higher TI throughout the flood layer, and a progressive decrease towards the surface. The discontinuity is also visible on the gray scale image (right). On this image, we note that the flood layer was deposited in several episodes marked by a sandy layer at the base that contains laminations typical of a deposition by traction (Crémer et al. 2002) and a sharp basal contact that denote the presence of erosion at the top of pre-flood sediments. Each episode is associated with high TI in the sandy layer, followed by lower TI values. According to Crémer et al. (2002), the high TI values in the sandy layer are related to a high carbonate content. This inorganic carbon originates from the exposed marine clays eroded during the flood. Its concentration in the flood layer is up to 0.6% compared to the underlying sediments where it is about 0.08% (Mucci et al. 2000a, St-Onge et al. 1999). As carbonate is nearly absent in the finer pre-flood sediments, their TI is lower.

Geotechnical Signature

From a geotechnical point of view, the 1996 layer is differentiated by its higher water content, its higher liquidity index that corresponds to a very low consistency, and by its lower undrained shear strength both in intact (C_u) and remolded state (C_{ur}) (Maurice et al. 2000) compared to the underlying pre-flood deposits. In general, as shown on a typical profile of a sample taken at the station 9 (Fig. 4), the water content decreases with depth, as does the liquidity index, and C_u and C_{ur}, all due to self-weight consolidation process. The interface between the flood and the pre-flood sediments is marked by a lower water content at the interface, and/or an important increase of water content just below the interface. The lowest water content values are associated with the sandy layer that contains less water than finer sediments. The interface is also identifiable by an increase of C_u and C_{ur} below the sandy layer. Note that it is impossible to measure this parameter in the sandy layer because the method of measurement, the Swedish fall cone, is adapted for sediment finer than sand. This is why there is no value between 26 and 33 cm in Figure 4. Below the interface, the C_u and C_{ur} increase mainly because of bioturbation. Maurice et al. (2000) noted that bioturbation influenced the consolidation behavior of sediments. In fact, the burrowing organisms drain and mix the sediments contributing to an increase of the shear strength by reducing the water content as well as liquidity index. Then, where burrowing organisms are active, mainly in the first 5 cm (Fig. 5), we might expect an increase of the water content with depth as the organisms activity decreases (not shown). Maurice et al. (2000) also inferred that if the thickness of the layer was greater than the limit depth of activity for the organisms, which is 40 cm for the Saguenay Fjord, a high water content and a weak resistance would persist below this limit.

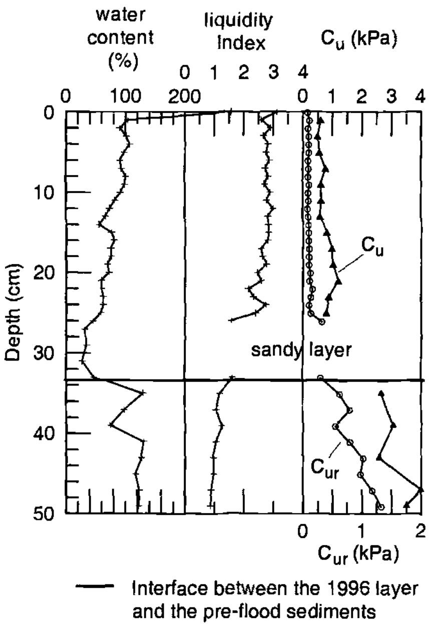

Figure 4 – *Profile of geotechnical properties for station 9 in 1998.*

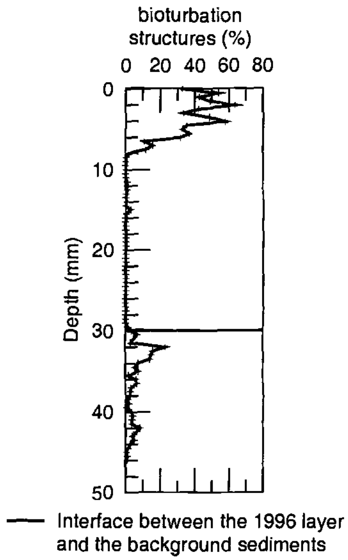

Figure 5 - *Profiles of percentage of bioturbation structures for station 9 taken in 1999 (from de Montety et al. 2000).*

Biological Signature

The large amount of sediment transported and deposited in the upstream portion of the fjord represented a short-term disaster for the benthic communities. In September 1996, two months after the flood, Pelletier et al. (1999) reported that in the Baie des Ha! Ha!, the meiofauna had been reduced in population by more than 97%. One of the dominant pre-flood species (nauplii) was absent in all the stations. Two families of meiofauna (kinorhynches and ostracodes) were found in only one station located downstream of the area of influence. The same authors also registered a dramatic reduction of the macrofauna. In two of the stations monitored two months after the flood and located about 6 km west of station 9, the macrobenthic organisms were totally absent. Even if the populations were abundant in most of the investigated stations, they were less abundant than those reported by Bossé et al. (1996) before the flood.

Figure 5 shows the relation between the percentage of biogenic structures and depth for a core taken in 1999 at station 9. These were determined with a CAT-scan. This tool makes it possible to quantify the occupation rate of organisms through sediment profiles, and then to identify the old sediment surface that is marked with an increase of occupation rate compared to the base of the 1996 sediment layer. The counting of trace fossils of organisms was done on every layer of 1 to 3 cm. As shown in Fig. 5, in the first 5 cm, the biogenic structures comprise a mean of 60%. The majority of benthos found between 0 and 1 mm are nematodes. Polychetes are more abundant in subsurface layers. On this figure, it can also be observed that the biogenic structures rapidly decrease with depth. As a result, between 8 and 30 cm, bioturbation is almost absent, but a peak appears at 30 cm, which peak corresponds to ancient biogenic structures present at the surface of the pre-flood sediments. It can be noted here an evidence of erosion during the flood. In fact, the top of the pre-flood sediments contains a lower level of benthic activities than the top of the flood deposit.

Geochemical and Radioisotopic Signatures

The pre-flood sediments of the Saguenay Fjord generally consist of gray-black anoxic sandy muds with organic carbon concentrations (C_{org}) ranging from 0.5 to 3% (by weight) although more than 5% can be found in the sandy muds of the Bras Nord (Smith and Walton 1980). The sedimentary organic matter is dominantly of terrestrial origin and much of the recent accumulations are from upstream pulp-and-paper and sawmill outfalls (Pocklington and Leonard 1979, Louchouarn et al. 1997).

Dissolved oxygen is depleted within the first five millimeters below the sediment-water interface (Mucci and Edenborn 1992, Deflandre et al. 2002). Sulfate reducing conditions are encountered within the first two centimeters, as evidenced by porewater sulfate depletion and/or the appearance of acid volatile sulfides (AVS) in the solid sediments (Mucci et al. 2000b). The shallow oxygen penetration depths and the rapid onset of sulfate reduction reflect the high oxidant demand of these sediments or, in other words, the amount and accumulation rates of degradable organic matter. Under steady-state conditions, reactive (i.e., extractable in 1N HCl) Fe and Mn accumulate in the thin layer of oxic sediments. The concentration of authigenic Fe and Mn oxides near the sediment-water interface results from the reductive dissolution of authigenic and detrital oxides buried below the oxygen penetration depth and the diffusion of dissolved Fe(II) and Mn(II) to the oxic zone where they are oxidized and precipitated as oxides (Mucci et al. 2000a).

From a geochemical point of view, the 1996 flood layer can be most easily differentiated from the indigenous sediment by its inorganic carbon content. The flood material contains up to 0.6% C_{inorg} whereas it is nearly undetectable in the normal Fjord sediments (~0.08%) (Fig. 6). The inorganic carbon content of the pre-flood sediments is low because any calcareous material that settles at the sediment-water interface is readily dissolved during oxic diagenesis (Mucci et al. 2000a). In contrast, the C_{inorg} delivered with the flood material will be preserved under the anoxic conditions that rapidly developed throughout most of the deposit (Mucci et al. 2000a). Thus, the C_{inorg} is likely to represent a useful test for the flood layer identification in the future.

The C_{org} content of the flood deposit is about one third to half of the pre-flood sediment and its C_{org}/N molar ratio (~18) is similar to that of the indigenous sediment and also attests to its predominantly terrestrial origin. In some cases, a peak of C_{org} is observed at and just below the base of the flood deposit and may be related to the rapid burial of organisms trapped at the original sediment-water interface (Deflandre et al. 2002).

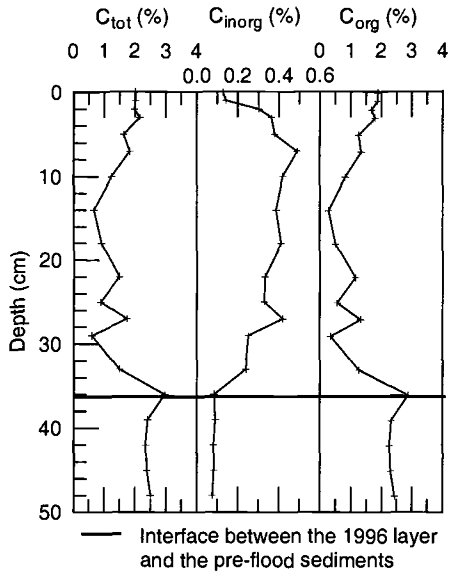

Figure 6 - *Geochemical profiles of cores taken at station 9 in 1999 in 1997 (from Savard 2000).*

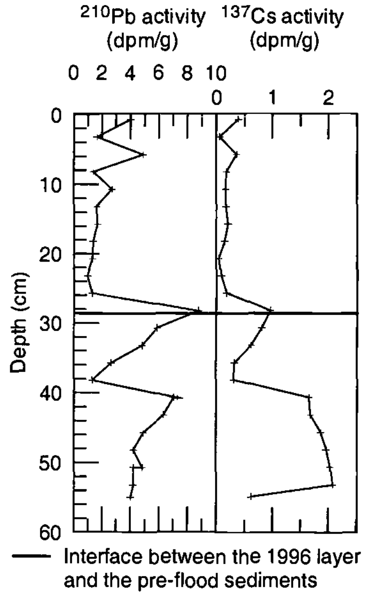

Figure 7 - *Radioisotope profiles of cores taken near station 9 (from Savard 2000).*

The vertical distribution of ^{210}Pb and the ^{137}Cs was measured in a core at station 9. The results reveal that the activity of these radioisotopes is a good indicator of the position of the flood layer interface in the Baie des Ha! Ha! (Fig. 7), where the lower contact is sharp. In contrast, this contact is difficult to identify in cores recovered in the Bras Nord (not shown), because of a mixing of the layer due to bioturbation (Savard 2000). In the flood layer, the activity of these radioisotopes is low compared to the pre-flood sediments. The main reason why the ^{137}Cs activity is low in the flood layer is because the major source of ^{137}Cs is the atmospheric thermonuclear tests started in 1952 (Eisenbud 1963). As the sediments eroded and transported down to the Saguenay Fjord following the accidental event are older than these tests (deposited about 10 000 years ago), they are almost exempt of that contamination compared to the pre-flood sediments that are contaminated by atmospheric deposition of ^{137}Cs. The ^{210}Pb, which has a natural origin, is also lower in the flood deposits because in this layer ^{210}Pb is more decomposed than in the recent pre-flood sediments.

Local Spatial Variability

The variability of properties can result from different aspects inducing errors on the parameters we want to compare. The origin of variability is mainly natural and technical. The natural variability comes from the settling of sediments from the flood. The lateral variability of the thickness of the 1996 layer is very important (Maurice et al. 2000). This is primarily due to the presence of sedimentary bed forms such as channels, dunes, mounts, etc. on the seafloor. Hill et al. (unpublished) observed in seismic records that the major variations in sedimentation of the flood sediments are caused by of meso-scale bottom roughness in the order of meters that existed before the flood, and that were also created during the flood. The flood layer was deposited by gravity involving sliding and by turbidity current flow (Crémer et al. 2002). These sedimentation processes cause divergent-fill style of sediment accumulation where sedimentation occurs preferentially in topographic lows. According to Hill et al. (unpublished), the meso-scale roughness on the seafloor of the Baie des Ha! Ha! may have an impact on the sedimentological and geotechnical properties of the bed (because of the potentially large variability in depositional conditions and grain size), erodability (because of the hydrodynamic effects of the meso-scale topography on the bottom boundary layer), biological recolonization (because of the inherent heterogeneity of the new seafloor and the hydrodynamic effect on the boundary layer) and consequently on bioturbation, bio-irrigation and geochemical processes. To evaluate the natural variability of the flood layer thickness, a spatial variability study was conducted on 29 box cores at stations V1 and V2. The results indicate that the thickness of the 1996 layer varies from 20 to 44 cm with a mean value of 28 cm and a standard deviation of 5.1 cm.

The technical variability concerns essentially the accuracy of the positioning system that increases the variability of data. The positioning of the ship was provided by a DGPS, which has an accuracy of 5 m. In addition, another variation is introduced by the drifting of the sampler that is non negligible with water depth of about 100 to 200 m, as found in the Saguenay Fjord. This drifting has been evaluated by comparing the position of the ship and the position given by an acoustic positioning system, the Trackpoint II, that gives the underwater position of a target, here the sampler, relative to reference point on the ship. The accuracy of this system is 0.5% of slant range, which correspond to about 1 m for a water depth of 200 m. The difference in position given by the ship and the Trackpoint II varies from 1 to 75 m, with a mean value of 33 m. Thus, the precision of the position of a sampling station is evaluated to be 33 m for the drifting of the sample plus the 5 m accuracy on the position of the ship, then 38 m. This means that, even if the position given by the ship is always the same for a given station, the sample can be off the desired station of an average of 38 m. This is large enough to introduce variability in the measured characteristics, as discussed previously. When using the Trackpoint II to position the sampler underwater relatively to the ship, the error on position of the sampler is reduced to about 6 m. In addition, the real position of all sampling stations, which is supposed to always be the same for a given station are, in reality, as distant as 880 m for Station 9. Therefore, it is clear that the sediment characteristics and the flood layer thickness vary drastically inside that distance range.

Comparing Criteria for Defining the 1996 Layer

From all data acquired in this project, it seems possible for each discipline to use one or more properties to define the 1996 flood layer. Due to the presence of the sandy layer and its light color compared to the pre-flood sediments, it is usually possible to identify the flood layer by visual observation alone, especially in the Baie des Ha! Ha!

From a physical point of view, density appears to be the most useful criteria to evaluate the position of the interface between the indigenous sediments and the flood sediments. The densities, measured with MST or CAT-scan, reflect the water content of sediment, its grain size distribution, degree of compaction and its mineralogy. Furthermore, a density contrast exists even when there is no sandy layer at the base of the flood layer, or when the sediments are bioturbated. The best geotechnical parameters are the undrained shear strength and the liquidity index, which are both related to the density state of sediments. Once again, these indicators of the interface between the old and the new sediments are more evident with the presence of a sandy layer and when there is no or little activity from benthic organisms. From a biological point of view, the quantification of the biogenic structures using the CAT-scan technology is a valuable tool to identify the interface between the background and the flood sediments. However, this signature can also be erased by the bioturbation below the interface. Finally, the best geochemical parameter to define the flood layer is indisputably the inorganic carbon content. As mentioned earlier, in a regular sedimentation regime, the inorganic carbon is dissolved during oxic diagenesis, but is preserved in a rapid sedimentation event as during a flood.

From a physical and geotechnical point of view, the presence of the sandy layer creates a sharp variation on profiles caused by the different properties of sandy sediments compared to clayey sediments. Because the sandy layer is almost absent in the Bras Nord, these properties are not always reliable in that sector of the fjord. In addition, bioturbation can erase physical, geotechnical and biological signatures with time as generally observed in the Bras Nord (results not shown), but they will be preserved if the thickness of the 1996 layer is greater than the depth limit of organism activities. Thus, the C_{inorg} seems to be the most reliable tool to identify the 1996 flood layer in the Saguenay Fjord environment because it does not seem to be affected by bioturbation and is still present in the absence of a sandy layer. Since the flood layer is thinner in the Bras Nord, it will be more difficult to identify it in the future. However, in most of the area covered by the deposit in the Baie des Ha! Ha!, the signature of the flood layer should be identifiable using the diagnostic criteria discussed above.

Influence of the Variability on the Results and on the Temporal Evolution of the 1996 Layer

One of the primary objectives of the Saguenay Project was to monitor the evolution of the 1996 flood layer. To do so, samples were taken each year and sometimes twice a year at the same station and their profiles were compared. To compare adequately the data from year to year, it is imperative that samples share the same geographical position, sedimentation regime, and flood layer thickness. Unfortunately, comparisons are not possible due to the significant spatial variability of the bulk sediment characteristics mentioned above.

A solution to this problem is to normalize the sediment depth profile to the measured thickness of the flood layer. An example is shown in Figure 8a for the concentration of porewater or dissolved iron at station 9. The interface between flood and pre-flood deposits was determined from the vertical distribution of C_{inorg}, but only the depth is shown on Figure 8a (horizontal lines). As we see, the thickness of the flood layer varies considerably at this station, from 22 to 33 cm. Consequently, an interpretation of the temporal evolution of a given sediment property, for example the concentration of iron, is complicated by the variability in the thickness of the 1996 layer. After the normalization, the thickness of the flood layer is always the same and dimensionless (Fig. 8b). Following this transformation, it becomes easier to evaluate the temporal evolution of sediment properties because the scale of comparison is the same. Thus, on Figure 8b, we see that the normalized porewater iron peak increases and rises over with time. This simple solution, however, does not allow for the fact that the behavior of a property could differ according to the thickness of the deposit. For example, a contaminant could migrate to the new sediment-water interface if the flood layer is thin or, could be confined within it if it is thick enough. Even if the flood layer thickness normalization does not solve all the variability problems, it greatly helps to constrain the effects of its spatial variability on the analysis-interpretation of the profiles of diverse properties measured through sediment cores.

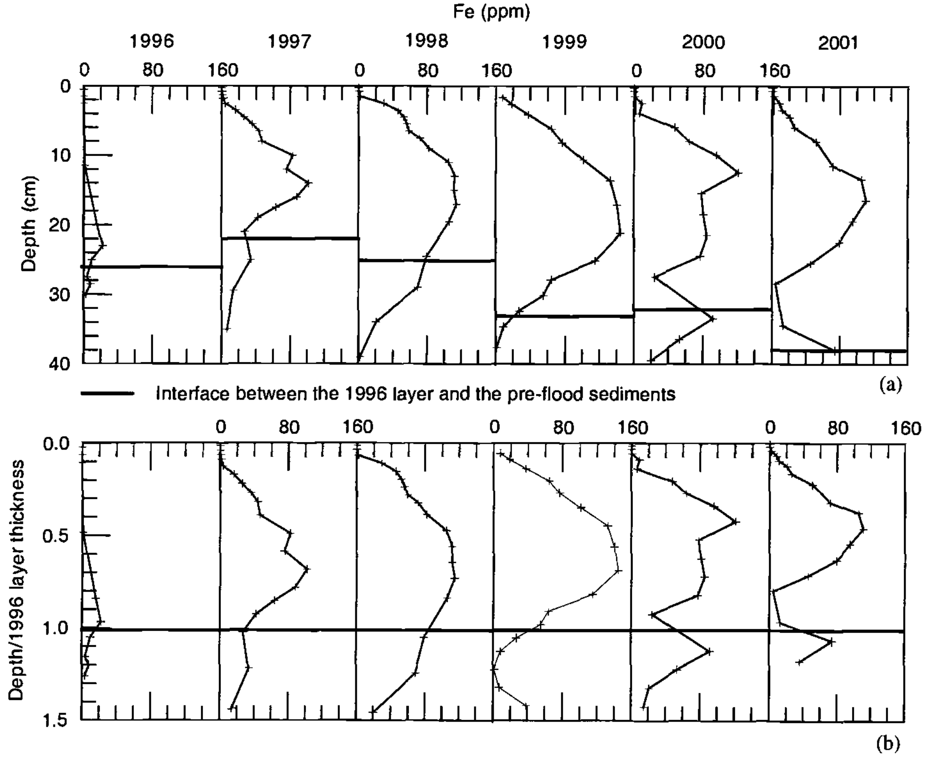

Figure 8 – *Time- series analyses of dissolved iron at station 9 between 1996 and 2001 as a function of a) depth and b) normalized depth.*

Conclusions

Physical, geotechnical, biological, and geochemical data suggest a discontinuity between the 1996 flood deposit and pre-flood deposit. Most important, is the fact that all the investigators involved in this project reached similar conclusions with respect to the thickness of the layer, irrespective of the parameter measured. As a first approximation, visual observations provide very reliable estimates in most of the sectors covered by the flood layer, particularly in the Baie des Ha! Ha!, where the layer is generally thicker than in the Bras Nord and where it is marked by a sandy layer at its base. In the Bras Nord, bioturbation through the thinner flood deposit has intermixed both the upper and lower boundaries between the flood layer and the pre-flood sediments, which makes the discontinuity more difficult to recognize. Nevertheless, some properties such as density, undrained shear strength, degree of bioturbation, and inorganic carbon content are useful to differentiate the discontinuity in most of the covered area. Among them, it seems that the inorganic carbon content is the most useful parameter to distinguish flood deposit from pre-flood sediments in the Saguenay Fjord, and in contrast to the other aforementioned parameters, it is unaffected by the presence of a sandy layer at the base of the deposit.

This paper confirms that the variability of the thickness of the flood layer is important and must be considered in temporal studies. A normalization of the depth relative to the 1996 layer thickness may be a way to cope with its variability.

Acknowledgment

This project was funded by a strategic grant from the Natural Sciences and Engineering Research Council of Canada (NSERC) and through the sponsorship of Alcan Inc. The authors wish to thank all the staff and students involved in this project for their assistance in the field and in the laboratory as well as the captains and crew of the research vessels used during this study. Special thanks go to G. St-Onge, J.-F. Crémer, L. de Montety, and J. Savard for their contribution to this paper.

References

Boespflug, X., Long, B.F. and Occhietti, S., 1995, "CAT-scan in Marine Stratigraphy: a Quantitative Approach." *Marine Geology,* Vol. 122, pp. 281-301.

Bossé, L., Ste-Marie, B., and Fournier, J., 1996, "Inventaire et Biogéographie des Invertébrés des Fonds Meubles du Fjord du Saguenay." *Rapport Technique Can. Sci. Halieutiques Aquat.* 2132.

Crémer, J.-F., Long, B., Desrosiers, G., de Montety, L., and Locat, J., 2002, "Application de la Scanographie à l'Étude de la Densité des Sédiments et à la Caractérisation des Structures Sédimentaires: Exemple des Sédiments Déposés dans la Rivière

Saguenay (Québec, Canada) Après la Crue de Juillet 1996." *Canadian Geotechnical Journal*, Vol. 39, pp. 440-450.

Deflandre, B., Mucci, A., Gagné, J.-P.,Guignard, C., and Sundby, B., 2002, "Early Diagenesis Process in Coastal Marine Sediments Disturbed by a Catastrophic Sedimentation Event." *Geochimica et Cosmochimica Acta.* in press.

de Montety, L., Long, B., Desrosiers, G., Crémer, J.-F., and Locat, J., 2000, "Quantification des Structures Biogènes en Fonction d'un Gradient de Perturbation dans la Baie des Ha! Ha! à l'Aide de la Tomodensitométrie Axiale." *Proc. of the 53rd Canadian Geotechnical Conference, Montreal,* pp. 131-135.

Drake, D.E. ,1999, "Temporal and Spatial Variability of the Sediments Grain-Size Distribution on the Eel Shelf: the Flood Layer of 1995." *Marine Geology*, Vol. 154, pp. 169-182.

Eisenbud, M., 1963, "Environmental Radioactivity." McGraw-Hill Book Co., New York, 430 p.

Hill, P., Cervantes, O., Beneton, G. and Côté, P., Unpublished, "Bottom Roughness Characteristics of the Baie des Ha! Ha!, Saguenay Fjord, Quebec, Canada: a Constraint on Mapping Bed Thickness of a Natural Capping Layer."

Holler, P. and Kögler, F.C., 1990, "Computer Tomography: a Nondestructive, High Resolution Technique for Investigation of Sedimentary Structures." *Marine Geology*, Vol. 91, pp. 263-266.

Leithold, E.L. and Hope, R.S., 1999, "Deposition and Modification of a Flood Layer on the Northern California Shelf: Lessons From and About the Fate of Terrestrial Particulate Organic Carbon." *Marine Geology*, Vol. 154, pp. 183-195.

Louchouarn, P., Lucotte, M., Canuel, R., Gagné, J.-P. and Richard, L.-F., 1997, "Sources and Early Diagenesis of Lignin and Bulk Organic Matter in the Sediments of the Lower St-Lawrence Estuary and the Saguenay Fjord." *Marine Chemistry,* Vol. 58, pp. 3-26.

Maurice, F., Locat, J., and Leroueil, S., 2000, "Caractéristiques Géotechniques et Évolution de la Couche de Sédiment Déposée Lors du Déluge de 1996 dans la Baie des Ha! Ha! (Fjord du Saguenay, Québec)." *Proc. of the 53rd Canadian Geotechnical Conference, Montreal*, pp. 123-130.

Mucci, A. and Edenborn, H.M., 1992, "Influence of an Organic-Poor Landslide Deposit on the Early Diagenesis of Iron and Manganese in a Coastal Marine Sediment." *Geochimica et Cosmochimica Acta*, Vol. 56, pp. 3909-3921.

Mucci, A., Guignard, C., and Olejczyk, P., 2000a, "Mobility of Metals and As in Sediments Following a Large Scale Episodic Sedimentation Event." *Proc. of the 53rd Canadian Geotechnical Conference, Montreal*, pp. 169-176.

Mucci, A., Richard, L.-F., and Lucotte, M., 2000b, "The Differential Geochemical Behavior of Arsenic and Phosphorus in the Water Column and Sediments of the Saguenay Fjord Estuary, Canada." *Aquatic Geochemistry*, Vol. 6, pp. 293-324.

Pelletier, E., Deflandre, B., Nozais, C., Tita, G., Desrosiers, G., Gagné, J.-P., and Mucci, A., 1999, "Crue Éclair de Juillet 1996 dans la Région du Saguenay (Québec). 2. Impacts sur les Sédiments et la Biote de la Baie des Ha! Ha! et le Fjord du Saguenay." *Canadian Journal Fisheries and Aquatic Science*, Vol. 56, pp. 2136-2147.

Perret, D., Locat, J., and Leroueil, S., 1995, "Strength Development With Burial in Fine-Grained Sediments From the Saguenay Fjord, Quebec." *Canadian Geotechnical Journal*, Vol. 32, No. 2, pp. 247-262.

Pocklington R., and Leonard, J.D., 1979, "Terrigenous Organic Matter in Sediments of the St-Lawrence Estuary and the Saguenay Fjord." *J. Fisheries Research Board Can.*, Vol. 36, pp. 1250-1255.

Savard, J., 2000, "Évolution Temporelle des Couches Accidentelles (Crues, Séismes, Glissements de Terrain) Récentes du Fjord du Saguenay d'Après des Profils de Radio-Isotopes de Courtes Périodes (^{228}Th/^{232}Th, ^{210}Pb, ^{137}Cs)." *M.Sc Thesis*, Université du Québec à Montréal, Montréal, Québec.

Schafer, C.T., Smith, J.N., and Seibert, G., 1983. "Significance of Natural and Anthropogenic Sediment Inputs to the Saguenay Fjord, Quebec." *Sedimentary Geology*, Vol. 36, pp. 177-194.

Schafer, C.T., Smith, J.N., and Côté, R., 1990, "The Saguenay Fjord: a Major Tributary to the St. Lawrence Estuary. In Oceanography of Large-Scale Estuarine System: the St-Lawrence." Vol. 39, ed. M.I.El-Sabh and N. Sylverberg, pp. 378-420.

Smith, J.N. and Walton, A., 1980, "Sediment Accumulation Rates and Geochronologies Measured in the Saguenay Fjord Using the Pb-210 Dating Method." *Geochimica et Cosmochimica Acta*, Vol. 44, pp. 225-240.

St-Onge, G., Leduc, J., Bilodeau, G., de Vernal, A., Devilliers, R., Hillaire-Marcel, C., Loucheur, V., Marmen, S., Mucci, A., and Zang, D., 1999, "Caractéristiques des Sédiments Récents du Fjord du Saguenay (Québec) à Partir de Traceurs Physiques, Géochimiques, Isotopiques et Micropaléontologiques." *Géographie physique et Quaternaire*, Vol. 53, no. 3, pp. 339-350.

St-Onge, G. and Hillaire-Marcel, C., 2000, "Inventaire des Couches Accidentelles Récentes dans le Fjord du Saguenay à Partir des Propriétés Physiques de Carottes de Forages." *Proc. of the 53rd Canadian Geotechnical Conference, Montreal*, pp. 145-151.

Yu, W., Lin, C.A. and Benoit, R., 1997, "High Resolution Simulation of the Sever Precipitation Event Over the Saguenay Region, Quebec, in July 1996. " *Geophysical Research Letters*, Vol. 24, pp. 1951-1954.

Alex J. Zeman[1] *and Timothy S. Patterson*[1]

Characterization of Contaminated Sediments in Hamilton Harbour, Lake Ontario

Reference: Zeman, A. J. and Patterson, T. S., "**Characterization of Contaminated Sediments in Hamilton Harbour, Lake Ontario**" Contaminated Sediments: Characterization, Evaluation, Mitigation/Restoration, and Management Strategy Performance, ASTM STP 1442, J. Locat, R. Galvez-Cloutier, R. C. Chaney, and K. R. Demars, Eds., ASTM International, West Conshohocken, PA, 2003.

Abstract: Sediments in many harbors and connecting channels of the Great Lakes have been negatively impacted by industrial, agricultural and municipal discharges and by atmospheric deposition. Contaminated sediments may pose risks to both human health and to aquatic environments. All 42 U.S. and Canadian Areas of Concern (AOCs), designated by the International Joint Commission (IJC), have problems associated with the occurrence of contaminated sediments. Remedial Action Plans, which have been prepared for these areas, include sediment remediation plans. Appropriate and cost-effective sedimentological, geotechnical and geochemical investigations are required to determine the degree and extent of contamination. The methodology used in sediment characterization includes in-situ penetration tests, core sampling, acoustic bottom-classification systems, side-scan surveys and in-situ porewater samplers. Contaminated sediments are typically characterized for chemical concentrations of contaminants of interest in terms of both areal extent and vertical distribution. Site specific examples of sediment analyses and characterization for remediation projects are discussed for three sites within Hamilton Harbour, Ontario, where very heterogeneous sediments exist.

Keywords: Great Lakes, sediment, remediation, toxicity, capping, dredging

---

[1] Aquatic Ecosystem Management Research Branch, National Water Research Institute, 867 Lakeshore Road, Burlington, Ontario L7R 4A6.

Introduction

Drafting an adequate cleanup strategy for the remediation of a harbor or river containing contaminated sediments requires detailed information on the sediment properties and the nature and extent of contamination. There are many technologies available for characterizing the necessary geotechnical and geochemical information from sediments, both *in-situ* and in the laboratory. There are also several options for the remediation of contaminated sediments, each with its own available technologies that may be implemented at any given site. The characterization techniques, remedial options and equipment utilized for the remediation of sites containing contaminated sediments will be briefly described. Within the Great Lakes, the International Joint Commission (IJC) designated 42 areas in both Canada and the U.S. containing contaminated sediments as Areas of Concern (AOCs). The IJC has identified remediation of contaminated sediments as a priority for investigation. Three sites that have been under study within Hamilton Harbour (a high-priority AOC) will be briefly described in this paper.

Remediation Technologies

Sediment remediation techniques can be generally subdivided into two broad classes: a) non-removal technologies which do not rely on dredging, and b) removal technologies in which sediment is dredged from a site and is either stored elsewhere without treatment or treated and stored in a confined disposal facility (CDF). Removal technologies typically use environmental dredging (as opposed to navigation and construction dredging), which is focussed on removing sediment from targeted regions with great accuracy while restricting the amount of resuspension of contaminated sediment.

Non-Removal Technologies

Natural and Enhanced Sediment Isolation - In many cases where contaminated sediments in harbors or bays have been investigated, the committees or government bodies involved in organizing potential clean up plans have elected to leave the problem alone. Sometimes the very delays involved in cleanup strategies (lack of funding, disagreements between organizations) continue for so long that in effect, the natural attenuation approach is implemented, even if not by choice. The natural attenuation approach follows the principle that natural sedimentation will gradually cover over and isolate contaminated sediments from the water column and eventually from the benthic invertebrates. Although bioturbation (feeding, burrowing, and locomotory activities of sediment-dwelling benthos) produces vertical sediment mixing, the zone of bioturbation (in the Great Lakes region typically less than 10 cm) will be eventually moved into clean sediments. In addition to sedimentation as a function of natural remediation, toxic organic compounds are left to natural biodegradation. The natural sedimentation process may be accelerated with the addition of a thin layer of clean sand (about 15 cm thick) which is known as enhanced natural recovery. These passive methods of remediation are only effective where bottom currents and wave vortices are weak enough that surficial sediments are not disturbed, and where no other sources of sediment disturbance occur, such as heavy shipping traffic. The continued success of natural and enhanced sediment isolation is dependent on the prevention of further contaminated discharges into the aquatic environment.

In-Situ Sediment Treatment - Sediments in both marine and freshwater environments have been treated *in-situ* as an economical means for remediation, where the natural attenuation approach has been rejected. The type of *in-situ* remediation chosen is dependent on the nature of contamination. PAHs and total petroleum hydrocarbons (TPHs) have been treated *in-situ* by aeration and the addition of nutrients mixed with the oxidant calcium nitrate (Murphy et al. 1995) which caused significant biodegradation of PAHs. Where freshwater eutrophication is a concern, sediments may be treated with chemicals such as aluminum sulphate (alum), lime, calcite and ferric chloride (Klapper 1991).

In-Situ Capping - *In-situ* capping is the covering over of contaminated sediments with a clean layer (usually sand) thick enough to isolate the sediment from benthos and other aquatic organisms (Palermo et al. 1998). This remedial alternative is suitable for situations when the sediment is contaminated with a wide range of compounds, e.g. with several persistent organic contaminants and toxic metals. The application of the capping layer must be placed so as not to significantly disturb the surficial sediment (i.e. the capping material must not be too coarse or too heavy so that it will not penetrate the very soft sediment). This has been shown to be achievable using medium to coarse sand as the capping material over very soft silty clay (Zeman and Patterson 1997). Once the capping material has been placed, the cap may be further protected from water currents by an additional overlying layer of gravel or boulders.

Removal Technologies

Improved and newly designed dredges have been created for environmental cleanup projects with the goals of minimizing sediment resuspension, and providing for the more accurate and complete removal of contaminated sediments (Environment Canada - OR 1998; Dredging Supply Company Inc. 2002). Several of these dredges are herein briefly described.

Cable Arm Environmental Bucket - This Canadian dredge is designed to remove contaminated sediment on a flat plane, using a precision clamshell aggregate bucket, so that a level, horizontal cut is completed as opposed to a curved cut, typical of other dredges. Cables anchored at the four corners of the bucket ensure this type of cut.

Mud Cat - The Mud Cat is a U.S. made dredge designed to operate in shallow marine environments. It features an effective sediment removal system consisting of a boom-mounted horizontal auger and a centrifugal slurry pump. There is also dual convergence at the auger head. The dredge is designed to minimize the resuspension of the sediment while maximizing the solids content of the dredged material. An hydraulic forward tilt and manual transverse tilt of a truss boom allows for use on sloping underwater sediment.

Pneuma Pump - The Pneuma Pump was developed in Canada and consists of a barge mounted dredge utilizing guide cables operated above the water surface. The dredge is pulled by a winch system with a speed of about 4-5 m per minute. The Pneuma Pump was successfully used in the cleanup of Collingwood Harbour, which became the first AOC in North America to become delisted.

Visor Grab - The Visor Grab was developed in the Netherlands, and utilizes a sealed dredge bucket. It has a standard backhoe bucket with a controlled visor, operated by hydraulic cylinders on each side of the bucket. The bucket can be used on standard excavators.

Amphibex - The Amphibex is a Canadian designed dredge using a barge equipped with spuds, stabilizers and an excavator. An hydraulic arm and bucket with attached pumps allows the Amphibex to hydraulically dredge sediment without requiring any suction. Positive pressure is used instead, which increases the solids content and minimizes excess water. The Amphibex has proved to be less expensive than conventional dredges, meeting regulatory requirements.

Viscous Excavator - This U.S. designed dredge uses an enhanced rotary cutterhead element that removes viscous sediment more efficiently than conventional dredges. The hollow cutterhead uses circular rings that rotate and pass the dredged material through it.

Sediment Toxicity

For areas of Canadian jurisdiction in the Great Lakes, the Ontario Ministry of Environment and Energy (MOEE) sets the provincial sediment quality guidelines (PSQGs) for sediment toxicity. Determining what can be classified as toxic sediment in legal terms is no simple task. Toxicity must be determined in relation to the effects contaminants have on organisms for any given area. The obvious disadvantage to this is the fact that different species of organisms react differently to contaminants. As a result, the MOEE does not rely on single-species data to develop PSQGs. Another disadvantage is the fact that some species develop a level of immunity to contaminants over time. The tolerance of species so exposed will thus differ to that of unexposed communities of the same species. The species of organism to be used for a standard, and the mortality rate from exposure to any given chemical or element must thus be established with great care. This includes the determination of a time of exposure and a percentage rate of mortality after this elapsed time. Based on the long term effects that contaminants in sediment have on sediment dwelling organisms, the MOEE further classifies sediment into three categories (Persaud et al. 1994):

No Effect Level - Fish and sediment dwelling organisms are not affected.
Lowest Effect Level - Majority of sediment dwelling organisms are not affected.
Severe Effect Level - "Likely to affect the health of sediment dwelling organisms".

Sediment with this rating requires further testing to determine if it is acutely toxic. Acute toxicity is generally measured as the percentage of an effluent in clean water that causes a 50% lethality rate to test organisms over a 96-hour period (Ontario Ministry of the Environment 1988).

An approach created by researchers at the National Water Research Institute (NWRI) classifies sediment toxicity based on the effects observed on four benthic invertebrate species (*Chironomus riparius, Hexagenia limbata, Hyalella azteca and Tubifex tubifex*). Software has been developed to classify sediment into three categories based on this method, namely, non-toxic, potentially toxic and toxic (Reynoldson and Pascoe 2000).

For comparison, in nearly all of U.S. National Oceanic and Atmospheric Administration's (NOAA's) sediment toxicity studies, three separate bioassays are used to measure toxicity. The three bioassays ensure that a range of species and assessment end points (e.g., mortality, reproductive impairment, physiological stress) would be tested to provide a wide perspective on adverse biological effects. The NOAA's bioassays are used to determine: (1) amphipod survival following a 10-day exposure to bulk (or) whole sediment; (2) successful fertilization of sea urchin (or other invertebrates) following exposure of gametes to pore water; and (3) decreased light production, indicative of metabolic stress, by a luminiscent marine bacterium, *Vibro fisheri*, when exposed to an organic extract of sediment (Hameedi et al. 1999).

Mapping of Contaminated Sediments

Acoustical Mapping

The texture of sediments is an important factor for mapping sediment beds as contaminants are usually found in much higher concentrations in finer sediments. In addition, core samples are more difficult to retrieve from sandy sediments. A map of surficial sediment texture may thus not only be a good indication of where contaminated sediments are more likely to be found, but may show areas of sediment where core samples can be more easily retrieved. If areas containing sandy, surficial sediments are known, the planning of sampling at these sites may be changed accordingly (e.g. the use of vibracoring instead of gravity coring).

Over the years, various technologies have been used for mapping marine and freshwater beds using acoustical equipment, primarily for navigational and fisheries purposes. As these technologies expanded and improved, some were utilized for the mapping of sediment texture and type. Some systems presently in use were developed especially for this purpose. An example of this is the acoustic marine-bed classification system known as RoxAnn^{TM}, which has been successfully used within the Great Lakes on various projects in determining surficial sediment type (Rukavina and Caddell 1997). RoxAnn works on the principle that various textures of surficial sediment reflect acoustic signals differently. The type of echo received by RoxAnn is interpolated and instantly classified within the software system used in conjunction with the unit.

An acoustical coring analysis method was developed by Caulfield Engineering to classify sediments for dredging operations (Tuchman et al. 1997). Acoustic Core^{TM} is an acoustic remote sensing tool which was jointly field tested with the U.S. Army Corps of Engineers R&D Center and which is now commercially available. Both core samples and acoustical measurements were made at several sites in Great Lakes harbors and rivers to compare the accuracy of the acoustical profiles. The profiles of sediment distribution were reported to have an accuracy of 95% in estimating density in marine sediment.

A multiple-frequency echo sounding system known as DSLP (Detection of Sediment Layers and Properties) can provide high-resolution analysis of the stratification of suspended sediments and individual sediment layers of unknown physical and sedimentological properties (Eden et al.1999, Kern and Westrich 1999). DSLP uses a complex digital signal to determine sediment type. The DSLP method can be used to determine required volumes of sediments to be dredged for sediment remediation projects.

Chemical Mapping

Chemical mapping of contaminated sites is best done in three dimensions, which requires the sampling of sediment below the sediment/water interface. This is done by taking core samples, whereby a tube usually made of clear acrylic is either dropped or pushed through the sediment. Core samples may then be cut and subsampled at any depth measured from the top of the core. Where duplicate core samples of the upper sediment from the same location are desired, a large box corer with a retractable bottom is often used to scoop up almost 1 m^3 of sediment. Two or more short core tubes are then pushed through the sediment by hand and pulled out.

The mapping of chemical compounds within contaminated sediments has proven to be a challenge at many sites. Deposited compounds from spills or dumped material tend to be very site specific and initially cover a small area, often spreading out into a thin layer of only several millimetres thick. Over several years, natural sedimentation will bury such a layer. Subsampling cores at intervals that are too far apart may result in contaminated layers being missed, especially if the sediment color and texture are very similar to the neighboring sediment within the core. Contaminated sediments also tend to be very fine, and are thus easily disturbed by currents, propeller wash, and anchor dragging from passing ships. In industrial areas, contaminant spills not only come from various sources, but usually differ in chemical makeup, frequency of occurrences and volume. As a result, the composition of sediments in industrial areas is often very heterogeneous and, in extreme cases, can significantly vary among sediment samples collected only several metres away. Accurate three-dimensional chemical mapping is thus very difficult in cases like this, and the site sediment can only be properly mapped with a high density of sampling locations. The constant disturbance, migration, and settlement of sediments results in the rendering of chemical maps obsolete over several years, depending on the rate of change.

Chemical mapping may be done for hundreds of different elements and chemical compounds found within contaminated sediment. The sampling technologies used for extracting and measuring these chemicals vary in cost and procedures. One or more sets of chemicals may be identified as being the primary contaminants in industrial sediment (e.g. PAHs), but the extent of contamination of other chemical compounds may be unknown and even unsuspected. Since budget limitations usually prevent the analyses for all known hazardous substances that may be found in sediment, priority contaminants must be established based on aquatic ecosystem health and budgetary limitations. The determination of such priority contaminants is usually based on previous biological monitoring (e.g. deformity and mortality rates of fish and animal species, and determinations of sediment toxicity from bioassays of benthic invertebrates). It is wise to test a small percentage of samples for hazardous compounds that are not known to be in high concentrations at the site, but are potentially present. If unexpected high concentrations of additional compounds are found, further testing for these compounds may be deemed prudent on other cores.

Samples taken from an initial set of sampling sites usually reveal areas of sediment that require more detailed mapping, and thus a secondary set of samples. It is often the case where one sample from a set may reveal unusually high concentrations for some contaminants in comparison to other samples taken nearest to it. This may indicate a small localized spill or dump site of contaminated sediment, which may be deemed important enough to map in greater detail to aid in determining a remedial strategy.

In principle, the density of sampling stations should be as great as possible, but usually the total number of cores and samples is determined by time requirements and budgetary constraints. For smaller surveys, the position of sampling stations depends primarily on the size and shape of the water body. Different sampling strategies and sampling grid designs (e.g. square grids, nested grids, parallel line sampling grids with equal and unequal spacing, ray sampling grids) can be chosen for more complex surveys (Golterman et al. 1983).

Once areas of contaminated sediments are sufficiently mapped to reveal calculated volumes and measured concentrations, remedial options may be considered. Volumes are determined by setting a contaminant concentration limit, and measuring the vertical range in each core where concentrations meet or exceed the limit, in addition to the horizontal distances between the cores. Computer software programs may then be used to calculate the volume and three dimensional profile of the contaminated sediment deposit(s).

Chemical mapping of contaminated sediments is closely tied to risk assessments of contaminated sites, considering both ecological risks quantified on the basis of laboratory toxicity experiments and human-health risks, where assessments result e.g. in fish consumption guidelines or cancer risk levels (Förstner 2002).

Geotechnical Investigations

In-Situ Tests

Physical *in-situ* testing of the geotechnical properties of sediment is usually conducted to determine the strength and consolidation of the sediment (Richards and Zuidberg 1985). Sediment is composed of solid particles and pore water, often with the presence of gas, and is always under static pressure from the overlying water column. Geotechnical tests look at one or more of these attributes and their relationships.

Cone penetration testing may be conducted on *in-situ* sediments to obtain a quick and economical general understanding of shear strength tendencies of site sediments. A device known as a free-fall penetrometer, called STING^{TM} (Jasco Research Ltd. 2001) which is shaped like a long rod with a fin, has been used for determining approximate shear strength values at sites where contaminated sediments exist. The penetrometer is dropped from a boat and allowed to fall and sink into the sediment bed. An electronic measuring device attached to the instrument measures the rate of reduced speed upon impact of the tip with the sediment. This gives an indication of the shear strength of the sediment, which can aid in the interpretation of sediment grain size. For example, if the penetrometer penetrates through 50 cm of sediment with an abrupt stop at 50 cm, it may be assumed that the upper 50 cm sediment layer is comprised of soft, fine-grained sediments underlain by a different type of sediment with much higher shear strength (e.g., an overconsolidated glaciolacustrine sediment). A general knowledge of the site sediment stratification is necessary, however to avoid misinterpretation. Both sand and hard clay layers will greatly slow down or stop the penetrometer.

Specialized cone penetrometers have been equipped with electrodes to measure sediment temperature, electrical conductivity, resistivity and shear wave velocity. Other penetrometers have been designed to sample pore water and to be used for outflow hydraulic conductivity testing (Campanella et al. 1993). Dialysis samplers, known as "peepers" (Hesslein 1976) have been deployed into sediment at study sites to extract pore water through a porous membrane into chambers filled with distilled water (Zeman and Patterson 2000). The peepers remain vertically oriented in the sediment, over a time period of several weeks. The diffusive equilibrium that results within the peepers allows for the capture of major ions and nutrients.

In-situ testing of sediment also includes the use of field vane tests, porewater pressure tests and seepage measurements. Field-vane tests are used for determining the undrained shear strength and sensitivity of soft cohesive sediments. A four-bladed vane fastened to the bottom of a vertical rod, is gently pushed into the sediment and is then rotated. The relationship between torque and angular rotation is recorded so that undrained shear strength may be calculated. Porewater pressure may be determined by the use of differential piezometers, which are used to measure the extent of underconsolidation in soft fine-grained sediments. Seepage meters may be installed in nearshore sediments to monitor the interaction between groundwater and open water bodies. This allows for measurement of the horizontal and vertical sediment permeability, and the quantity and direction of groundwater flow (Zeman and Patterson, 2002).

Laboratory Tests

Where in-situ testing is deemed to be too costly or impractical, laboratory testing on samples is required to determine geotechnical parameters. One of the most basic classification tests performed on sediments is grain size. Sediment samples are generally classified by their grain size and plasticity according to the Unified Soil Classification System (Terzaghi and Peck 1968, ASTM Standard D 2487, Standard Classification of Soils for Engineering Purposes). Under this system, sediments are classified into three major groups: coarse-grained, fine-grained, and highly organic (peaty). The grain size of sediment samples factors into the results of many laboratory tests. Such tests include moisture content, shear strength, plasticity, consolidation, viscosity and specific surface area. The moisture content of sands is around 30%, whereas the moisture content of soft, fine grained sediment may be as high as 400% or greater. Shear strength can range from < 1 kPa for very soft sediments, to > 80 kPa for hard clays. The specific surface area for clay minerals varies from 5-20 m^2/g for kaolinite to 700-800 m^2/g for smectite group minerals with expandable internal surfaces (Mudroch et al. 1997).

Site-Specific Examples From Hamilton Harbour, Ontario

Overview of Hamilton Harbour

Hamilton Harbour is located on the western end of Lake Ontario and has an area of approximately 31 square kilometres (Fig. 1). The harbor has been designated as one of the 42 AOCs within the Great Lakes by the IJC. It contains contaminated sediment that exceeds the MOEE sediment quality guidelines at the "severe effect" level for both metals and organic compounds (Persuad et al. 1994). The southern shore of the harbor borders mainly on industrial land. The eastern shore is comprised of a narrow sand bar used primarily as a transportation corridor. The north shore has a mix of land use, being mainly residential and recreational. PAHs and heavy metals are most concentrated near the industrial shoreline.

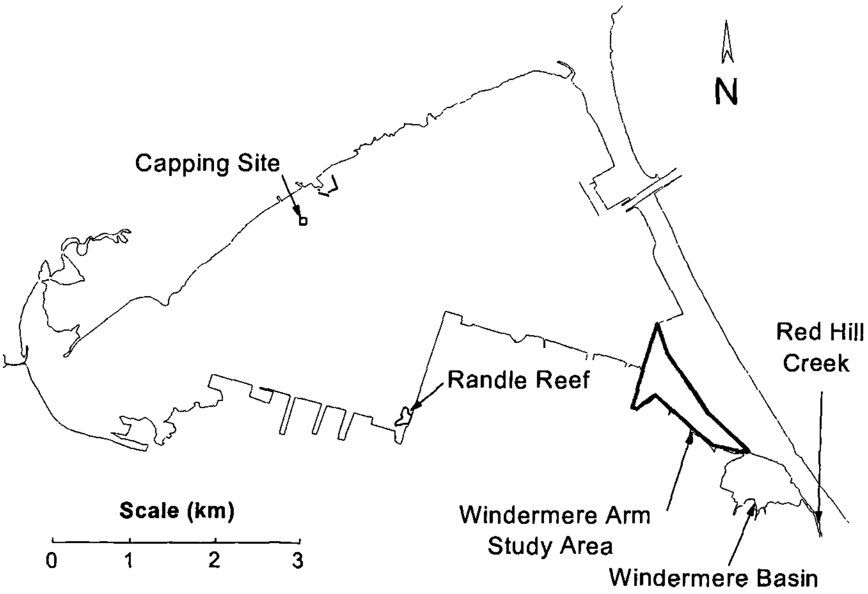

Figure 1 - *Study areas in Hamilton Harbour*

Hamilton Harbour In-Situ Capping Project

A one hectare pilot size capping project was completed near the north shore of the harbor in 1995 (Zeman and Patterson 1997). The contaminants of concern were trace metals and PAHs that had migrated northward from the south shore industrial area. A sand cap averaging about 34 cm in thickness was successfully placed over very soft contaminated sediments. Because of the sand cap, post-capping cores had to be taken by vibracoring. The cores showed a very sharp sediment/cap interface and a significant difference in trace metal concentrations between the sediment and the sand cap (Fig. 2).

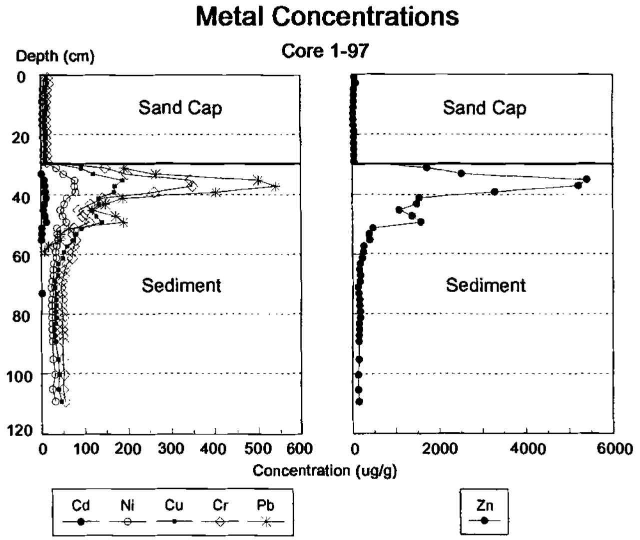

Figure 2 - Metal concentrations in core from capping site in Hamilton Harbour

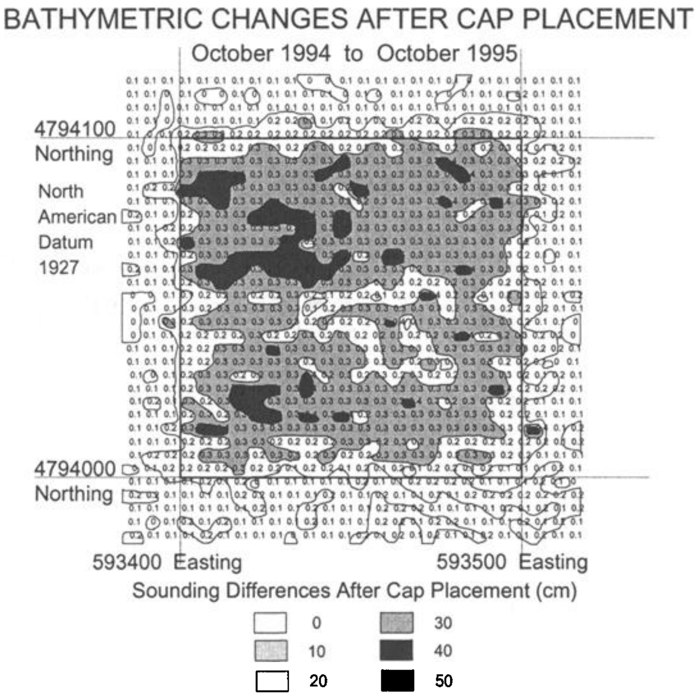

Figure 3 - *Bathymetric changes after capping*

Multibeam echo-soundings were taken of the site before, during and after cap placement (Fig. 3). This consisted of sounding intervals that were approximately 5 m apart, together producing a grid pattern of depths. Changes in bathymetry were most evident within the capping area.

The placement of the cap was clearly delineated by using the acoustic sounder RoxAnn. As with the multibeam echo soundings, RoxAnn mapping was conducted before, during and after capping.

Randle Reef Site

The Randle Reef "hot spot" is located near the south shore of Hamilton Harbour (Fig. 1). It is considered to contain the most highly contaminated sediment for PAH concentrations in the harbor. Due to the softness of the sediment, several sets of gravity cores were easily collected. Subsamples for PAHs were taken at varying intervals from the cores and mapped using a contouring software program (Fig. 4). Since the sediment at the site was found to be extremely heterogeneous, chemical maps of the site showed widely varying concentrations within a relatively small area. The maps significantly changed in appearance depending on how the extent of contamination was expressed (e.g. maximum PAH concentrations found vs. maximum depths of highly contaminated sediment). The maximum concentration of PAHs found at the site was 17 000 ppm near the middle of the hot spot area.

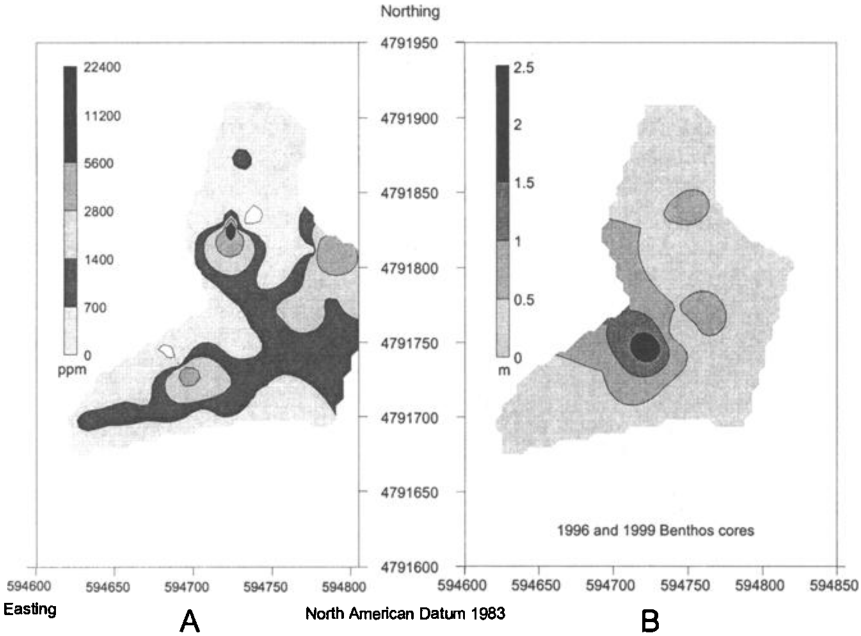

Figure 4 - *Maximum PAH concentrations regardless of depth (A), and maximum depth of PAH concentrations > 700 ppm (B), Randle Reef Study Site*

Discussions on potential remedial measures for the Randle Reef hot spot have been ongoing for several years. Acoustical, penetration, and chemical mapping conducted at the site was instrumental in determining the extent of the hot spot, both in area and volume. Due to the area coverage and volume of contamination, the remedial process is greatly limited by financial resources available. Various options of remediation have been considered, including dredging. For this option, it was proposed to remove approximately 20 000 m^3 of the most toxic sediments with sum PAH concentrations greater than 700 µg/g PAH minus naphtalene. Several *ex situ* sediment treatment options have been assessed for applicability (Environment Canada 1999).

A final remedial project for Randle Reef has yet to be undertaken, although stakeholders (committee members) have tentatively agreed to a confinement and capping plan. A structure is to be built at Randle Reef that will be large enough to confine the on-site sediment in addition to dredged sediment from other contaminated sites in the harbor. The structure will likely be capped above the water level to form an island or peninsula (McGuinness 2002).

Windermere Arm Site

Windermere Arm is a narrow channel situated in the southeast portion of the harbor, covering an area of approximately 80 hectares (Fig. 1). The western shoreline of the Arm is industrial. The northern section of the Arm is a well used shipping corridor. Red Hill Creek flows into a basin which empties into the Arm from the south. An old landfill site and an operating sewage treatment plant are situated alongside the Red Hill Creek.

Although sediment contamination in the Arm is not as severe as that found in Randle Reef, concentrations of PAHs and PCBs are well above the MOEEs "lowest effect level" guidelines, whereas concentrations of at least seven trace metals exist above the "severe effect" level. Digital photographs taken of opened cores (Fig. 5) do not always give a clear indication of where the most highly contaminated sediment may be found. The sediment in Windermere Arm is not as heterogeneous as sediment found at Randle Reef, but chemical contamination is still extensive, and chemical compounds often reach their peak values independent of each other at various depths in the sediment (Table 1).

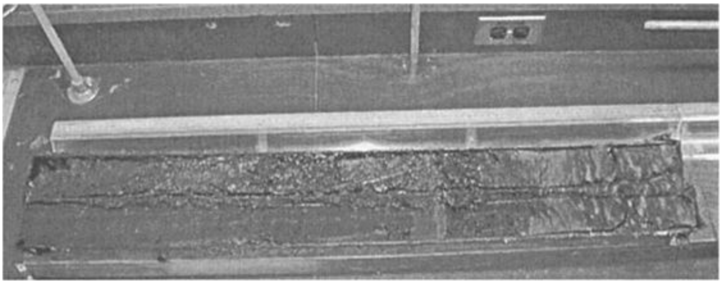

Figure 5 - *Sediment core from Windermere Arm*

Full chemical characterization of the sediment at Windermere Arm has yet to be finalized. It is expected that a management strategy will be completed in 2004.

Table 1 - *PAH, PCB and lead comparisons between two cores from Windermere Arm.*

Core	Depth, cm	PAHs, ppm	PCBs, ppm	Lead, ppm
A6A	0	22.99	1.84	91.38
	10	113.81	-----	2,302.00
	41	0.28	Not Detected	<2.25
A8	0	3.93	0.34	<5.0
	30	0.25	159.00	<5.0
	50	0.07	Not Detected	<5.0

Conclusions

The cleanup of AOCs and other sites with contaminated sediments require adequate mapping and characterization of contaminants within the sediment. This is to ensure that the volume of contaminated sediments and its geotechnical and geochemical properties are known. From this information, the appropriate remedial technologies may be selected for any cleanup plan, subject to budget limitations. Authoritative sediment toxicity guidelines are necessary to determine whether contaminant levels in sediments at any site warrant a cleanup plan.

From the three sites examined in Hamilton Harbour, it is clear that acoustical mapping along with geotechnical and geochemical testing have provided significant information for site delineation and sediment composition. Accurate placement of the sand cap for the 1995 capping project was confirmed through both acoustical mapping and cores collected at the site. The tentative cleanup strategy for Randle Reef was based largely on sediment data collected from the site. Ongoing sampling and testing of Windermere Arm sediments is expected to identify areas within the Arm to be selected for a likely future cleanup project.

References

Campanella, R. G., Davies, M. P., and Boyd, T., 1993, "Characterizing Contaminated Soil and Groundwater Systems with In-Situ Testing," *Proc.1993 Joint ASCE-CSCE National Conference on Environmental Engineering*, July 12-14, Montreal, Québec.

Dredging Supply Company Inc., 2002, URL: http://www.dscdredge.com/viscous_excavator.html, Reserve, Louisiana.

Eden, H., Müller, V., and Vorrath, D., 1999, DSLP Method, a New Surveying Technology. In: DVW-Schriftenreihe Band 37, "Gewässermessung und Hydrographische Informationssysteme", pp. 106-115, Konrad Wittwer Verlag, Stuttgart.

Environment Canada, Environmental Protection Branch - Ontario Region, Great Lakes 2000 Cleanup Fund, 1998, *The Remediation Technologies Program Great Lakes 2000 Cleanup Fund, Technical Report*, Downsview, Ontario.

Environment Canada, Environmental Protection Branch - Ontario Region, Great Lakes 2000 Cleanup Fund, 1999, *Randle Reef Sediment Remediation Project, Environmental Screening Report*, Draft Report, Downsview, Ontario.

Förstner, U., 2002, "Sediment Sampling, Sample Preparation, Grain Size Corrections, and Chemical Criteria", In: *Environmental Monitoring Handbook*, Burden, F.R., McKelvie, I., Förstner, U. and Guenther A. (eds.), McGraw-Hill Companies, Inc., New York, pp. 14.1-14.35.

Golterman, H. L., Sly, P. G., and Thomas, R. L., 1983, "Study of the Relationship Between Water Quality and Sediment Transport", Technical Papers in Hydrology No. 26, UNESCO, Paris.

Hameedi, M. J., Long, E. R., and Harmon, M. R., 1999, "Sediment Toxicity", In: NOAA's State of the Coast Report, National Oceanic and Atmospheric Administration, Silver Spring, MD. URL: http://state-of-coast.noaa.gov/bulletins/html/sed_15/sed.html

Hesslein, R.H., 1976, "An In-Situ Sampler for Close Interval Pore Water Studies," Limnology and Oceanography, Vol. 21, pp. 912-914.

Jasco Research Ltd., 2001, STING Mk.II. Seabed Terminal Impact Newton Gradiometer. Product Specifications, URL: http://www.jasco.com/downloads/sting.pdf, Victoria, BC.

Kern, U., and Westrich, E., 1999, *Methoden zur Erkundung, Untersuchung und Bewertung von Sedimentablagerungen und Schwebstoffen in Gewässern (Methods for Mapping, Investigation and Assessment of Sediment Deposits and Suspended Sediment in Water Bodies),* Schriften, Deutsche Vereinigung für Wasserwirtschaft (DVWK), No. 128, Bonn. Germany.

Klapper, H., 1991, *Control of Eutrophication in Inland Waters*, Ellis Horwood, New York.

McGuinness, E., 2002, "Harbour Stakeholders Agree to Cap Hot Spot," *The Hamilton Spectator*, April 25, 2002, Hamilton, Ontario.

Mudroch, A., Azcue, J. M. and Mudroch P. (eds.), 1997, *"Manual of Physico-Chemical Analysis of Aquatic Sediments"*, CRC Press Boca Raton, FL.

Murphy, T., Moller, A., Brouwer, H., 1995, "In-Situ Treatment of Hamilton Harbour Sediment," *Journal of Aquatic Ecosystem Health,* Vol. 4, pp. 195-203.

Ontario Ministry of the Environment., 1988, "*Toxicity of Pulp and Paper Effluent in Ontario,*" Queen's Printer, Toronto, Ontario.

Palermo, M., Maynord, S., Miller, J., and Reible, D., 1998, "*Guidance for In-Situ Subaqueous Capping of Contaminated Sediments,*" EPA 905-B96-004, Great Lakes National Program Office, Chicago, Illinois.

Persuad, D., Jaagaumagi, R., and Hayton, A., 1994, "*Guidelines for the Protection and Management of Aquatic Sediment Quality in Ontario,*" ISBN 0-7729-9248-7, Ontario Ministry of the Environment, Water Resources Branch, Toronto, Ontario.

Reynoldson, T. R., and Pascoe, T., 2000, "*Development and Application of the BEAST Software for Using Biological Sediment Guidelines Developed for the Great Lakes. Abstracts,*" 35th Central Canadian Symposium on Water Pollution Research, Burlington, Ontario.

Richards, A. F., and Zuidberg, H. M., 1985, "In-Situ Determination of the Strength of Marine Soils," *Strength Testing of Marine Sediments: Laboratory and In-Situ Measurements, ASTM STP 883*, R.C. Chaney, K.R. Demars, Eds., Philadelphia, PA, pp. 11-13.

Rukavina, N.A., and Caddel, S., 1997, "Applications of an Acoustic Sea-Bed Classification System to Freshwater Environmental Research and Remediation in Canada," *Proceedings of the Fourth Conference on Remote Sensing for Marine and Coastal Environments*, Orlando, Florida, pp. I-317-I-329.

Terzaghi, K., and Peck, R. B., 1968, *Soil Mechanics in Engineering Practice*, 2nd Ed., First Corrected Printing, Wiley, New York.

Tuchman, M., Bolattino, C., and Miller, J., 1997, "*Solving Great Lakes Contaminated Sediment Problems*," Proceedings of the National Conference on Management and Treatment of Contaminated Sediments. Cincinnati, Ohio, May 13-14, 1997.

Zeman, A. J., and Patterson, T. S., 1997, "*Results of In-Situ Capping Demonstration Project in Hamilton Harbour, Lake Ontario*," International Symposium on Engineering Geology and the Environment, Athens, Greece, June 23-27, 1997.

Zeman, A. J., and Patterson, T. S. 2000, "*Results of Physical, Chemical and Biological Monitoring at the In-Situ Capping Site in Hamilton Harbour*," Contribution 00-088, National Water Research Institute, Burlington, Ontario.

Zeman, A. J., and Patterson, T. S., 2002: "Sediment Physical Parameters and Techniques", in: "*Environmental Monitoring Handbook*", Burden, F. R., McKelvie, I., Förstner, U., Guenther, A. (Editors), McGraw-Hill Companies, Inc., New York, pp. 15.1-15.20.

Ann-Laure Moreau,[1] Jacques Locat,[2] Philip Hill,[3] Bernard Long,[4] and Yvon Ouellet[5]

In situ Flume Measurements of Sediment Erodability in Saguenay Fjord (Quebec, Canada)

Reference: Moreau, A-L., Locat, J., Hill, P., Long, B., and Ouellet, Y., "**In situ Flume Measurements of Sediment Erodability in Saguenay Fjord (Quebec, Canada),**" *Contaminated Sediments: Characterization, Evaluation, Mitigation/Restoration, and Management Strategy Performance, ASTM STP 1442*, J. Locat, R. Galvez-Cloutier, R. C. Chaney, and K. R. Demars, Eds., ASTM International, West Conshohocken, PA, 2003.

Abstract: The erodability of surficial sediment in Saguenay Fjord, Quebec, was investigated over a three-year period at fourteen sites in Baie des Ha! Ha! and the North Arm using a benthic flume, *Miniflume*. Previous studies showed that Saguenay Fjord sediment characteristics vary greatly on small and large scales. The critical shear stress (τ_c) reflect this variability, with τ_c between 0.07 and 0.48 Pa. The measured critical shear stress and erosion rates were consistent with those of other *in situ* studies in other areas. The variability in the results is linked to the great spatial variability of benthic sediments rather than to temporal variability. Some of the results were integrated in the Parchure and Mehta (1985) erosion law since the upper portion of the active sediment layer is typically a stratified bed. The identification of erosion parameters (critical shear stress, erosion rate, parameters α and Ef in erosion law) and their high variability is the first step in defining the erosion susceptibility hazard in Saguenay Fjord.

Keywords: in situ measurements, erodability, erosion rate, critical shear stress, Saguenay Fjord, contaminated sediments, annular flume.

---

[1] Ph.D. student, Department of Geology and Geological Engineering, Laval University, Quebec, Canada G1K 7P4.

[2] Professor, Department of Geology and Geological Engineering, Laval University, Quebec, Canada G1K 7P4.

[3] Marine Sedimentologist, Natural Resources Canada, Geological Survey of Canada, P.O. Box 6000, Sidney, B.C., V8L 4B2.

[4] Professor, INRS-ETE, 880 Chemin Ste-Foy, C.P. 7500, Québec, Canada G1V 4C7.

[5] Professor, Civil Engineering Department, Laval University, Quebec, Canada G1K 7P4.

Introduction

A flash flood that occurred in July 1996 in the Saguenay area (Quebec) (Figure 1), deposited a bed of cohesive sediment, on average10-60 cm thick (but locally up to 5 m thick in the proximal delta environment) over an area of 65 km² of the deep fjord basin of the upper reaches of the Saguenay Fjord (Pelletier et al. 1999). This new layer, called the 1996 layer, is expected to act as a capping layer over underlying contaminated sediments. Industrialization of the upper reaches of the Saguenay valley during the 19th and 20th centuries resulted in significant pollution of the benthic environment in the fjord, with organic matter, heavy metals and polyaromatic hydrocarbons (PAH) being the principal pollutants (Schafer et al. 1990). This research is part of a multidisciplinary research project aimed at determining the efficiency of the 1996 layer to act as a capping layer. This paper reports on studies of the erodability of surficial sediment in Saguenay Fjord. The underlying hypothesis is that contaminants that diffuse through the 1996 layer from underlying sediments may be re-suspended through current-induced erosion of the surficial layer.

Over most of the study area the 1996 layer consists of cohesive silty clay. There are two possible approaches to the study of cohesive sediment erosion: laboratory methods (Villaret 1987, Dennett 1995) and in situ methods (Amos et al. 1992, 2000, Amos and Gibson 1994, Maa et al.1993, 1998). Due to the complexity of the natural bed sediments and dependence of the sediment properties on physical, chemical and biological properties, it was decided to study erodability in situ so as to avoid the need to transfer sediment from the field to the laboratory. To achieve our objectives a medium size annular flume, called *Miniflume*, was used (Amos et al. 2000). Constant geometry, existence of a completely-developed boundary layer above the sediments, no pumps to break down the suspended aggregates (such as fecal pellets and flocculated sediment) are the principal advantages of an annular flume (Widdows et al. 1998). Paradoxically, the principal disadvantage results from the geometry since the curvature of annular flumes brings about the occurrence of secondary radial flows (Maa et al. 1993, Ravens and Gshwend 1999). However this disadvantage can be minimized by reducing the channel width (Fukuda and Lick 1980). The medium size of the *Miniflume* allows easy deployment and provides measurements that take into account the most significant physical and biological parameters affecting erodability (Widdows et al. 1998).

Erodability is often characterized by the erosion threshold (τ_c) (Pa) and erosion rate (E) (kg.m^{-2}.s^{-1}) although there is not a uniform definition for the erosion threshold (Young and Southard 1978, Amos et al. 1992, Maa et al. 1998, Ravens and Gschwend 1999). In the same way, erosion rate (E) has been described by several mathematical expressions. Ariathurai and Arulanandan (1978) used linear expressions, Mehta et al. (1982) and Parchure and Mehta (1985) proposed an exponential expression, while Kusuda et al. (1984) used a power-law expression. All these expressions are based on excess bed shear stress. There are also power law expressions based on applied bed shear stress (Lavelle et al. 1984) that imply that a critical value of the bed shear stress does not exist, and a generalized exponential expression based on bed shear strength (Lee et al. 1994, Dennett 1995). Some of these expressions are appropriate for a uniformly deposited bed (linear expression) while others apply to stratified deposits (exponential expression based on excess bed shear stress). 1996 layer corresponds to several pulses of sedimentation due to turbidity currents (Crémer et al. 2002). It is composed of sediments (sable and silt) set up by traction overlain by sediments (silty clay) set up by settling (Crémer et al. 2002), which correspond to a stratified deposit (Villaret 1987).

In this study, the results of three annual deployments are presented and discussed. The spatial and temporal trends are examined for stations distributed over the study area (Figure 1). Some of the results were compared to the Parchure and Mehta (1985) erosion law since the upper portion of the active sediment layer is typically a stratified bed.

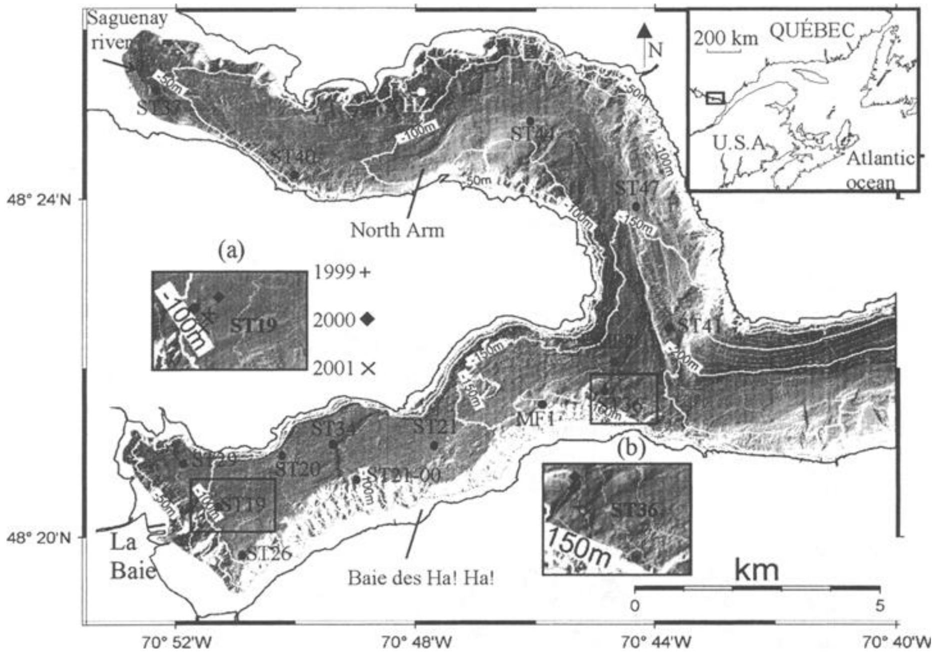

Figure 1 - *Location of Saguenay Fjord and Miniflume Deployment Sites. (a) ST19 Position in 1999, 2000 and 2001 and (b) ST36 Position in 1999, 2000 and 2001.*

Environmental Setting

The Saguenay Fjord is the largest fjord in eastern Canada. It joins the St. Lawrence estuary at Tadoussac about 180 km northeast of Quebec City (Figure 1). The Fjord occupies a drowned valley, 93 km long and 1-6 km wide, incised into the crystalline rocks of the Canadian Shield. It has a typically U-shaped cross-section and has high rock walls from 366 m above to 274 m below sea level. The Fjord may be divided into three sections: the main Fjord, Baie des Ha! Ha! and the North Arm. The study area includes the North Arm and Baie des Ha! Ha!. It is characterized by sandy, silty clay sediments and water depths ranging from 40 to 180 m. The North Arm is the area where fresh waters from the Saguenay River encounter the marine waters from the Fjord (Drainville 1967). Ninety percent of the freshwater runoff into the Fjord is derived from this river, which is about 63 km long and has a mean monthly discharge rate of 1500 $m^3 \cdot s^{-1}$. The natural flow regime of the river has been regulated by a series of hydro-electric dams built between 1923 and 1943 (Schafer et al. 1990).

Miniflume

Description and Data Obtained

The *Miniflume* is an annular benthic flume made of acrylic. It is 30 cm high, has a 29 cm outer diameter and a 20 cm inner diameter, resulting in a 4.5 cm wide channel with a total bed area of 0.0346 m^2 and a maximum flow volume about 0.01 m^3 (Figure 2). The flume is open at the base and totally enclosed at the top. Below the top lid, there are four square equidistant paddles embedded in a second, rotating lid. The flume, a batteries pack housing and an electronics housing are mounted on a tubular frame (Figure 2), which is placed on the sediments. This frame provides stability for the flume, while four springs maintain a downward pressure on the flume (10 kg force) once deployed, thus allowing the flume to encapsulate the local bed properties as well as those of the near bed waters. A camera (Figure 2) can be installed on the frame, but during this study it only functioned in 1999 and only for some stations. A Seapoint® Optical Backscatter Sensor (OBS) monitors turbidity at a height of 12 cm above the base. At the same height, opposite the OBS, a sample port was installed for purposes of sensor calibration.

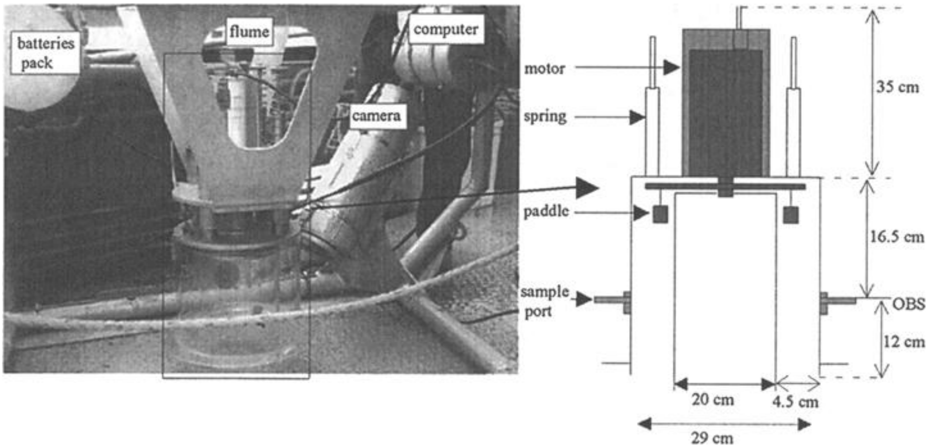

Figure 2 - *Photo of Miniflume on Its Frame and Schematic Diagram Showing Miniflume in Cross Section.*

The raw data recorded during an experiment include motor voltage (mV) and OBS response (mV). The relationship between the motor voltage (M), lid rotation (R), and azimuthal current speed 10 cm above the bed (u_{10}) is: $R = 1.22\times10^{-4} M$ (m.s^{-1}), and $u_{10} = 0.54 R$ (m.s^{-1}). Due to the non-linear response of the motor for a given gear ratio, the minimum speed of the lid is 0.16 m.s^{-1}. Before and after each deployment, the lid rotation was verified. Determination of friction velocity (u_*) (m.s^{-1}) and bed shear stress τ_b from the *Miniflume* are described in Amos et al. 2000.

Experimental Procedure

An identical four-phase experimental protocol was used over the three years of deployment. The first phase incorporates a start delay. The depth of the deployment sites varied between 47 and 192 m, and even if the flume was paid out very slowly to minimize seabed disturbance on landing, a sediment cloud would be created on impact. In order to obtain data which correspond as closely as possible to sediment erodability in undisturbed conditions, a one hour delay was maintained before recording the OBS data. This delay was determined using video recording. They show that after one hour the cloud had completely disappeared. The second phase was a period of recording during a still-water episode in order to determine the initial concentration in the flume without applied shear stress and thus the offset of the OBS (Figure 3). The duration of this period was 5 - 30 minutes. In the third phase (erosion), flow was increased in a series of eight steps. The first four steps were of equal duration with times between 5 and 30 minutes. The final four steps were twice as long. The final lid speed was selected based on the expected erosion characteristics of each site. Since the minimum lid speed is 0.16 m.s^{-1},the first steps of erosion phase can present the same value for shear stress applied on the bed (Figure 3). The last phase was a settling period of five steps, four with approximately 0.16 m.s^{-1} lid speed and one with a 0 m.s^{-1}. All steps had a duration between 5 and 30 minutes. Between each settling step, the lid was accelerated to the maximum speed for 1 to 3 minutes in order to resuspend settled material.

Determination of Erosion Rate (E) and Critical Shear Stress (τ_c)

Erosion rate (E) (kg.m^{-2}.s^{-1}) was evaluated as the rate of change of suspended mass (S) in the flume. In order to determine the mass concentration of sediment in suspension (S), the OBS sensor was calibrated in a laboratory with in situ sediment from each deployment site because many characteristics of the sediments, such as color (level of blackness), mineralogy (variation of refraction index of particles), shape of the particles, percentage of fines compared to sand, can influence OBS response (Sutherland et al. 2000, Hatcher et al. 2000). Suspended sediment concentration was increased gradually and, for each increase, samples were collected from the sample port. Each sample was filtered through pre-weighed, 25 mm, glass fibre GFC® filters, dried for 48 hrs at 40°C, and re-weighed. Each calibration curve consists of 5 to 7 points and the correlation coefficient (r^2) was between 0.97 and 1. Knowing the concentration of sediment in suspension (S) the erosion rate (E) can be determined from:

$$E = \frac{\Delta m}{\Delta t} = \frac{S_{t+\Delta t} - S_t}{\Delta t} \times \frac{V}{a} \tag{1}$$

where m is the eroded dry mass, V is the flume volume and a is the flume bed area. Study of trends in the erosion rate through time (Amos et al. 1997), allows determination of the erosion type (I or II) as defined by Mehta and Partheniades (1982). Type I erosion shows an asymptotic decrease in erosion rate with time whereas Type II erosion shows continuous erosion rate with time.

At the beginning of the erosion process, the particle size of suspended sediment is so small that they are not easily detectable and determination of the threshold of erosion is not possible, even with a sophisticated apparatus. An alternative method is the use of a mathematical extrapolation. One of the calculation methods consists of applying a stress on the bed until erosion ceases (Amos et al. 1997). It is supposed that erosion continues until the critical shear stress of the new exposed surface exceeds the stress induced by the moving fluid. The speed of the liquid is then increased in a series of steps. A regression of sediment concentration (OBS response) with bed shear stress is applied. Logarithmic plots are used because they provide a better fit for the lower levels of erosion (Amos et al. 1997). The intercept of the straight line regression with the offset of the OBS during the still-water episode, or the fit of the regression line for a series of steps gives the critical shear stress (τ_c) (Amos et al. 1994).

Site Deployment

Over three years, 50 in situ deployments were made at 14 different stations: 6 stations in the North Arm and 8 in Baie des Ha! Ha! (Figure 1). Nine deployments gave unusable results due to a bad connection between the OBS, motor and computer or open communication between water in the flume and the ambient water. Forty one deployments gave usable results. These correspond to results, which allowed the determination of an erosion threshold. Twenty six present a concentration plateau during each erosion step. For 6 stations, ST19, ST34, ST21, ST41, ST47, ST44, we obtained usable results for the three years. For several stations several deployments were carried out during the same year. Two usable results were obtained at stations ST19, ST34, ST36 in 2000 and 2001, at stations ST21, ST40, ST37, HZ in 2001, at station ST41 in 1999 and three at station ST47 in 2001 (Table 1). Typically, a station corresponds to a circular area with a diameter between 45 and 416 m except for ST21. The deployment at ST21 in 2000 is about 1600 m from deployments in 1999 and 2001 due to a positioning error. For the other stations, the difference between deployment locations is related to the difficulty in deploying the *Miniflume* in deep water.

Table 1 - *Critical Shear Stress (τ_c) (Pa), Maximum Bed Shear Stress (τ_{max}) (Pa) Applied during each Miniflume Deployment. Real τ_{max} Correspond to the Last Bed Shear Stress using for Determined (τ_c), After Real τ_{max} there was Saturation (Pa). E_{mean} is the Mean Erosion Rate for all the Erosion Phases ($kg.m^{-2}.s^{-1}$), conc is the Minimum and Maximum Concentration Recorded during Erosion Phases, Type is the SSC Response Type.*

	2001						2000						1999					
station	τ_c (Pa)	τ_{max} (Pa)	real τ_{max} (Pa)	conc ($mg.l^{-1}$)	E_{mean} ($kg.m^{-2}.s^{-1}$)	type	τ_c (Pa)	τ_{max} (Pa)	real τ_{max} (Pa)	conc ($mg.l^{-1}$)	E_{mean} ($kg.m^{-2}.s^{-1}$)	type	τ_c (Pa)	τ_{max} (Pa)	real τ_{max} (Pa)	conc ($mg.l^{-1}$)	E_{mean} ($kg.m^{-2}.s^{-1}$)	type
ST29													0.42	0.8	0.8	354-639.1	4.88E-05	A
ST19	0.1	2.59	0.91	191.6-2237.6	5.13E-05	A	0.22	1.09	1.09	102.3-298.9	5.05E-06	B	0.35	2.22	1.7	99.2-2237.6	3.42E-04	A
ST19	-	1.15	1.15	-	-	A	0.29	1.15	1.15	102.8-135.5	6.17E-07	B						
ST20													0.24	0.8	0.8	181-5-774.8	7.70E-05	A
ST26													-	-	-	-	-	
ST34	0.48	1.42	1.09	378.1-2220.5	2.40E-04	A	0.34	1.42	1.42	3.4-1004.9	5.47E-05	B	0.38	1.42	1.42	1574.9-2220.5	1.15E-04	A
ST34	0.26	0.8	0.8	193-1327.2	7.28E-05	A	0.14	1.42	0.8	20.2-2220.5	8.55E-05	A						
ST21	0.20	1.15	0.65	616-1538.4	1.13E-04	A	0.23	1.15	1.15	194.7-1529.1	8.29E-05	A	0.38	1.8	0.7	333.9-1538.4	-	A/B
ST21	0.27	0.8	0.61	334.1-1538.4	1.72E-04	A												
MF1	-	2.59	-	-	-		0.33	1.15	1.15	102.3-394.3	1.65E-05	B						
MF1	0.19	2.05	0.8	85.7-1894.5	1.49E-04	A												
ST36	-	1.42	-	-	-		0.31	1.15	1.15	157.4-245.8	2.42E-06	B	-	-	-	-	-	
ST36	0.30	1.42	1.09	408.9-1820.7	1.44E-04	A	0.35	1.15	1.15	157.8-253.7	5.02E-06	B						
ST36	0.25	1.15	0.88	455.6-1820.7	1.61E-04	A												
MF2							0.16	1.15	1.15	102.2-1562.9	7.35E-05	A						
ST41	0.19	1.15	1.15	32.1-1388.9	9.20E-05	A	0.15	1.15	1.15	40.5-1388.9	6.76E-05	A	0.38	1.42	1.09	0.9-1388.9	1.78E-04	A
ST41													0.13	0.8	0.8	10.6-279.4	1.37E-05	A
ST47	0.07	1.42	0.8	423.9-1637.3	2.18E-04	A	0.29	1.15	1.15	174.2-870.4	3.58E-05	B	0.31	0.8	0.8	-	-	B
ST47	0.16	1.15	0.65	296.7-1637.3	2.06E-04	A												
ST47	0.14	0.8	0.61	218.5-1637.3	1.23E-04	A												
HZ	0.42	1.41	1.09	387-2146.7	8.36E-05	A												
HZ	0.17	1.15	1.15	202.2-1802.2	1.54E-04	A												
ST44	0.22	1.42	1.42	180-2041.9	1.12E-04	A	0.09	1.15	1.15	157.2-907.4	2.77E-05	B	0.15	2.22	0.87	154.3-2041.9	1.68E-04	A
ST40	0.22	1.15	0.88	187.1-2066.6	1.61E-04	A	0.12	1.15	1.15	161-2066.6	9.90E-05	A	-	-	-	-	-	
ST40	0.23	1.42	1.09	328.1-2066.6	3.12E-04	A												
ST37	-	2.59	-	-	-		-	1.15	1.15	-	-	B	-	-	-	-	-	
ST37	0.14	2.59	1.01	82.7-1709.9	2.65E-04	A												
ST37	0.21	1.42	1.09	44.1-1709.9	8.57E-05	A												

Results

Suspended Sediment Concentration Profiles

For each profile, the time dependent erosion response is characterized by a maximum erosion rate immediately after application of a higher shear stress (Piedra Cueva and Mory 2001). The OBS response, i.e. the suspended sediment concentration (*SSC*), following an acceleration step can be divided into two groups: most of the profiles (Type A) show a rapid increase of *SSC* followed by a concentration plateau or a slower increase until the next step (Figure 3 and Table 1). Ten profiles (Type B) show an increase at the beginning of the step of the SSC followed by a decrease while the rotation speed was held constant (Figure 3 and Table 1). Nine of the ten Type B profiles were obtained in 2000 (ST19, ST34, MF1, ST36, ST47, ST44, ST37) and one in 1999 (ST47).

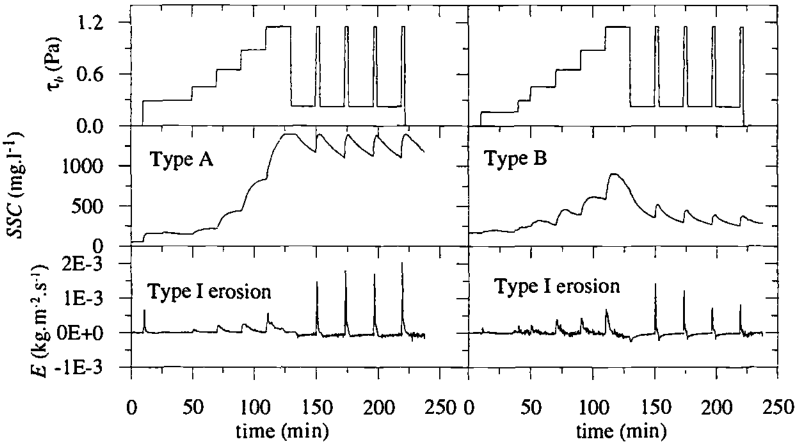

Figure 3 - *Bed Shear Stress (τ_b, Pa) and Suspended Sediment Concentration (SSC, mg.l^{-1}) (Pa) Obtained using Laboratory OBS Calibration and Erosion Rate (kg.m^{-2}.s^{-1}) (Equation 1) for an Example of Type A SSC Profile (ST41, 2000) (left) and Type B SSC Profile (ST44, 2000) (right).*

The same station may show different *SSC* profiles, Type A or Type B, between deployments in the same year (Table 1: ST34 in 2000; Figure 4a) or from one year to the next (Table 1: ST19, MF1, ST36, ST47, ST44; Figure 4d). For deployments at the same station in the same year, with identical bed shear stress profiles, the suspended sediment concentration response is quantitatively similar (Figure 4c) with the exception of experiments at station ST34 in 2000 and at station ST41 in 1999. At station ST34 (2000), the same bed shear stress profile was applied but the duration of steps was doubled. The concentration obtained for the longer steps were significantly greater (Figure 4a). At station ST41 (1999), a much higher concentration increase was observed during the first step for one of the experiments, presumably due to the presence of a very loose layer at the seabed (Figure 4b). From one year to the next, however, the suspended sediment concentration at the same station may differ by an order of magnitude, as is the case with ST19, MF1, ST36 (Figure 4d), ST47 and ST44 (Table 1). Concentrations obtained for Type B response are always lower than the concentration for Type A (Table 1).

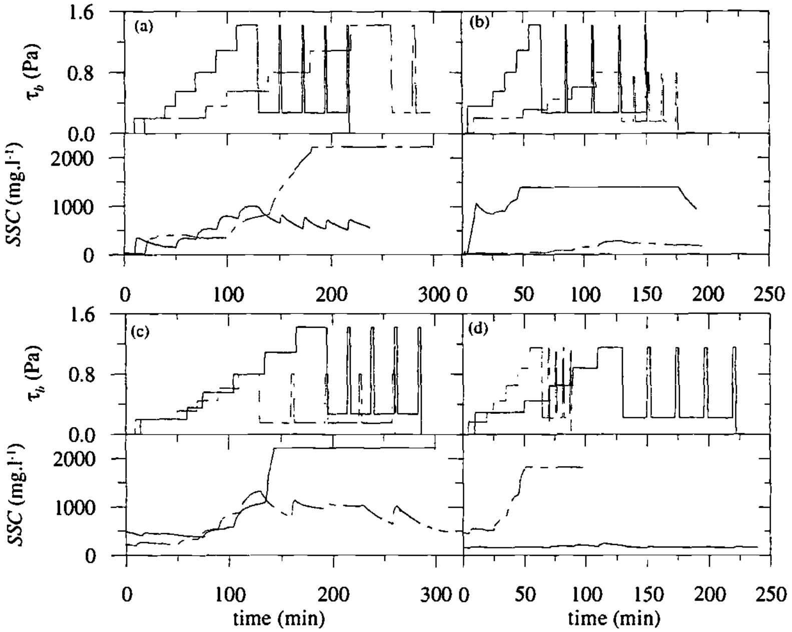

Figure 4 - *Bed Shear Stress (τ_b, Pa) and Suspended Sediment Concentration (SSC, mg.l^{-1}) Obtained for Different Stations: (a) Station ST34 for Two Deployments in 2000 with Duration of Steps Doubled Between the Two. Dashed Line Represent the Second Deployment [ST34-00(2)]; (b) ST41 for Two Deployments in 1999, Dashed Line Represent the Second Deployment [ST41-99(2)]; (c) Station ST34 for Two Deployments in 2001; for the Same Bed Shear Stress, Concentrations are Similar; (d) ST36 in 2000 (Solid Line) and in 2001 (Dashed Line) (ST36-01(3)). Type B Shows Concentration Ten Times Smaller than Type A.*

Erosion Rate

For all the stations, the erosion rate shows an asymptotic decrease with time for each step (Figure 3) corresponding to Type I erosion as defined by Mehta and Partheniades (1982). The peak erosion rate (E_{max}) and mean erosion rate (*Em*) were evaluated for each acceleration step. The peak erosion rate is the maximum value within any increment of flow (Amos et al. 1992, 1996, Widdows et al. 1998, Houwing 1999). It varies between 1.02×10^{-5} and 2.55×10^{-3} kg.m^{-2}.s^{-1}. In contrast to Amos et al. (1996), no significant relationship was found between E_{max} and the applied bed shear stress. *Em* appeared to show a relationship with the applied current speed (U_{10}) taking the exponential form:

$$E_m = 6.31\times10^{-7}.10^{(11.47\,U_{10})},\quad r^2 = 0.63,\quad n = 101 \qquad (2)$$

Considering the diversity of sites, the correlation is notable. Amos et al. (1998) judged the correlation for a mudflat in the Humber estuary with a $r^2 = 0.55$ and n = 100 to be noteworthy. The mean erosion rate for the total erosion phase (E_{mean}) varies between 3.42×10^{-4} and 6.17×10^{-7} kg.m^{-2}.s^{-1} and is smaller for Type B response (Table 1). Stations in the North Arm always show a E_{mean} higher than 2×10^{-5} kg.m^{-2}.s^{-1}. Figure 5 shows a plot of E_{mean} and (τ_c) as a function of along-axis distance, measured from La Baie city in Baie des Ha! Ha! and from station ST37 in the North Arm. The graph shows no relation between E_{mean} and distance. Similarly, there is no temporal trend in erosion rate (Table 1, Figure 5).

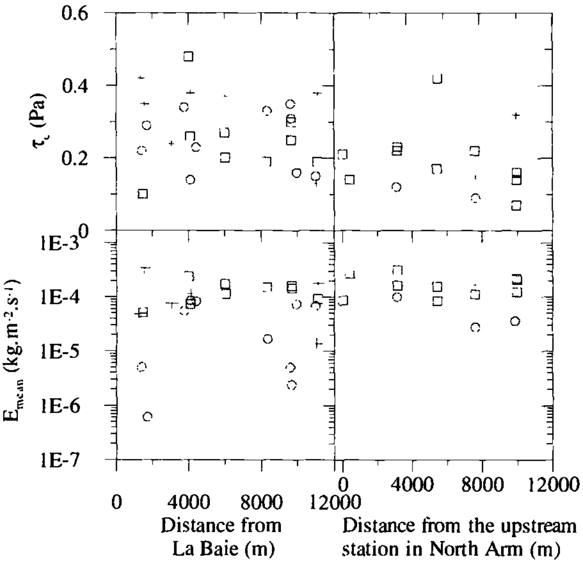

Figure 5 - *Erosion Threshold and Mean Erosion Rate Along Axis Distance are Measured from La Baie city in Baie des Ha! Ha! and from the Upstream Station in the North Arm (Station ST37-01(3)). Crosses Represent 1999 Data, Circles 2000 Data and Squares 2001 Data.*

Critical Shear Stress

For each usable result, the critical shear stress (τ_c) (Pa) and bed shear stress of the last step before saturation (*real* τ_{max}) were determined (Table 1). The *real* τ_{max} varies between 0.61 and 1.7 Pa and τ_c between 0.07 and 0.48 Pa. The average value of τ_c is 0.24 Pa with a standard deviation of 0.10. The value of τ_c for stations ST21, MF1, ST47 is greater when they show a Type B response (Table 1) and is of the same order for Type A and B responses for station ST34, ST36 and ST44. For the same station, τ_c values in Baie des Ha! Ha! are more variable than in the North Arm. As for erosion rate, there is no temporal trend in critical shear stress (τ_c), the spatial variability is important on small and large scale (Figure 5).

Erosion law

The time-rate of increase of suspended sediment mass per unit bed area, m, is given in the functional form:

$$\frac{dm}{dt} = f(\tau_b - \tau_s,\ \upsilon_1,\ \upsilon_2, \dots \upsilon_n) \tag{3}$$

where τ_b is the bed shear stress, τ_s is the bed shear strength, (τ_b-τ_s) is the excess bed shear stress, and , v_1, v_2,..., v_n are parameters which define erosion resistance (Mehta 1989). The bed shear strength may be used interchangeably with the critical shear stress τ_c. From experiments on unconsolidated cohesive sediments in stratified deposits, Parchure and Mehta (1985) determined an exponential expression based on excess shear stress:

$$\ln \frac{E}{E_f} = \alpha(\tau_b - \tau_s)^{1/2} \tag{4}$$

where E_f is defined as the floc erosion rate (kg.m^{-2}.s^{-1}), α is an empirical coefficient (m.N$^{-½}$), τ_s or $\tau_{c(z)}$ is the bed shear strength (Pa), and E is the erosion rate over ten minutes for each acceleration step. The value of Δt used in (1) is always equal to 10 minutes in order to homogenize the results (Hydraulics Research Station 1980, Amos et al. 1996). In equation (7) $\tau_b - \tau_s$ is determined from concentration profiles that showed a plateau for each erosion step. A concentration plateau indicates that there is no more erosion and that the bed shear stress equals the critical shear stress. Twenty six deployments demonstrate this behavior (Table 2).

The α values from the twenty six tests vary between 3.92 and 23.92 m.N$^{-½}$, and the floc erosion rate between 3.74×10^{-9} and 1.56×10^{-5} kg.m^{-2}.s^{-1} (Figure 6). Floc erosion rate and α are connected by an exponential relation (5):

$$E_f = 1.10\times10^{-4} \exp[-0.43\ \alpha],\ r^2 = 0.92,\ n = 26 \tag{5}$$

Table 2 - *Values of Erosion Threshold* τ_c *(Pa), Floc Erosion Rate* E_f *(kg.m*$^{-2}$*.s*$^{-1}$*) and Empirical Coefficient* α *(m.N*$^{-1/2}$*) for Stations having Concentration Plateau for Erosion Steps. –99 Results obtained in 1999, -00 in 2000 and –01 in 2001. (1) Results obtained for the First Test, (2) the Second and (3) the Third at the "Same" Station.*

Station	τ_c	α	E_f	Station	τ_c	α	E_f
ST19-99	0.35	3.92	8.77E-06	ST41-00	0.15	11.99	4.67E-07
ST19-1	0.1	5.04	1.28E-05	ST41-01	0.19	12.55	3.88E-07
ST20-99	0.24	12.72	5.41E-07	ST47(2)-01	0.16	16.85	2.68E-07
ST34-99	0.38	12.06	2.04E-07	ST47(3)-01	0.14	12.92	1.06E-06
ST34(1)-01	0.48	7.42	7.81E-06	ST44-99	0.15	11.97	5.88E-07
ST34(2)-01	0.26	5.45	1.56E-05	ST44-01	0.22	12.25	3.14E-07
ST21-00	0.23	6.19	6.56E-06	HZ(1)-01	0.42	7.97	4.35E-06
ST21(2)-01	0.27	9.35	8.25E-06	HZ(2)-01	0.17	13.07	4.58E-07
MF1-01	0.19	12.08	4.36E-07	ST40-00	0.12	23.62	4.45E-09
ST36(2)-01	0.30	5.65	1.10E-05	ST40(1)-01	0.22	23.92	3.74E-09
ST36(3)-01	0.25	8.98	4.57E-06	ST40(2)-01	0.23	13.82	3.64E-07
MF2-00	0.16	12.60	3.94E-07	ST37(2)-01	0.14	7.72	4.79E-06
ST41(2)-99	0.13	10.83	4.24E-07	ST37(3)-01	0.21	14.78	1.31E-07

The erosion law determined by Mehta et Parchure 1985 for stratified sediment fits quite well for each set of results, but a general law would have a determination coefficient (r^2) equal to 0.58:

$$E = 4.98.10^{-6} \times \exp\left[7.26(\tau_b - \tau_s)^{1/2}\right], \quad r^2 = 0.58, \quad n = 101 \tag{6}$$

Discussion

Type B Response

Similar Type B behavior has been observed in other in situ studies in lower Chesapeake Bay and Baltimore Harbor (Maa et al. 1993, 1998). These investigators suggested several possible explanations: (1) a leakage from the flume; (2) decrease of the skin friction shear stress due to suspension of surface sediment; (3) greater annulus acceleration at the beginning of a step resulting in a larger initial bed shear stress than can be maintained during the rest of the step, resulting in redeposition of the larger sediment particles. Maa et al. 1998 concluded that leakage was the predominant factor in their experiments, caused by a dynamic pressure difference and imperfect sealing between the rotating ring and the two side walls. In the present study, Type B profiles are always associated with lower *SSC* (Figure 3, Figure 4d and Table 1) suggesting that a decrease of the skin friction shear stress due to the suspension of surface sediment is not a significant factor. Leakage from the *Miniflume*, while possible given the often irregular meso-scale morphology of the Fjord bottom, is considered unlikely. The VIMS *Sea Carousel* used by

Maa et al. (1993, 1998) is much larger than *Miniflume*, and probably allows more leakage. It is more likely that mechanical limitations of the motor, resulting in a larger initial bed shear stress (hypothesis 3) explains the Type B occurrences. A small decrease in concentration during the first step in Type A profiles, when annulus acceleration is maximal, supports this interpretation.

Erosion Rate and Critical Shear Stress

Two different interpretations of erosion Types have traditionally been suggested. Type I erosion (depth-limited) is manifested as a decrease in the erosion rate as a function of depth while Type II erosion (unlimited) occurs as a continuous function of time. Conceptually, Type I erosion has been viewed as a surface phenomenon caused by entrainment of small aggregates and flocs (Amos et al. 1992, 1997). Type II erosion is characterized by failure along thin planes of weakness within the sediments, probably related to the sediment microfabric generated after deposition (Amos et al. 1992), enlargement of surface irregularities, and subsequent undercutting and release of large aggregates. Type II erosion is typically associated with erosion of deeper sediment. However, Sanford and Maa (2001) suggest a formulation that relates the two types. If the time scale of the shear stress step is long compared to the time scale for depletion of erodible sediment, then the erosion will appear to be Type I (Parchure et Mehta 1985, Maa et al. 1998, Piedra Cueva et Mory 2001). Otherwise, it will appear to be Type II (Gust et Morris 1989, Tolhurst et al. 2000). The same sediment bed can exhibit Type I erosion or Type II erosion, or some intermediate state (Amos et al. 1996) depending on the nature of the forcing (Sanford and Maa 2001).

Since all the experiments in the present study show Type I erosion whatever bed shear stress is applied, it is likely that the time scale for depletion of erodible sediment is shorter than the time scale of the erosion step of the experiment and the bed shear stress applied was only sufficient to cause shallow erosion.

E_{mean} and τ_c are variable, both in time for single stations and between different stations; there is no obvious trend. Variability is more noticeable in Baie des Ha! Ha! but probably only because more measurements were obtained in this area (Figure 5). To the authors' knowledge, this is the deepest water in which in situ experiments have been made. The quality of the in situ flume measurements at these depths is more difficult to establish than for shallower water. Nevertheless, for the experiments when the video camera was recording, it was observed that the frame maintained a stable base for the flume and that there was no communication between the flume and the ambient water. While, in spite of all the precautions, some results were still unusable and may be attributed to equipment problems, it is more likely that the natural heterogeneity of surficial sediment in Saguenay Fjord is a significant factor in the variability. Locat et al. (2000) defined several geomorphologic units in Saguenay Fjord, which contributes to highly variable meso-scale topography (Hill et al. 1999). Heterogeneity in bioturbation of the recently deposited bed (Maurice 2000) also strongly influences surficial roughness resulting in local heterogeneity of the physical properties (water content, particle size, reflectivity) of surficial sediment (Schmitt 2001).

Prediction of Suspended Sediment Concentration in Miniflume

Comparison with previous studies - The α and E_f values determined for the different sites in Saguenay Fjord have a large range (Table 2, Figure 6) but they have been determined over a small range of square root of excess shear stress (0.14 to 0.67 Pa) (Figure 7). In order to compare these results with previous investigations, published data from both in situ and laboratory studies were used (Table 3).

Table 3 - *Values of Floc Erosion Rate E_f (kg.m^{-2}.s^{-1}) and Empirical Coefficient α(m.N$^{-1/2}$) for Previous Studies.*

Investigators	Bed	α	E_f
- Partheniades (1965)	bay mud	8.3	6.67E-08
- Lee (1979)	lake mud	8.3	7.00E-07
- Thorn and Parsons (1977)	estuarial mud	8.3	7.00E-07
- Thorn and Parsons (1979)	estuarial mud	4.2	3.10E-06
- Dixit (1982)	kaolinite	25.6	1.00E-06
27 Parchure et Mehta (1985)	kaolinite+ tap water	18.4	8.33E-07
28 Parchure et Mehta (1985)	kaolinite+ salt water (35 ppt)	17.2	2.33E-06
29 Parchure et Mehta (1985)	lake mud + varying salinity water	13.6	5.33E-06
33 Caywood (1999)	kaolinite	2.48	2.36E-04
34 Caywood (1999)	Chalk bluff	2.07	8.86E-05
37 Caywood (1999)	mix	2.01	4.58E-05
38 Caywood (1999)	sand mix	2.34	2.18E-05

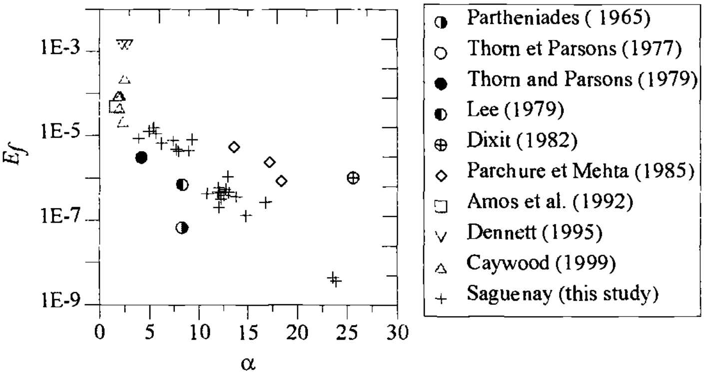

Figure 6 - *Floc Erosion Rate (Ef, kg.m^{-2}.s^{-1}) Versus α(m.N$^{-1/2}$) for This Study (Crosses) and Previous Studies.*

The α and E_f values from previous investigators correspond to sediment deposited in shallower water. Parchure and Mehta 1985 explained the differences between α values for the different authors in terms of a number of factors, including the bed preparation procedure, the characteristics of the apparatus used, the influence of temperature, the effect of relatively high sediment concentrations on bed shear stress, the influence of sediment type and the errors in estimating the magnitude of bed shear stress. The range of values obtained with *Miniflume* suggests that sediment characteristics (bioturbation, grain size...) are most important. Since, during this in situ study the same apparatus was used, there was no bed preparation, all stations presented the same temperature characteristics, relatively high sediment concentrations had no major effect on bed shear stress. Indeed, the algorithm of Amos et al. (1997) shows that drag reduction increases with both increasing *SSC* and applied shear stress and predicts a reduction in the friction velocity (u_*) of 1.24 % related to the maximum *SSC* (2.24 g.l^{-1}) and shear stress (1.7 Pa). Therefore, during the experiments drag reduction would not be significant.

The erosion rate for surficial sediments in Saguenay Fjord varies with the square root of excess shear stress within the same range as previous studies (Figure 7).

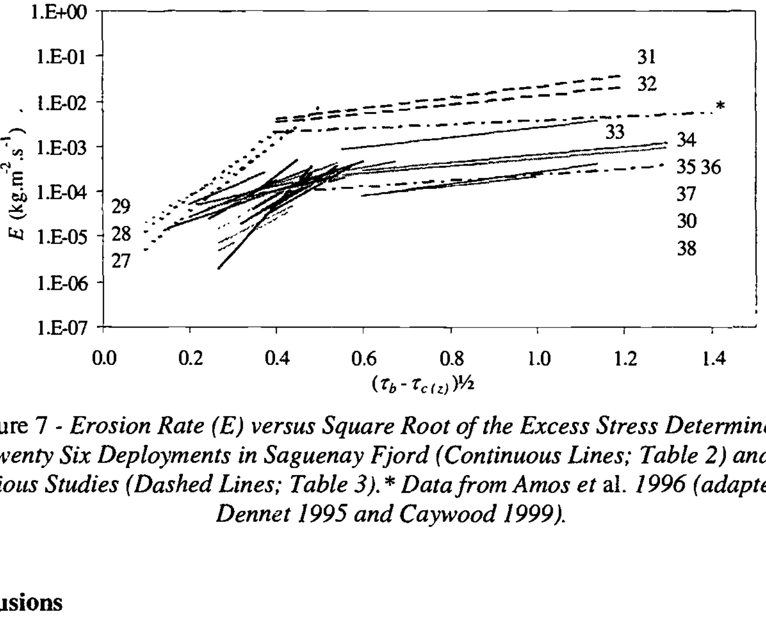

Figure 7 - *Erosion Rate (E) versus Square Root of the Excess Stress Determined for Twenty Six Deployments in Saguenay Fjord (Continuous Lines; Table 2) and for Previous Studies (Dashed Lines; Table 3).* Data from Amos et* al. *1996 (adapted from Dennet 1995 and Caywood 1999).*

Conclusions

The variability of the physical, chemical and biological properties of the area led to prefer an in situ study rather than a laboratory study in spite of the great depth of the Fjord. For the first time at such depths, a circular benthic flume, *Miniflume,* was used to measure the erodability of cohesive sediments. Typically, a station corresponds to a circular area within a diameter between 45 and 416 m.

Over three years, 41 deployments gave results which allowed the determination of an erosion threshold (τ_c). The values of τ_c ranged between 0.07 and 0.48 Pa.

Two types of *SSC* profiles were obtained. Type A, the most common profile, shows a concentration plateau for each acceleration step. Type B shows an increase at the beginning of the step followed by a decrease as the lid speed was held constant. Type B profiles were interpreted to be related to variations in lid rotation during the erosion step.

Excess lid acceleration at the beginning of a step appears to suspend larger particles, which redeposit during the latter period of the step.

For all the stations, the erosion rate shows an asymptotic decrease with time for each step corresponding to Type I erosion. The time scale for depletion of erodible sediment is shorter than the time scale of the erosion step and the bed shear stress applied was only sufficient to cause shallow erosion.

Mean erosion rates were between 3.42×10^{-4} and 6.17×10^{-7} $kg.m^{-2}.s^{-1}$ and were smaller for Type B profiles.

The erosion law determined by Mehta et Parchure 1985 for stratified sediment fits quite well for each Type A profile, but a general law would have a determination coefficient (r^2) equal to 0.58. Erosion rate versus square root of the excess stress for surficial sediments in Saguenay Fjord varies in the same range as previous studies.

Variability of Erosion thresholds, parameters α and *Ef* in erosion laws are partly related to the experimental conditions but mostly to the diversity of benthic sediment in Saguenay Fjord. No significant temporal variations were noticeable.

If surficial sediments contain contaminants diffused upwards from underlying sediments, they might be re-mobilized if the bottom current speed were sufficient. Erodability of surficial sediments and their associated pollutants in Saguenay Fjord is therefore of concern. Determination of benthic hydrodynamic conditions will be the second step in defining the erosion susceptibility hazard in Saguenay Fjord.

Acknowledgments

The authors thank the Geological Survey of Canada (Atlantic) for loan of the *Miniflume* and C. L. Amos for taking the time to demonstrate its use on the R/V Alcide C. Horth and during a cruise in the Woods Hole region. Financial support was provided by the Natural Sciences and Engineering Research Council of Canada, and Alcan of Canada Ltd. We greatly appreciate the assistance of the captain and crew of the R/V Alcide C. Horth. Geological Survey of Canada Contribution No. 2002110.

References

Amos, C. L., Daborn, G. R., Christian, H. A., Atkinson, A., and Robertson, A., 1992, "In situ erosion measurements on fine-grained sediments from the Bay of Fundy," *Marine geology*, Vol. 108, pp. 175-196.

Amos, C. L., and Gibson, J., 1994, "The stability of dredge material at Dumpsite B, Miramichi Bay, New Brunswick, Canada," *Geological Survey of Canada Open File Report*, N° 3020.

Amos, C. L., Sutherland, T. F., and Zevenhuizen, J., 1996, "The stability of sublittoral, fine-grained sediments in a subarctic estuary," *Sedimentology*, Vol. 43, pp 1-19.

Amos, C. L., Feeney, T., Sutherland, T. F., and Lutemauer, J. L., 1997, "The stability of fine-grained sediments from the Fraser River Delta," *Estuarine, Coastal and Shelf Science*, Vol.45, No.5, pp.507-524.

Amos, C. L., Brylinsky, M., Sutherland, T. F., O'Brien, D., Lee, S., and Cramp, A., 1998, "The stability of a mudflat in the Humber estuary, South Yorkshire, UK," *Sedimentary Processes in the Intertidal zone*. Geological Society, London, Special Publications, Vol. 139, pp. 25-43.

Amos, C. L., Sutherland, T. F., Cloutier, D., and Patterson, S., 2000, "Corrasion of a remoulded cohesive bed by saltating littorinid shells," *Continental shelf Research*, Vol. 20, pp. 1291-1315.

Ariathurai, R., and Arulanandan, K., 1978, "Erosion rates of cohesive soils," *Journal of Hydraulics Division, ASCE*, Vol. 104, No. HY2, pp. 279-283.

Caywood, C. L., 1999, "Determination of erosion rates of cohesive sediments in the Carson and Truckee Rivers," *Master of Science, University of Nevada, Reno,* 135 pp.

Crémer, J-F., Long, B., Desrosiers, G., de Montety, L., and Locat, J., 2002 "Application de la scanographie à l'étude de la densité des sédiments et à la caractérisation des structures sédimentaires : exemple des sédiments déposés dans la rivière Saguenay , Québec, Canada) après la crue de juillet 1996," *Journal Canadien de Géotechnique*, Vol. 39, pp. 440-450.

Dennet, K. E., 1995, "Flume studies of the erosion of cohesive sediments," *Thesis, Georgia Institute of Technology,* 238 pp.

Dixit, J. G., 1982, "Resuspension potential of deposited kaolinite beds," *Master of Science, University of Florida, Gainesville.*

Drainville, G., 1967, "Étude océanographique et ichtyologique du fjord du Saguenay," *Mémoire de maîtrise, Universitḉ du Québec à Montréal,* 166 pp.

Fukuda, M. K., and Lick, W., 1980, "The entrainment of cohesive sediments in freshwater," *Journal of Geophysical Research,* Vol. 85, No. C10, pp. 2813-2824.

Gust, G., and Morris, M. J., 1989, "Erosion thresholds and entrainment rates of undisturbed in situ sediments," *Journal of coastal Research*, Vol. 5, special issue, pp. 87-100.

Hatcher, A., Hill, P., Grant, J., and Macpherson, P., 2000, "Spectral optical backscatter of sand in suspension: effects of particle size, composition and color," *Marine Geology*, Vol. 168, pp. 115-128.

Hill, P. R., Côté, P., Locat, J., and the students of the UQAR Mission Stage, 1999, "Evidence for gravity-flow processes as the mechanism for basin-sedimentation in Baie des Ha! Ha!, Saguenay fjord, from sidescan sonar data," *Abstract, Canadian Meteorological and Oceanographic Society, Annual Meeting*, Montreal, May 31 - June 1, 1999.

Houwing, E-J., 1999, "Determination of the critical erosion threshold of cohesive sediments on intertidal mudflats along the Dutch Wadden sea coast," *Estuarine, Coastal and Shelf Science*, Vol. 49, pp. 545-555.

Hydraulics Research Station, 1980, "River Scheldt surge barrier. Study of estuarine sediments," *Internal Report*, No. EX928.

Kusuda, T., Umita, T., Koga, K., Futawatari. T., and Awaya, Y., 1984, "Erosional process of cohesive sediments," *Water Science and Technology*, Vol. 17, pp. 891-901.

Lavelle, J. W., Mofjeld, H. O., and Baker, E. T., 1984, "An in situ erosion rate for a fine-grained marine sediment," *Journal of Geophysical Research*, Vol. 89, No. C4, pp. 6543-6552.

Lee, D. Y., 1979, "Resuspension and deposition of lake Erie sediments," *Master of Science, Case Western Reserve University, Cleveland, Ohio.*

Lee, S. C., Mehta, A. J., and Parchure, T. M., 1994, "Cohesive sediment erosion: Part I-Test devices and field instrument assemblies; Part II- Relationship between the erosion rate constant and bed shear strength," *UFL/COEL/MP-94/02, Coastal and Oceanographic engineering*, University of Florida.

Locat, J., Urgeles, R., Schmitt, T., Martin, F. and Hoareau L., 2000, "The morphological signature of natural disasters in the upper Saguenay fjord area, Québec, Canada," *53rd Canadian Geotechnical Conference*, Vol. 1, pp. 109-116.

Maa, J. P. Y., Wright, L. D., Lee, C-H., and Shannon, T. W , 1993, "VIMS sea carousel : a field instrument for studying sediment transport," *Marine Geology*, Vol. 115, pp. 271-287.

Maa, J. P. Y., Sanford, L., and Halka, J. P., 1998, "Sediment resuspension characteristics in Baltimore Harbour, Maryland," *Marine Geology*, Vol. 146, pp. 137-145.

Maurice, F., 2000, "Caractéristiques géotechniques et évolution de la couche de sédiments déposée lors du déluge de 1996 dans la Baie des Ha! Ha! (fjord du Saguenay, Québec), " *Mémoire de maîtrise, département de géologie et génie géologique, Université Laval.*

Mehta, A. J., 1989, "On estuarine cohesive sediment suspension behavior," *Journal of Geophysical Research*, Vol. 94, pp. 14306-14314.

Mehta, A. J., and Partheniades, E., 1982, "Resuspension of deposited cohesive sediment beds," *Eighteenth Conference Coastal Engineering*, pp.1569-1588.

Mehta, A. J., Parchure, T. M., Dixit, J. G., and Ariathurai, R., 1982, "Resuspension potential of flocculated fine sediments," *Estuarine Comparisons*, V.S. Kennedy, Academic Press, New York.

Parchure, T. M., and Mehta, A. J., 1985, "Erosion of soft cohesive sediment deposits," *Journal of Hydraulics Engineering, ASCE*, Vol. 111, No 10, pp1308-1326.

Partheniades, E., 1965, "Erosion of cohesive sediments," *Journal of Hydraulics division, ASCE*, Vol. 91, No. HY1, pp. 105-139.

Pelletier, E., Deflandre, B., Nozais, C., Tita, G., Desrosiers, G., Gagné, J-P., et Mucci, A., 1999, "Crue éclair de juillet 1996 dans la région du Saguenay (Québec). 2. Impacts sur les sédiments et le biote de la baie des Ha! Ha! et du fjord du Saguenay," *Canadian Journal of Fisheries and Aquatic Sciences*, Vol. 56, pp. 2136-2147.

Piedra Cueva, I., and Mory, M., 2001, "Erosion of a deposited layer of cohesive sediments," MCAnally, W.H. Mehta, *Coastal and estuarine fine transport processes*, Elsevier, Amsterdam, pp. 41-52.

Ravens, T. M., and Gschwend, P. M., 1999, "Flume measurements of sediment erodibility in Boston harbour," *Journal of Hydraulic Engineering*, Vol. 125, No. 10, pp. 998-1005.

Sanford, L. P., and Maa, J. P. Y., 2001, "A unified formulation for fine sediments," *Marine Geology*, Vol. 179, pp. 9-23.

Schafer, C. T., Smith, J. N., and Côté, R., 1990, "The Saguenay Fjord : A major tributary to the St. Lawrence Estuary," *Coastal and Estuarine studies*, Vol. 39, pp. 378-419.

Schmitt, T., 2001, "Caractéristique acoustique et évolution des sédiments superficiels de la couche de 1996 dans la Baie des Ha! Ha! et le Bras Nord, fjord du Saguenay, Québec," *Mémoire de maîtrise, département de géologie et génie géologique, Université Laval.*

Sutherland, T. F., Lane, P. M., Amos, C. L., and Downing, J., 2000, "The calibration of optical backscatter sensors for suspended sediment of varying darkness levels," *Marine Geology*, Vol. 162, pp. 587-597.

Thorn, M. F. C., and Parsons, J. G., 1977, "Properties of Grangemouth Mud," *Report No. EX 781*, Hydraulics Research Station, Wallingford, England.

Thorn, M. F. C., and Parsons, J. G., 1979, "Properties of Belawan Mud," *Report No. EX 880,* Hydraulics Research Station, Wallingford, England.

Tolhurst, T. J., Black, K. S., Paterson, D. M., Mitchener, H. J., Termaat, G. R., and Shayler, S. A., 2000, "A comparison and measurement standardization of four in situ devices for determining the erosion shear stress of intertidal sediments," *Continental Shelf Research,* Vol. 20, No.10-11, pp. 1397-1418.

Villaret, C., 1987, "Étude expérimentale et numérique des lois d'érosion pour des sédiments cohésifs," *thèse, Université scientifique, technologique et médicale de Grenoble.*

Widdows, J., Brinsley, M. D., Bowley, N., and Barrett, C., 1998, "A benthic annular flume for in situ measurements of suspension feeding/biodeposition rates and erosion potential of intertidal cohesive sediments," *Estuarine, Coastal and Shelf Science,* Vol. 46, pp. 27-38.

Young, R. N., and Southard, J. B., 1978, "Erosion of fine-grained marine sediments : sea-floor and laboratory experiments," *Geological Society of American Bulletin,* Vol. 89, pp. 663-672.

Section II: Mitigation and Restoration Methods

Thiam Soon Tan,[1] *Godakuru P Karunaratne,*[1] *Victor Choa,*[2] *and Myint Win Bo*[3]

Reclamation Using Waste Sediment by Sand Capping Technique

Reference: Tan, T. S., Karunaratne, G. P., Choa, V. and Bo M. W., "**Reclamation Using Waste Sediment by Sand Capping Technique,**" *Contaminated Sediments: Characterization, Evaluation, Mitigation/Restoration, and Management Strategy Performance, ASTM STP 1442,* J. Locat, R. Galvez-Cloutier, R.C. Chaney, and K. R. Demars, Eds., ASTM International, West Conshohocken, PA, 2003.

Abstract: Disposal of unwanted seabed sediment arising from dredging activities is an increasingly intractable problem. One solution is to use the sediment as fill material for land reclamation, as a replacement for sand, the traditional fill. As the water content of sediment is high, even a small fill will ensure rapid consolidation. The underlying philosophy is to place a layer of sand on top of the slurry to accelerate consolidation. This paper summarizes the research carried out in Singapore. A pilot test and a large-scale project will be described and the results from monitoring discussed. A physical framework will then be provided to explain the sand capping of the sediment, followed by the introduction of a simplified model to connect the two key aspects of the mechanics of sand capping, namely the accumulation of sand on the sediment and the way the slurry gained shear strength to resist this load. This simple model was able to produce results consistent with that observed in the field.

Keywords: slurry, sedimentation and consolidation, yield shear stress, sand capping

Introduction

Singapore was a very small country of area 580 square kilometers at the time of its independence in 1965. To alleviate this highly restrictive condition, land reclamation was a top priority national effort in the last 37 years. As indicated in Figure 1, which shows the increase in land area since 1965, the city-state has grown to an estimated 680 square kilometers today, an increase of 17%, and still growing by the day. Ongoing and already approved projects will add at least another 50 square kilometers in the next ten

---

[1] Associate Professor, Centre for Soft Ground Engineering, National University of Singapore, Kent Ridge Crescent, Singapore 117576
[2] Professor, Nanyang Technological University, Singapore
[3] Executive Geotechnical Engineer, SPECS Consultant Pte, Singapore

years while those being planned will add another 50 square kilometers in the following decade. The fill volume, mainly sand, needed to support such activities is enormous.

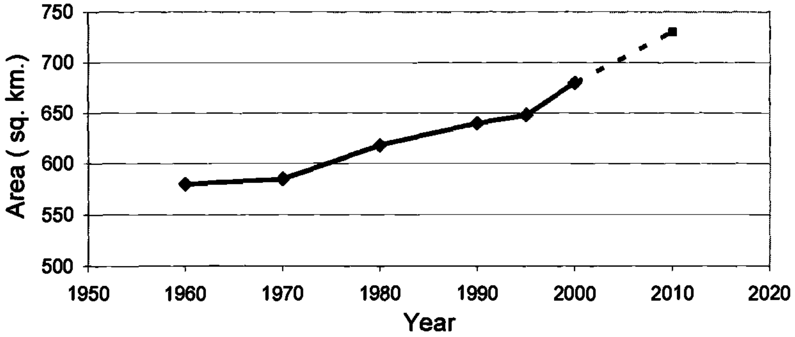

Figure 1 – *Increase in Land Area of Singapore*

On the other hand, there has been a significant increase in the supply of dredged sediment and marine clay as a result of reclamation activities, dredging activities to maintain shipping lanes and exploitation of subterranean space, the disposal of which is becoming an increasingly intractable problem. In recognition of the fact that these two problems provide an ideal situation for marriage, significant research activities have focused on how to use such materials directly as alternate fills in reclamation works. As reclamation volume is always very large, it is important that any technique developed will require minimal re-handling.

Two approaches have been developed to make use of such soils, in accordance to the type of sediment obtained. If the sediment is very soft, in most cases with water content much higher than liquid limit, then the sediment in the form of slurry is used directly in the reclamation and the important challenge is to find ways to apply a small load on the slurry as soon as possible so as to accelerate the consolidation process. In this case, research has focused on finding an effective way to place a thin layer of capping sand on the clay slurry, a method referred to as sand capping (Townsend et al. 1989). If the sediment is sufficiently stiff for it to be in the form of lumps, the second method will use these lumps directly in the reclamation, and the challenge is to develop effective post treatment after the formation of the reclaimed land to ensure large inter-lump voids are effectively closed.

Both techniques have been tested in pilot projects and then subsequently used in large reclamation projects. A 40 hectares pilot project was carried out from 1988 to 1990 to evaluate both methods and also to develop specific techniques to execute such a reclamation project (Karunaratne, et al. 1990 and 1991). This pilot project was carried out after a smaller scale project was carried out with the aim to build a fill with alternate clay and sand layers, often referred to as the sandwich method (Lee et al. 1987). At around the same time, to form a sand key for the building of a containment bund for a reclamation project in the northeastern part of Singapore, seabed sediment was dredged and, mainly in the form of lumps, was disposed in a reclamation site. This site was characterized very recently using a radio-isotope cone (Karthikeyan et al. 2001 and

2002). Another project was the creation offshore of a 180 hectares containment bund in eastern Singapore in 1986 to contain the hydraulic dumping of fine material washing from sand quarrying activities. This area was reclaimed in the mid-1990s as part of the reclamation works for the extension of Changi International Airport (Bo et al. 1998). More recently, since 1999, a new mega project has commenced work, whereby dredged and excavated clay lumps are being used directly as a major source of fill material.

The use of marginal soil as reclamation fill represents one of the most effective approaches towards sustainable development of infrastructure related to the use and generation of earth. Seabed sediment, regarded as waste previously and has to be disposed in increasingly scarce land or offshore disposal sites when generated, is now effectively a material of value when used as fill. Though there are two different approaches depending on whether the sediment is very soft or in reasonable stiff lumps, this paper will only concentrate on the topic of using very soft sediment as a fill, and will discuss the approach adopted in Singapore. The use of clay lumps, which is the subject of intense research activities presently, will not be described. The paper will first describe results from two actual projects where the sand capping method was applied. Using the results from these projects as a basis, the mechanics of the treatment method will then be discussed. A simple model will then be introduced to link together the four key parameters in the operation, namely the amount of sand that is being spread each time, its grain size distribution, depth of water it has to descend to reach the clay and the shear strength of the slurry. These four parameters will, in turn, affect the two key aspects of the mechanics of sand capping, namely the rate of accumulation of sand on the sediment and the formation of a permanent sand layer or otherwise of the sand accumulating. These ideas will then be used to explain the field performance described.

Changi South Bay Project (CSB Project)

This pilot test was carried out from 1988 to 1990 and had been reported by Karunaratne et al. (1991). The project site was located to the south of Changi International Airport. Figure 2 shows a plan of this project. A central dyke was formed to partition the whole area into two large compartments and two sub-dykes were also built for the purpose of facilitating the sand spreading operation. A thin sand mat, 0.3 m to 0.5 m thick, was first laid on top the seabed. Then clay slurry was discharged from a single outlet in Segment C1 for Pond C and one in Segment A2 for Pond A.

After adequate time was set aside for sedimentation, typically about one week, a sand layer of thickness varying from 5 cm to 20 cm was spread onto the pumped sediment. To control this spreading, a perforated pipe system was used. Sand with water was pumped through the perforated pipe, and a winch system was then used to move this spreader on the surface of the pond in a controlled fashion. The thickness of sand spread was controlled by the speed the pipe system was towed and the rate of pumping of the sand. The purpose was to form a thin sand cap on top of this slurry. To ensure that the sand could be formed on top of the slurry, the sand was spread in thin layers and in many passes to form the cap. The selection of the thickness of sand to spread and the number of passes needed is a crucial design consideration and is a key focus of this paper. After adequate time of consolidation by the sand cap formed, a second layer of clay slurry was pumped into the pond and after that, another layer of sand was spread on top of it in a similar fashion. To monitor the effectiveness of the spreading, the density profile was measured after each spreading using a gamma-ray probe. As the fill was a slurry, this probe could be lowered directly into the sediment using its own weight. The accuracy of this particular density probe, which used a 8.3 mCi Cesium 137 source, was 10 kg/m^3

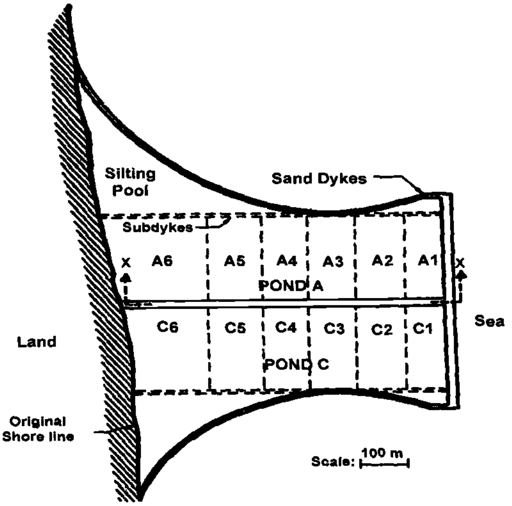

Figure 2 – *Layout of Pond in the Changi South Bay Project*

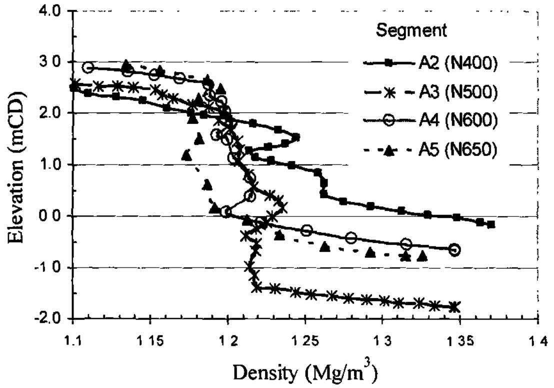

Figure 3 – *Density Profiles at Different Distances from Pumping Outlet*

One problem encountered, when the clay slurry was pumped out from a single outlet, was the dispersion of the clay slurry with coarser particles settling near to the pumping point and finer particles depositing further away. This is clearly reflected in the density profiles at different distances away from the pumping, which is shown in Figure 3 for points in Segment A. Note that at Segment A2, the density at the surface is about 1.17

Mg/m^3, that is, a water content of just over 300% but shows an obvious increase with depth. In Segment A5, the furthest away, the density at the surface is also about 1.17 Mg/m^3, but the density shows only a slight increase with depth. Subsequently in this project, instead of pumping from a single outlet, the clay was pumped using the same perforated pipe system as the one used for spreading sand. In that case, a nearly uniform distribution was obtained.

The next important aspect of the operation was the formation of the sand cap on top of the clay slurry. As the density profile of the pumped slurry clay changed with distance, as shown vividly in Figure 3, the sand spreading sequence had to be adjusted to take this into account. As shown in Figure 4, in Segment C2, the density of the slurry was about 1.17 Mg/m^3 (just over 300% water content) but showed a significant increase with depth, just as for Segment A2 in Figure 3. Thus for this segment, the spreading was carried out using first a 5 cm pass followed by a 10 cm pass, then a 15 cm pass and finally a 20 cm pass.

As shown in Figure 4, before spreading, the density at the surface is about 1.17 Mg/m^3 just as in Figure 3. However, the density increases with depth. After the first spreading of 5 cm in Segment C2, it is clear that sand was trapped above the elevation of -0.5 mCD (meter above chart datum). After the second spreading of 10 cm, a new sand layer with a little mixture with slurry was clearly built on top of the first layer and the bulk of the sand was now trapped above 0.0 mCD. Note that the density profiles are not stationary as in between one spreading and the next; the slurry would have started consolidating and compressed due to the trapped sand, and thus the surface of the sand trapped after the first spreading would have settled some amount. Unfortunately, no data was collected for the third spreading of 15cm and Figure 4 only showed the result for the fourth spreading of 20 cm. At this stage, it was clear a clean sand layer was formed above the elevation of 0.5 mCD, as indicated by the very high density of around 1.8 Mg/m^3, achievable only with sand.

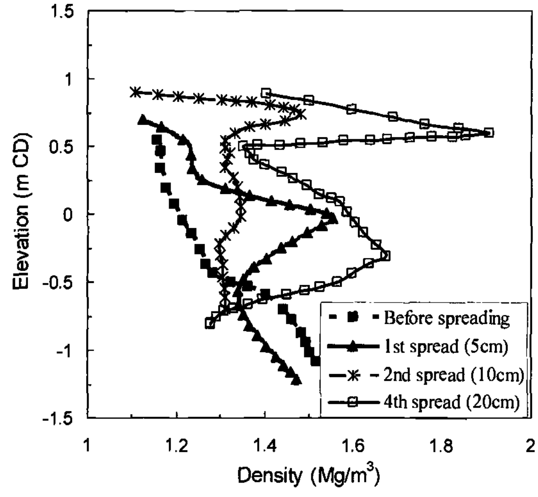

Figure 4 – *Density Profiles at C2 after Different Stages of Sand Spreading*

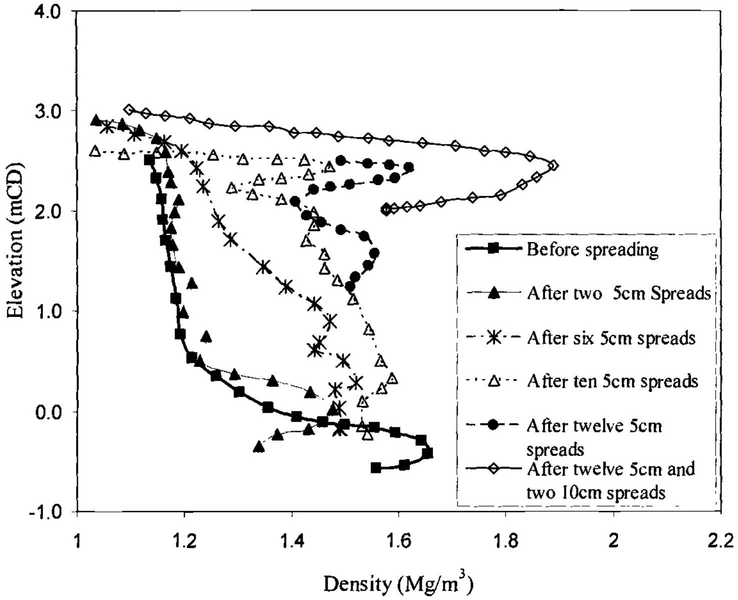

Figure 5 – *Density Profiles at C6 after Different Stages of Sand Spreading*

For Segment C6, which was the furthest away from the pumping outlet, the density near the surface was also close to 1.17 Mg/m^3, but showed negligible increase with depth, just as for Segment A5 in Figure 3. Clearly, the slurry was much weaker, and thus the sand had to be spread in thin layers. As this was an actual project, 5 cm was considered the thinnest layer practical to control. As such, at this location, the sand was spread in passes of 5 cm until a layer was built up. After that, the spreading thickness was increased. The density results after selective passes were shown in Figure 5. After 2 passes of 5 cm, the density profile showed that most of the sand penetrated into the clay slurry. However, even though the sand had totally penetrated, it could also be observed that there was a slight increase in density, indicating that some amount of the sand spread was trapped at the upper portion of the slurry. This sand that was trapped at the upper portion would play an important role in arresting the penetration of future passes. This was now clearly seen in the results after an additional four passes, that is, after 6 passes totaling 30 cm of sand, there was a much more significant built up of sand, especially towards the top now. However, at this stage, there was still no visible sand layer being formed. Subsequently, the behavior became much more similar to that observed in Segment C2 and discussed above. After an additional 4 passes of 5 cm each, a sand layer mixed with slurry was clearly formed at the surface with density of around 1.4 Mg/m^3, or a water content of about 120%. After this, a sand layer was formed near the surface and finally, a clean sand layer, with density of about 1.8 Mg/m^3 could be seen to form after 80 cm of sand had been spread in twelve passes of 5 cm and 2 passes of 10 cm.

The Silt Pond Project (SP Project)

In 1986, a containment sand bund was constructed around a previously burrowed pit in the sea to provide a disposal area for silt and clay washings from sand quarrying activities. This containment is nearly rectangular in shape with length of about 2000 m and width of 750 m at one end to 1050 m at the other end. The total area is about 180 hectares. Pumping activities stopped towards the end of the 1980s when such quarrying activities were phased out, and the slurry was allowed to consolidate under its own self-weight. Around 1995, reclamation of this pond commenced. To a large extent, the lessons learned from the previous pilot test were applied to this project, which could be viewed as a full scale implementation of the pilot test.

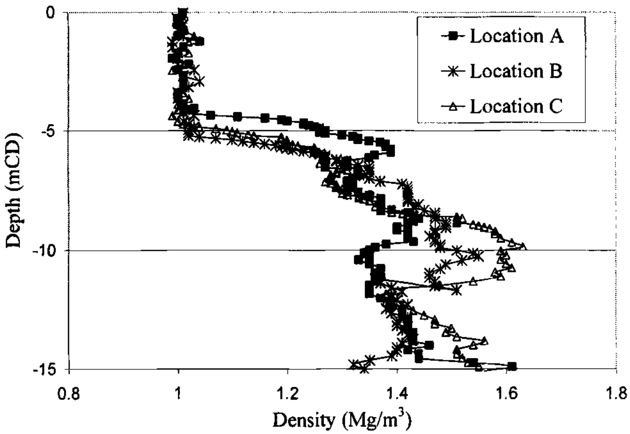

Figure 6 – *Initial Density Profiles at Different Locations in the Silt Pond Project*

Sub-surface investigations were carried out first in 1992 and then in 1994. These tests indicated that the density near the surface is around 1.2 Mg/m^3 or a water content of 270%, with an average value of about 1.3-1.35 Mg/m^3 or about 150% to 170% as shown in Figure 6, which gave typical density profiles at three different locations in the silt pond. As can be seen, the clay slurry, after many years of self-weight sedimentation and consolidation, had settled to an elevation of -4 to -5 mCD. As these were field measurements, it was difficult to obtain very precise values. Nevertheless, it could be seen that the surface water content was ranging from 1.17 Mg/m^3 to 1.2 Mg/m^3 (water content of 300% to 270%). More importantly, the density could be seen to increase very rapidly with depth from a value of about 1.2 Mg/m^3 to a value of 1.4 to 1.5 Mg/m^3 within a depth of 5 m. The difference between this profile and that observed in the CSB project shown in Figure 3 was principally due to the different stages of consolidation as a result of differing length of time the slurry was left alone.

As the water content of the slurry is still considerably large, it was recognized that conventional sand dumping or hydraulic pumping would not work as the large quantity of sand would break easily through such soft clay. But this profile was ideally suited for the placement of thin sand layers as shown in the results from the pilot test at the CSB project. Thus, the method developed at the pilot test in CSB project was applied here, namely spreading the sand in thin layer through a perforated pipe system that is being moved on the surface of the pond. As this was an actual and large scale project, the density distribution was determined only a few times, and a somewhat less detailed record was available. The density distributions at three different stages after dumping were shown in Figure 7. Though the exact detail of the spreading was not well established, but the sand was spread in thickness of about 20 cm in each pass.

As shown in Figure 7, it could be observed that the bulk of the sand spread just before the first measurement on 9 January 1995 had been trapped at the upper portion near the surface, but at this first measurement, no clean sand layer had been formed yet. However, by the second measurement date, a clean sand layer, indicated by density as high as 1.9 Mg/m^3 could be clearly seen. Subsequent spreading increased the thickness of the sand layer formed. Also, from the bottom of the sand layer formed, the amount of compression occurring between 20 March and 9 April, a total of 20 days, could be clearly observed to be about 0.5 m. It is also important to note that the formation of a nearly 2 m thick sand layer had occurred without any breaking in of the sand layer.

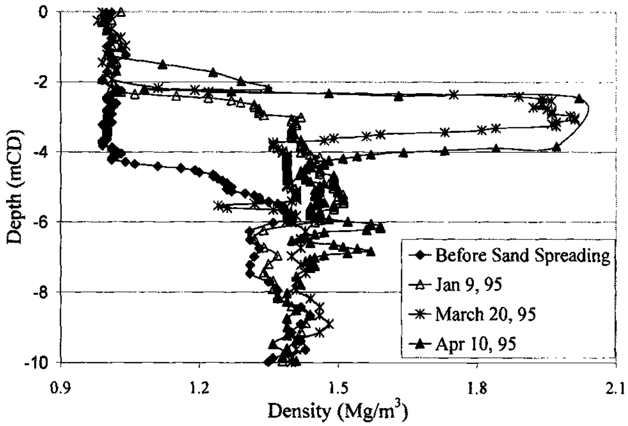

Figure 7 – *Density Profiles at One Location after Different Stages of Sand Spreading*

Basic Principles in the Mechanics of Sand-capping

As can be seen from the above description, the use of soft sediment as a fill to be treated by providing a sand-cap has proven to be a technically and economically feasible approach even for a very large reclamation. A number of different aspects of mechanics are involved in the entire process and these will be discussed next.

To be hydraulically transported, the slurry clay typically has water content 3 to 6 times of the liquid limit, at which state, the slurry has virtually no shear strength. On its own, this slurry will undergo combined self-weight sedimentation and consolidation. The theory of sedimentation and consolidation under self-weight for one-dimensional problem is well established (Tan et al. 1990 and Tan 1995) and will not be discussed further. At the end of the sedimentation period, the self-weight consolidation process would have just started. At the CSB project, the sedimentation phase was observed to take about a week to 10 days. At the end of this stage, at the segment furthest away from the pumping outlet, the slurry was nearly uniform with a water content of about 270% - 300% (density from 1.17 Mg/m^3 to 1.2 Mg/m^3), as was observed in Segment A5 in Figure 3 and Segment C6 in Figure 4 for the CSB project. Such a profile is an indication that sedimentation is over but consolidation has just begun and thus the density has not adjusted to the self-weight gradient imposed by gravity. On the other hand, at A2 where the particle sizes were larger, the density profile showed a more significant increase with depth compared to that at A5 where the particle sizes were much finer. Clearly, the rate of sedimentation and consolidation at these two locations were different.

On other hand, for the SP project, the slurry had been left to settle under its own self-weight for a number of years, and at the end of that period, the density profile is increasing with depth. This is a good indication that sedimentation is over and to a large degree, the soil has consolidated under its own self-weight (Tan et al. 1990a). The very rapid increase with depth of the density in the slurry in the upper portion of the slurry highlights another very important aspect of the consolidation behavior of such a soft clay. That is, a very small load can induce a very large compression when the water content is very high. In effect, the success of the sand capping method depends on this simple observation. Nevertheless, the water content at and near the surface was still very high, principally because the effective stress available there was nearly zero. A measurable yield shear stress of a few Pascals can now be achieved for this slurry. Incidentally, the water content at the surface of the slurry is about 3 times liquid limit, and this ratio seems to be close to a boundary between sedimentation and consolidation observed by Tan et al. (1990a), where the yield shear strength of a slurry shows a sudden change around this ratio (Tan et al. 1990b).

The time needed for the slurry to gain sufficient strength by self-weight is too long for most practical purposes. Even if adequate time is set aside for self-weight consolidation, the absence of effective stress at the surface in a self-weight situation, will result in a very weak surface layer, such as that seen in the results from the SP project, and a way has to be found to increase the shear strength, especially at the surface. If the void ratio versus pore pressure relationship of a slurry is examined (Tan et al. 1988), then it can be seen that only a small load is needed to quickly induce a large increase in the density. In the approach adopted in Singapore, this has been successfully achieved by providing a sand cap through careful spreading of thin passes of sand through a moving perforated pipe system.

Inoue et al. (1991) had found that the controlling factors in the mechanics of sand capping were the grain-size of the sand spread, the thickness of the sand spread, the height of supernatant water and the shear strength of the slurry. When a sand mass is spread onto the seawater, initially the motion of the sand particles is highly turbulent, but the sand particles will quickly reach their respective terminal velocities and settle, as shown in Figure 8. Particulate segregation will occur as heavier particles are falling faster than lighter ones. The front of the falling sand mass will then impinge on to the surface of the clay slurry. As shown in Tan et al. (2002), as individual particles, most of them will be trapped and a very thin sand layer is then formed on top of the clay surface. Trailing sand particles coming down and impinging on the trapped front particles will then impose additional load. Depending on the interaction between the strength of the slurry, and the rate of loading imposed by the trailing sand, this thin layer of sand will either hold with increasing thickness or "break" into the clay. In the latter case, the penetrated sand particles will either be arrested at the upper portion of the slurry or sink to the bottom of the slurry. As shown in the field projects, the trapped sand also played an important role.

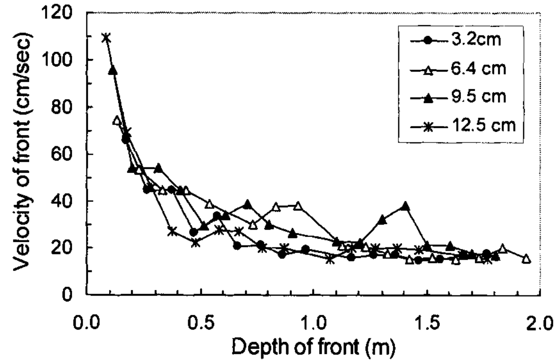

Figure 8 – *Velocity of Front of Falling Sand Particles for Different Thickness of Sand Spread*

The precise mode the thinly formed sand layer would break was difficult to assess, but in all the experiments conducted in the laboratory, the failure was observed to be not a punching type such as in the case for a shallow foundation. Instead, at a certain stage, a weak point caves in and the sand particles then flow into this plume, suggesting that this is an instability problem. Thus far, no stability analysis could be found to take into account this complex interaction described above where the loading and resistance are both changing with time, and the resistance itself is also a function of the loading.

The above description identifies two key aspects in the mechanics of sand capping, namely the rate of loading of the sand layer and the rate the slurry clay will gain strength at the surface over the initial yield shear strength as a result of the ongoing consolidation. On the other hand, the rate the slurry clay gained strength over its initial value is governed by the load imposed and time. The important point is whether the slurry can have enough strength right from the start, and if not, whether it can gain strength fast enough to be able to hold the increasing load imposed by the falling sand.

Thus a key parameter to establish is the rate of sand accumulating on top of the slurry surface. Usually, when this method is used, the sand is spread in thin layer, and to a large degree, particulate settling is occurring. Based on Inoue et al. (1991) observation that particles reach terminal velocity very quickly, Tan et al. (2002) has developed a simple model to explain this accumulation. The terminal velocity of a particle is determined using an extended Stokesian model of a spherical particle settling in a fluid, but taking into account the actual drag coefficient if the flow is not in low Reynolds Number regime (Batchelor 1973). To take into account the fact that the sand particles are actually not spherical, an approach recommended by Zimmels (1986) was adopted. To account for the grain size distribution, the sand particles are divided into smaller range of particle sizes and the average terminal velocity in each range is determined. Thereafter, the dispersion of a column of sand can be calculated based on the terminal velocity determined for each range and the amount of particles in that range based on the grain size distribution curve. In Tan et al. (2002), this model was shown to be able to describe the behavior of this sand accumulation in experiments, a typical set of comparison is shown in Figure 9. The important point to note is that this simplified model is able to take into account three of the four key parameters, namely grain size distribution and thickness of the sand spread and the height of supernatant water above the slurry.

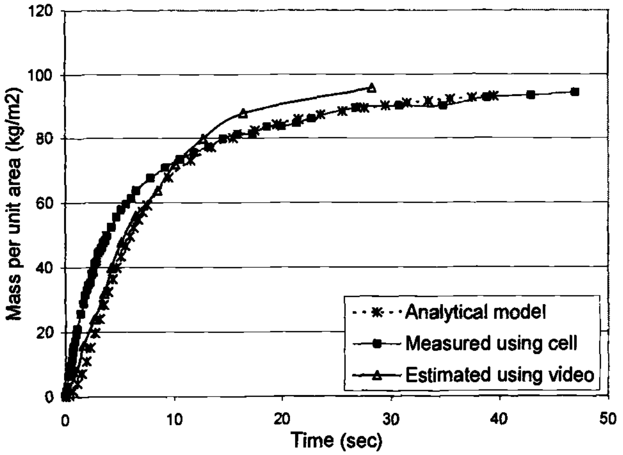

Figure 9 – *Sand Accumulation Experiment: Height of Water = 1.5m, Thickness of Sand Spread = 7.5cm*

To explain the interaction between the two aspects of the mechanics, namely the rate the sand is accumulating on top of the slurry surface and the rate the slurry is gaining shear strength, a simple "bearing capacity type" of concept was introduced by Tan et al. (2002) to explain the subsequent break-in of the sand under the right conditions. From the results of sand accumulation tests by Tan et al. (2002) and the simplified model introduced, and noticeable in Figure 9, in most cases the rate of accumulation of sand is nearly linear until near the end of the accumulation period. If this linear relation is assumed, the loading on the clay surface with time, $\sigma_L(t_a)$ is:

$$\sigma_L(t_a) = k_l \, r_L \, t_a \tag{1}$$

where t_a is the elapsed time after the sand layer begins to accumulate on the clay surface and k_l is a constant to account for the interaction with other particles.

The shear strength of the slurry, especially at the surface, will also increase with the overburden load applied as a result of consolidation. Thus the shear strength increase is also a function of two factors; time and the rate of sand accumulation, r_L. A faster rate of sand accumulation would mean a larger surcharge is applied in a given time and, in turn the surface, which will consolidate almost immediately, will be able to gain strength faster. As a first order estimate, this resistance, or "bearing capacity" of the slurry is assumed to be also linear and of the form:

$$\sigma_R(t_a) = k_2\,(\tau_y + k_3\, r_L\, t_a) \qquad (2)$$

where k_2 is a "bearing capacity factor" and k_3 is to account for the increase in shear strength due to an increase in vertical load. τ_y is the yield shear stress of the slurry initially. For failure to occur, the rate of loading must be significantly faster than the rate of increase in shear resistance so as to exceed the combined shear resistance provided by the initial yield shear stress and the subsequent increase due to consolidation, and the amount of sand spread must be enough for this to occur. These two conditions are specified as follows:

(a) $\sigma_L(t_{af}) \geq \sigma_R(t_{af})$ (3a)

(b) $t_{af} \leq t_{au}$ (3b)

where t_{af} is the time to failure and t_{au} is the time needed for the entire amount of sand spread to accumulate at the surface at a constant rate of r_L. Figure 9 shows that the residual amount of sand deposited after time t_{au} is small. At the onset of failure, $\sigma_L(t_{af}) = \sigma_R(t_{af})$ and a simple manipulation will give:

$$t_{af} = \alpha \frac{\tau_y}{r_L} \qquad (4a)$$

where $$\alpha = \frac{k_2}{k_1 - k_2 k_3} \qquad (4b)$$

If r_L is expressed in load/unit area/time, then α is dimensionless. The above derivation showed that the ratio τ_y / r_L holds the key to understanding sand capping. In the conceptual model developed, the idea is very simple. If the sand is deposited completely at the rate r_L in a time that is less than t_{af}, then failure cannot occur, else failure would occur. This simple idea is illustrated graphically in Figure 10. The three unknown parameters k_1, k_2 and k_3 are combined into a single parameter, which facilitates back-analysis. Though Eq. 4a is a very simple equation, it actually encompasses all the key ideas discussed previously. It relates the two key aspects of the mechanics of sand capping, namely the rate of sand accumulating at the surface and the rate the shear strength is increasing. The rate of accumulation of sand has taken into account the grain size distribution, the amount of the sand used and the height of water the sand has to fall through. Thus, this simple model is able to bring all the different ideas together. Clearly, the most important limitation in this derivation is the assumption of linearity for increase in loading and shear strength. However, this does not distract from the key idea that the instability can be describe by the interaction between the two key aspects of mechanics.

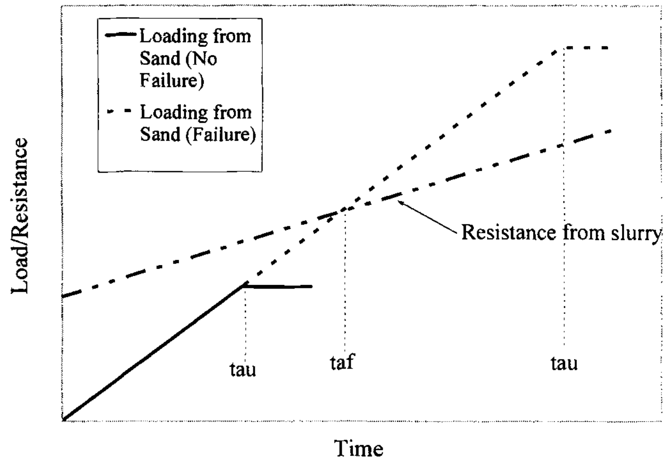

Figure 10 – *Schematic Interpretation of the Interaction between Sand Loading and Gain in Shear Resistance by Slurry*

Though the linear assumptions are expected to be true for only very short duration, nevertheless, it can be used to provide a rough guide to interpret the field results. For a given spread per pass in S Pascal (product of thickness per pass and the effective unit weight), t_{au} is given by:

$$t_{au} = (S)/r_L \tag{5}$$

where r_L is in Pa/s. If the ratio of t_{af}/t_{au} is now calculated based on Eqs. 4a and 5, then, this will yield

$$\frac{t_{af}}{t_{au}} = \alpha \frac{\tau_y}{S} \tag{6}$$

In Eq. 6, the ratio has to be greater than 1 for failure not to occur. To do this, either τ_y has to be large or S has to be small. In the former, this means the slurry has to be stronger (lower water content) and in the latter, it means that sand has to be spread in thinner layer. In Tan et al. (2002), back analysis of results from 37 tests indicates a value of α of 260. A 5 cm pass, equivalent to about 400 Pa under submerged condition, will require the slurry to have a yield shear stress larger than 1.5 Pa. On the other hand, a 20 cm pass, equivalent to 1600 Pa will need a yield shear stress higher than 6 Pa for failure not to occur. The clay slurry at the CSB project has a liquid limit of about 80%, and was shown in Tan et al. (1991) to have a yield shear stress of about 1.5 Pa at 300% whereas to achieve 6 Pa, its water content has to reduce to about 240%. These two values are in reasonable concurrence with the observed behaviors shown in Figures 4 and 5.

It is recognized that the present treatment is simplified. The rate of loading by the sand spread is likely to be non-linear when the water depth is great. The gain in yield shear stress as a result of the ongoing consolidation is also unlikely to be a linear function of time for significant period of time. Nevertheless, the above derivation does provide a coherent way to demonstrate the importance of the ratio of the initial yield shear stress of the slurry over the weight/unit area of the sand spread in controlling sand capping.

Conclusions

The problem of treating a large volume of slurry clay is increasingly important due to the scarcity of land in major urban centers. In Singapore, the solution adopted is to use such dredged material as reclamation fill, and to treat this, a sand cap is built on top of the slurry. In this paper, results from two actual projects were described. These two projects, one for 40 hectares and the other for 180 hectares, clearly showed the feasibility of this method.

The mechanics of sand capping is discussed. The controlling parameters in sand capping are the thickness and grain size of sand spread, height of water and the initial yield shear strength of the slurry (or water content of the slurry). The first three parameters govern the rate the sand is accumulating on top of the slurry while the rate the slurry will gain strength over its initial value is a function of this loading and time. If the loading is fast enough, failure will occur with the sand layer caving into the slurry. If not, then a clean sand layer will be formed as can be seen from the result from the two projects reported. A simple conceptual model was presented to demonstrate this idea.

A simplified model is able to show that the key parameter is the ratio of the initial yield shear stress over the expected loading. When this is applied to the field project, it seems to provide a reasonable guide as to what to expect in the field. Conclusions cannot be firmer than this at the present stage as the assumptions involved are highly simplified and also the field conditions are not as simplified as that assumed in the derivation. However, this does not distract from the fact that the above derivation and subsequent results do clearly demonstrate what are essential in the mechanics of sand capping.

Acknowledgments

The assistance of Dr. R. G. Robinson and Mr. M. Kathikeyan in preparing the figures is gratefully acknowledged. The results of the laboratory works reported here were basically drawn from the works of two former students, Dr. T. Inoue and Dr. T. C. Goh, of the senior author.

References

Bo, M. W., Arulrajah, A., Choa, V., and Na, Y. M., 1998, "Land reclamation on slurry like foundation," *Proceedings, International Symposium on Problematic Soils, IS-Tohoku*, A.A. Balkema, pp. 763-766.

Inoue, T., Tan, T. S., and Lee, S. L., 1990, "An investigation of Shear Strength of Slurry Clay," *Soils and Foundations*, Vol. 30, No. 4, pp. 1-10.

Inoue, T., Tan, T. S., and Lee, S. L., 1991, "Sand Penetration into Clay Slurry," *GEO-COAST '91*, Sept, 1991, Yokohama, pp. 317-322.

Karunaratne, G. P., Yong, K. Y., Tan, T. S., Tan, S. A., Liang, K. M., Lee, S. L., and Vijiaratnam, A., 1990, "Layered clay-sand scheme reclamation at Changi South Bay," *Proceedings of the 10th Southeast Asian Geotechnical Conference*, 16-20 April 1990, Taipei, ROC, Vol.1, pp. 71-76.

Karunaratne, G. P., Yong, K. Y., Tan, T. S., Tan, S. A., Lee, S. L., and Vijiaratnam A., 1991, "Land reclamation using layered clay-sand scheme," *GEO-COAST '91*, Sept, 1991, Yokohama, pp. 335-340.

Tan T. S., 1995, "From sedimentation to consolidation: A geotechnical perspective," *Proceedings, Compression and Consolidation of Clayey Soils*, May, 1995, Hiroshima, Japan, Yoshikuni and Kusakabe (eds), Balkema, pp. 937-948.

Tan, T. S., Yong, K. Y., Leong, E. C., and Lee, S. L., 1990a, "Sedimentation of Clayey Slurry," *Journal of Geotechnical Engineering*, ASCE, Vol. 116, No. 6, pp. 885-898.

Tan, T. S., Yong, K. Y., Leong, E. C., and Lee, S. L., 1990b, "Behavior of Clay Slurry," *Soils and Foundations*, Vol. 30, No. 4, pp. 105-118.

Tan, T. S., Goh, T. C., Karunaratne, G. P., Inoue, T., and Lee, S. L., 1991, "Yield Stress Measurement by a Penetration Method," *Canadian Geotechnical Journal*, Vol. 28, pp. 517-522.

Tan, T. S., Goh, T. C., Karunaratne, G. P., and Lee, S. L., 1994, "Shear Strength of very soft clay sand mixes," *Geotechnical Testing Journal*, ASTM, 17, No. 1, pp. 27-34.

Tan, T. S., Goh, T. C., and Karunaratne, G. P., 2002, "A study of the mechanics of sand spreading and penetration into a slurry," Submitted to the *Canadian Geotechnical Journal*.

Townsend, F. C., McVay, M. C., Bloomquist, D. G., and McClimans, S. A., 1989, "Clay waste reclamation by sand/clay mixture or capping," *Journal of Geotechnical Engineering*, Vol. 115, No. 11, pp. 1647-1666.

Zimmels, Y., 1986, "Accelerated and steady particle flows in Newtonian Fluids," *Encyclopedia of Fluid Mechanics*, Gulf Publishing Company, Houston, Vol. 5: Slurry Flow Technology, pp. 93-153.

Dave Ta-Teh Chang,[1] Chao-Ping Sung,[2] Bor-Ling Chen,[2] and Nuan-Hsuan Ho[3]

Durability Study for Geotextile Tube Use in Talimu River Sediment Control

---

Reference: Chang, D. T.-T., Sung C.-P., Chen B.-L., and Ho N.-H., **"Durability Study for Geotextile Tube Use in Talimu River Sediment Control,"** *Contaminated Sediments: Characterization, Evaluation, Mitigation/Restoration, and Management Strategy Performance, ASTM STP 1442*, J. Locat, R. Galvez-Cloutier, R. C. Chaney, and K. R. Demars, Eds., ASTM International, West Conshohocken, PA, 2003.

Abstract: To rebuild dikes for Talimu River regulation project, insitu sediments is considered to be contained by geotextile tube (geotube) for use as dike core. Stress analysis and matrix shape analysis are required to determine the geotube size. Based on experience and the local climatic conditions of Xing Jiang, China, durability of the geotubes is considered the most critical factor for sediment control. The geotube material used in this study is woven geotextile made in Taiwan - GTM-1 and GTM-2. The tests were conducted in accordance with ASTM Test Method (D 4355) for deterioration of geotextiles from exposure to ultraviolet light and water. After UV exposure for 200 and 500 hours, the results showed that the residual tensile strengths of the geotextiles are greater than 90 % and 70 % of the ultimate tensile strength, respectively. More results showed that reduction in tensile strength is insignificant even after UV exposure for over 600 hours. Another durability test is the geotextile's resistance to freezing and freeze-thaw cycles. Initially the geotextiles were placed in a temperature chamber and cured at −20 °C, −30 °C, −40 °C for 6 days. The results showed that the geotextiles still retained greater than 90% of its ultimate tensile strength. For the freeze-thaw cycles (−40 °C−40 °C, −10 °C−20 °C), results also indicate that the selected geotextiles provide good freeze-thaw resistance.

Keywords: sediment control, geotextile tube (Geotube), UV resistance, freezing resistance

---

[1] Professor,[2] Research Assistant, Civil Engineering Department of Chung Yuan Christian University, 22 Pu-Jen, Pu-Chung Li, Chung Li, Taiwan, ROC 320.

[3] Ph.D candidate, Department of industry engineering and management, Chunghua University, and also Director General of Bureau of Taiwan High Speed Rail, Ministry of Transportation and Communications, R.O.C.

Introduction

The Talimu River at Xing Jiang flows over 1200 km, making it one of the longest rivers in China. In the last 30 years, the Talimu River has suffered from reduced water flow, channel sedimentation, and a damaged shipping channel resulting in overflow of river water and severe loss of water. Thousands of hectares of agriculture development are facing land degradation problems, with more than 130 000 hectares of agriculture land having become desert. The situation is expected to deteriorate if the problem is not addressed properly. A local government environmental committee was established to study the rehabilitation of the Talimu River and the ecology system on both sides of the river. So far, a number of hydraulic structures have been built. The rehabilitation has been undertaken in two phases. An initial short-term investment of up to USD 40 millions is called for to urgently implement a regulation to manage the river water flow so as to restore the total volume conveyed to 550 millions cubic meters per day. Long-term investment is forecast in the USD 150 millions bracket in order to provide a total volume of 750 millions cubic meters conveyance and eventually to guarantee the supply of water for both industrial and household use.

Channels used in this project are mostly of conventional design where an embankment dike was built on both sides of the river. A conventional design of this type has the drawback of forming a wide but shallow channel. The region sits at the border of a desert and the major soil profile here is fine, loose sand on which it is difficult for dikes of this type to remain stable. As such, liquefaction is commonly encountered here even if the slope of the embanked dike is reduced from 1:2 to 1:3.5 ; see Figure 1 (Casagrande 1975). Through a gradual process, the embankment dike will erode back towards the river, with sediment blocking the waterway and causing the river to overflow, resulting in a significant drop in the conveyance capacity. The committee decided after extensive discussions to using geotubes filled with sediments as the dike core. This method has two advantages: more stable embankments are constructed, and at the same time, the waterway is dredged because the sediments are pumped into the geotube. The structures, once completed, are more resistant to erosion and are thus easier to maintain. This study focused on the durability of geotube and its use as the dike core.

Original Designed Channel Cross Section

Embankments along the Talimu River were built by hydraulic fill. Initially, the slope designed was 1:2.0. After experiencing total collapse of quite a few sections of the embankment dike, the gradient of the slope was reduced to 1:3.5. There are three different types of channel design cross-sections which contain a 6 – 8 cm concrete plate, a 0.4 – 0.5 mm thick geomembrane, a 3 – 20 cm layer of coarse sand/gravel layer, and a geotextile filter.Typical sediments in this region is classified as ML or SM based on its grain size and for its non-plasticity of fines (see Figure 2). This type of soil has poor resistance to erosion. At the same time, capillary action and freeze-thaw conditions could adversely affect the slope, foundation and core stability. Using twenty percent of the effective grain size (D_{10}) as the estimate effective pore size, the height of capillary rise can be obtained, which is approximately 16 m. There is a substantial variation in temperature in this region. During winter, the temperature can typically drop to –20 °C, sometimes go as low as –40 °C with the wind chill; in the summer, the temperature can be as high as 40 °C. An embankment core consisting of geotubes can isolate or at least moderate the freeze-thaw effect, reduce capillary action, enhance the restraining forces of soil and increase erosion resistance.

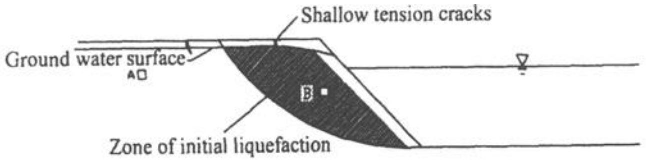

(a) Start of liquefaction

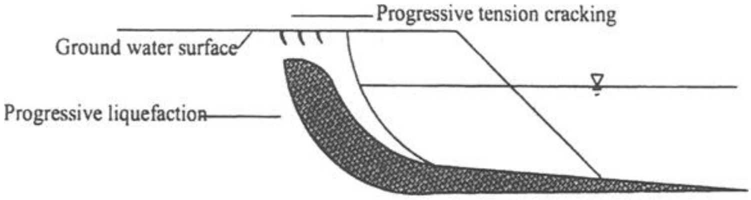

(b) Progressive liquefaction

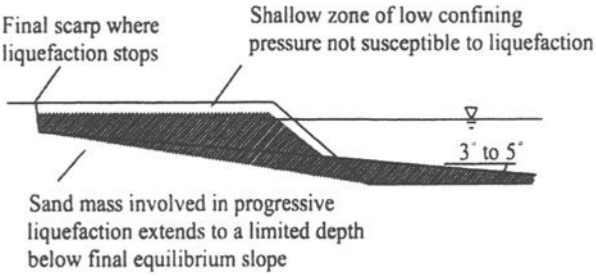

(c) Section through slide area after failure

Figure 1 — *Liquefaction in Loose Sand Adjacent to a Waterfront (Casagrande 1975)*

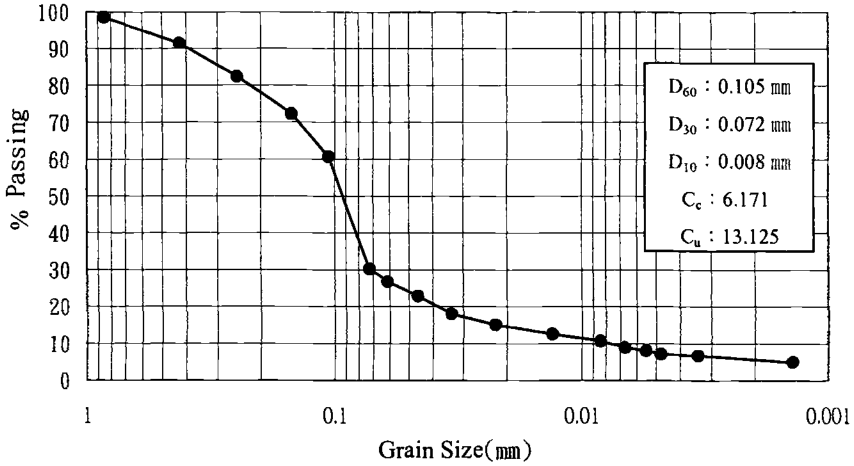

Figure 2 — *Grain Size Distribution Analysis for Typical Sediment Sample*

Research Approaches

To ensure long-term performance of the geotube, it is essential that the geotube be made of geotextile material of sufficient strength and durability. In this study, geotextile materials developed and manufactured by Taiwanese manufacturers were used to conduct the optimum design, aging test and durability test. It is anticipated that results from the analysis will serve as guidelines for future design, manufacture and application of geotubes.

Optimum Design for Tube Matrix Size

At the initial or intermediate stage of the installation, the geotube has a cylindrical cross section. As can be seen in Figure 3(a), when the geotube is flat, the height of the installed geotube (H) approaches zero ($H = 0$), the radius of both corners (rounded ends) of the geotube approaches zero ($R'=0$) and the larger R, representing a arc of an infinitely large circle approaches infinity ($R \rightarrow \infty$). The tensile modulus of the geotextile under this condition equals zero. On the contrary, when the geotube becomes cylindrical in shape, $H/2 = R = R'$, the tensile modulus of the geotextile theoretically approaches infinity. The tube height-to-width ratio is normally kept at below 0.8, so that the designed tensile modulus of the geotextile is not too high. The matrix shape of geotube also can be expressed in a simplified manner as in Figure 3(b). The cross section shows that both ends are semi-circular in shape while the upper and lower sides are flat.

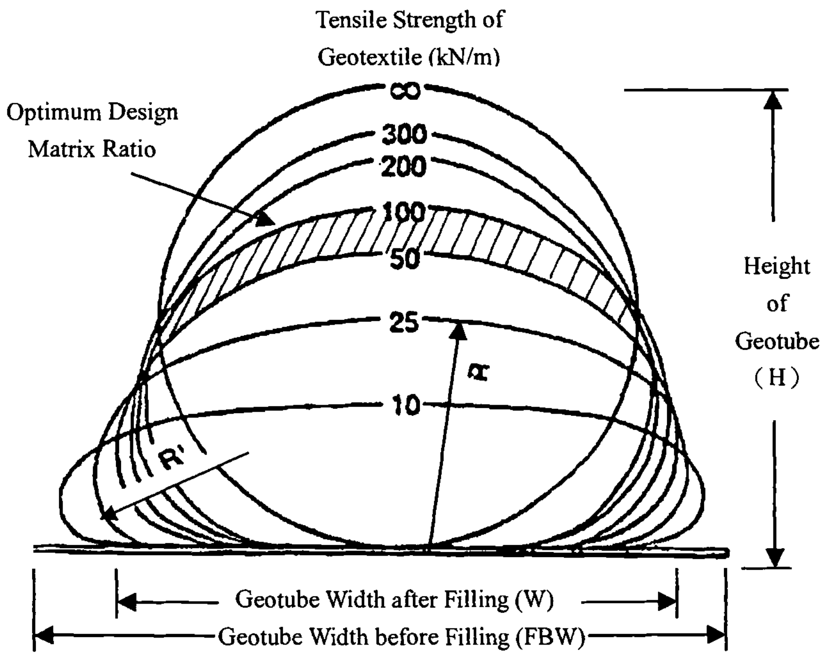

(a) *Relationship of Stress Tensile Strength of Geotextile and Shape of Tube*

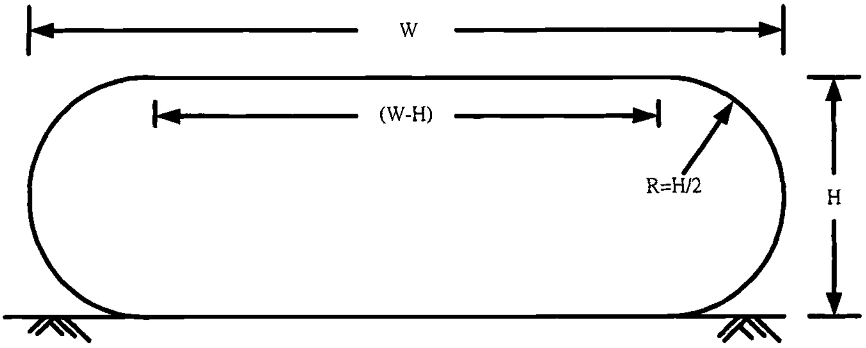

(b) *Simplified Tube Cross Section*

Figure 3 — *Size and Shape of Geotube for Calculation (from Leshchinsky et al 1996)*

Aging and Durability Evaluation of Geotube Material

The geotube is made of a woven geotextile. In accordance with ASTM Test Method for Tensile Properties of Geotextiles by the Strip Method (D 1682), one can measure and observe the changes in tensile strength. Aging conditions were simulated by exposure to ultraviolet light and the use of a temperature chamber (Schneider 1988, Sprague and Goodrum 1987). The operating range of the temperature chamber used in this study is between –40 °C and 40 °C. The tests were conducted in accordance with ASTM Test Method for Deterioration of Geotextiles from Exposure to Ultraviolet Light and Water (D 4355). Duration of UV exposure can be as long as 1000 hours, after which changes in tensile behavior were analyzed. Both wet and dry woven geotextiles were subjected to freeze-thaw cycles to study the effects of temperature on the tensile strength of the geotextiles.

Basic Properties of Woven Geotextiles

Materials used in this study are Taiwan products, GTM-1 and GTM-2 denoted as Sample A and Sample B, respectively. Basic properties of the woven geotextiles are given in Table 1.

Table 1 —*Basic Properties of Woven Geotextiles Used in the Laboratory Study*

Test Items	Test Method		GTM-1 (sample A)	GTM-2 (sample B)
Thickness (mm)	ASTM D 5199		1.095	1.128
Mass per unit area (g/m^2)	ASTM D 5261		345.2	361.1
Strip tensile strength and elongation (kN/m; %)	ASTM D1682	MD[1]	66 (19.7)	82 (23.6)
		CMD[2]	64 (18.6)	70 (15.9)
Trapezoid tearing strength (kg)	ASTM D4533	MD[1]	118.6	133.7
		CMD[2]	104.7	124.2
Grab breaking load (kg)	ASTM D4632	MD[1]	258.5	270.5
		CMD[2]	224.5	234.5
Wild strip tensile strength and elongation (kN/m; %)	ASTM D4595	MD[1]	57 (23.1)	71 (26.8)
		CMD[2]	56 (22.8)	62 (17.7)
Apparent opening size (μm; O_{95})	ASTM D 4751		229	248
Coefficient of permeability (cm/sec)	ASTM D 4491		2.4×10^{-2}	2.7×10^{-2}

[1] MD = machines direction
[2] CMD = cross machine direction

Durability Behavior Studies for Geotextiles

UV Resistance

After exposing the woven geotextiles of Sample A and Sample B to UV light for 200 hours in accordance with ASTM D 4355, the residual strip tensile strengths of the geotextiles were measured to be 91 % and 93 % respectively, of the tensile strength before UV exposure. After 500 hours of UV exposure, the residual strip tensile strengths were 76 % and 78 % respectively. This complies with the requirements of typical design guide (Holtz et al. 1998), wherein residual tensile strength after 500 hours of UV exposure shall not be less that 70 % of the ultimate tensile strength. Figure 4 shows the residual tensile strengths under UV exposure. From the curves, it is found that for UV exposure beyond 600 hours, the additional strength loss is insignificant. This is probably because of the white powder deposits formed on the geotextile surface, which blocked the effect of further UV exposure. It is recommended that the chemical composition of the white power deposit be examined and to understand the mechanism of weakening of the effect of UV light. According to Raumann's findings (1982) untreated polypropylene is sensitive to UV light, a suitable stabilizer should be added for improving UV resistance. In this study, carbon black is added to the raw material of geotextile A and B. Selection of proper additives is another important topic in manufacturing stable geotextile material.

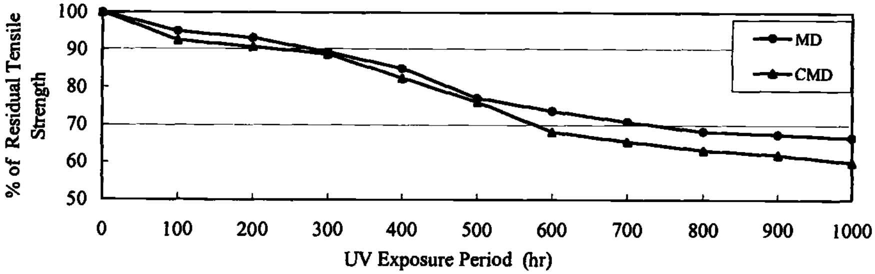

(a) *Sample A*

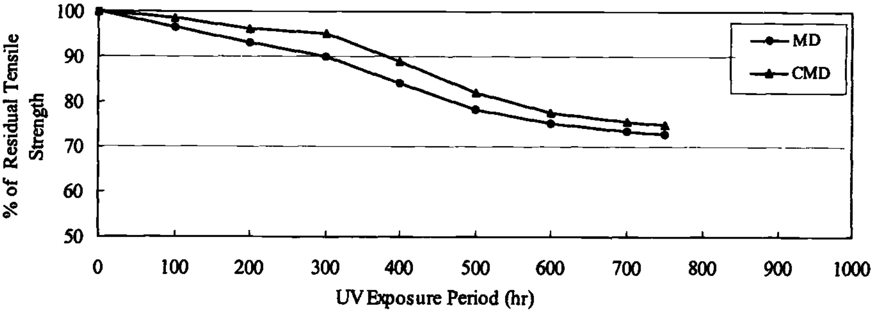

(b) *Sample B*

Figure 4 - *The Strength Residual under UV Exposure*

Strength Stability Subject to Temperature Variation

Wet geotextile and air-dried geotextile were cured at –20 °C, –30 °C and –40 °C for 2, 4 and 6 days. The cured specimens were returned to room temperature (21 ± 1°C) before the strip tensile test was carried out to identify the effects of freezing condition on geotextile tensile strength. The annual temperature ranges in Xing Jiang Province varies from –40 °C to 40 °C. The temperature at Urumqi City ranges from –10 °C in winter to 20 °C in summer. Wet and air-dried geotextiles were again subjected to freeze-thaw cycles from –40 °C to 40 °C and from –10 °C to 20 °C. When the temperature chamber attained the intended temperature, it was maintained for at least 4 hours before switching to another temperature. This study used a specially designed temperature chamber that can achieve a temperature gradient of 1 °C/1.5 min. Geotextiles were treated with 15, 30, 45 and 60 freeze-thaw cycles. The tensile strength of the geotextiles was measured after these curing cycles.

Referring to the table at the right hand side in each of Figures 5 through 10, definitions for all digits can be described below. the first digit in the test designator is either "A" or "B". "A" or "B" denotes the type of geotextile used (refer to Table1). The second digit, either "1" or "2" denotes the machine direction, either 1 = MD or 2 = CMD (cross-machine direction) denotes machine direction (MD) and "2" denotes cross-machine direction (CMD). The third digit is either "D" or "W", wherein "D" denotes dry condition and "W" denotes wet conditions. The last two digit is either of "20", "30" or "40"; in which "20" denotes a curing temperature of –20 °C, "30" denotes a curing temperature of –30 °C, and "40" denotes a curing temperature of –40 °C. Each plotted data is an average value obtained from these six specimens. A total of 852 specimens were prepared for strip tensile tests.

As can be seen from Figures 5 through 8, the effect of temperature and curing period on tensile strength is insignificant. As the number of curing days increases, the tensile strength reduction becomes less dependent on the curing time. For dry and wet conditions, (D versus W specimens) there was no significant difference noted in the tensile strength reduction curves. For all of these tensile strength reductions, the results indicated the residual strength still remains above 90% of the ultimate tensile strength. From Figures 9 and 10, it can be seen that with an increasing number of freeze-thaw cycles, the strength reduction per cycle tends to increase. The strength reduction of wet geotextile is slightly higher than that of air-dried geotextile. This perhaps occurs as the freeze-thaw cycle causes water to squeeze and stretch the pore size of the geotextile and hence undermines the matrix structure of the geotextile. In all cases, the tensile strength still remains above 80%. It must be noted that the adverse effects of freeze-thaw cycles on tensile strength are greater than that of freezing only.

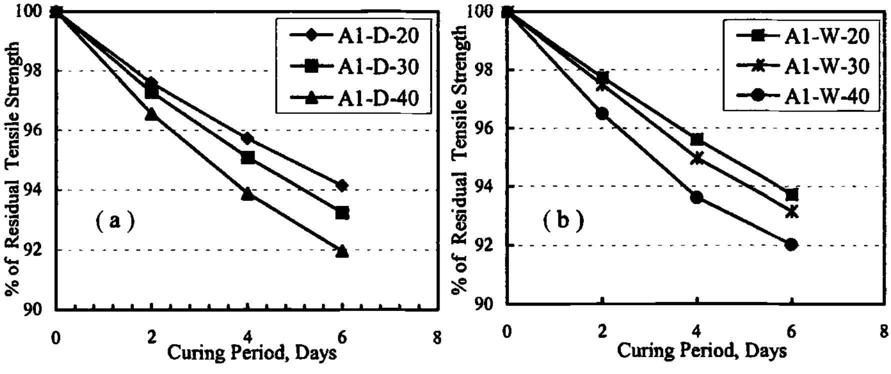

Figure 5—*Sample A with MD Tensile Strength under Varied Curing Temperature*

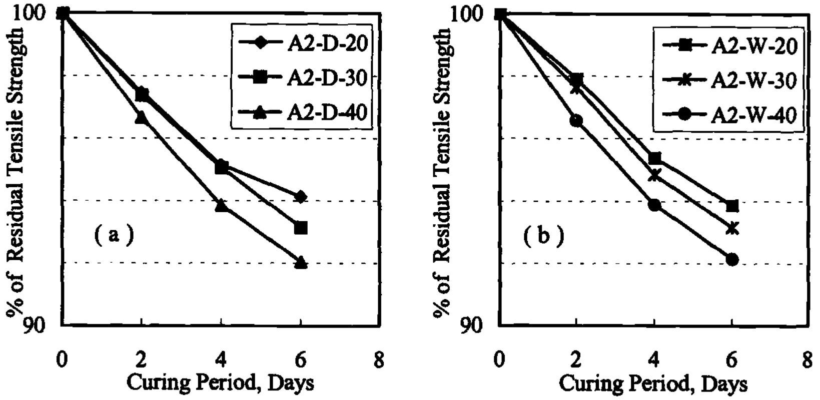

Figure 6—*Sample A with CMD Tensile Strength under Varied Curing Temperature*

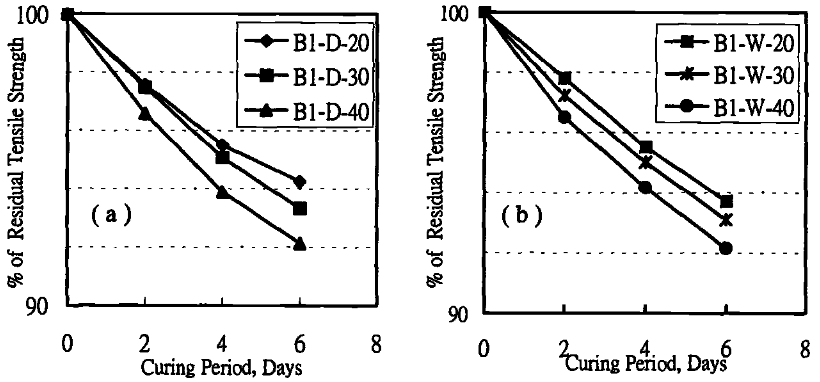

Figure 7—*Sample B with MD Tensile Strength under Varied Curing Temperature*

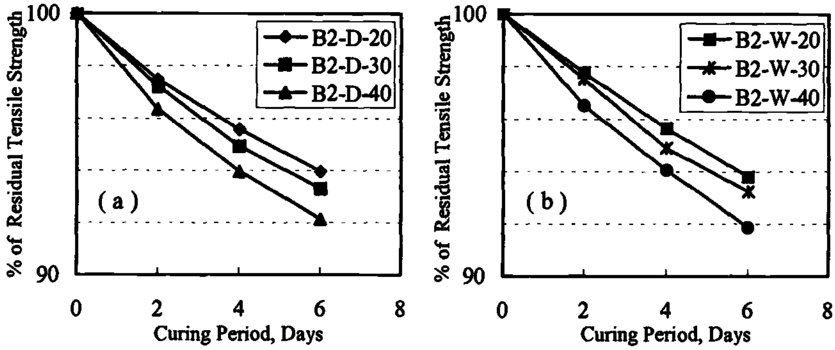

Figure 8—*Sample B with CMD Tensile Strength under Varied Curing Temperature*

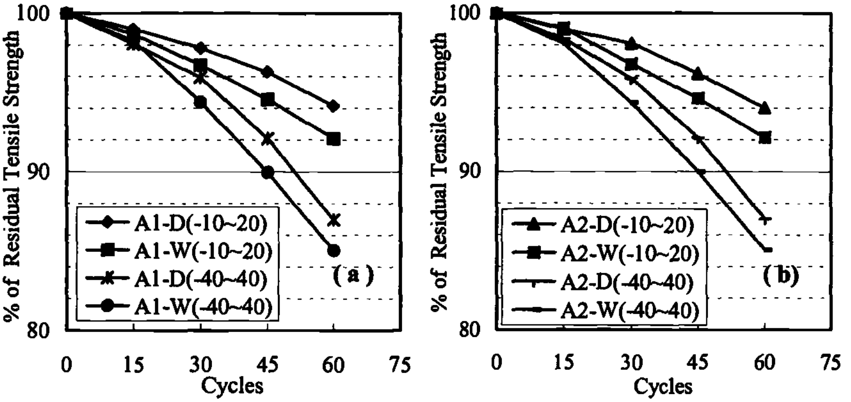

Figure 9—*Sample A with MD and CMD Tensile Strength under Freeze-Thaw Cycles*

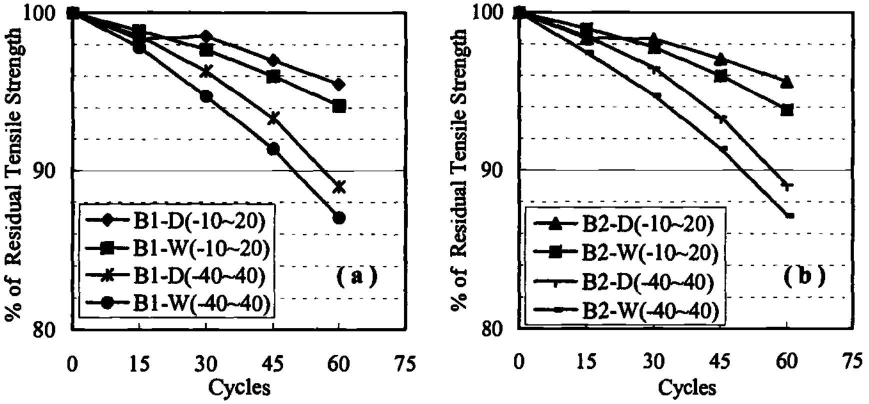

Figure 10—*Sample B with MD and CMD Tensile Strength under Freeze-Thaw Cycles*

Review of Requirement for Geotube Tensile Properties

The geotubes used in this study were unseamed. To cope with the machine width (5.5 m), the perimeter of the geotube is set at 5 m. Based on the simplified cross section as shown in Figure 3(b), a preliminary dimension can be estimated. In the case of a single geotube, if the perimeter is 5 m, the water pressure can be assumed to be 0.3 kg/cm^2, then the perimeter stress of the geotube is 1.8 MPa (tensile stress of geotextile requires 17.5 kN/m), the limit stress is 7.16 MPa (maximum tensile stress requires 70 kN/m); the geotube maximum height is 1.4 m, while the H/W ratio is 0.8. With grouped tubes, the interlocking mechanism between geotextile and soil shall be considered, such as consolidated drain strength, shear strength, normal stress and surcharge. The resulting tensile strength for geotextile much lower than single tube in factored in. According to typical analysis results as given above, a suitable geotube material, sample B, is therefore selected for ongoing project details.

Conclusions and Recommendations

1. Carbon-black treated geotextile manufactured in Taiwan after subjection to UV exposure still possesses a tensile strength that fully complies with relevant design manual and is considered applicable in the Xing Jiang area, which has very harsh climatic conditions.
2. The effect of freezing temperatures on the tensile strength of geotextile A and B is insignificant. For a curing period of up to 6 days, the tensile strength remains greater than 90%.
3. The effect of freeze-thaw cycle on the tensile strength of geotextile is insignificant. In all cases, the tensile strength remains greater than 90%, except for Sample A after subjected to 60 cycles of the –40 °C—40 °C cycle. In this particular case, the tensile strength drops to slightly lower than 90 %.
4. For single tube and mechanically calculated and group tubes, all stress levels meet the properties of Sample A and Sample B.
5. It is suggested that Sample B be used in the project as it has a higher tensile strength.

Reference

Casagrande, A., 1975, "Liquefaction and Cyclic Deformation of Sands, a Critical Review," *Proceedings of the Fifth Panamerican Conference on Soil Mechanics and Foundation Engineering*, Buenos Aires; reprinted as Harvard Soil Mechanics Series, No.88, pp. 27.

Holtz, R. D., Christopher, B. R., Berg, R. R., 1998, "Geosynthetic Design and Construction Guidelines Participant Notebook," Publication No. FHWA HI-95-038. Federal Highway Administration, U.S. Department of Transportation.

Leshchinsky, D., and Leshchinsky O., Ling H. I., and Gilbert P. A., 1996, "Geosynthetic Tubes for Confining Pressurized Slurry: Some Design Aspects," *Journal of Geo-technical Engineering, ASCE*, Vol. 122, No.8.

Raumann, G., 1982, "Outdoor Exposure Tests on Geotextiles," *Proc.Second International. Conference. Geotextiles*, Las Vegas, NV, IFAI, pp.541-546.

Shneider H., 1988, "Long-Term Performance of Polypropylene Geosynthetics," *Geosynthetic Research Institute*, Drexel University, Philadelphia, P.A., pp. 95-109.

Sprague C.J and Goodrum R. A., 1994, "Selecting Standard Test Methods for Experimental Evaluation of Geosynthetic Durability," *Transportation Research Record, No. 1439*, TRB, National Research Council, Washington, D.C., pp. 32-40.

Sibylle Dueri[1] and René Therrien[2]

Factors Controlling Contaminant Transport Through the Flood Sediments of the Saguenay Fjord: Numerical Sensitivity Analysis

Reference: Dueri, S. and Therrien, R., **"Factors Controlling Contaminant Transport Through the Flood Sediments of the Saguenay Fjord: Numerical Sensitivity Analysis,"** *Contaminated Sediments: Characterization, Evaluation, Mitigation/Restoration, and Management Strategy Performance, ASTM STP 1442,* J. Locat, R. Galvez-Cloutier, R. C. Chaney, and K. R. Demars, Eds., ASTM International, West Conshohocken, PA, 2003.

Abstract: In July 1996, two days of intense rainfall caused severe flooding in the Saguenay region and led to the discharge by rivers of several million cubic meters of clean sediments to the Fjord. This turbidite layer, composed of clean sediments, represents a potential barrier for the migration of heavy metals and PAHs from the underlying contaminated sediments towards the new sediment-water interface. A numerical model has been developed to simulate the vertical migration and remobilization of dissolved contaminants in the capping layer. The model includes the main physical, chemical and biological factors affecting the contaminant flux in the cap. Calibration of the model has been achieved through comparison with the data collected during the field and laboratory characterization of the sediments of the Saguenay Fjord. A detailed sensitivity analysis, based on factorial design, shows that the model parameters associated with bio-irrigation have the greatest impact on the model output and by extension on the effectiveness of a capping layer.

Keywords: Saguenay Fjord, sediment cap, contaminant migration, numerical model, sensitivity analysis, factorial design

---

[1] PhD Student, Département de Géologie et génie géologique, Université Laval, Québec, Canada G1K 7P4.

[2] Professor, Département de Géologie et génie géologique, Université Laval, Québec, Canada G1K 7P4.

Introduction

The capping of contaminated sediments with clean material is a promising alternative for the isolation of contaminants from the water column and the prevention of further pollution. This approach has the advantage of being applicable even if the contamination extends over a large surface. A capping layer is designed to physically isolate the contaminants from the benthic fauna, stabilize the sediment, and prevent or at least reduce the contaminant flux towards the new water-sediment interface. Any attempt to predict the long-term effectiveness of the cap requires an understanding of the physical, chemical and biological factors affecting the migration of contaminants in the sediments.

The TRANSCAP-1D numerical model was developed to simulate the migration of dissolved contaminants through a subaqueous capping layer. The model considers the physical, chemical and biological processes affecting the fate of a dissolved contaminant in a sedimentary environment and can be used to predict the effectiveness of a sediment cap in isolating the contaminant from the water column. The transport equation includes advection, diffusion, chemical reactions and the effect of bio-irrigating worms.

The model has been applied to the Saguenay Fjord, where a major flood led to the deposition of a natural capping layer over contaminated sediments. Since the catastrophic flood, which occurred in 1996, the geotechnical and geochemical characteristics of the capping layer, as well as the recolonisation of the benthic fauna, have been extensively studied in the context of a multidisciplinary research project. The objective of this research project is to assess the effect of the new capping layer on the migration of contaminants towards the new sediment-water interface. A large database was available for the model calibration and the response of the numerical model was successfully matched to measured concentrations of dissolved arsenic in the Saguenay Fjord. These results will be presented in a separate paper that focuses on the calibration of the model.

Sensitivity analysis is commonly used in engineering to assess the influence of a model input on the output. The simplest form of sensitivity analysis consists in increasing or decreasing the value of one input parameter at a time by some fraction, or perturbation, and then evaluate the corresponding variation in the model output. This procedure is repeated for each parameter tested and the parameter causing the greatest modification in the model output is deemed the most important. Although this approach is simple and commonly used, there is no guideline for the selection of parameters to evaluate and for the magnitude of the perturbation to impose. In addition, since parameters are evaluated one by one, any significant combined effect of two or more parameters is never detected.

Kabala (2001) presents an overview of sensitivity analysis, with an application to pumping tests in aquifers. The definition of sensitivity of model output to input parameters given by Kabala (2001) is more precise than the general definition given above, because it is expressed in a mathematical form as the differential in the model output with respect to selected input parameters. By using this definition, sensitivities can be calculated with more precise mathematical techniques, such as the direct method that requires differentiating the governing equations, or the adjoint method that requires solving the governing equation and its mathematical adjoint.

Other approaches have been developed in chemical engineering to determine the combined effect of several parameters on model output. An example is a two-level factorial design, which is used to determine the influence of *n* parameters on some observed value with a minimum number of experiments (Box et al. 1978). Two levels, or values, are selected for each parameter and a total of 2^n experiments are sufficient to test the impact of each parameter, as well as every possible combination of parameters, on the experimental output. By limiting the number of trials and still considering all combined effects, the method is well suited for a rapid identification of the main parameters for the model, which could then be studied or characterized in more detail. The application of this method to the sensitivity analysis of numerical models has been very limited, especially in the environmental domain, but it is well suited for that purpose. A good example of the application of the factorial design to simulation results is presented by Elliott et al. (2000), where the method was used to determine the kinetic parameters with a significant effect on an anaerobic treatment process.

A large variability and uncertainty associated with several physical, chemical and biological parameters was observed for the Saguenay Fjord. This situation requires a detailed approach in order to identify the crucial parameters affecting the fate of contaminants in sediments. To investigate the sensitivities of the model parameters that are either variable or uncertain, a factorial design approach is presented here for the model simulating the migration of contaminants in sediments of the Saguenay Fjord. The purpose of the sensitivity analysis presented here is to deepen our understanding of the effect of variable input values on the model output and to identify the factors that have the greatest influence on the contaminant migration towards the new sediment-water interface.

Model Equations and Parameters

The TRANSCAP-1D model simulates advection, diffusion, chemical reactions and the effect of the burrowing activity of the benthic fauna. The consolidation of the sediment and associated fluid advection are not included. The sediment is represented as a dual porosity medium composed of sediment-pores and bio-irrigated tubes. The mathematical formulation consists of two partial differential equations, corresponding to the contaminant transport in the two media. These equations are coupled via a non-local exchange term that represents the mass transfer of contaminant between the sediment and the tubes. The formulation is mathematically similar to the one describing solute transport in a dual-porosity medium, in the context of groundwater flow (for example, Zheng and Bennett 2002).

The equation describing solute transport in the sediment porewater is given by:

$$n_S \frac{\partial C_S}{dt} = n_S \cdot \frac{D_S}{R}\left(\frac{\partial^2 C_S}{\partial z^2}\right) - n_S \cdot \frac{v_S}{R} \cdot \frac{\partial C_S}{\partial z} - \beta(C_S - C_T) \qquad (1)$$

where C_S and C_T are the solute concentration [ML^{-3}] in the sediments and the tubes, respectively, n_s is the sediment porosity [-], v_s is the fluid velocity in the sediment [LT^{-1}],

R is the solute retardation factor [-], and β is a first-order mass transfer coefficient [T^{-1}]. The dispersion coefficient of the solute in the sediments, D_s [L^2T^{-1}], is given by:

$$D_S = D_d + \alpha_L \cdot v_S \tag{2}$$

where D_d is the effective diffusion coefficient [L^2T^{-1}] and α_L is the sediment dispersivity [L]. Note that when the fluid velocity is small in the sediment, which is the case for low-permeability material, the dispersion coefficient is approximately equal to the diffusion coefficient.

The equation describing solute transport in the tubes is given by:

$$n_T \frac{\partial C_T}{\partial t} = n_T D_m \frac{\partial^2 C_T}{\partial z^2} - n_T v_T \frac{\partial C_T}{\partial z} + \beta(C_S - C_T) + S \tag{3}$$

where n_T is the porosity of the tubes [-], D_m is the dispersion coefficient for the tubes [L^2T^{-1}], given by an expression similar to equation (2), and v_T is the fluid or irrigation velocity in the tubes [LT^{-1}]. In equation (3), S is a general source or sink term [$ML^{-3}T^{-1}$] representing the release of contaminant from mineral dissolution associated to bio-irrigation. This term is defined later in this section.

The mass transfer coefficient β and the porosity of the tubes n_T decrease exponentially with depth, following the distribution of bio-irrigated tubes (Martin and Banta 1992). The mass transfer coefficient β can be split in two coefficients β_1[T^{-1}] and β_2 [L^{-1}], representing the maximal value of the mass transfer coefficient at the surface of the sediment and the coefficient of exponential decrease respectively:

$$\beta(z) = \beta_1 \cdot \exp[\beta_2(z - z_{max})] \tag{4}$$

As illustrated by Boudreau (1997), the value of the non-local term β_1 [T^{-1}] at the surface of the sediment can be estimated using the parameters of Aller's cylindrical diffusion model (Aller 1980):

$$\beta_1 = \frac{2 \cdot D_d \cdot r_1}{(r_2^2 - r_1^2)(\delta - r_1)} \tag{5}$$

where r_1 is the inner radius of the tubes/burrows [L], r_2 is the half-distance between two tubes/burrows [L] and δ is the distance [L] from the burrow axis to a point where the concentration equals the horizontally integrated value.

The porosity of the tubes $n°_T$ at the surface is calculated using cylinders to approximate their geometry:

$$n^\circ_T = m \cdot r_1^2 \cdot \pi \tag{6}$$

where m represents the quantity of tubes per unit area [L^{-2}]. The exponential decrease with depth of the tube porosity can be represented with the same coefficient β_2 [L^{-1}]:

$$n_T(z) = n_T{}^{\circ} \cdot \exp[\beta_2(z - z_{max})] \quad (7)$$

The source term S of the equation for the tubes (3) represents the chemical reactions responsible for the remobilization of contaminants. The representation of the chemistry is very simplified and the model only considers the dissolution caused by the reoxidation of reduced contaminants adsorbed or coprecipitated with iron-monosulfide (FeS). The dissolution is a consequence of the exposition of the anoxic sediment, containing sulfides, to oxygenated water advected in the tubes by bio-irrigation. As observed by Furukawa (2001) the irrigated burrow walls are the interface between oxic-anoxic milieus and are characterized by steep geochemical gradients and rapid chemical mass transfer. In the model, the dissolution term is composed of a kinetic factor γ [L^{-1}] and a coefficient L [ML^{-3}], representing the maximal dissolved contaminant concentration for a given FeS concentration in the sediment. The representation of the chemical reaction was specifically adapted for the dissolution and the remobilization of arsenic (As), which was extensively studied in the Saguenay Fjord. In the anoxic zone, As is adsorbed or coprecipitated with FeS, but the oxidation of the Fe-sulfides leads to the remobilization of this contaminant. The coefficient L is derived from the linear correlation between the released As and initial solid FeS that was observed during resuspension tests of Saguenay sediments (Saulnier and Mucci 2000). The source term can be expanded in the following way:

$$S = \gamma(L - C_T) \quad (8)$$

$$L = k_1 C_{FeS} + k_2 \quad (9)$$

where k_1 and k_2 are regression parameters that can be viewed as dissolution coefficients and C_{FeS} [ML^{-3}] is the concentration of FeS.

Initial and boundary conditions are required to solve both equations (1) and (3). To impose the initial conditions one specifies the initial solute concentration in the two domains, sediments and tubes. Boundary conditions are required at the top and bottom of the domain and can be either a prescribed concentration or prescribed mass flux for both domains.

The two governing equations (1) and (3) are discretized with the finite volume method. The equations are coupled through the mass exchange term and a simultaneous solution for the concentration in the sediment and tube is obtained for each finite volume. The system of equations is thus solved in a fully-coupling fashion, avoiding the use of iteration that is necessary when the equations are decoupled. The block tridiagonal matrix resulting from the discretization and assembly of the terms is solved with the Thomas algorithm adapted to block matrices. The numerical solution was tested by comparing to the semi-analytical solution MPNE of Neville et al. (2000), which has been developed for one-dimensional solute transport in a dual-porosity medium with multiple non-equilibrium processes. The numerical model reproduces almost perfectly the concentrations computed with the analytical solution (results not presented).

Design of the Sensitivity Analysis

The first step of the two-level factorial design is to determine the number of factors, or parameters, that have to be tested and define the two levels, which are the minimum and maximum value for each input parameter. Each factor is assumed independent of the other factors, but a factor can be composed of a set of dependent input values. For *n* factors at two levels each, a total of 2^n simulations are necessary for a full factorial design.

The choice of the parameters to be tested is based on the available information about the processes affecting the migration of contaminants in the sediments of the Saguenay Fjord. At the study site the sediments show a low permeability but are intensively bio-irrigated. Thus bio-irrigation, dissolution and retardation are supposed to influence the migration of contaminant. Consequently, a factorial design with five factors was selected: three factors related to bio-irrigation (number of tubes per square meter, depth of the tubes and bio-irrigation velocity) one factor related to the reactions (dissolution coefficients) and the retardation factor. The fluid velocity in the sediment v_s was not considered for the sensitivity analysis because in the sediments of the Saguenay Fjord there is no evidence for such advection. This parameter was therefore set equal to zero for all simulations.

The minimum and maximum values of each tested parameter were determined from the available information, which includes data measured at the Saguenay Fjord and data derived from the literature. The values of the parameters are discussed in the following paragraphs and are presented in Table 1.

The depth of bio-irrigation is represented in the model by two parameters: the maximum depth attained by the tubes, *biox*, and the corresponding coefficient β_2, where β_2 describes the exponential decrease of both the mass transfer between tubes and sediment β and the tube porosity n_T. The two parameters, *biox* and β_2, are related since the maximum depth corresponds to the location where the mass transfer β and the tube porosity n_T exponentially tend to zero. According to field observations and to measured bioturbation intensities (De Montety et al. 2000), the minimal value of the bio-irrigation depth *biox* was set to 0.06 m and the maximal value to 0.26 m. This corresponds to values of β_2 equal to 70 m^{-1} and 16 m^{-1}, respectively.

Table 1 - *Minimum and Maximum Values for the Tested Factors*

Factor	Parameters	Name (Units)	Minimum	Maximum
Bio-Irrigation Depth B_1	Depth of Tubes	biox (m)	0.06	0.26
	Mass Transfer Coefficient	β_2 (m^{-1})	70	16
Number and Dimension of Tubes B_2	Porosity of Tubes at Surface	n_{T0} (-)	0.00039	0.00471
	Mass Transfer Coefficient	β_1 (day^{-1})	0.0157	0.119
Retardation Factor R		R (-)	5	45
Bio-Irrigation Velocity V		v_T (m/day)	0.2	5
Dissolution Coefficients D		k_1 (g^2 mol^{-1} L^{-1})	1	1.7
		k_2 (µg L^{-1})	1	1.3

The number and the dimension of the tubes in the upper sediment layer are an indicator of the intensity of bio-irrigation in this zone. This factor affects two input values of the model: the tube porosity at the surface n^o_T and the mass transfer coefficient β_l. To calculate these parameters, one must first set the minimum and maximum values of the inner radius of the tubes r_l, as well as the number of tubes per square meter, m. The value of m also defines the half-distance between two tubes r_2 according to:

$$r_2 = \frac{1}{2\sqrt{m}} \tag{10}$$

The value of r_l results from observation on sediments sampled with a box-corer in the Saguenay Fjord during summer 1999 and 2000 and varies between 0.0005 m and 0.001 m. The minimum and maximum value of the number of tubes m, visually determined from photographs of the undisturbed bottom sediments taken during the summer 2001, are equal to 500 and 1500 tubes per square meter, respectively. Thus, the mass transfer coefficient β_l may vary between 0.0157 day^{-1} and 0.119 day^{-1}, whereas the tube porosity n^o_T varies between 0.00039 and 0.00471.

The value for the retardation factor, R , has been estimated for model calibration on two measured arsenic concentration profiles and taking into account the average of the range of values presented by Fuller (1978) for arsenic. The minimum and maximum values of R have thus been set to 5 and 45, respectively.

The values for the bio-irrigation velocity v_T were derived from data measured during laboratory tests carried out on polychaete families living in shallow water (Riisgard 1989, Riisgard 1991). In the calibrated model, the irrigation velocity is equal to 1 m day^{-1}. The minimum and maximum values for the factorial design were determined by modifying this value by a factor of five. Thus, we obtain a minimum bio-irrigation velocity of 0.2 m day^{-1} and a maximum value of 5 m day^{-1}.

The minimum and maximum values of the dissolution coefficients were derived from the values of dissolved As and solid FeS measured at two sampling stations of the Saguenay Fjord in 1998 (Saulnier and Mucci 2000). To define the levels of these parameters, it has been assumed that the dissolution coefficients, determined by means of the measured data, correspond to the minimum and maximum values of the coefficient. Thus, we assume that k_l varies between 1 and 1.7 and that k_2 varies between 1 and 1.3.

Four series of simulations were carried out for the sensitivity analysis (Table 2). The first two series of simulations considered five variable factors, including a variable dissolution coefficient, and were thus composed of $2^5 = 32$ simulations. The series 3 and 4 simulated the response of the model for a non-reactive contaminant and the dissolution coefficient was therefore equal to zero. This means that there were only four factors to test and the factorial design was composed of $2^4 = 16$ simulations. To evaluate the influence of the thickness of the capping layer, two of the series were performed with a cap thickness of 20 cm (series 1 and 3) and the other two with a cap thickness of 10 cm (series 2 and 4). The initial concentration of contaminant was extrapolated from the arsenic concentration measured in the sediments of the Saguenay Fjord in 1998.

Each series was composed of simulations representing every possible combination of the minimal and maximal values of each factor (Table 3). The results of the simulation of each series were sorted in a standard order and thereafter the Yates algorithm was applied in order to calculate the effect of each factor and of the combination of factors (Box et al. 1978). These effects represent the change in the response as we move from the maximum value to the minimum value of a factor.

Table 2 – *Description of the Series of Simulations for the Sensitivity Analysis*

Series of Simulations	Thickness of Cap	Reactions	Number of Simulations
1	0.2 m	Yes	32
2	0.1 m	Yes	32
3	0.2 m	No	16
4	0.1 m	No	16

Table 3 - *Simulation Protocol for the Factorial Design of Four Tested Factors: Variable Input Values Used for a Set of 16 Simulations*

Simulation	Factors					
	Depth of Bio-Irrigation B_1		Quantity and Dimensions of Tubes B_2		Retardation Factor R	Bio-Irrigation Velocity V
	biox	β_2	n_{T0}	β_1	R	v_T
1	0.06	70	0.00039	0.0157	5	0.2
2	0.26	16	0.00039	0.0157	5	0.2
3	0.06	70	0.00471	0.119	5	0.2
4	0.26	16	0.00471	0.119	5	0.2
5	0.06	70	0.00039	0.0157	45	0.2
6	0.26	16	0.00039	0.0157	45	0.2
7	0.06	70	0.00471	0.119	45	0.2
8	0.26	16	0.00471	0.119	45	0.2
9	0.06	70	0.00039	0.0157	5	5
10	0.26	16	0.00039	0.0157	5	5
11	0.06	70	0.00471	0.119	5	5
12	0.26	16	0.00471	0.119	5	5
13	0.06	70	0.00039	0.0157	45	5
14	0.26	16	0.00039	0.0157	45	5
15	0.06	70	0.00471	0.119	45	5
16	0.26	16	0.00471	0.119	45	5

Results

The sensitivity analysis was performed over a simulation time of ten years after the capping event. Two types of model output were considered for the analysis: the total mass of contaminant that left the system from the upper boundary, and the concentration of contaminant in the upper sediment layer at the end of the simulation. The results of the sensitivity analysis were represented in a normal probability plot. This type of plot is generally used to test the normality of a distribution, but in our case it allows a straightforward identification of the factors with a significant influence on the output of the model. Each point on the graph corresponds to the effect of one or a combination of factors. The effects represent the average variation of the response for a changing factor over all conditions of the other factors and does not have units (Box et al. 1978). The points that fall on or near the straight line are normally distributed and thus these effects cannot be distinguished from the normally distributed error. On the opposite, the effects that deviate from the straight line and therefore from the normal error distribution point out significant factors. The sum of squares indicates the deviation of the effect from the normal distribution and thus this value can be used to quantify the importance of a factor for the response.

Contaminant Mass Released from the Upper Boundary of the Sediment After 10 Years

The result of the first set of simulations, representing the migration of a reactive contaminant through a cap of 0.2 m, is displayed in Figure 1. The graph illustrates that the factors with the greatest influence on the released mass are those associated to bio-irrigation (irrigation velocity *V*, number and dimension of tubes B_2 and depth of the tubes B_1). There is also a second group of factors affecting the output of the model. This group is composed of the combination of bio-irrigation factors with the factor of dissolution *D*.

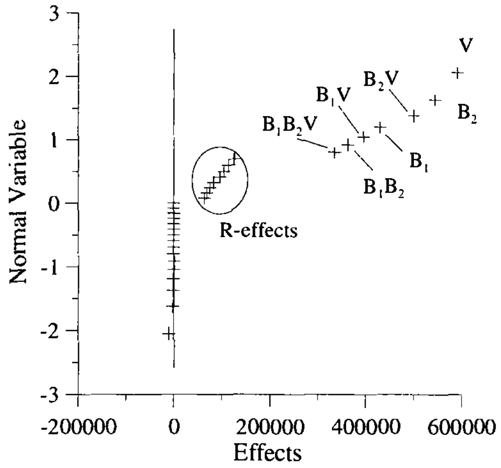

Figure 1 - *Effect of Tested Factors on the Mass Release of a Reactive Contaminant. Cap Thickness of 20 cm. Significant Effects Identified by the Variable Name.*

As these effects show a smaller deviation from the normal distribution, their influence on the result is less significant. The result of the second series of simulations, representing a reactive contaminant migrating through a cap of 10 cm, shows a very similar trend to the previous series. The similarity is best illustrated by comparing the sums of squares, presented in Table 4.

Table 4 - *Sums of Squares for a Reactive Contaminant Migrating Through a Cap of 20 cm (Series 1) and a Cap of 10 cm (Series 2).*

Sum of Squares %	Series 1	Series 2
V	22.47	22.53
B_2	19.10	19.01
B_2V	16.13	16.17
B_1	11.96	11.79
B_1V	10.08	10.10
B_1B_2	8.46	8.57
B_1B_2V	7.23	7.25
SOFS Total	95.43	95.41

Figure 2 shows the results of the third series of simulations, representing a non-reactive contaminant migrating through a sediment covered by a cap of 20 cm. In this case the contaminant release is strongly affected by the bio-irrigation depth B_l, followed by the combination of bio-irrigation factors B_l, B_2 and V. The retardation factor R also exhibits a significant deviation from the normally distributed values. Figure 3 illustrates the results of series 4, representing the effects for a non-reactive contaminant migrating through a cap of 10 cm. In this case, the depth of the tubes B_l is the only important factor identified on the graph.

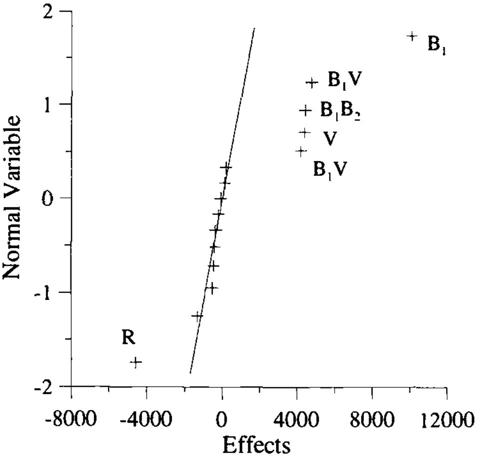

Figure 2 - *Effect of Tested Factors on the Mass Release of a Non-Reactive Contaminant. Cap Thickness of 20 cm. Significant Effects Identified by the Variable Name.*

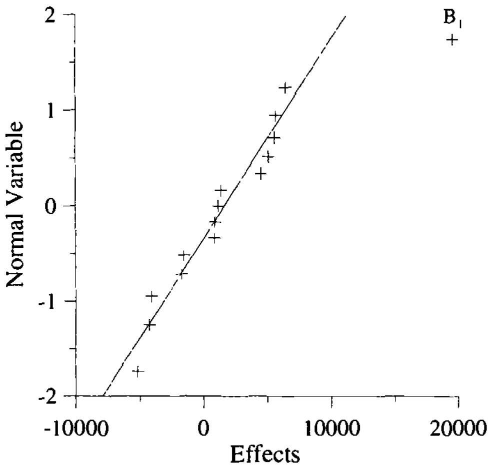

Figure 3 - *Effect of Tested Factors on the Mass Release of a Non-Reactive Contaminant. Cap Thickness of 10 cm. Significant Effect Identified by the Variable Name.*

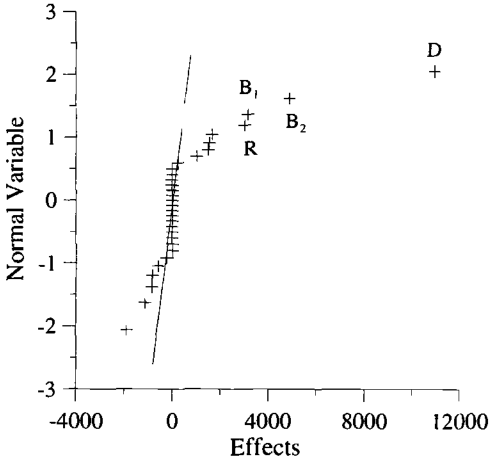

Figure 4 - *Effect of Tested Factors on the Surface Concentration of a Reactive Contaminant. Cap Thickness of 20 cm. Significant Effects Are Listed.*

Contaminant Concentration in the Upper Sediment Layer After 10 Years

In this section, the sensitivity analysis was used to determine the significant factors affecting the contaminant concentration in the upper sediment layer, from the four series of simulations described previously. Figure 4 shows the result of the first series of simulations, considering a reactive contaminant and a cap thickness of 20 cm. The graph shows the significant influence of the dissolution coefficients D, the bio-irrigation depth B_1, the number and dimensions of the tubes B_2 as well as the retardation factor R.

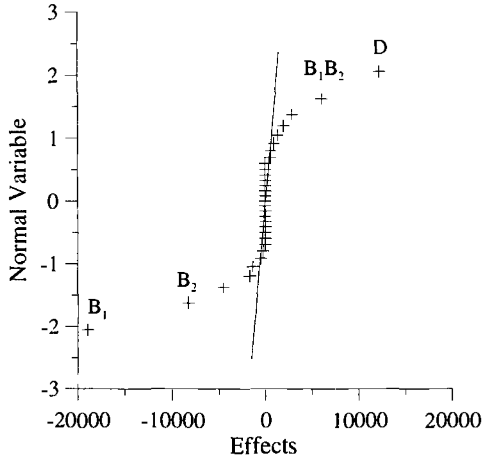

Figure 5 - *Effect of Tested Factors on the Surface Concentration of a Reactive Contaminant. Cap Thickness of 10 cm. Significant Effects Are Listed.*

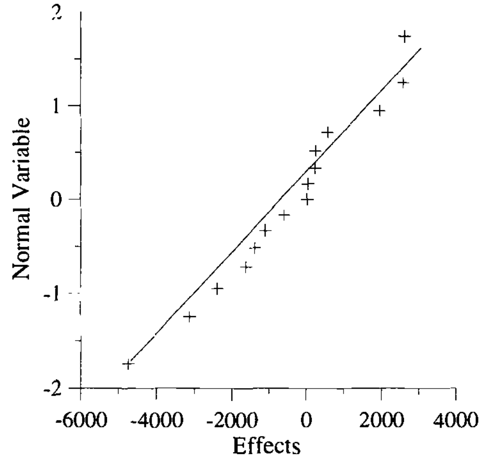

Figure 6 - *Effect of Tested Factors on the Surface Concentration of a Non-Reactive Contaminant. Cap Thickness of 20 cm.*

Shown in Figure 5 are the results of the factorial design for a reactive contaminant migrating through a cap of 10 cm. In this set of simulations the most significant factor is the bio-irrigation depth B_1, followed by the dissolution coefficients R. The combination of the depth and the number and dimensions of the tubes B_1B_2 is also an important factor, whereas the retardation factor R does not play a significant role.

The series representing a non-reactive contaminant are illustrated in Figures 6 and 7. The graphs do not display any outliers and none of the factors shows a significant deviation from the normally distributed population, represented by the straight line. Thus, they do not reveal any significant factor affecting the concentration in the surface layer.

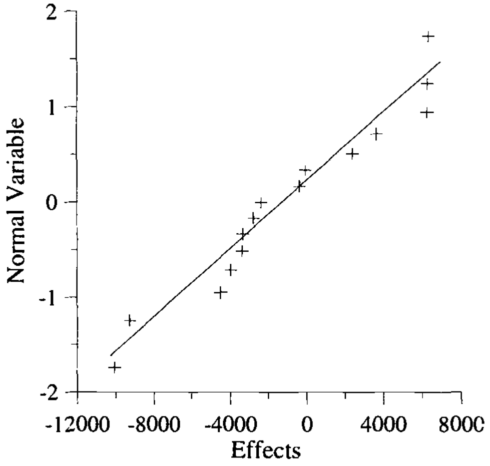

Figure 7 - *Effects of Tested Factors on the Surface Concentration of a Non-Reactive Contaminant. Cap Thickness of 10 cm.*

Table 5 summarizes the significant effects highlighted by the sensitivity analysis. The first two columns define the variable characteristics of the physical system (cap thickness) and of the contaminant (possibility of dissolution). The third and the fourth columns review the significant effects determined by the factorial design, depending on the considered output variable, i.e., the released mass or the surface concentration.

Table 5 - *Review of the Factors Having a Significant Effect on the Output of the Model.*

Parameters		*Response*	
Cap Thickness	Dissolution	Released Mass	Surface Concentration
0.2 m	Yes	V, B_2, B_1	D, B_2, B_1, R
0.1 m	Yes	V, B_2, B_1	B_1, D, B_2
0.2 m	No	B_1, V, R	-
0.1 m	No	B_1	-

The contaminant mass released over a period of ten years is mainly affected by bio-irrigation factors (B_1, B_2, V). The dissolution factor D does not display a significant effect on this type of output. The comparison between the series with a cap of 10 cm versus a cap of 20 cm indicates that the results depend upon the reactivity of the contaminant. For the ranges of cap thickness tested in this study and considering a reactive contaminant, the thickness variation does not lead to relevant differences in the results of the factorial design. Conversely, the effect of the cap thickness is evident for a non-reactive contaminant. The results for the surface concentration of contaminant ten years after capping show that in the case of a reactive contaminant, a variable cap thickness slightly influences the results of the factorial design. For a cap thickness of 20 cm, the most important factor is the dissolution coefficient *D*, whereas if the cap is only 10 cm thick, the depth of bio-irrigation B_l becomes the most important factor. In both cases, the bio-irrigation velocity *V* does not affect the results. Comparing the results of both output variables, one observes that for a reactive contaminant the bio-irrigation velocity V dominates the mass release, whereas the surface concentration is regulated by the dissolution coefficients *D*. The model is generally very sensitive to bio-irrigation parameters, except for the surface concentration of a non-reactive contaminant.

Conclusions

The factorial design has been successfully used to determine the most significant parameters for the transport of dissolved contaminant through a capping layer. Two types of responses were considered for the sensitivity analysis: the total mass of contaminant that left the system from the upper boundary in the first ten years after capping and the concentration of contaminant in the upper sediment layer after ten years. Both responses represent a potential harm for the aquatic fauna, since they indicate an exposure pathway for the organisms living in the marine environment. The results of the study pointed out that for the studied conditions the significant parameters are a function of the response variable, the contaminant type (reactive or non-reactive) and to a lesser extent the cap thickness. The sensitivity analysis showed that the bio-irrigation parameters are generally very important for the prediction of the released contaminant mass. It also demonstrated that the concentration of contaminant in the upper sediment layer depends on the bio-irrigation parameters as well as the dissolution coefficient.

The minimum and maximum values of each tested parameter were derived from the data collected at the Saguenay Fjord and from the available information reported in the literature. The present study identifies the input values with a significant effect on the result, thus highlighting the parameters that should be studied carefully in order to reduce the uncertainty and get a better approximation of the performance of the capping layer. However the most accurate characterization will not be able to eliminate the variability of the input values. Therefore, an uncertainty analysis will be performed to determine the distribution of the response considering the variability of the input parameters.

References

Aller, R. C., 1980, "Quantifying Solute Distributions in the Biotubated Zone of Marine Sediments by Defining an Average Microenvironment," *Geochimica et Cosmochimica Acta*, Vol. 44, pp. 1955-1965.

Box, G. E. P., Hunter, W. G., Hunter, J. S., 1978, *Statistics for Experimenters: an Introduction to Design, Data Analysis, and Model Building*. John Wiley, New York.

Boudreau, B. P., 1997, *Diagenetic Models and Their Implementation: Modelling Transport and Reactions in Aquatic Sediments*. Springer-Verlag, Berlin Heidelberg.

De Montety, L., Long, B., Desrosiers, G., Crémer, J. F. and Locat, J., 2000, "Quantification des Structures Biogènes en Fonction d'un Gradient de Perturbation dans la Baie des Ha! Ha! à l'Aide de la Tomodensitométrie Axiale," *Proceedings of the 53th Canadian Geotechnical Conference*, Vol. 1, pp. 169-175.

Elliott, M., Zheng, Y. and Bagley, D. M., 2000, "Determining Significant Anaerobic Kinetic Parameters Using Simulation," *Environmental Technology*, Vol. 21, pp. 1181-1191.

Fuller, W. H., 1978, *Investigation of Landfill Leachate Pollutant Attenuation by Soils*, US EPA, Municipal Environmental Research Laboratory, Cincinnati, OH.

Furukawa, Y., Bentley, S. J. and Lavoie, D. L., 2001, "Bioirrigation Modeling in Experimental Benthic Mesocosms," *Journal of Marine Research*, Vol. 59, pp. 417-452.

Kabala, Z. J., 2001, "Sensitivity Analysis of a Pumping Test on a Well with Wellbore Storage and Skin," *Advances in Water Resources*, Vol. 24, pp. 483-504.

Martin, W. R. and Banta, G.T., 1992, "The Measurement of Sediment Irrigation Rates :A Comparison of the BR^- Tracer and $^{222}RN/^{226}RA$ Disequilibrium Techniques," *Journal of Marine Research*, Vol. 50, pp. 125-154.

Neville C.J., Ibaraki, M. and Sudicky, E.A., 2000, "Solute Transport with Multiprocess Nonequilibrium: a Semi-Analytical Solution Approach," *Journal of Contaminant Hydrology*, Vol. 44, pp. 141-159.

Riisgard, H. U., 1989, "Properties and Energy Cost of the Muscular Piston Pump in the Suspension Feeding Polychaete Chaetopterus Variopedatus," *Marine Ecology Progress Series*, Vol. 56, pp. 157-168.

Riisgard, H. U., 1991, "Suspension Feeding in the Polychaete Nereis Diversicolor," *Marine Ecology Progress Series*, Vol. 70, pp. 29-37.

Saulnier, I. and Mucci, A., 2000, "Trace Metal Remobilization Following the Resuspension of Estuarine Sediments : Saguenay Fjord, Canada," *Applied Geochemistry*, Vol. 15, pp.191-210.

Zheng, C. and Bennett, G.D., 2002, *Applied Contaminant Transport Modeling*. 2nd Edition, John Wiley, New York.

Osman A. El-Rayis[1]

Steps for Restoration of a Polluted Egyptian Closed Lagoon on the Alexandria Mediterranean Coast

---

Reference: El-Rayis, O. A.,“ **Steps for Restoration of a Polluted Egyptian Closed Lagoon on the Alexandria Mediterranean Coast,”** *Contaminated Sediments: Characterization, Evaluation, Mitigation/Restoration, and Management Strategy Performance, ASTM STP 1442,* J. Locat, R. Galvez-Cloutier, R. C. Chaney, and K. R. Demars, Eds., ASTM International, West Conshohocken, PA, 2003.

Abstract: Lagoon (or Lake) Maryout Main Basin is one of the lagoon's four sub-basins, polluted with organic and metals contaminants from untreated sewage and industrial effluents from Alexandria City. Since 1993, these effluents have become primary treated before discharging into this basin through two point sources; one source is at a new site, as a step in rehabilitating the lagoon. Surface sediment samples were collected 3 years later, from the Main Basin as well as from the other three basins of the lagoon to determine the level of nine priority metal pollutants as well as organic carbon (Org-C). The data reveal that the sediments of the Lagoon Main Basin, particularly that in vicinity of the new point source, became spoiled and remarkably enriched with all the studied contaminants. In addition, some of the studied metals are at levels comparable to those of the median effect-range of Long and Morgan recommended by the EPA. This means that either diversion or advanced treatment is necessary to eliminate these effluents.

Keywords: restoration, polluted Lagoon Maryout, sediments, organic carbon and metals, Alexandria, Egypt

Introduction

Lagoon Maryout is a closed lagoon without a natural connection to the Mediterranean Sea. Most of the lagoon is situated south of Alexandria and is completely separated from the sea by a high (to ~ 20 m), rather well lithified carbonate ridge of late Pleistocene age (Ali and West 1983). The long, narrow extension of the lagoon southwest of Alexandria occupies the lowest part of the depression between two carbonate ridges (named Abu Sir and Gable Maryout ridges). This lagoon extension parallels the coastline. Lagoon Maryout is presently a small remnant of its precursor and now is artificially divided with dikes into four sub-basins named Main, Fisheries, Northwest, and Southwest Basins (Figure 1). The respective areas of these basins are 6000, 1000, 3000 and 7500 acres. The average depth of the lagoon is about 1 m.

---

[1] Professor, Oceanography Department, Faculty of Science, University of Alexandria Moharrem Bek 21511, Alexandria, Egypt.

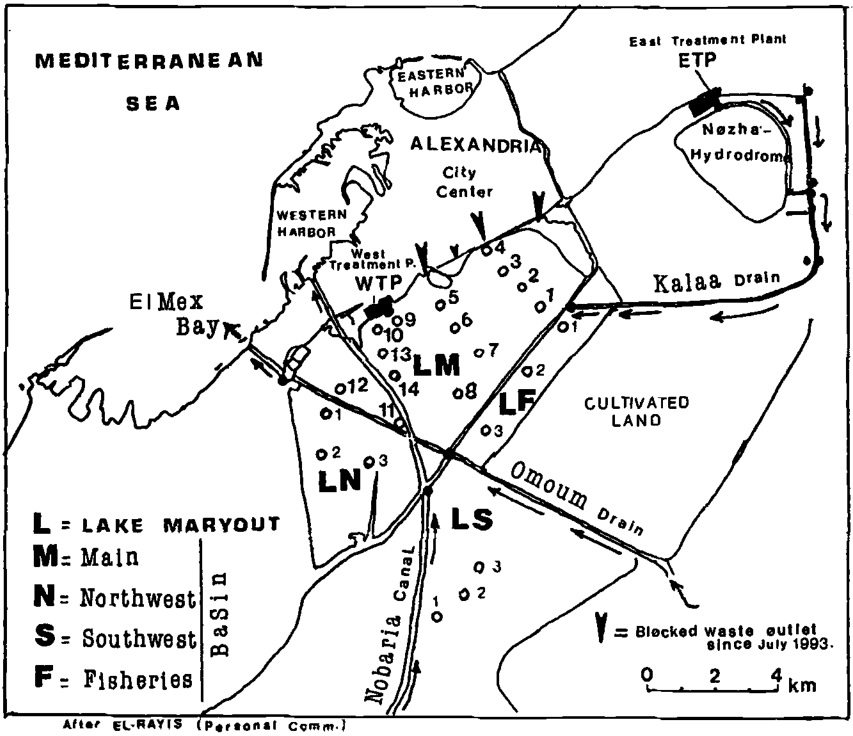

After EL-RAYIS (Personal Comm.)

Figure 1- *Lagoon Maryout and Its Four Basins and Locations of the Sampling Stations.*

The Main Basin, since 1993, receives flow from three main sources: (1) Kalaa (agricultural) Drain that also carries the discharge from a treatment plant called East Treatment Plant (ETP), (2) Directly from the West Treatment Plant (WTP) outlet, and (3) Omoum (agricultural) Drain. The other three basins receive flows from a variety of canals and drains but do not receive any effluent from the ETP or WTP. It is worth mentioning that the water level in the lagoon and in the Omoum Drain downstream portion must be regulated and always kept at 3.7 m below the sea surface level to allow for the drained waters mainly from the neighboring agricultural lands, of Alexandria and Bohaira Provinces, to flow gravitationally into them. This is accomplished by the El Mex Pumping Station (Figure 1), which pumps the water from the downstream portion of the drain across the lithified ridge on to the sea at El Mex Bay. Before 1993, the lagoon Main Basin received most of the raw industrial and sewage effluents of Alexandria City, without treatment, through four drains (Figure 1), named Industrial, Gheit El-Enab and Kabbary Drains at the northern side of the lagoon beside the Kalaa Drain.

The historical sediment quality data and metal concentrations in the sediments from Lagoon Maryout, before 1993, have been reviewed by El-Rayis and El-Nady (1997). The bottom of the lagoon in 1968 (El-Wakeel and Wahby 1970) was covered with a badly sorted sand-silt-clay sediment. The lagoon sediments were grayish to blackish gray in color, having smelled of hydrogen sulfide in regions covered with rooted water plants. The average median grain size of sediments in the Main, Northwest, Southwest and

Fisheries Basins are 58, 6, 28 and 26 microns, respectively. These sediments were derived mainly from the suspended load of silt and clay carried into the lagoon through the drains, enriched with calcareous shells and constituting a sand-silt clay admixture. The sand is constituted of the calcareous shells and the shell fragments of lamellibranches, gastropods and tubeworms. These cover large areas of the lagoon bottom. The carbonate (as calcium carbonate) content of the lagoon sediments averaged 41%. The organic matter content in 1968 averaged 8%, reflecting the high productivity of the lagoon in that date.

Over time, especially after 1960 –after industrialization of Alexandria - it seems likely that the nature of the bottom of at least the Main Basin was altered from its original condition. This by the continuous supply of sewage and industrial wastes, carrying large loads of suspended matter, from the above mentioned four main point sources (Figure 1). The respective suspended matter loads from the Kalaa, Industrial, Gheit El-Enab and Kabbary Drains were 42500, 433100, 30100 and 110400 kg/d (Environmental Impact Statement CDM, 1978). After settling, this suspended matter eventually formed the sludge bed on the bottom of the Main Basin. In 1987, El-Rayis and El-Sabrouti (1997) studied the organic matter percentage (see Figure 3k) of the sediments of the Main and Northwest Basins and found respective averages 19.8 and 8.5%. Also, they found that the sediments containing high organic matter content (>18%) are those at the eastern half of the Lagoon Main Basin particularly those in front of the fore mentioned four point sources. The concentration of metals (Cu, Zn, Fe and Mn) in the sediments collected from the Lagoon Main Basin in 1979 was measured by El-Rayis and Saad (1990). They showed that the metal concentrations tend to be also higher at the far eastern side of the lagoon mimicking the 1987 distribution of organic matter (El-Rayis and El-Sabrouti 1997). This deterioration of the lagoon conditions especially the evasion of the malodorous hydrogen sulfide gas has impacted the fish diversity, quality and quantity. This has led to a real social problem to the local fishermen besides the loss of a considerable source of animal protein.

The present work is a study of the level and distribution of eleven elements including Cu and Zn and Org-C in the sediments of the Main and the other basins of Lagoon Maryout collected in 1996. This is as a part of a pilot study to provide an understanding and evaluation of the existing conditions in the lagoon Main Basin after the erection of the ETP and WTP. The water quality of the lagoon is studied and mentioned elsewhere (El-Rayis et al 1998), the distribution of some of the water quality parameters in the lagoon waters are presented in Figure 2. The present results, however, beside those for the water quality of the lagoon may be of value to the decision makers in choosing a solution for next phase of restoration of this important lagoon.

Materials and Methods

Twenty-three locations were sampled on Lagoon Maryout. Fourteen of the stations were distributed throughout the Main Basin, LM, and there were three stations in each of the Fisheries, LF, Northwest, LN, and Southwest, LS, Basins. The locations of the sampling stations are shown in (Figure 1). All sediment samples were collected with a 6"x 6" petite Ponar dredge that sample an area of 0.023 square meters and to a depth of about 20 cm. The geotechnical data collected from borings in the lagoon to gather information on stratigraphy of its sediments indicated that up to 30 cm sludge is found on the bottom of the Main Basin, accumulated along the last forty years, (Geotechnical Report 1996). The solid sediment (macrophytes were discarded) was placed into an appropriately labeled plastic container and stored at 4°C until ready for shipment to EAESTI's Analytical Laboratory in Sparks, Maryland, USA. Analyses were performed using Standard Operating Procedures Manual (SOPs) based on guidelines provided by the US-Environmental Protection Agency (SW 846 Method) and APHA, 1995. Method detection limit for the studied trace elements was < 0.9 ug/g dry weight sediment. Blanks were carried through the entire sample preparation and analytical process. Also duplicate samples were processed on a routine basis to determine precision. In addition spiked samples and reference materials were employed to determine accuracy. Finally the

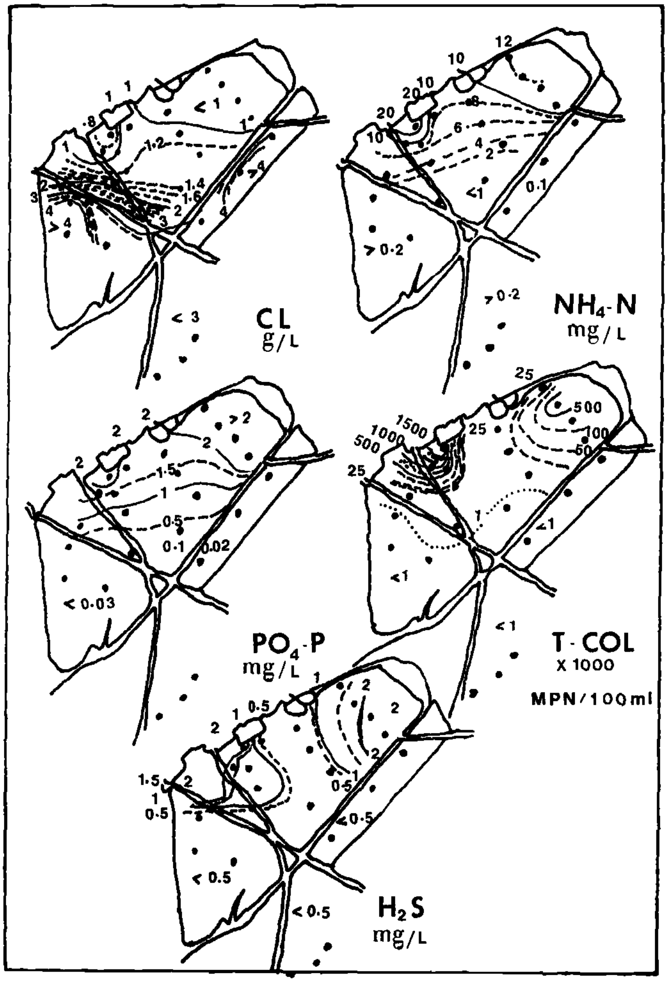

Figure 2 – *Distribution of the Values of Some of the Water Quality Parameters in the Surface Waters of Lagoon Maryout, 1996.*

concentration of all calibrated standards were verified against a quality control check sample obtained from outside source. The reference materials 2704 Buffalo River sediments and 2710 and 2711 Montana Soil of high and normal levels respectively were used.

Results and Discussion

Table 1 – *Analytical Results (and Matrix Interrelation Coefficients) of the Studied Metals (mg/kg Dry Weight) and Organic-C (OC %) in the Sediments of Lagoon Maryout.*

Stat.No	Hg	Sb	Ag	Ni	Cr	Pb	Zn	Cu	Cd	OC
LM01	110	330	470	668	1050	3700	1050	625	260	9.6
LM02		350								10.7
LM03	110		310	590	796	1720	605	267	170	16.1
LM04										10.9
LM05							276	121	42	9.7
LM06	32	110	190	355	432	672	240	139	94	10.6
LM07							129	77	41	8.6
LM08	36	140	220	519	545	847	213	129	69	13.4
LM09	28	220	110	217	319	471	182	72	68	9.0
LM10	73	240	140	442	662	3200	986	395	226	22.4
LM11										4.9
LM12	8	130	370	18	35	27	13	6	16	11.2
LM13	22	41	160	400	451	280	115	48	32	37.8
LN01		36	150	206	228	114	86	21		9.4
LN02	17	52	160	163	178	101	74	23		14.7
LN03	31	63	250	71	107	75	55	25		11.3
LF01	15	48	110	85	133	95	81	9		4.5
LF02	20	69	180	92	95	204	84	18		6.5
LF03	19	73	130	73	89	110	101	21		5.2
LS01	18	95	200	37	66	52	43	5		4.3
LS02	18	100		31	21	42	21	3		3.0
LS03	17	41	140	156	198	132	68	18		6.2
Hg	1.0	0.85	0.57	0.83	0.91	0.89	0.90	0.90	0.90	0.22
Sb		1.0	0.54	0.63	0.76	0.86	0.84	0.86	0.84	-0.04
Ag			1.0	0.43	0.50	0.50	0.46	0.58	0.35	0.05
Ni				1.0	0.98	0.79	0.78	0.82	0.71	0.48
Cr					1.0	0.89	0.89	0.91	0.88	0.41
Pb						1.0	0.99	0.98	0.98	0.26
Zn							1.0	0.97	0.98	0.27
Cu								1.0	0.96	0.23
Cd									1.0	0.02
OC										1.0

The results of the lagoon sediment analyses for different elements are presented in (Table 1) and as areal distributions shown in (Figure 3).

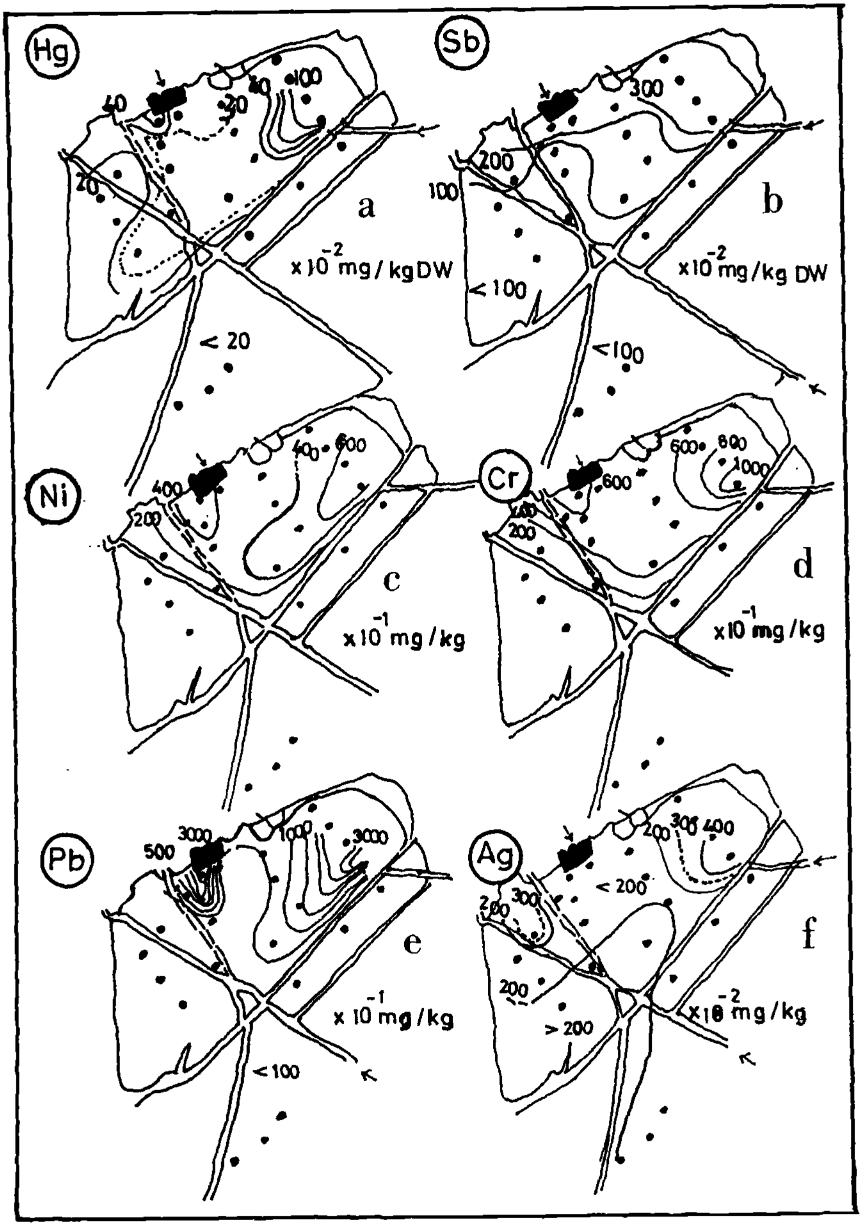

Figure 3 a-f – *Areal Distribution of Some Metals and Organic Carbon in the Surface Sediments of Lagoon Maryout, 1996*

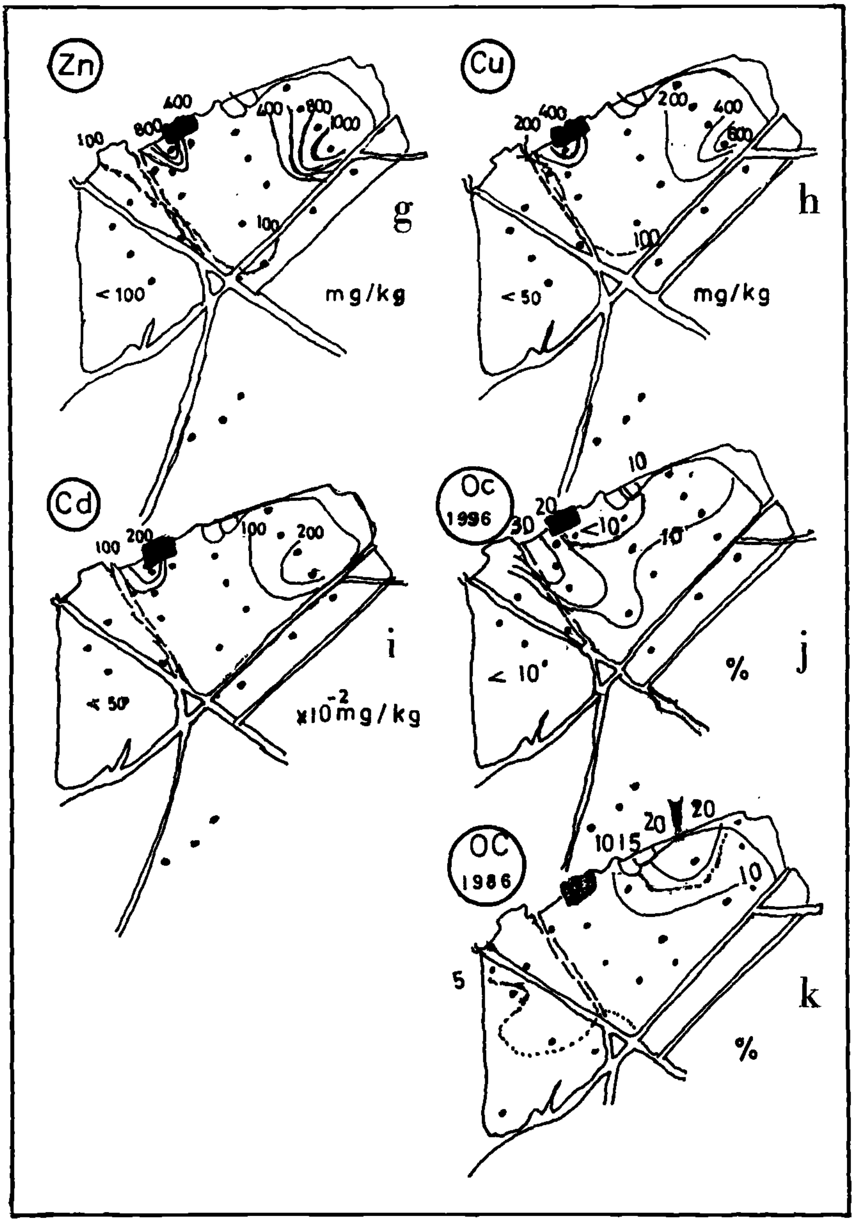

Figure 3 g-k – *Areal Distribution of the Other Metals and Organic Carbon in 1996 (and of the Organic Carbon Studied in 1986) in the Surface Sediments of Lagoon Maryout.*

From the figure, one can notice that most of the highest metal concentrations are found in the sediments of the lagoon Main Basin compared with those in the sediments of the other three basins. In addition, within the Main Basin these high values particularly those of the metals are generally found in two quite distinct areas. One at its eastern side in front of the outlet of Kalaa Drain and the other at the northwest corner, in vicinity of the WTP discharge site. This distribution pattern also correlated with the water quality parameters (Figure 2). Silver showed a slight deviation in the position of the polluted area in front of the WTP as it become more westward in the sediments close to the course of Nobaria Canal (Figure 3). The high values of the Org-C in the Lagoon Main Basin are mainly for the sediments at the northwestern side off the WTP outlet. This is reflected on the interrelation coefficients between the studied parameters in the sediments (Table 1). Apart from these, and as mentioned, the other sediments of the other basins are less contaminated with these studied elements.

Comparing the current figures of the Org-C and the metals Cu and Zn (Figures 3) with their counterparts obtained before 1986 (El-Rayis and Saad 1990 and El-Rayis and El-Sabrouti 1997) one can easily note that: (1) The sediments contaminated with metals after 1993, the erection time of the WTP and its discharge site, become not only restricted to the eastern side of the Lagoon Main Basin but also to those in a new sediment area at the northwestern side in front of the new point source. (2) The high concentrations of the Org-C after 1993 become restricted more to the sediments off the new source WTP outlet, while the sediments at the eastern side of the Main Basin, particularly those off the old source Gheit El-Enab, besides those off the Kalaa Drain, show quite lower contents of Org-C. This means that after 1993 the distribution pattern of the Org-C actually is not mimicking that of the metals (Table 2), unlike before 1993. These results refer to the high impact of the direct discharge from WTP, compared to the other discharge from the ETP that is indirectly reaching the lagoon through Kalaa Drain, in the nearby sediments. In addition, there is a degradation of considerable proportion of the organic matter from the spoiled sediments in front of the three old point sources after about 3 years from blockage. -It is worthy to assure that the ETP does not dispose its effluent directly into the lagoon but on to Kalaa Drain. It discharges its effluent into the Kalaa agricultural Drain, at a site distant about 2 km landwards from the drain outlet. i.e. it mixes with the agricultural drainage water before reaching the lagoon-. Obviously, this process beside the dilution effect it gives a better chance for occurrence of a partial degradation to the organic matter load (its biodegradable part, BOD_5, on average represents about 40 % of the total, COD, bio plus non-bio degradable, El-Rayis et al 1998) with a possible precipitation of considerable part of the suspended particulate organic matter to the bottom of the drain before reaching the lagoon.

The noticeable good association of most of the studied metals (significance $\rho > 0.5$) with each other rather than with organic matter confirms their immobilization and the degradation of the organic matter in the sediments.

The levels of the nine studied metals here are compared with those previously reported in literature for Lagoon Maryout. For example, Sb concentrations in the Main Basin in the present work (1996) ranged from 0.6-6.1 mg/kg compared to WWCG (1994) ranges of 20-71 mg/kg in 1993. The other basins of the lagoon in 1996 exhibited a concentration range of 0.41-1.2 mg/kg compared to the values of 13 and 21 mg/kg reported in WWCG (1994). Arsenic in sediments of Main Basin and other basins ranged from 0.35-11.3 and 2-4.7 mg/kg compared to 0.06-0.1 reported by Mostafa (1994) and 4-

16 mg/kg by WWCG (1994). Cadmium in 1996 shows concentrations ranged from 0.42-2.6 mg/kg in Main Basin and from 0.38-0.53 mg/kg in the other basins. There are no literature concentrations for this metal. Chromium concentrations in the Main Basin and other basins in 1996 ranged from 3.5-105 mg/kg and 2.1-22.8 mg/kg respectively. These concentrations are similar to those found earlier and reported in the literature (for example WWCG 1994). Copper in the sediments of the Main Basin in 1996 ranged from 5.6-625 mg/kg. This concentration range is similar to literature data except for that reported in WWCG (1994). Copper measured in other basin sediments in 1996 ranged from 3.4-31.4 mg/kg, similar to literature data. Lead concentrations in sediments of Main Basin in 1996 ranged from 2.7-370 mg/kg and from 4.2-20.4 mg/kg in other basins. Similar to the discussion related to literature reported Pb in sediments, the concentrations reported by WWCG (1994) of 110-3200 mg/kg is considerably higher than those found in 1996. Mercury concentration range in 1996 in the Main Basin was 0.28-2.1 mg/kg that are similar to 1991-1992 and 1993 data that show a concentration range of 0.18-1.77 mg/kg. In 1996, three samples in other basins exceeded the detection limit and ranged from 0.37-0.60 mg/kg. Nickel in 1996 sediments of the Main Basin ranged from 1.8-66.8 mg/kg that is closest to the data reported by the United States laboratory results in WWCG (1994) of 31-107. Nickel in other basins ranged from 4.6-20.6 mg/kg. Silver in Main Basin in 1996 ranged from 2.1-8.9 mg/kg, slightly lower than Ag in 1993 that ranged from 3.4-11.8 mg/kg. Relatively high concentrations of Ag found in the sediments of the Southwest Basin (2-13.5 mg/kg). Finally, Zn in 1996 the main Basin shows concentrations ranged from 12.6-1050 mg/kg while other basin concentrations ranged from 13-116 mg/kg. Main Basin literature Zn concentrations were similar to those found in 1996 (100-1000 mg/kg, El-Rayis and Saad 1990; WWCG 1994).

The elevated concentrations for the metals Hg, Ni, Pb, Cd, Zn and Cu (Table 2) are found to be at levels above those corresponding of the median effect-range of Long and Morgan recommended by the EPA. This may have possible effect on bottom fauna and other organisms (including edible fish) that live in this polluted basin. Subsequently this situation makes the Main Basin as a possible source health-hazard for fish and humans who consume them.

Table 2 – *Levels of Priority Metal Pollutants in the Lagoon Maryout Main Basin Sediments with Respect to Those of Median (ER-M) and Long (ER-L) Effect-Range of Long and Morgan Recommended by the EPA.*

Element	No.of results	No. of detects	ER-L mg/kg	No. above ER-L	ER-M mg/kg	No. above ER-M	Highest value mg/kg
Sb	15	12	2.00	6	25.00	0	6.10
As	15	15	33.00	0	85.0	0	11.30
Cd	15	10	5.00	0	9.00	0	2.60
Cr	15	15	80.00	1	145.00	0	105.00
Cu	15	15	70.00	12	390.00	2	625.00
Pb	15	15	35.00	12	110.00	5	370.00
Hg	15	12	0.15	12	1.30	2	2.20
Ni	15	15	30.00	7	50.00	3	66.80
Ag	15	9	1.00	9	2.20	8	8.90
Zn	15	15	120.00	12	270.00	7	1050.00

The previous and aforementioned two important findings seem to point to the following conclusions: (1) Most of the organic wastes in the lagoon are biodegradable.(2) Most of the metals in the sediment are immobilized and most probably non-bioavailable, unlike organic matter. Therefore, dredging of the spoiled sediments highly contaminated with the toxic metals is seriously recommended. (3) The waste effluent from the WTP must be either further treated (at least secondary treated) prior to discharge into the lagoon or diverted.

The suggested diversion of the sources in addition to dredging of the lagoon's spoiled sediments is adopted by the government for the next step for rehabilitation of the lagoon. Further, the diverted effluents of the two treatment plants will be subjected to a secondary treatment process before reuse for inland (neighboring desert) irrigation.

Acknowledgment

This work is carried out for the Alexandria General Organization for Sanitary Drainage (AGOSD) and the U.S Agency for International Development (USAID) as part of Alexandria Wastewater Project - Phase II (USAID Contract No. 263-0100-C -00-5117-00). The grant offered by USAID for carrying out this research work is gratefully acknowledged.

References

Ali, Y. A. and West, I. A., 1983, "Relationships of Modern Gypsum Nodules in Subkhas of Loess to Compositions of Brines and Sediments in Northern Egypt", *Journal of Sediment Petrology,* Vol. 53, pp. 1151-1168.

APHA (American Public Health Association), 1995, Standard Methods for the Examination of Water and Wastewater, 19th ed.

El-Rayis, O. A. and El-Nady, F. E., 1997, Chapter 3 in: Technical Report of Chemical and Biological Characterization of Lagoon Maryout, Alexandria Wastewater Project Phase II. Prepared for Metcalf & Eddy International.

El-Rayis, O. A., El-Nady, F. and Hinckely, D., 1998, Existing Environmental Conditions in Lagoon Maryout South of Alexandria, Egypt: 1- Water Quality. Proc. 8th Int. Conf. "Environ. Prot. Is a Must ". Alexandria 5-7 May 1998, NIOF, Euro-Arab Coop. Center (VEA), Int. Sci. Assoc. (ISA) & Social Fund for Development (SFD), pp. 33-43.

El-Rayis, O. A. and Saad, M., 1990, "Heavy Metal Pollution in Lagoon Maryout, on the Southeastern Coast of the Eastern Mediterranean Sea", *Journal of King Abdulaziz University for Marine Sciences, Jeddah,* Vol. 1 pp. 17-26.

El-Rayis, O. A. and El-Sabrouti, M. A., 1997, "Lake Maryout: Pollution Problems and Proposals for Restoration", *Fresenius Environmental Bulletin,* Vol.6, pp.598-604.

El-Wakeel, S. K. and Wahby, S. D., 1970, "Texture and Chemistry of Lake Mariut Sediments", *Archive Hydrobiology*, Vol. 67, pp.368-395.

Environmental Impact Statement (CDM), 1978, Environmental Impact Statement for the Alexandria Wastewater Plan Study. Vol. I, Prepared by Camp Dresser and Mckee (CDM) Inc., Environmental Planning Division with Marine Environmental Services CHAS. T., Main International Included Arab Technology and Economic Consulting Office.

Geotechnical Report, 1996, Technical Memorandum No. 3. Volume 2 "*Lake Maryout Geotechnical Data Report*", Alexandria Wastewater Project – Phase II, USAID Project No. 263-0100.

Mostafa, A. H., 1994, Environmental Studies on the Water and Sediments of Lake Mariut, with Reference to Pollution Chemistry, Ph.D. Thesis Alexandria University, 396 p.

US-Environmental Protection Agency, 1986, Acid Digestion of Sediments, Sludge and Soils, SW 846 Method, Third Edition, September 1986.

WWCG (Wastewater Consulting Group), 1994, Report on Preliminary Investigations of Lake Maryout Water Quality: Past, Present and Future, 1994.

Moir D. Haug,[1] S. Lee Barbour,[1] and Chris A. Johns[2]

Rehabilitation of Brine-Saturated Sediments

Reference: Haug, M. D., Barbour, S. L., and Johns, C. A., "**Rehabilitation of Brine-Saturated Sediments,**" *Contaminated Sediments: Characterization, Evaluation, Mitigation/Restoration, and Management Strategy Performance, ASTM STP 1442,* J. Locat, R. Galvez-Cloutier, R. C. Chaney, and K. R. Demars, Eds., ASTM International, West Conshohocken, PA, 2003.

Abstract: A large quantity of brine-saturated fine-grained sediments (insolubles) is produced each year as a by-product of potash mining. These sediments have traditionally been disposed of in clay-lined ponds to minimize their environmental impact. Many of these ponds are now nearing capacity and there is a desire to find techniques to wash the brine from these sediments so they can be taken outside the waste management areas and used for other purposes. Laboratory studies have shown that brine can be removed from these insolubles by flushing with fresh water; however, the feasibility of de-brining by this method had not been established at field scale. As a result, a field study of three prototype de-brining systems was conducted at the Potash Corporation of Saskatchewan Inc. (PCS) Allan Potash mine. The three treatment systems investigated were: a gravity drainage pond, a reverse-flushing pond with a sand and gravel filter, and a reverse-flushing pond with a geotextile filter.

Keywords: potash, reclamation of insolubles, slimes, brine removal, gravity drainage pond, reverse-flushing pond

---

[1] Professor, Department of Civil Engineering, 57 Campus Drive, University of Saskatchewan, Saskatoon, SK, S7N 5A9.

[2] Geo-Environmental Engineer, MDH Engineered Solutions, 111 Research Drive, Saskatoon, SK, S7N 3R2.

Introduction

The disposal of waste products from potash mining is facing increased attention from both industry and regulators. Laboratory studies have shown that brine can be removed (flushed) from insolubles with freshwater permeation; however, the feasibility of de-brining by this method has not been established at field scale. This paper describes the results of a pilot-scale field study conducted to evaluate the effectiveness of different pond drainage system designs for brine removal. The primary issues explored during this study involved the determination of how efficiently such a pond drainage system would perform in the field, and which type of drainage/pond design is best suited to maximize performance.

The approach that was used for this research was to design, construct and instrument three test cells at PCS Allan, Saskatchewan (Figure 1). One of the test cells was designed as a gravity drainage pond in which the slimes were surcharged with fresh water to flush the brine into an underdrain system. The other two test cells were designed as reverse-flushing systems in which the underdrain system was pressurized with fresh water to flush the slimes in an upward direction. These test cells were designed based on seepage and contaminant transport modeling to evaluate field performance over a relatively short time period. The layout of the treatment system is shown in Figure 2.

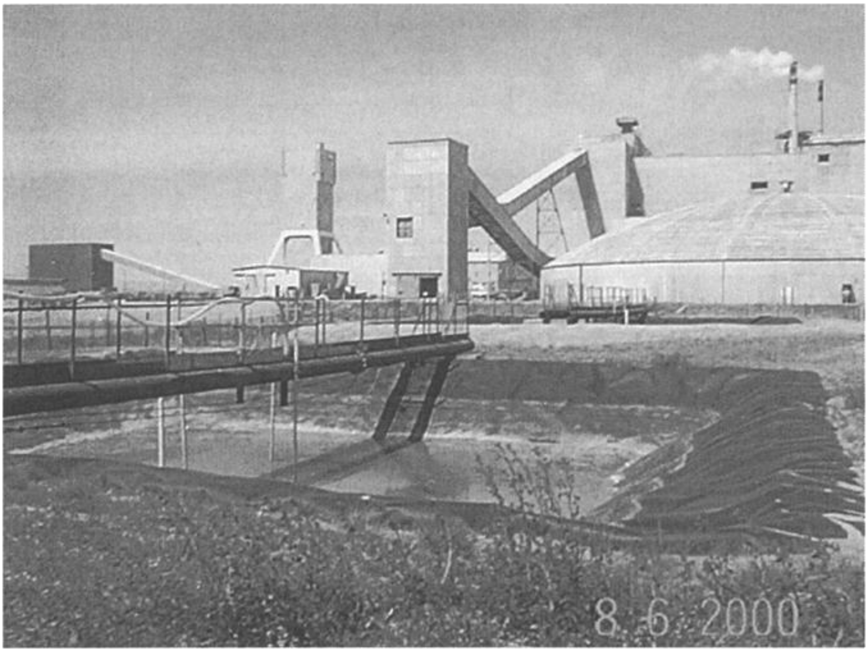

Figure 1 – *Photograph of a Test Cell at PCS Allan, Saskatchewan*

Background

Traditionally, in the treatment and disposal of potash mine waste, the water-insoluble fine-grained wastes (slimes) have been mixed together with brine and coarse salts and pumped as a slurry to tailings piles for deposition. This practice was generally considered to be the most economical method of waste disposal. Potash mining in the province has grown however, and several mines now produce significant amounts of slimes as a by-product of potash production. These slimes contain high concentrations of sodium chloride (salt) brine as well as water insolubles. According to Hart (1988), the insoluble portion of this waste can be up to 10% of the total waste mass. These water insolubles come from "clay" seams mined adjacent to the ore and consist of sand, silt and clay sized particles. It is now understood that the long-term disposal of the slimes at surface facilities would be more easily accomplished if the salt concentrations were reduced. Recent unpublished research conducted by PCS Inc. has shown that it may be possible to reclaim the insolubles portion of the waste stream if the sodium chloride saturated brine is separated from the insolubles.

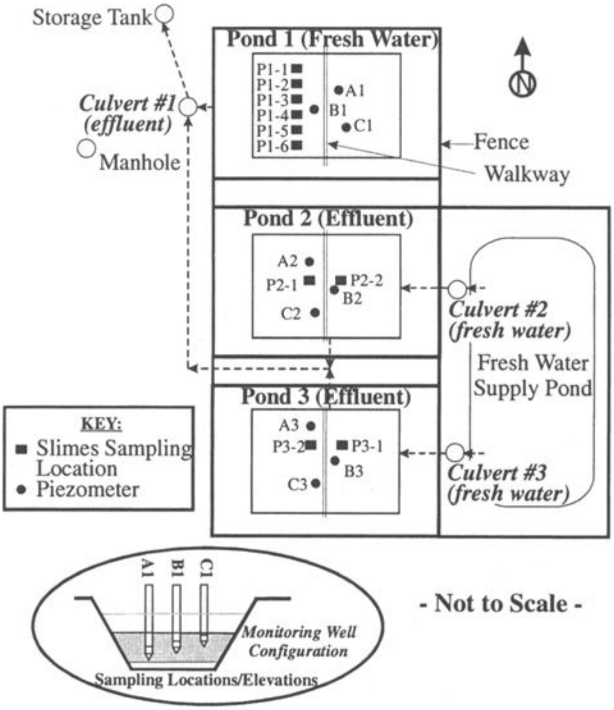

Figure 2 - *Slimes Washing Pilot Project Site Plan, Including Slimes Sampling Points*

Characteristics of Slimes

The characteristics of potash insolubles have been the focus of several studies. A study investigating the potential for using insolubles as a component in a tailings pile cover material was carried out by Haug (1988). Insolubles from the PCS Allan mine were tested to determine the composition of slimes. Table 1 summarizes the results of this analysis, which found that the major mineral components of potash insolubles at PCS Allan are dolomite, halite, and sylvinite.

Table 1 - *XRD Analyses of PCS Allan Insolubles (after Haug 1988)*

Component/Mineral	Proportion (%)
Quartz	10.8
Sylvinite	19.9
Dolomite	27.4
Halite	21.3
Anhydrite	12.5
Kaolinite	6.2
Illite	1.9

Brine from the thickener discharge pipe at the PCS Allan mine was also analyzed as part of the 1988 study. Table 2 shows the results of this analysis, which found that the major mineral constituents of the brine are sylvite and halite.

Table 2 - *Chemical Analysis of PCS Allan Process Brine (after Haug 1988)*

Constituent	Percentage
Sylvite	10.8
Halite	18.7
Calcium	0.17
Magnesium	0.13
Sulphate	0.17
Water	70.03

The hydraulic conductivity (k) of these "washed" slimes was measured with a constant head permeameter and found to be in the range of 9 x 10^{-6} cm/s at a density of 1070 kg/m^3 and a water content of 29%. This test was run on 270 mm diameter samples under a gradient of 2.7 for approximately 2.5 hours. In contrast, the k of the natural (containing salt) insolubles using fresh water was found to be 3 x 10^{-5} cm/s on a similar sample under a gradient of 4.2 for 8 hours. Theoretical calculations of k based on consolidation testing of the washed insolubles suggested that the hydraulic conductivity of the insolubles should be in the 3 x 10^{-7} cm/s range. The slimes layer hydraulic conductivity during treatment in the test ponds was expected to play a critical role in the effectiveness of each system.

Drainage Systems Design and Operation

Three treatment systems were evaluated in this project: a gravity drainage pond, a reverse-flushing pond constructed with an aggregate filter, and a reverse-flushing pond constructed with a geotextile filter. The gravity drained pond provided the simplest design and effort of operation. However, the reverse-flow systems had several attractive features including the following:

- It was expected that there would be reduced consolidation of the slimes during treatment and that the hydraulic conductivity of the sediments would remain higher than those in the gravity pond. This would be most advantageous for long-term treatment of thick layers of slimes.
- If additional untreated slimes layers were added to the upflow system, the clean water would flow through the cleanest slimes first. This would result in fresh untreated sediments being added without adverse contamination of the cleaned sediments below.
- This system would allow for staged filling-flushing operations. The hydraulic head applied to the underdrain system would be the only limiting factor to the depth of slimes that could be effectively flushed.
- Upward flushing away from the drainage system would minimize clogging of the drainage system with fine-grained wastes or precipitates.

All three ponds were constructed with base dimensions of three meters by five meters, to a depth of approximately three meters (Figure 3). The pond side slopes were cut to an angle of 2 horizontal:1 vertical. The sidewalls and the bottom of the ponds were lined with a 60 mil high density polyethylene (HDPE) geomembrane liner. Detailed design of the aggregate filter drain and geotextile followed the published recommendations provided by Terzaghi (1929), U.S. Army Corps of Engineers (1955, 1975), and the U.S. Bureau of Reclamation (1987).

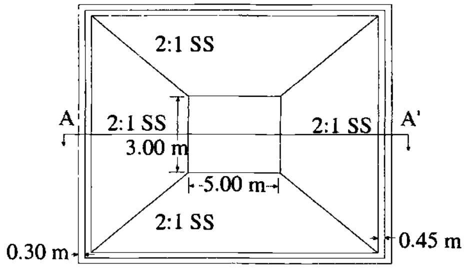

Note: 5 % slope on bottom of Pond #1

- Not to Scale -

Figure 3 - *Upward and Downward Flow Systems – Plan View*

The ponds were constructed and filled with slimes in 1998. The three ponds were instrumented with 1″ diameter piezometers with screened intervals at three different depths within the slimes layer, as shown on Figure 2. Monitoring of the porewater quality and hydraulic head in the system commenced in December 1998. Porewater samples and head measurements were obtained approximately every two weeks until May 2000.

Gravity Drainage System Pond (Pond 1)

The gravity drainage system was composed of a specially lined pond with an underdrain bedded in an aggregate filter. The insolubles were placed over top of the drainage system. After slimes placement, the excess brine was decanted and the insolubles surcharged with a fresh water cover. The head of fresh water flushed the brine within the insolubles downwards into the underdrain system. The underdrain system conducted the effluent to a collection basin (Culvert 1 on Figure 2).

Figure 4 shows the construction details of the gravity drainage pond. This system consisted of approximately 0.60 m of screened drainage rock (25.4 mm) covered with 0.15 m (6″) filter sand. A 0.15 m (6″) diameter slotted HDPE pipe was installed in the gravel to conduct the effluent to the collection basin. Approximately 0.57 m of slimes were added to Pond 1.

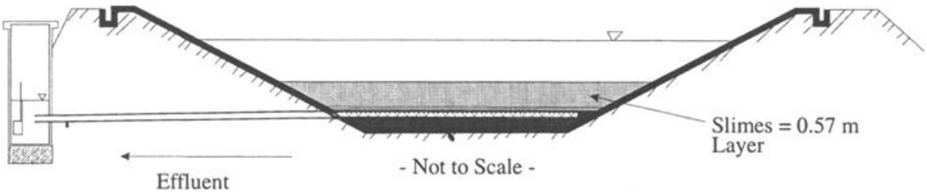

Figure 4 – *Cross section of Pond 1 (Gravity Flow)*

Reverse-Flow Ponds (Ponds 2 and 3)

The reverse-flushing treatment systems were also composed of specially lined treatment ponds with slimes placed over top of underdrain structures; however, an adjacent fresh water supply pond was connected to the underdrain system at a higher hydraulic head than the treatment pond. This caused the fresh water to flow upwards through the slimes layer, with the brine effluent collecting in the treatment pond above the slimes layer. For effective treatment, the upward gradient across the slimes must be sufficient to promote adequate flushing, but not so great as to cause piping and short circuiting through the slimes layer.

Pond 2 is a reverse-flow system that was constructed with a geosynthetic filter separating the slimes from the inflow piping. Figure 5 shows the design details of Pond 2. The fresh water inlet pipe was fed from a large supply pond adjacent to the treatment pond. Fresh water flowed through the piping system underneath the slimes and was flushed upwards through an approximately 0.79 m slimes layer. A 0.4-m-thick screened drainage rock layer was placed around the slotted HDPE inlet pipe and separated from the overlying slimes by a non-woven geotextile (Amoco 4553).

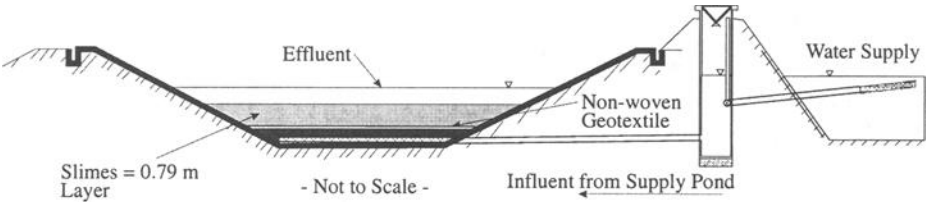

Figure 5 - *Cross section of Pond 2 (Reverse-Flow with Geotextile Filter)*

Pond 3 is a reverse-flow system that was constructed with an aggregate filter separating the slimes from the inflow piping. Figure 6 shows the design details of Pond 3. The underdrain system was comprised of a 0.13-m-thick layer of filter sand placed over 0.63 m of drainage rock that surrounded the inlet pipe. This pond contained approximately 0.61 m of slimes.

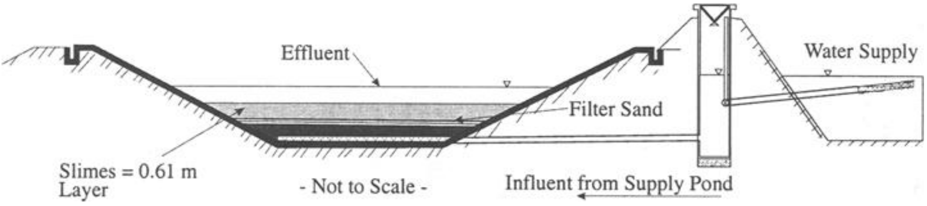

Figure 6 - *Cross section of Pond 3 (Reverse-Flow with Sand Filter)*

Sampling and Analyses

Water samples were taken every two weeks from the sampling points shown on Figure 2. Samples were analyzed for a variety of parameters including electrical conductivity, density, total dissolved solids, and chlorides. The test period for slimes porewater analysis commenced in December 1998 and was completed in June 2000. The various methods of testing the slimes porewater in the laboratory are shown in Table 3.

Table 3 - *Laboratory Methods for Slimes Porewater Analyses*

Parameter	*Method*
Density	Pipetting/Gravimetric
Chloride	Titration with Silver Nitrate
TDS	Major Ions (Carb-bicarb-SO_4-Na-Ca) analyzed by ion chromatography or titrated with EDTA
Electrical Conductivity	EC meter max = 200 000 uS/cm

Porewater samples were tested by trained technicians at an analytical laboratory. Selected samples were also submitted to a separate accredited analytical laboratory for comparison. Samples of treated slimes were collected from each pond in June 2000 at the end of the testing period. Subsamples of the slimes were tested for several parameters including electrical conductivity, density, chlorides, pH, sodium, calcium, magnesium, and potassium content.

Results of Testing

The water chemistry results indicated that all three systems removed brine from the insolubles. The gravity drainage pond (Pond 1) was the most effective of the three brine flushing systems, but this was the result of difficulties operating the reverse-flow ponds during freezing conditions.

Pond 1: Gravity Drainage Pond

Table 4 contains a summary of the averaged data collected from the three piezometers in the slimes layer of Pond 1. The gravity drainage system removed more than 92% of the brine from the porewater in the slimes. A plot showing the change in chloride concentration with time for the slimes porewater, the influent (Pond 1), and the effluent (Culvert 1) is shown in Figure 7. The surface of the gravity flow pond was frozen between January and March 1999, but the results indicate that significant brine removal occurred in that time interval.

Table 4 - *Summary of Porewater Chemistry (Pond 1)*

Parameter	Initial Concentration	Final Concentration	Removal
EC (uS/cm)	200 000	15 000	92.5%
Chloride (mg/L)	170 000	3400	98.0%
TDS (mg/L)	320 000	6600	97.9%
Density (mg/cm^3)	1.20	1.01	95.0%

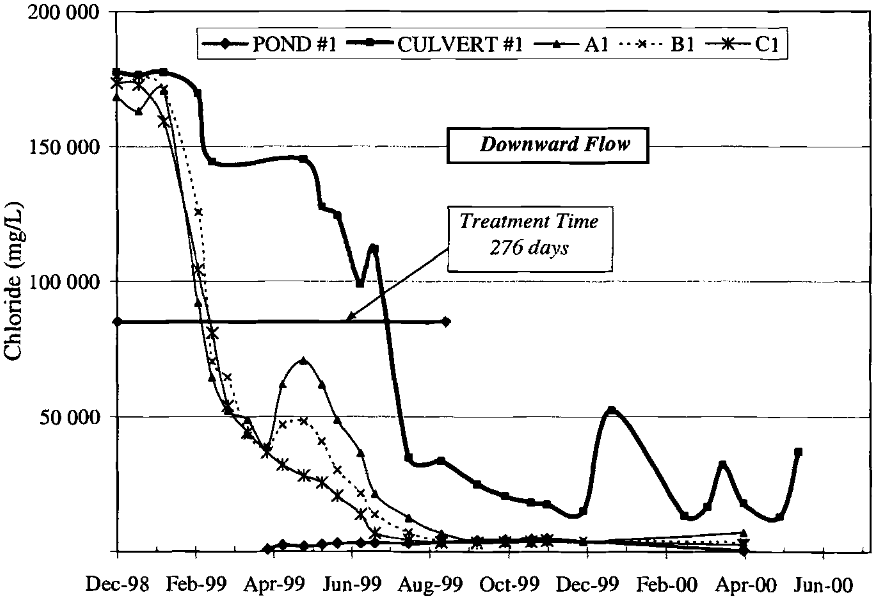

Figure 7 – *Pond 1: Chloride Versus Time (98% Reduction, Downward Flow)*

In June 2000, the slimes layer was sampled and analyzed for several parameters. Figure 2 shows the location of the slimes samples obtained from Pond 1. Table 5 contains the average chemical analysis results with depth for each of the subsamples tested.

Table 5 - *Summary of Slimes Chemical Analysis (Pond 1)*

Sample	EC (uS/cm)	Dry Density (g/cm^3)	Chloride (mg/L)	Sum of Cations (Mg, Na, K, Ca) (mg/L)
P 1-1	6 180	0.998	9 020	8 630
P 1-2	5 950	1.032	9 250	8 342
P 1-3	14 710	1.052	33 200	27 150
P 1-5	6 570	n/a	n/a	n/a
P 1-6	6 290	0.992	n/a	n/a

The lateral consistency in the EC results indicate that brine was being removed evenly across the pond, with the exception of the extreme edge of the pond at P 1-3. The EC, TDS, and chloride results for the slimes samples are similar to the porewater chemistry results. This indicates that the porewater chemistry results reflect bulk changes in the slimes chemistry and not local effects near the piezometer tips.

The chloride concentration data presented on Figure 7 indicates that the system reached an adequate level of treatment after approximately 276 days of operation. A field evaluation of the system and laboratory k testing of the sampled slimes indicates that the hydraulic conductivity of the slimes layer was approximately 2 x 10^{-6} cm/s in Pond 1 at the end of the testing period. The volume of fresh water that flushed through the system over the effective treatment time was estimated to be 91 m^3, or approximately 5 pore volumes.

Pond 2: Reverse-Flushing Pond with Geotextile Filter

Table 6 summarizes the porewater chemistry data collected from the piezometers in Pond 2. There was an approximately 60% reduction in brine concentration in the treated insolubles, most of which occurred at the end of the treatment period when ice was off the pond surface (Figure 8).

Table 6 - *Summary of Porewater Chemistry (Pond 2)*

Parameter	Initial Concentration	Final Concentration	Removal
EC (uS/cm)	200 000	165 000	17.5%
Chloride (mg/L)	170 000	67 000	60.6%
TDS (mg/L)	316 000	128 000	59.5%
Density (mg/cm^3)	1.20	1.08	60.0%

One of the reasons for the relatively poor results were the operational problems encountered during cold weather operation. The surface of the effluent pond was frozen during the winter months, which impeded the measurement of head levels in the pond. This made it difficult to maintain the optimum gradient across the slimes layer. In one instance, the critical gradient was exceeded and piping was observed in the slimes layer next to one of the piezometers. The piping appeared to "self heal" when the hydraulic gradient was reduced. The installation of an air bubbler system or a wind powered turbine to keep ice off the water surface would significantly reduce these operational difficulties.

Table 7 - *Summary of Slimes Chemical Analysis (Pond 2)*

Sample	EC (uS/cm)	Dry Density (g/cm^3)	Chloride (mg/L)	Sum of Cations (Mg, Na, K, Ca) (mg/L)
P 2-2	46 400	1.045	87 800	80 275

Figure 2 shows the sample locations for Pond 2, while Table 7 shows the average results of the slimes chemical analysis measured at the end of treatment.

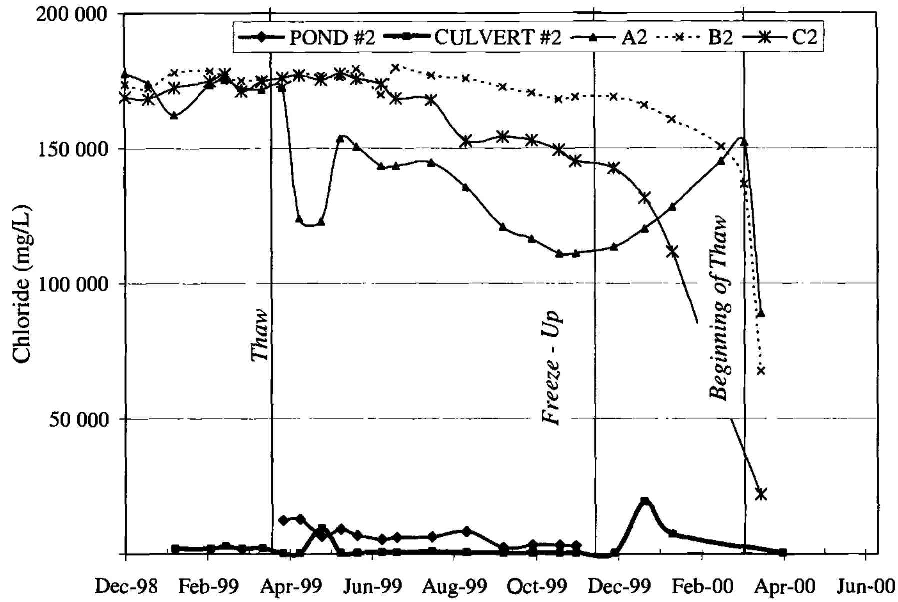

Figure 8 – *Pond 2: Chloride Versus Time (60% Reduction, Upward Flow)*

Pond 3: Reverse-Flushing Pond with Aggregate Filter

Table 8 summarizes the porewater analytical data collected from the piezometers in Pond 3. The brine removal efficiency was near 75% (Figure 9), approximately 15% lower than Pond 1. Pond 3 experienced the same operational difficulties as Pond 2; however, the area of piping failure appeared to be somewhat larger. It is unclear whether the more significant piping problem was due to the difference in filter construction or the result of a locally thinner slimes layer over the drain. Again, a method of maintaining an ice free area on the pond surface would have improved the pond operations and likely the effectiveness of brine removal. Figure 2 shows the sampling locations in Pond 3 and Table 9 shows the average results of the slimes chemical analysis. The measurements of electrical conductivity, TDS and chloride were similar to Pond 2 results.

The presence of a denser fluid overlying a less dense fluid, such as occurred in Pond 2 and 3, could also have lead to instability in the plug flow front resulting in "fingering" across the fresh water/brine interface. This may have acted to enhance the onset of piping as described above. This possibility was anticipated in the original design; however, it was felt that the relatively low hydraulic conductivity of the slimes would restrict the development of an unstable interface between the fresh water and the brine.

Table 8 - *Summary of Porewater Chemistry (Pond 3)*

Parameter	Initial Concentration	Final Concentration	Removal
EC (uS/cm)	200 000	102 000	49.0%
Chloride (mg/L)	170 000	36 000	78.8%
TDS (mg/L)	304 000	72 000	76.3%
Density (mg/cm^3)	1.20	1.05	75.0%

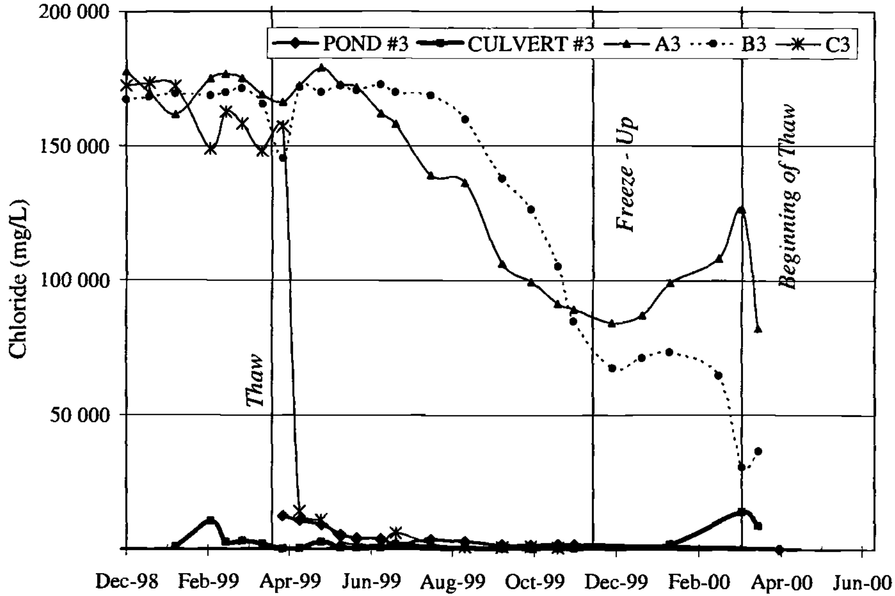

Figure 9 – *Pond 3: Chloride Versus Time (75% Reduction, Upward Flow)*

Table 9 - *Summary of Slimes Chemical Analysis (Pond 3)*

Sample	EC (uS/cm)	Dry Density (g/cm^3)	Chloride (mg/L)	Sum of Cations (Mg, Na, K, Ca) (mg/L)
P 3-2	36 700	n/a	83 000	75 525

Conclusions

In this paper, the feasibility of the-brining by flushing with fresh water has been established based on a field pilot-scale treatment system operated at the PCS Allan Potash mine in Saskatchewan. Of the three treatment systems investigated, the gravity drainage pond provided the simplest design and operation, and achieved greater than 95% removal of chlorides and total dissolved solids. The brine reduction in the gravity pond was achieved by flushing with approximately five pore volumes of fresh water over 276 days. Two reverse-flow systems were evaluated that have several attractive features; however, these systems encountered operational difficulties that adversely affected the treatment system's effectiveness. The surface of all the ponds froze during the winter, but only the reverse-flow ponds became difficult to operate because accurate control of the gradient across the thin slimes layer was not possible. The reverse-flow ponds achieved 60 to 75% removal of chlorides and TDS, but because an undetermined quantity of freshwater flushed through each reverse-flow pond, the results are not directly comparable to the gravity flow pond results. Detailed evaluation of the reverse-flow system would require the maintenance of an ice free zone in the ponds to permit more accurate operational control.

The demonstrated ability to remove brine from potash insolubles by flushing with fresh water presents a potential design alternative for the permanent disposal of potash insolubles.

Acknowledgments

This research project was funded by the Saskatchewan Potash Producers Association. Jeff Stoicescu, P.Eng., was instrumental in the successful treatment system construction and the development of the field monitoring program. Field sampling and monitoring were diligently carried out by April Slotsve and several assistants. This paper was written by Brenda Bews, P.Eng., based on reports produced by MDH Engineered Solutions.

References

Hart, R.T., 1988, "Preliminary Observations and Investigations into the Suitability of Insols as a Capping Material for Potash Tailings Piles," Internal Report # ID-3749K, Hart Environmental Consulting, Research at PCS Cory, SK for the Saskatchewan Potash Producers Association (SPPA), 38 pp.

Haug, M.D., 1988, "Potential Cover Materials," Internal Report on the University of Saskatchewan Research Program for SPPA, Saskatoon, SK.

Terzaghi, K., 1929, "Effect of Minor Geological Details on the Safety of Dams," American Institute of Mining and Metallurgical Engineers, Technical Publication 215, pp. 31-44.

U.S. Army Corps of Engineers, June 1955, "Drainage and Erosion Control-Subsurface Drainage Facilities for Airfields," Part 13, Chapter 2, Engineering Manual, Military Construction, Washington, D.C., 15 pp.

U.S. Army Corps of Engineers, October 1975, "Guide Specification for Plastic Filter Cloth," CW 02215.

U.S. Bureau of Reclamation, 1987, "Design of Small Dams," United States Government Printing Office, Denver, Colorado.

Catherine N. Mulligan[1] and Behnaz Dahr Azma[1]

Use of Selective Sequential Extraction for the Remediation of Contaminated Sediments

---

Reference: Mulligan, C.N. and Dahr Azma, B.“**Use of Selective Sequential Extraction for the Remediation of Contaminated Sediments,**" *Contaminated Sediments: Characterization, Evaluation, Mitigation/Restoration, and Management Strategy Performance, ASTM STP 1442*, J. Locat, R. Galvez-Cloutier, R. C. Chaney, and K. R. Demars, Eds., ASTM International, West Conshohocken, PA, 2003.

Abstract: The interaction of contaminants with sediments is a very complex phenomenon and means are required to understand this matter more fully. To determine the speciation of metals in sediments (the distribution of elements among chemical forms or species), specific extracts are used in a process called sequential selective extraction. This method can be used to determine if heavy metals are removable by remediation techniques or to predict removal efficiencies. Sequential extraction can be employed for the evaluation of the most appropriate sediment remediation technology and for monitoring remediation procedures. A biosurfactant, rhamnolipid, was used to remove organic-bound copper and carbonate-bound zinc. Exchangeable, carbonate, reducible oxide and organic fractions are amenable to washing techniques, and residually bound contaminants are not economical or feasible to remove. This information is important in designing the most appropriate conditions for sediment washing.

Keywords: Sequential extraction, sediment washing, remediation, heavy metals, biosurfactants

Introduction

Cadmium, copper, lead, mercury, nickel and zinc are considered the most hazardous heavy metals and are included on the EPA's list of priority pollutants (Cameron 1992). Recently, the EPA has announced that the decontamination of sediments will receive the highest priority. Sources of metals include domestic and industrial effluents, the atmosphere, runoff and the lithosphere. Once heavy metals are

---

[1] Associate Professor and Ph.D. student, respectively, Department Building, Civil and Environmental Engineering, Concordia University, 1455 de Maisonneuve Blvd W., Montreal, Quebec, Canada H3G 1M8.

allowed to pass through the municipal waste treatment facility, they return to the environment where they are persistent, cannot be biodegraded and can thus follow a number of different pathways. The metals can adsorb onto the soil, run off into rivers or lakes or leach in the groundwater, an important source of drinking water. Exposure to the heavy metals through ingestion or uptake of drinking water (particularly where water is reused) and foods can lead to accumulation in animals, plants and humans.

Sediments dewatering is frequently necessary after dredging to remediate and treat contaminants. Methods include draining of the water in lagoons with or without coagulants and flocculants, or using presses or centrifuges. Treatment methods are similar to those used for soil and include pretreatment, physical separation, thermal processes, biological decontamination, stabilization /solidification and washing (Mulligan et al. 2001a). However, compared to soil treatment, few remediation techniques have been commercially used for sediments. Solidification /stabilization techniques are successful but significant monitoring is required since the solidification process can be reversible. In addition, the presence of organics can reduce treatment efficiency. Vitrification is applicable for sediments but expensive. Only if a useful glass product can be sold will make this process be economically viable. Thermal processes are only applicable for removal of volatile metals such as mercury and costs are high. Biological processes are under development and have the potential to be low cost. Since few low cost metal treatment processes for sediments are available, there exists significant demand for further development. Pretreatment may be one of the methods that can reduce costs by reducing the volumes of sediments that need to be treated. Methods to determine the requirements for remediation are necessary for optimal design.

Methods of Determining Speciation

Solid- State Methods

The term speciation is related to the distribution of an element among chemical forms or species. Heavy metals can occur in several forms in water and soils. Interest has increased in these techniques to relate the degree of mobility with risk assessment (i.e., the more mobile the metal is, the more risk associated with it (Bourg 1995)). Not only is total metal concentration of interest, but it is now accepted that understanding the environmental behavior by determining its speciation is of paramount importance.

Metal speciation of solid-state sediments may be obtained by spectroscopic methods such as X-ray absorption fine structure in sediments (XAFS) (Helz et al. 1996). Detection limits as low as μg/g can be achieved at ambient atmospheric temperatures for wet sediments. Since synchrotron radiation is required for XAFS, only a few researchers have access to this type of equipment. X-ray absorption near-edge structure (XANES) or extended X-ray absorption fine structure (EXAFS) can be used to determine the valence states of elements.

Peterson et al. (1997) were able to determine Cr(III) and Cr(VI) in contaminated soils at levels of 20 to 50 μg/g by XANES. Szulczewski et al. (1997) compared the XANES analysis and extraction of different species of chromium. They found that only 10% of the total Cr was in the form of Cr(VI) and that only small amounts of this form could be extracted as exchangeable and with a phosphate buffer. Chemical methods supported that only a small amount was extractable but were not able to detect pools of Cr(VI) identified by XANES. Efforts are continuing to correlate chemical extractability and solid-state characterization.

Selective Sequential Extraction

To determine the speciation of metals in soils, various methods are used. One method is to use specific extractants. By sequentially extracting with solutions of increasing strengths, a more precise evaluation of the different fractions can be obtained (Tessier et al. 1982). A soil or sediment sample is shaken over time with a weak extractant, centrifuged and the supernatant is removed by decantation. The pellet is washed in water and the supernatant removed and combined with the previous supernatant. A sequence of reagents is used following the same procedure until, finally, mineral acid is used to extract the residual fraction. Heavy metal concentrations are then determined in the various extracts by atomic absorption, inductively coupled plasma (ICP) or other means. Numerous techniques and reagents have been developed and have been applied to soils (Shuman 1985), sediments (Tessier et al. 1982), sludge-treated soils (Petrozelli et al. 1983) and sludges.

These methods are not standardized and even the results can vary with the same reagents, pH, temperature, extractant strength and solid to volume of extractant ratio. None of the extractions is completely specific, however the extractants are chosen in an attempt to minimize solubilization of other fractions and provide a distribution of the partitioning of the heavy metals. The chemical agents are used to destroy the bonds of the heavy metals to the various sediment components. The extracting agents increase in strength throughout the sequence.

To extract the exchangeable fraction, ammonium acetate, barium chloride or magnesium chloride at pH 7.0 is generally used (Lake 1987). They cause the displacement of the ions in the soil or sediment matrix bound by electrostatic attraction. Pickering (1986) showed that magnesium chloride leached low quantities of other sulfides, organic matter, aluminum and silicon. Other agents such as calcium chloride, potassium nitrate and sodium nitrate can also be used (Yong 2001).

The reducible phase (iron and manganese oxides) is extracted with hydroxylamine hydrochloride with acetic acid at pH 2.0. The hydroxylamine hydrochloride reduces the ferrous and manganese hydroxides to soluble forms. Other components such as organic matter and clay components are not solubilized to any great extent (Tessier et al. 1979). The carbonate phase (calcite and dolomite) is extracted at pH. 5.0 with sodium acetate acidified with acetic acid. This solubilizes the carbonates, releasing carbonate-entrapped metals. Organic matter, oxides or clay components are not solubilized.

Hot hydrogen peroxide in nitric acid is used to oxidize the organic matter. The oxidized organic matter then releases metals that are complexed, adsorbed and chelated. These agents are used so that the silicates are not affected by this treatment (Yong 2001). In the final step, the silicates and other materials are dissolved by strong acids at high temperatures. This residual fraction is usually used to complete the mass balances for the metals.

Uses of Speciation

Monitoring of Soil Remediation

Kabata-Pendias (1992) demonstrated that the speciation of trace metals in natural soils depends on the physical and chemical characteristics of the soil. Soil pH, redox, organic, carbonate, clay and oxide contents all influence metal speciation and mobility. Simple and complex cations are the most mobile, exchangeable cations in organic and inorganic complexes are of medium mobility and, chelated cations are slightly mobile. Metals in organic or mineral particles are only mobile after decomposition or weathering and precipitated metals are mobile under dissolution conditions (e.g., change in pH). Kabata-Pendias (1992) also showed the speciation of trace metals such as zinc, copper, cadmium and lead. Zinc and cadmium are mostly organically bound, exchangeable and water soluble. Copper is mainly organically bound and exchangeable. Whereas, lead is slightly mobile and bound to the residual fraction. Chlopecka (1993) showed, however, that the cadmium and zinc speciation of the soils depended significantly on the application of sewage sludge on the soil. The speciation of the metals changed from the oxidizable to the acetic acid extractable once the sludge was added to the soil due to microbial oxidation of the organic matter in the sludge (Hooda and Alloway 1994). Fertilizer addition, water and air pollution can also affect speciation.

The effect of soil pH, constituents and heavy metal types were evaluated. In a study by Ramos et al. (1994), sequential extraction techniques were used to evaluate the mobility of cadmium, zinc, lead and copper in contaminated soil in a national park. Cadmium was found to be the most mobile and would likely be the most bioavailable.

A potential method to determine if the heavy metals can be removed by remediation techniques or predict removal efficiencies is to determine speciation with selective extractive techniques. It is believed that exchangeable, carbonate and reducible oxide fraction may be amenable to soil washing techniques (Li et al. 1995). Removal of organically and residually bound fractions may not be economical to recover or necessary due to lack of bioavailability. Ravishankar et al. (1994) evaluated several sludges for Al, Cu, Fe, Mn and Zn speciation to predict bioleaching processes. They concluded that more stabilized sludges contained higher contents of organically bound metals and that sludges vary considerably making bioleaching prediction difficult. Gombert et al. (1994) used sequential extraction to determine if cesium, cobalt and chromium could be removed by soil washing. Since less than 20% was extracted after dissolving 20% of the soil mass, soil washing was abandoned as an option.

Barona and Romero (1996) used sequential extraction to show that 0.1 M EDTA could extract lead from various fractions of a contaminated soil by multiple regression analysis. Van Benschoten et al. (1997) also assessed lead removal during batch washing. Electrokinetic remediation of copper was monitored by Ribiero and Mexia (1997). The immobilization by zeolite, hydroxyapetite and an iron-oxide waste of cadmium and lead in an arable soil at an industrial site has been evaluated (Chlopecka and Adriano 1997).

Recently, sequential extraction techniques have been studied as a tool in various applications. Yong et al. (1993) examined sequential extraction to obtain a better appreciation of the ability of clay soil barriers to contain contaminants in landfill barriers. Dahlin et al. (2001) examined the speciation of heavy metals in soils to determine if they were mobile, extractable and plant-available. Samples with lead, arsenic and chromium were collected from two Superfund sites. They found that using Tessier's sequential extraction procedure with data from optical and scanning-electron microscopy, X-ray diffraction and chemical analyses was the best approach during early stages of site analyses. Man-made materials and large particles can make the use of sequential extraction unsuitable.

Monitoring of Sediments by Sequential Extraction

To develop remediation strategies, the ease of release of the contaminants must be investigated. In sediments, speciation has been determined by selective sequential extraction by Galvez-Cloutier (1994). The effect of pH on lead was examined. As the pH increased to 4 from 1.3, precipitation of hydroxyl and carbonate species occurs. Stabilization takes place at pH 4.5 since the speciation is stable. Most of the lead remained in the residual fraction which represents the lattice of the silicate minerals.

Yong (1995) compared an illite soil with sediments. Sequential selective extraction showed that lead can be released easily from the exchangeable ion fraction. This fraction was negligible for the sediment sample at pH values greater than 4. The use of more aggressive extractants in the selective extraction process for the removal of oxide and carbonate fractions suggests that these conditions may not be normally found in the natural environment of the sediments for release of lead. However, for remediation of dredged sediments this information is highly useful. The fraction associated with the residual fraction would require total destruction of the sediment and thus is not likely to occur naturally and would not be practical for remediation. Further work by Galvez-Cloutier and Dube (1998) indicated that sequential extraction results of zinc and cadmium, in particular, varied according to the pH and that particle size was not a major consideration for sediments.

Characterization of sediments was performed by Savvides et al. (1995). Heavy metal contamination included Cu, Cr, Ni, Pb, Zn and Fe. Using sequential extraction, they found that although the significant amounts of the metals were found in the residual fraction, acid extraction was able to remove the heavy metals from the organic and carbonate.

Dredged sediments can be applied to soils to enhance fertility. If these sediments are contaminated, there is the possibility that metals may leach from the sediments once they are removed from the reducing environment and placed in an oxidizing one. Sequential extraction can be utilized to evaluate the likelihood of metal mobilization before application and over time to identify changes in metal mobility (Singh et al. 1998).

Fitch and Burken (1998) studied metal removal by lab-scale wetlands. Influent levels of lead and zinc were 100 ppb and 200 ppb, respectively and removal rates were 90% for lead and 70 to 80% for zinc. Sequential extraction of the sediments was employed to determine the removal mechanism. It showed that coprecipitation with iron oxides led to substantial removal of lead and zinc.

Recently, Chartier et al. (2001) showed that sequential extraction could be used to determine which metal fractions were extracted from sediments before and after biological treatment. They showed that between 90 and 100% of Pb, Zn, and Cd that was biologically removed was from the fractions bound to carbonate and oxide fractions and

70 to 80% of the Ni from the same fractions. Approximately, 63% of the copper, on the other hand, removed the organic and sulfide fractions, which were the major copper fractions. Almost none of the Cr was removed.

Selective Sequential Extraction for Remediation of Contaminated Sediments with Biosurfactants

Clearly, more work is needed in the field of sequential extraction for the evaluation of remediation technologies. The use of sequential extraction procedures to characterize the sediments and the sequential extractions were performed after washing with biosurfactants. These surfactants are less toxic and more biodegradable than most synthetic ones available. They are commercially available and have been studied for various environmental applications. The most notable is the application of rhamnolipids for the release of three times as much oil as water alone from the beaches of the Alaska after the Exxon Valdez tanker spill (Harvey et al. 1990). Due to their anionic and hydrophilic/hydrophobic nature, biodegradable surfactants including rhamnolipids, surfactin, and sophorolipids, by-products of bacteria or yeast, have been able to remove metals from an oil-contaminated soil by disruption of the pollutant/soil bonds (Mulligan et al. 1999). Sequential extraction has been used to develop strategies and monitor the remediation of the soil through multiple washing steps (Mulligan et al. 2001b). In this paper, sequential extraction was used to monitor remediation of sediments by the biosurfactant rhamnolipids. Different concentrations of rhamnolipid with and without sodium hydroxide were used to extract the heavy metals and sequential extraction was used before and after surfactant washing to determine which metal fractions were removed by the surfactants. Sodium hydroxide was added as it was previously shown to enhance the biosurfactant washing step (Mulligan et al. 1999).

Experimental Methods

Characterization of the Sediment

The metal-contaminated sediment sample was obtained from a canal area which was surrounded by metal and steel industries. The sample was air-dried. The grain size distribution of the sediment indicated 10% sand, 70% silt and 20% clay. X-ray analysis indicated the presence of quartz (30%), feldspar (36%), illite (2%), kaolinite (27%), chlorite (3%) and carbonate (0.5%) as performed by Mulligan et al. (2001c). Total organic matter was 20% (w/w). The sediments were digested by the method recommended by Environment Canada (1990) and then analysed by a Perkin Elmer Atomic Absorption Aanalyst 100 Spectrophotometer for heavy metal content. These results are summarized in Table 1.

Sediment Washing Procedures

Batch washing experiments were used to evaluate the feasibility of using biosurfactants for the removal of heavy metals from sediments. The rhamnolipid biosurfactant (JBR215) was obtained as a 15% solution (w/v) from Jeneil Biosurfactant

Co. It is produced from sterilized and centrifuged fermentation broth. Two major types of rhamnolipids, RLL (R1) and RRLL (R2), are present in the solution. The molecular weight of RLL ($C_{26}H_{48}O_9$, rhamnolipid type I) is 504 and of RRLL ($C_{32}H_{58}O_{13}$, rhamnolipid type II) is 650 as determined by the supplier.

Table 1 - *Characterization of Sediment Sample for Total Heavy Metal Content*

Parameter	Concentration (mg/kg)
Chromium	145
Copper	140
Nickel	76
Lead	572
Zinc	4,854

The biosurfactant solution was diluted with distilled water or 1% NaOH as required. A quantity of 1.5 g from the sediment of each particle size was placed in individual 50mL vials. 15.0mL of surfactant solution was added to each vial. The samples were kept in the temperature incubator at constant temperature (25°C) for 1 day. Blank samples including 15.0mL distilled water and 1.5 g sediment were provided. Vials were placed on the side in order to achieve the maximum contact surface between the sediment particles and the biosurfactant. The pH of the rhamnolipid with NaOH was 10 and without NaOH was 6.0. Blanks included the same additives as for the biosurfactant studies without the presence of the biosurfactant. The series of washings was performed by washing the soil for 24 h, and then removing the supernatants (3,000 x g, 30 min). All experiments were performed in triplicate. Results were reproducible to ± 10%. The solutions from each sample were collected. The samples were digested and the concentrations of copper and other metals in each sample were measured by the Atomic Absorption Spectrophotometer. In order to release the heavy metals trapped in the biosurfactant micelles, the organic copper colloids were oxidized by adding 30% H_2O_2 slowly until no reaction was observed. The method chosen for biosurfactant digestion was 3030E, which is recommended by APHA (1995) and approved by the EPA.

Sequential Extraction Procedures

The procedure used for the sequential extraction was similar to that of Yong et al. (1993) shown in Table 2. Sediment samples (1.5 g) were washed with the surfactant solutions and controls and then subsequently dried prior to sequential extraction. Each of the fractions was collected and the concentrations of heavy metals were determined by atomic absorption spectrometry. The amounts of copper, lead, zinc, chromium and nickel extracted from each of the extractants were then calculated.

Table 2 - *Sequential Extraction Procedure* (Yong et al. 1993)

Sequence	Chemical Reagents	Fraction
1	Extraction of metals by surfactants and controls overnight with 15 mL of solution	Soluble
2	Extraction of metals with 8 mL of 1 M $MgCl_2$ (pH 7) for 1 h	Exchangeable
3	Extraction of metals with 8 mL of 1 M NaOAc[1] adjusted to pH 5 with acetic acid for 5 h	Carbonates
4	Extraction of metals with 20 mL of 0.04 M $NH_2OH.HCl$ in 25% (v/v) acetic acid (pH 2.5) at 96°C for 6 h	Oxides and hydroxides
5	Extraction with 3 mL of 0.02M HNO_3 and 5 ml of 30% H_2O_2 (pH 2) for 2 h at 85°C, followed by 3 mL of 30% H_2O_2 (pH 2) at 85°C for 3 h and then 5 mL of 3.2 M NH_4OAc[1] in 20% (v/v) HNO_3 diluted to 20 mL at room temperature for 30 min.	Organic matter
6	Digestion at 90°C with 25 mL of dilute aqua regia (50 mL HCl, 200 mL HNO_3 and 750 mL water) for 3 h	Residual fraction

[1] Ac – denotes acetate

Results and Discussion

Surfactant Washing

A series of washings was performed on the sediments using 0.5%, 1% and 2% rhamnolipid solutions with and without 1% NaOH. The control was 1% NaOH. Copper, zinc, lead, nickel and chromium were analyzed in the supernatants. All are plotted in Figure 1 with the exception of chromium since no chromium removal was detected. This was because chromium is usually found in the more mobile anionic form (CrO_4^{2-}) and therefore the anionic biosurfactant had no affinity for the chromium. Removal rates for zinc and nickel increased as the rhamnolipid concentration increased in an almost linear fashion without NaOH. However for lead and copper, highest removal rates occurred for 0.5% rhamnolipid with 1% NaOH. Increasing the biosurfactant concentration when NaOH was added did not enhance removal rates. Maximal removals were 7.3% nickel, 4.9% zinc, 1.7% lead and 15.6% copper. However, since zinc was in the highest concentration, this metal was removed the most. For example, for a 2% rhamnolipid concentration, approximately 250 mg/kg of zinc were removed compared to 20 mg/kg of copper (0.5% rhamnolipid with NaOH). If an average molecular weight of 575 is assumed for the rhamnolipid, then it can be calculated that 10 moles of the biosurfactant removed 1 mole of zinc. Significant amounts of zinc (129 mg/kg) were also removed with 0.5% rhamnolipid and NaOH.

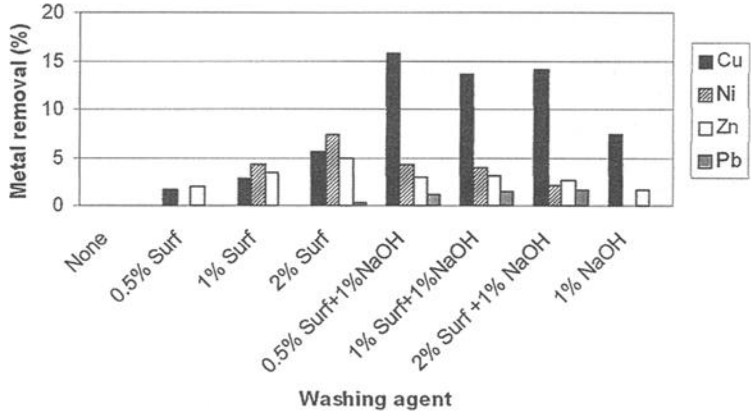

Figure 1 - *Percentage of Copper, Nickel, Zinc, and Lead Removed from Sediments by Various Washing Agents, 0.5%, 1% and 2% Rhamnolipid With and Without 1% NaOH. 1% NaOH Was Also Evaluated.*

Sequential Extraction of the Sediment Before Washing

Sequential extraction procedures were used on the sediment to determine the speciation of the heavy metals before surfactant washing. The exchangeable fractions of all metals were small. The carbonate and oxide fractions accounted for over 60% of the zinc present in the sediments (Tables 3 and 4). The organic fraction constituted over 80% of the copper, and 50% of the chromium and lead. A major proportion of nickel was found in the residual fraction. In a study by Ramos et al. (1994), copper, lead, cadmium and zinc were sequentially extracted from soils with organic contents of approximately 15%. Similar to this research, they found that copper was associated with the organic matter or residual fractions, lead and zinc were primarily found in the oxide fraction.

Sequential Extraction of the Sediments after Biosurfactant Washing

Sequential extraction of the sediments was performed after washing with the biosurfactant. The results of these experiments for copper, zinc and nickel are shown in Figures 2, 3 and 4. Rhamnolipid could remove the organically-bound copper when NaOH was added and the oxide fraction when no NaOH was used since the pH was 6 and more appropriate for copper removal associated with the oxide fraction. For zinc, there was a major decrease in the carbonate fraction when no NaOH was added with the biosurfactant, since this is removed more easily than the oxide fraction. In the presence of

NaOH and the biosurfactant, there was removal from the organic fraction of zinc. For nickel, the oxide and carbonate fractions decreased as the biosurfactant concentration increased. There were also significant reductions in the organic fraction, upon addition of NaOH with 0.5 and 1.0% surfactant. Chartier et al. (2001) also showed similar trends.

Table 3 - *Sequential Extraction Characterization of Metal Contaminants in Sediment Before Washing With the Biosurfactant*

Metal	Fraction (% of total)				
	Exchangeable	Carbonate	Oxide	Organic	Residual
Chromium	1	1	21	51	25
Copper	1	1	4	86	12
Lead	1	8	34	54	2
Nickel	0	9	23	29	39
Zinc	4	18	46	22	10

Table 4 - *Heavy Metal Affinity for Various Fractions in the Sediments (pH of Each Matrix Was Not Adjusted)*

Heavy metal	Affinity for each fraction
Chromium	Organic>residual> oxide> carbonate, exchangeable
Copper	Organic>residual> oxide > carbonate, exchangeable
Lead	Organic> oxide >carbonate> residual>exchangeable
Nickel	Residual>organic> oxide>carbonate> exchangeable
Zinc	Oxide> organic> carbonate>residual >exchangeable

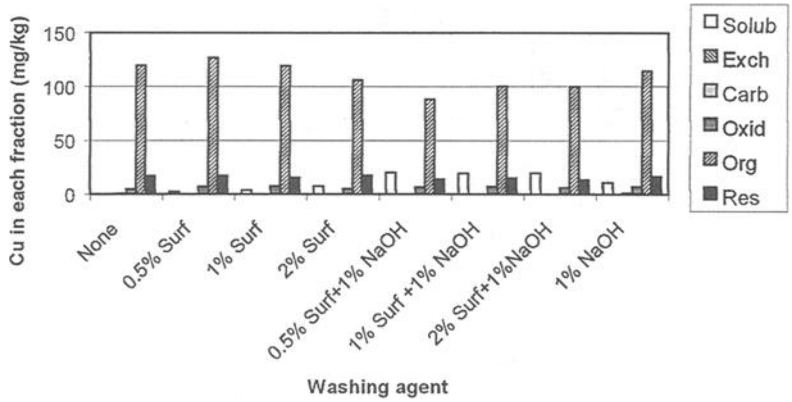

Figure 2 - *Sequential Extraction of Cu after Washing Sediments with Each Agent, 0.5%, 1% and 2% Rhamnolipid, With and Without 1% NaOH and 1% NaOH. The Fractions are Indicated as Solub for Soluble, Exch for Exchangeable, Carb for Carbonate, Oxid for Oxide, Org for Organic and Res for Residual.*

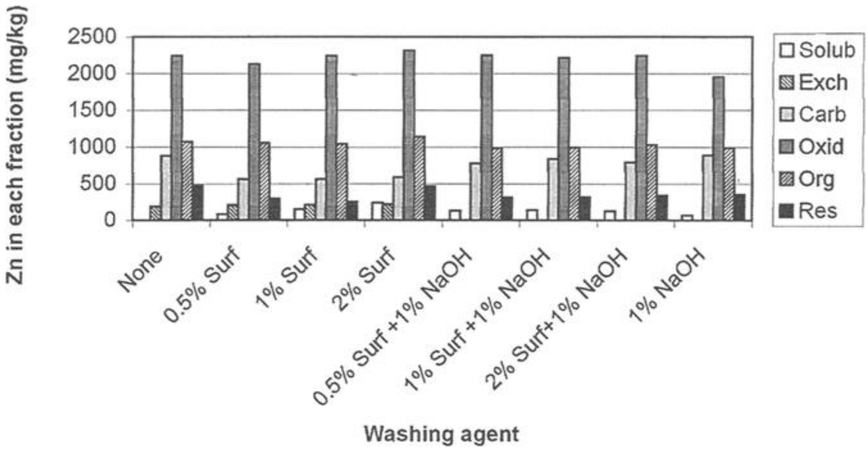

Figure 3 - *Sequential Extraction of Zinc After Washing Sediments with Each Agent, 0.5%, 1% and 2% Rhamnolipid (Surf), With and Without 1% NaOH and 1% NaOH. The Fractions are Indicated as Solub for Soluble, Exch for Exchangeable, Carb for Carbonate, Oxid for Oxide, Org for Organic and Res for Residual.*

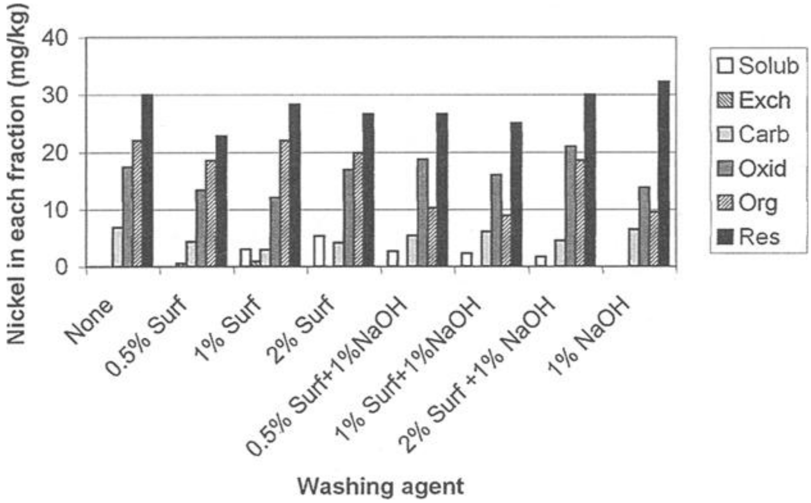

Figure 4 - *Sequential Extraction of Nickel after Washing Sediments With Each Agent, Water, 0.5%, 1% and 2% Rhamnolipid (Surf), With and Without 1% NaOH and 1% NaOH. The Fractions are Indicated as Solub for Soluble, Exch for Exchangeable, Carb for Carbonate, Oxid for Oxide, Org for Organic and Res for Residual.*

Treatability Protocol

When it has been determined that a dredged sediment sample has been contaminated with heavy metals, an assessment must be performed to determine how to remove the metals, and how much will be removed. Therefore, a scheme of assessment can be used as shown in Figure 5. A selective sequential extraction procedure can be integrated into the scheme with the characterization of the sediments. The most efficient pH values and types of reagents can be devised for extracting the heavy metals from the various fractions based on the selective sequential extraction and bench scale tests can be carried out. An overall remediation plan can then be designed followed by scale-up to field tests.

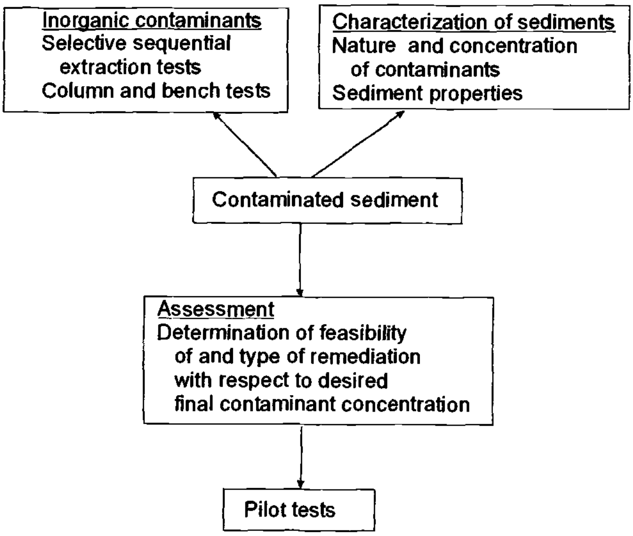

Figure 5 – *Protocol for Designing the Most Appropriate Remediation Strategy for Heavy-Metal Contaminated Sediment*

The purpose of the sequential extraction studies on sediments that have been previously washed with the surfactants was to determine from what fraction these surfactants are removing the metals. This information can then be used to determine if sediment washing is useful and if surfactant use is potentially effective and what surfactants might be useful and under what conditions. For example, if the metals are retained mainly in the residual fraction, it may be very difficult, if not impossible to use any of these surfactants to remove these metals.

In this research, only the residual fraction was untouched during soil washing procedures. All fractions under different conditions could be decreased. For example, under acidic conditions, the carbonate phase would be released. However, under basic conditions (co-addition of the surfactants with NaOH) copper, zinc and nickel could be released since they were found in the organic phase.

Conclusions

The results in this study show that the organic phase-associated metals can be removed by rhamnolipid with sodium hydroxide. Conditions without NaOH addition were effective for removing the zinc and nickel in the oxide and carbonate phases. Residual fractions, the most difficult to remove, were not affected during the surfactant washing studies. This information is important in designing the appropriate conditions for soil washing. A combination of acidic and basic conditions, therefore, would increase the amounts of metals removed in the case of carbonate, oxide and organic-associated metals.

Sequential extraction procedures can provide indications but not specific information on chemical binding of metals. This information can then be used to determine remediation procedures and to monitor the procedures during the treatment phase. It was shown that copper could be removed from the organic-bound fractions and zinc could be removed from the oxide-bound fractions during washing with rhamnolipid biosurfactants. More exact information from surface analytical methods such as electromicroscopy, X-ray absorption spectroscopy (XANES, EXAFS) and X-ray diffraction can be obtained but these equipments are not widely available. The combination of sequential extraction with analytical techniques such as chromatography would lead to more selectivity and improvements in treatability testing and in the design of remediation techniques.

References

American Public Health Association (APHA) American Water Work Association (AWWA) Water Pollution Control Federation (WPCF), 1995, *Standard Methods for the Examination of Water and Wastewater,* 17th Edition.

Barona, A. and Romero, F., 1996, "Fractionation of Lead in Soils and Its Influence on the Extractive Cleaning with EDTA," *Environmental Technology*, Vol. 17, No. 1, pp. 63-70.

Bourg, A.C.M., 1995, *Speciation of Heavy Metals and Implications For Their Mobility. Heavy Metals,* Springer, Berlin, pp. 19 -32

Cameron, R.E., 1992, *Guide to Site and Soil Description for Hazardous Waste Site Characterization.* Volume 1: Metals. Environmental Protection Agency, 1992, EPA.

Chartier, M., Mercier, G., and Blais, J.F., 2001. "Partitioning of Trace Metals Before and After Biological Removal of Metals from Sediments," *Water Research,* Vol. 35, No. 6, pp. 1435-1444.

Chlopecka. A., 1993, "Forms of trace metals from inorganic sources in soils and amounts found in spring barley," *Water, Air and Soil Pollution,* Vol. 60, No. 1-2, pp. 127-134.

Chlopecka, A. and Adriano, D.C., 1997, "Influence of zeolite, apatite ad Fe-oxide on Cd and Pb uptake by crops", *Science of the Total Environment,* Vol. 207, No. 1-2, pp. 195-206.

Dahlin, C.L., Williamson, C.A., Collins, W.K., and Dahlin, D.C., 2001, "Can Sequential Extraction Determinations Effectively Define Heavy Metal Species in Superfund Site Soils," *Annual International Conference on Soils, Sediments and Water*, University of Massachusetts.

Environnement Canada, 1990, Service de conservation et protection Region Quebec *Methode d'analyse des metaux dans sediments, les boues et les sols.*

Fitch, M.W., and Burken, J.G., 1998, *Metals Removal by Constructed Wetlands*: Final Report to The Doe Run Company, The Doe Run Company, May 26, 1998, 12 pp.

Galvez-Cloutier, R., 1994, "A Study of Heavy Metals Accumulation Mechanism in Lachine Canal sediments," Ph.D. thesis, Department of Civil Engineering, McGill University, Montreal, Canada.

Galvez-Cloutier, R., and Dube, J-S., 1998, "An Evaluation of Fresh Water Sediments Contamination: The Lachine Canal sediments Case, Montreal, Canada. Part II: Heavy Metal Particulate Speciation Study," *Water, Air and Soil Pollution*, Vol. 102, No. 3, pp. 281-302.

Gombert II, D., 1994, "Treatability Testing to Evaluate What Can Work", *Nuclear Technology*, Vol. 108, No. 1, pp. 90-99.

Harvey, S., Elashi, I., Valdes, J.J., Kamelu, D., and Chakbarty, A.M., 1990, "Enhanced Removal of Exxon Valdez Spilled Oil From Alaskan Gravel by a Microbial Surfactant." *Bio Technology*, Vol. 8., No. 3, pp. 228 -232.

Helz, G.R., Miller, C.V., Charnock, J.M., Mosselmans, J.F.W., Pattrick, R.A.D., Garner, C.D.,and Vaughn, D.J., 1996, "Mechanism of Molybdenum Removal from the Sea and its Concentration in Black Shales: XAFS Evidence," *Geochimica Cosmochimica Acta*, Vol. 60, pp. 3631- 3639.

Hooda, P.S., and Alloway, B.J., 1994, "Changes in operational fractions of trace metals in two soils during two years of reaction time following sewage sludge treatment," *International Journal of Environmental Analytical Chemistry*, Vol. 57, pp. 289-311.

Kabata-Pendias, A., 1992, "Trace Metals in Soils in Poland - Occurrence and Behaviour," *Trace Substances in Environmental Health*, Vol. 25, pp. 53-70.

Lake, D.L., 1987, "Chemical Speciation of Heavy Metals in Sewage Sludge and Related Matrices. *Heavy Metals in Wastewater and Sludge Treatment Processes. Volume I: Sources, Analysis and Legislation.* (Lester, J.N., ed.), CRC Press Boca Raton, pp.125-153.

Li, W., Peters, R.W., Brewster, M.D., and Miller, G.A., 1995, "Sequential Extraction Evaluation of Heavy-Metal Contaminated Soil: How Clean is Clean?," *Proceedings of the Air and Waste Management Association, 88th Annual Meeting and Exhibition*, San Antonio, Texas, June 18-23.

Mulligan, C.N., Yong, R.N., and Gibbs, B.F., 1999, "On the Use of Biosurfactants for the Removal of Heavy Metals from Oil-Contaminated Soil," *Environmental Progress*, Vol. 18, No. 1, pp. 50-54.

Mulligan, C.N., Yong, R.N., and Gibbs, B.F., 2001a, "An Evaluation of Technologies for the Heavy Metal Remediation of Dredged Sediments," *Journal of Hazardous Materials*. Vol. 85, No. 1-2, pp. 145-163.

Mulligan, C.N., Yong, R.N., and Gibbs, B.F., 2001b, "The Use of Sequential Extraction Procedures for Soil Remediation," *Clay Science for Engineering* (K.Adachi and

M. Fukue, Eds.,) Balkema, Rotterdam, pp. 377-384.

Mulligan, C.N., Yong, R.N., and Gibbs, B.F., 2001c, "Heavy Metal Removal from Sediments by Biosurfactants," *Journal of Hazardous Materials*, Vol. 85, No. 1-2, pp. 111-125.

Pickering, W.F., 1986, "Metal Ion Speciation – Soils and Sediments (a Review)," *Ore Geology Review,* Vol. 1, pp. 83-146.

Peterson, M.L., Brown, G.E., Jr., Parks, G.A., and Stein, C.L., 1997, "Differential Redox and Sorption of Cr(III/VI) on Natural Silicate and Oxide Minerals: XAFS and XANES Results," *Geochimica Cosmochimica Acta,* Vol. 61, pp. 3399-3413.

Petrozelli, G., Giudi, G., and Lubrano, L., 1983, *Proc. Int. Conf. Heavy Metals in the Environment*, p. 475.

Ramos, L., Hernandez, L.M., and Gonzalez, M.J., 1994, "Sequential Fractionation of Copper, Lead, Cadmium and Zinc in Soils From or Near Donana National Park," *Journal of Environmental Quality,* Vol. 23, No. 1, pp. 50-57.

Ravishankar, B.R., Auclair, J.-C., and Tyagi, R.D.,1994, " Partitioning of Heavy Metals in Some Quebec Municipal Sludges," *Water Pollution Research Journal of Canada,* Vol. 29, No. 4, pp. 457-470.

Ribiero, A.B., and Mexia, J.T., 1997, "A Dynamic Model for the Electrokinetic Removal of Copper for Polluted Soil," *Journal of Hazardous Materials*, Vol. 56, No. 3, pp. 257-271.

Savvides, C., Papadopoulos, A., Haralambous, K.J., and Loizidou, M., 1995, "Sea Sediments: Contaminated with Heavy Metals: Metal Speciation and Removal," *Water, Science and Technology*, Vol. 32, No. 9-10, pp. 65-73.

Shuman, L.M., 1985, "Fractionation Method for Soil Microelements," *Soil Science,* Vol. 140, pp. 11-22.

Singh, S.P., Tack, F.M., and Verloo, M.G., 1998, "Heavy Metal Fractionation and Extractability in Dredged Sediment Derived Soils," *Water Air and Soil Pollution*, Vol. 102, No. 3, pp. 313-328.

Szulczewski, M.D., Helmke, P.A., and Bleam, W.F., 1997, "Comparison of XANES Analyses and Extractions to Determine Chromium Speciation in Contaminated Soils," *Environmental Science and Technology*, Vol. 31, No. 10, pp 2954-2959.

Tessier, A., Campbell, P. G. C., and Bisson, M., 1979, "Sequential Extraction Procedure for the Speciation of Particulate Trace Metals," *Analytical Chemistry,* Vol. 51, No.7, pp. 844-851.

Tessier, A., Campbell, P. G. C., and Bisson, M., 1982, "Particulate Trace Speciation in Stream Sediments and Relationships With Grain Size: Implication for Geochemical Exploration," *Journal of Geochemical Exploration*, Vol. 16, No 2, pp. 77-104.

Van Benschoten, J.E., Matsumoto, M.R., and Young, W.H., 1997, "Evaluation and Analysis of Soil Washing Seven Lead-contaminated Soils," *Journal of Environmental Engineering - ASCE*, Vol. 123, No. 3, pp. 217-224.

Yong, R.N., Galvez-Cloutier, R., and Phadingchewit, Y., 1993, "Selective Extraction Analysis of Heavy-Metal Retention in Soil," *Canadian Geotechnical Journal,* Vol. 30, No. 5, pp. 834-847.

Yong, R.N., 1995, "The Fate of Toxic Pollutants in Contaminated Sediments, " *Dredging,* *Remediation and Containment of Contaminated Sediments, ASTM STP 1293,* K.R. Demars, G.N. Richardson, R.N. Yong, and R.C. Chaney, Eds. American Society for Testing and Materials, Philadelphia, PA, pp. 13-39.

Yong, R.N., 2001, *Geoenvironmental Engineering, Contaminated Soils, Pollutant Fate and Mitigation,* CRC Press, Boca Raton, FL.

Ansm Kabir[1] and Miguel Picornell[2]

Effects of Overburden Stresses on Soil Reclamation by Electroosmosis

---

Reference: Kabir, A. and Picornell, M., "**Effects of Overburden Stresses on Soil Reclamation by Electroosmosis,**" *Contaminated Sediments: Characterization, Evaluation, Mitigation/Restoration, and Management Strategy Performance, ASTM STP 1442,* J. Locat, R. Galvez-Cloutier, R. C. Chaney, and K. R. Demars, Eds., ASTM International, West Conshohocken, PA, 2003.

Abstract: A fine-grained soil stock was cleaned of organic matter and soluble salts. Then the slurry was repeatedly washed with a barium-chloride solution to ensure a known pore solution chemistry. Test specimens were prepared by first consolidating the slurry in triaxial cells under varying cell pressures, and secondly by trimming the specimens to be placed into electroosmotic cells enclosed in rubber membranes with the same confining pressure applied on the membrane as had been used in the consolidation phase. The electroosmotic treatment was performed at constant voltage gradient and was continued until the electrical conductivity of the effluent was similar to that of deionized water. The "postmortem" investigations of the treated specimens show that the confining pressure has a significant effect on the removal of barium by the electroosmotic treatment.

Keywords: electroosmosis, effects of overburden, soil reclamation, barium

Introduction

Soil reclamation by electroosmosis is a technique that has been used to remove heavy metals from fine-grained soils. This process is an alternative to the conventional flushing of soil, with significant economic and technical advantages for fine-grained soils.

Electroosmosis is the transport of water under the influence of an electric current between a cathode and an anode. The method consists of applying an electric gradient across a soil mass to generate water flow. The application of DC current through the electrode results in the development of electrical, hydraulic and chemical gradients within the soil mass. It is assumed that the concentration of ions is initially uniform throughout the specimen and the application of electric potential creates a uniform electric gradient. The process results in the movement of ions due to the electric field and the flow of water towards the cathode well. During the process the pore fluid gets acidic (pH 1 to 4) at the anode and basic at the cathode (pH 11 to 13.5).

The existing technical literature abounds in research performed with laboratory specimens and bench-top experiments using low-charge soil media, such as sand and slurries of kaolinite (Lorenz 1969; Yong and Mourato 1990; Acar et al. 1994; Haran et al.

---

[1] Research Fellow, LMI, 2000 Corporate Ridge, McLean, Virginia 22120.

[2] Professor of Civil and Environmental Engineering, North Carolina A&T State University, Greensboro, NC 27411.

1995). The references published using low-charge materials are too numerous to be referenced exhaustively. There is a consensus that although kaolinite is commonly used in laboratory experiments, charged clays might retard ion transport (Chen et al. 1999). The presence of electrically charged clay minerals, as indicated by the cation-exchange-capacity "CEC" and the clay mineral content, has been demonstrated in laboratory experiments (Vane and Zang 1997; Puppala et al. 1997) and in field trials (Chen et al. 1990). The effect of the electric charge in the clay particles is to reduce the usefulness or efficiency of the electroosmosis treatment to remove electrolytes from contaminated soils (Puppala et al. 1997; Chen et al. 1999).

If the electric charge of the clay particles reduces the efficiency of electroosmosis, an increase of the density of the soil would result in smaller pore sizes. Thus the cations would have to move closer to the charged clay particles. Since the electrostatic attraction is inversely proportional to the square of the distance between electric charges, it appears reasonable to expect that at higher densities (for identical soil media) the efficiency of the electroosmosis treatment would be even lower.

In this manner, the depth of burial of the contaminated soil (that is, the applied confining pressure) should have an effect on the density of the soil stratum, and thus, on the efficiency or feasibility of electroosmosis decontamination of the stratum. Kelsh and Parsons (1997) have cataloged sites of the Department of Energy indicating burial depths of the contaminated layer. In most cases, the contaminated stratum is confined to the surficial soils to depths of 15 m (50 ft). In some isolated cases, the depth of burial of the contaminated stratum exceeds 152 m (500 ft). The effect of this large range of burial depths (and thus the associated confining pressures) can be expected to have a considerable influence on the density of the soil media, and thus on the efficiency of the electroosmotic treatment.

This paper describes the effects of confining pressure on the removal of Barium from a clayey soil (with a significant CEC) by electroosmosis treatment in a laboratory setting

Materials and Methods

Barium chloride reagent grade and soil from the flood plain of the Rio Grande in El Paso, Texas were the two main materials used in the study. Barium chloride was used to contaminate the fine grained soil due to following considerations: (1) Barium is a toxic metal common in industrial and nuclear waste, (2) Compounds of barium are highly toxic, and (3) The valence of barium is two, and thus the electrostatic interaction of the ions with electrically negative clay particles would be more apparent.

The collected soil sample was first dried and pulverized. Then the sample was washed through a number 200 sieve and the soluble components were removed by dissolution with diluted hydrochloric acid solutions. Then hydrogen peroxide, 30% by volume, was added to the soil suspension to oxidize the organic matter. These additions were repeated at day intervals until the peroxide did not react with the soil suspension. At this point the soil suspension was titrated to a pH 4 to complete the removal of carbonates present. These steps were implemented to ascertain that no other cat ion species would be present and thus interfere with the removal of barium by the electromigration treatment.

At this point, the soil suspension was repeatedly washed with solutions of barium chloride 0.01 N. For this purpose, the soil suspension was thoroughly mixed with some barium chloride solution and allowed to settle for periods ranging from 3 to 5 days. The resulting clear supernatant was then decanted and fresh barium chloride solution was added to replace the decanted supernatant and the suspension mixed thoroughly again. This process was repeated until the electrical conductivity of the clear supernatant decanted was nearly identical to the electrical conductivity of the fresh barium chloride solution.

The soil stock so prepared was characterized using identification tests such as the hydrometer analysis and the Atterberg Limits. The soil stock is made up of 78% silt size particles and 22% of clay size particles. The clean soil suspension exhibited a liquid limit of 48 and a plastic limit of 21. The contaminated soil stock exhibited a liquid limit of 54 and a plastic limit of 25. These results were the average of three determinations for each type of soil suspension.

For the preparation of specimens for consolidation, the stock slurry was concentrated by centrifugation at 3500 rpm for 45 minutes. The clear supernatant was discarded and the soil cake was scooped out of the centrifuge bottle and was thoroughly mixed with a spatula on a glass plate. This material was then placed in molds holding a rubber membrane to form specimens of 71.1 mm (2.8 in.) in diameter and 152.4 mm (6 in.) in length. The specimen enclosed in the membrane was placed in a triaxial cell, and a predetermined confining pressure applied on the membrane, while the specimen was allowed to undergo consolidation. The outflow of pore water was monitored and the process was continued until the outflow had essentially stopped. At this point, the specimen was removed from the triaxial cell and the specimen was trimmed down to 51 mm (2 in.) diameter and 127 mm (5 in.) in length. The trimmings were kept to analyze for the initial concentration of barium, the initial soil pH, the initial water content of the specimen, and the initial electrical conductivity of the soil.

The trimmed down specimens were placed in an electroosmotic cell. The specimens were isolated with a rubber membrane with the only exception of one specimen at zero confining pressure that was compacted and tested inside an acrylic tube. A sketch of the electroosmotic cell is shown in Figure 1. The electroosmotic cell was made of Plexiglas to facilitate the visual observation of the specimen during treatment. The cell was divided in three parts: the two end caps and the central cylindrical portion of the cell wall. The end caps had 50 ml capacity reservoirs associated with the electrode wells. At the cathode well, the reservoir was connected to a tube with a valve with the purpose of allowing the drainage of the well to measure the volume of fluid collected and the barium removed on a daily basis.

To avoid the trapping of gas bubbles forming at the electrodes by electrolysis of water, the electrodes were separated from the specimen with spacers. The specimens were in contact with filter paper and these were confined with porous stones. The spacers separated the electrode from the porous stone, and coincided within the electrode wells. The wells were equipped with access ports to monitor pH, electrical conductivity, and temperature of the fluid in the reservoir, and permitting the escape of gas forming.

A constant hydraulic head was maintained in the anode well using a Mariotte bottle as the source of de-ionized water to replenish the water moved by the electroosmotic flow

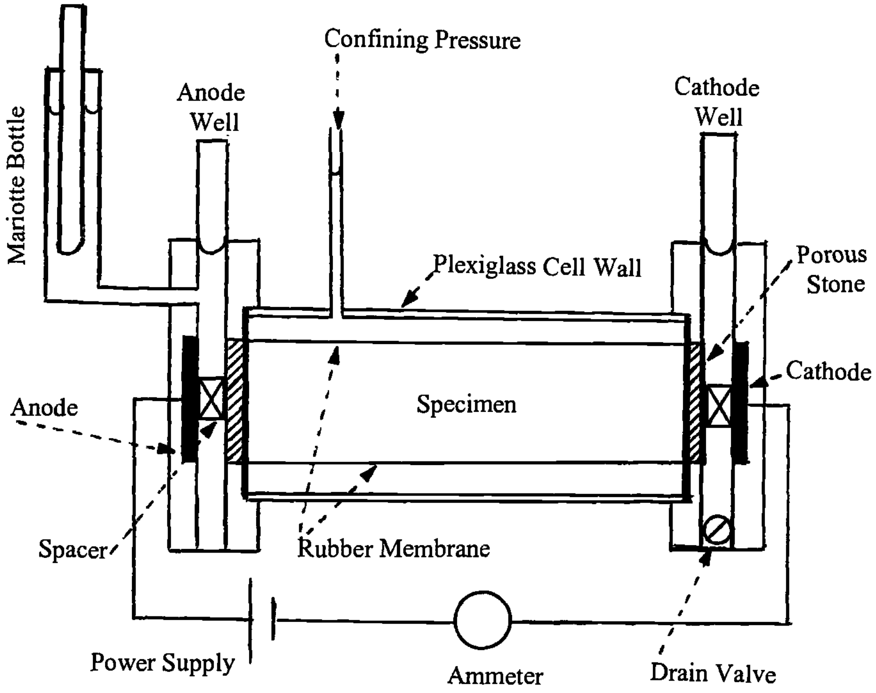

Figure 1 - *Sketch of Electroosmotic Cell Used in this Study*

towards the cathode. The water levels in the two wells were controlled to maintain a nearly zero hydraulic gradient during the electroosmotic treatment.

The cell wall was connected to a pressure control board. The pressure inside the cell was kept at the same pressure that had been used for the consolidation of each particular specimen. In this manner, four different tests were performed: test 1 for the specimen with no confining pressure applied; test 2 for a confining pressure of 172 kPa (25 psi); test 3 for a confining pressure of 241 kPa (35 psi); and test 4 for a confining pressure of 482 kPa (70 psi.)

An electrical gradient of 39 volt/m (1 volt/in.) was imposed on all specimens using a constant voltage power supply through graphite electrodes. The electrical gradient was kept constant for all the tests performed. The pH, the electrical conductivity, the temperature, the change in volume experienced by the specimen and the amount of effluent reaching the cathode well were monitored on a daily basis. The specimens were kept under electroosmotic treatment for periods of time ranging from one and a half months up to three months.

Upon completion of the treatment, the specimens were sliced into ten discs 12 mm (0.5 in.) thick. The slices were numbered from 1 to 10 starting at the anode side. The concentration of barium, pH, electrical conductivity, and moisture content was determined for each slice. The barium concentrations were determined on extracts from the slices obtained by the digestion method 3050 of the USEPA. The concentrations in the extracts were obtained analyzing the samples using a flame or a furnace Atomic Absorption Spectrophotometer.

Results and Discussion

Four different tests were performed to investigate the potential effects that overburden could have on the remediation of barium contaminated soils. The only difference between the specimens was the confining pressure used to consolidate and confine the specimen during electroosmotic treatment. The test 1 specimen was formed into an acrylic tube by compacting the soil slurry; no confining pressure was applied to consolidate or confine the specimen during treatment; this is referred as zero confining pressure. The initial moisture content of the soil trimmings was measured at 29.9%. The specimen for test 2 was consolidated and confined during treatment under 172 kPa (25 psi) confining pressure; before the initiation of the treatment phase, the soil had a moisture content of 24.4%. The specimen for test 3 was prepared and treated under 241 kPa (35 psi) confining pressure; the moisture content of the specimen was 22.8% upon completion of the consolidation phase. The specimen for test 4 was prepared and treated under a confining pressure of 482 kPa (70 psi) and resulted in a soil with a moisture content of 19.5% after the consolidation phase.

The differences in moisture content at the beginning of the treatment period indicate that the specimens had large differences in density, void ratio and pore sizes that could only be attributed to the confining stresses acting on the specimens. The treatment phase lasted 41 days for test 1 and the three remaining tests were all treated for 95 days. The complete set of all the data recorded has been presented elsewhere (Kabir 1996) and the more relevant findings are summarized in the remaining sections of this paper.

Acid/Basic Conditions in the Electrode Wells

Before the initiation of the treatment, the pH in both wells was nearly a pH of 7. As the treatment progressed, the pH in the anode well progressively decreased to a pH of 1.93 for test 1 and to a pH of 2.0 for test 3 and test 4. The only exception was test 2 in which the anode well stabilized at a pH of 3.This can probably be attributed to problems encountered for the full insertion of the pH probe into the anode well during this test.

By way of contrast, the pH in the cathode well increased as the treatment progressed, eventually stabilizing at a pH of 11.8 for test 1 and test 2, at pH of 12 for test 3, and at a pH of 13 for test 4. These results show a consistent pattern of increasing pH as the density of the soil specimen increased. This fact supports the contention that the higher densities restricted the diffusion of the hydroxyl ions into the soil mass resulting in higher concentration of hydroxyl ions in the cathode well.

Measurements of Electroosmotic Flow

The electroosmotic flow peaked early in the treatment phase and then decreased to non-measurable values towards the end of the process. During the first five days of treatment, the accumulated effluent collected in the cathode well decreased from 5.3 ml for test 1, to 4.4 ml for test 2, to 3.8 ml for test 3, and to 3.7 for test 4. These results show a consistent pattern of decreasing effluent for increasing density of the specimen with the associated decrease in porosity. Thus the higher the confining pressure, the lower will be the induced water flow by the same voltage gradient.

The lower electroosmotic flow rates translate to smaller coefficients of electroosmotic permeability. The coefficients of electroosmotic permeability in centimeters square per second and volt calculated from the above measurements decreased from $2.0*10^{-6}$ for test 1, to $1.96*10^{-6}$ for test 2, to $1.6*10^{-6}$ for test 3, and to $1.4*10^{-6}$ for test 4. These results are in general agreement with earlier reported findings (Casagrande 1952.)

Energy Consumption During the Treatment Process

The accumulated consumption of energy (in kilowatts hour per cubic meter of soil treated) at the end of the treatment process for each specimen did consistently increased from 3.0 for test 1, to 8.5 for test 2, to 8.7 for test 3, and to 9.1 for test 4. A further difference between the specimens was that the rate of energy consumption had leveled off for test 1, while it was still increasing at nearly constant rates for the remaining three tests.

These results by themselves indicate that the energy expenditures for cleaning the soil should increase as the soil contamination occurs in deeper layers. Nevertheless, these results have to be seen in light of the removal efficiency described later. These later results indicate that the removal of barium is, not only more costly, but the removal of barium is much less effective; in other words, the effect is more pronounced than could be inferred from the energy expenditures listed above.

A comparison of the energy expenditures of the three tests is presented in Figure 2. These results show that the energy expense per unit mass of barium removed increased for increasing confining pressures; that is, for increasing depths of burial of the contaminated soil. The energy consumption increased by 20% from test 2 to test 3 (for confining pressure increasing from 172 kPa to 241 kPa) and by 60% from test 2 to test 4 (for confining pressure increasing from 172 kPa to 482 kPa.)

Specimen Volumetric Changes Induced by the Electroosmotic Treatment

The specimens were initially trimmed down to 51 mm (2 in.). Upon completion of the treatment and extraction from the cell, the diameter of the specimen was measured at intervals of 12 mm (0.5 in.) along the length of the specimen. These results showed that the specimens consistently decreased in diameter near the ends of the specimen, and increased diameter towards the center of the specimen. The combined effect was a general decrease of the volume of the specimen on the order of 6 ml to 7 ml. Since the specimen expanded upon removal of the confining pressure, the 6 to 7 ml volume decrease is a lower bound of the actual volume changes experienced by the specimens. The effluent volume collected for tests 2, 3, and 4 was on the order of 12 ml. This effluent would be the result of fluid supplied by the anode well and fluid extracted from the pores of the specimen. Thus, 12 ml is an upper bound of the volume lost by the specimens during treatment. Both indicators show that the specimens lost some volume,

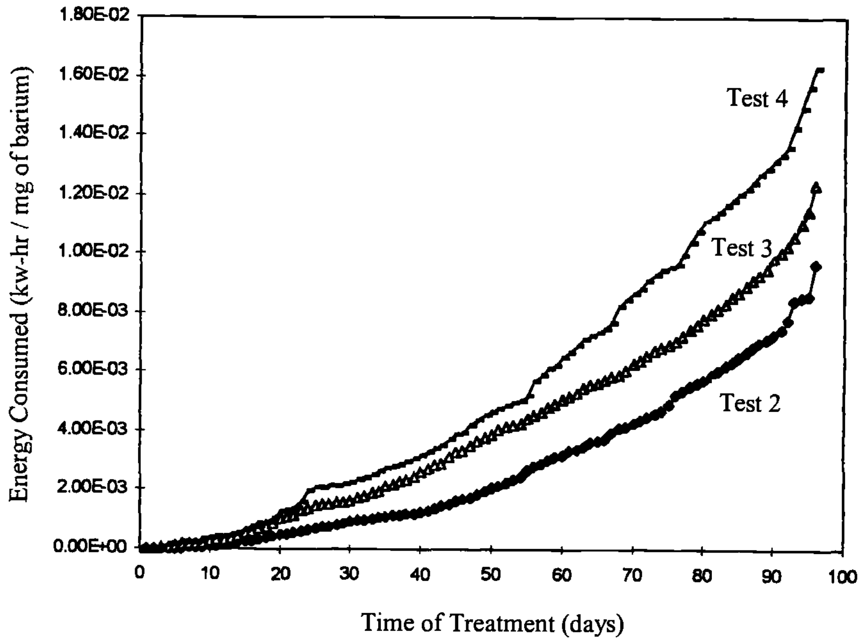

Figure 2 - *Cumulative Energy Spent per Unit Mass of Barium Removed*

from 6 ml to about 12 ml. This implies that the water removed at the cathode well was not thoroughly replaced by the constant pressure water supply. Thus in real applications, the soil will tend to shrink and to accommodate this shrinkage strain, the soil mass would have a tendency to crack.

Moisture Content of the Soil after Treatment

Upon removal of the specimen from the electroosmotic cell, the specimen was cut into ten slices and a portion of each slice was used to determine the water content of the soil after treatment. The results of all of these determinations are summarized in Table 1. This table also shows the moisture contents determined on the trimming of each specimen, before the treatment. The results shown in Table 1 are in conflict with the volumetric changes discussed earlier. The moisture content of the specimens, appear to have increased during treatment. This increase seems to be larger near the ends of the specimen and smaller towards the center of the specimen.

Although there is no conclusive evidence for this explanation, it appears that the differences in water content within the specimen are the result of the specimen preparation procedure. In this manner, the consolidation phase was probably not completed and gradients in water content existed within the specimen before the electroosmotic treatment was started. A similar explanation could be advanced to reconcile the moisture contents of the trimmings of the specimens before being subjected to the treatment process and the moisture contents of the specimens after treatment.

Table 1 – *Moisture Content (%) of the Soil Slices and Trimmings*

Slice Number[1]	Test 1	Test 2	Test 3	Test 4
1	43.2	32.6	21.5	19.2
2	42.3	28.2	20.4	19.6
3	34.0	27.9	20.8	19.7
4	33.9	27.1	18.5	20.7
5	37.2	28.9	20.8	21.2
6	36.4	28.9	22.7	20.0
7	35.6	31.1	20.3	19.9
8	34.8	23.6	20.5	19.8
9	50.0	30.3	24.7	19.6
10	32.8	32.8	26.6	15.4
Trimmings	29.9	24.4	22.8	19.5

[1] Slice 1 is at the anode well, and slice 10 is at the cathode well

Acid/Basic Conditions Along the Treated Specimens

A portion of each slice was mixed with de-ionized water in a 1:1 soil/water ratio by weight, and the pH of the supernatant was recorded. A summary of these measurements is presented in Table 2. The initial pH of the soil stock suspension was measured to be at a pH of 6.5. The measurements shown in Table 2 indicate very minor changes of the pH of the soil within the specimen. The trend appears to be that for the higher confining pressures, the central portion of the specimen appears not to have been affected, and only a limited zone around the electrode well appears to have experienced any significant pH changes.

The effects at the cathode well appear to be even more limited and no significant difference appears to have occurred beyond the first slice. These results are in stark contrast to the findings reported in the literature (Acar et al. 1990) about the penetration of the basic front being about one third of the specimen, and the penetration of the acid front being the remaining two thirds of the specimen. Most of the results published in the technical literature have been obtained using low charge clay, such as kaolinite, and thus have neglected the effect of the clay charge on the electro migration process. The results shown in Table 2, suggest a fairly strong pattern of increased isolation of the central part of the specimen as the pores become smaller and the movement of charged cat ions becomes more difficult.

Evaluation of Free Barium Removal by the Electroosmotic Treatment

As a result of the initial saturation of the soil stock with 0.1 N barium chloride solutions, the exchange complex of the clay was saturated with barium and the pore fluid consisted of a 0.1 N barium chloride solution. Thus the specimens contained free barium

Table 2 – *pH Measurements*[1] *of Specimen's Slices*

Slice Number[2]	Test 1	Test 2	Test 3	Test 4
1	4.88	4.45	4.46	3.54
2	4.22	5.85	5.49	4.23
3	5.92	6.34	5.88	6.09
4	6.06	6.82	6.42	6.68
5	6.02	6.83	6.58	6.66
6	6.39	6.84	6.64	6.69
7	6.41	6.87	6.71	6.74
8	6.46	6.94	6.72	6.77
9	6.76	6.93	6.80	6.88
10	7.49	6.94	7.30	9.31

[1] The pH measurements were performed on a 1:1 soil extract

[2] Slice 1 is at the anode well, and slice 10 is at the cathode well

in the pore water, and barium fixed on the exchange sites of the clay particles. A portion of each slice was used to determine the free barium in the pore water after the treatment. For this purpose, the soil was dispersed into de-ionized water and the volume brought to 100 ml. The concentration of barium in the water in equilibrium with the soil was considered as free barium. This amount of barium relative to the initial free barium (corresponding to the 0.1 N barium chloride solution) is an estimate of the barium left over by the electroosmotic treatment. The results obtained for all specimens are summarized in Table 3.

These results show a clearly defined trend of increasing percentage of free barium not removed by the electroosmotic treatment as the confining pressure on the specimen increases. The free barium left over in the specimen of test 1 is only about 1% of the initial barium present in the pore fluid. As the confining pressure increases for the tests 2, 3 and 4, the left over barium increases to 2%, 4%, and 7%, respectively. Furthermore, the free barium left near the cathode well increases significantly above the overall rates described above.

The removal of free barium was expected to be easier than the removal of the barium absorbed on the clay exchange sites. These results, show that most of the free barium is removed for all specimens; although, the confining pressure has an effect on the time frame of the cleanup operation and the energy expenditures necessary to accomplish the removal of free barium. The more plausible explanation is that the electric charge of the clay particles and the smaller pores existing in the specimen as the confining pressure increases forces a closer interaction between the cat ions and the clay charges. This appears to reduce the mobility of the barium ions and requires higher-energy expenditures to force the flow of ions towards the cathode.

Efficiency of Electroosmotic Treatment for Total Barium Removal

A portion of each slice was digested following the sludge digestion procedure 3050 of the USEPA, and the total concentration of barium was measured using an atomic

Table 3 – *Percentage*[1] *of Free Barium Remaining After Treatment*

Slice Number[2]	Test 1	Test 2	Test 3	Test 4
1	0.7	1.3	2.0	0.7
2	0.8	1.6	4.0	5.0
3	1.4	2.2	2.8	4.4
4	1.4	2.3	4.1	4.0
5	1.4	2.1	4.2	5.1
6	1.3	2.1	4.0	5.9
7	1.5	2.0	5.8	7.1
8	1.0	2.6	6.2	8.4
9	1.3	2.0	7.2	11.6
10	5.3	5.6	9.9	52.2

[1] The percentage is referred to the concentration of barium in the 0.01 N solution
[2] Slice 1 is at the anode well, and slice 10 is at the cathode well

absorption spectrophotometer. The amount of barium measured under these conditions includes the free barium in the pore water and the barium absorbed on the clay exchange sites. The efficiency was calculated as the percentage of barium removed with the treatment (this was calculated as the difference between initial barium minus the barium determined on the digested slice) referred to the total initial barium present in the specimen before the electroosmotic treatment. A summary of all the results for the four tests is presented in Table 4. These results show clearly that the confining pressure influences drastically the efficiency of barium removal. This implies, that under field conditions, the cleanup of deeper soil layers will require longer treatment periods and larger energy expenditures.

All the tests show a consistent trend of higher efficiency at the anode that then decreases gradually towards the cathode. This is the result of the transport of barium towards the cathode; thus, the first region to show signs of barium removal would always be near the anode well. The results for test 4 show an efficiency of about 72% at the anode, while the efficiency near the cathode is very nearly zero. The results for this test 4 indicate that the cleanup was in the beginning stages when the treatment process was stopped after 95 days.

At this point, it is worthwhile to recall that the energy expenditures for the electroosmotic treatment of test 1 were about one third of the energy expenditures in test 4. Furthermore, the clean up process in test 1 had lasted less than 10 days, while the cleanup process for tests 2, 3 and 4 was continued for 95 days and remained noticeably active for periods in excess of 50 to 60 days. Considering that the results shown in Table 4 indicate removal efficiencies for test 1 in excess of four times those achieved in tests 2, 3, and 4, the large effect of confining, or overburden, pressure is patently clear. The implication of these findings is that the depth of overburden above the contaminated soil will drastically affect the cleanup of clayey soils with non-negligible cat ion exchange capacities. These soils are by far the largest majority of soils found in nature.

Table 4 – *Efficiency of the Treatment as Percentage of Total Barium Removed*

Slice Number[1]	Test 1	Test 2	Test 3	Test 4
1	96	77	73	72
2	93	45	44	37
3	93	44	43	28
4	90	22	21	20
5	90	22	22	20
6	91	20	20	20
7	91	19	21	14
8	91	18	10	2
9	91	17	3	1
10	89	0	1	0

[1] Slice 1 is at the anode well, and slice 10 is at the cathode well

Conclusions and Recommendations

The results of the presently described laboratory program show conclusively that the overburden stresses can have a significant effect on the rate and the cost of the removal of contaminating cat ions from naturally occurring soil deposits by the electro migration imposed by an applied direct electric current. This is especially true for soil deposits with non-negligible exchange capacities.

Although the set of results available at this time is limited and does not permit a quantification of the effects in terms of cost increases and time delays that would be incurred, it appears that these two factors can be significantly affected by the cat ion exchange capacity of the soil in question, the ionic valence of the cat ion involved, and the magnitude of the overburden stresses. An important implication is that the extrapolation of bench trials in the laboratory cannot be used to predict the actual field performance unless the effect of the confining stresses on the cleanup process is adequately accounted for.

An additional concern associated with the extrapolation of results to other cases is related to the different behavior of each ionic species with the differences in the pH environment of the pore water. This is the result of the electrolysis of water, associated with the treatment process, that causes changes in the pH and these in turn cause differences in the solubility of the different ionic species.

The presently described study was limited since a single cat ion was used, for one soil type, and a constant voltage gradient was applied in all tests. The results described seem to indicate the need to extend the work to include more variables and permit clarification of the roll of all possible interferences caused by the presence of overburden stresses on the soil deposit undergoing restoration.

References

Acar, Y. B., Gale, R. J., Putnam, G. A., Hamed, J., and Wong, R. L., 1990, "Electrochemical processing of soils: Theory of pH gradient developed by diffusion, migration, and linear convection," *Environmental Science and Health*, Vol. 25 (6), pp. 687-714.

Acar, Y. B., Hamed, J., Alshawabkeh, A. N., and Gale, R. J., 1994, "Removal of Cd (II) from saturated kaolinite by application of electric current," *Geotechnique*, Vol. 44, pp. 239-254.

Casagrande, L., 1952, "Electroosmotic stabilization of soils," *Journal of the Boston Society of Civil Engineers*, Vol. 39, pp 51-83.

Chen, J. L., Al-Abed, S. R., Bryndzia, L. T., and Murdoch, L., "Cation transport and partitioning during a field test of electroosmosis," *Water Resources Research*, Vol. 35, No. 12, pp. 3841-3851.

Kabir, A., 1996, "Electroosmotic removal of barium from contaminated soils," *Thesis* presented to the Graduate School of The University of Texas at El Paso, in partial fulfillment of the requirements for the degree of Master of Science.

Haran, B. S., Zheng, G., Popov, B. N., and White, R. E., 1995, "Electrochemical decontamination of soils: Development of a new electrochemical method for decontamination of hexavalent chromium from sand," *Electrochemical Society Proceedings*, Vol. 95, No. 12, pp. 227-251.

Kelsh, D. J., and Parsons, M. W., 1997, "Department of Energy sites suitable for Electrokinetic remediation," *Journal of Hazardous Materials*, Vol. 55, pp. 109-116.

Lorenz, P. B., 1969, "Surface conductance and electrokinetic properties of kaolinite beds," *Clays and Clay Minerals*, Vol. 17, pp. 223-231.

Puppala, S. K., Alshawabkeh, A. N., Acar, Y. B., Gale, R. J., and Bricka, M., 1997, "Enhanced electrokinetic remediation of high sorption capacity soil," *Journal of Hazardous Materials,* Vol. 55, pp. 203-220.

Vane, L. M., and Zhang, G. M., 1997, "Effect of aqueous phase properties on clay particle zeta potential and electro-osmotic permeability: Implications for electrokinetic soil remediation processes," *Journal of Hazardous Materials*, Vol. 55, pp. 1-22.

Yong, R. N., and Mourato, D. 1990, "Influence of polysaccharides on kaolinite structure and properties in a kaolinite-water system," *Canadian Geotechnical Journal*, Vol. 27, pp. 774-788.

Thomas C. Sheahan,[1] Akram Alshawabkeh,[1] Loretta A. Fernandez,[2] and Karen S. Henry[3]

A Reactive Geocomposite to Remediate Contaminated, Subaqueous Sediments

---

Reference: Sheahan, T. C., Alshawabkeh, A., Fernandez, L. A., and Henry, K. S., "**A Reactive Geocomposite to Remediate Contaminated, Subaqueous Sediments,**" *Contaminated Sediments: Characterization, Evaluation, Mitigation/Restoration, and Management Strategy Performance, ASTM STP 1442*, J. Locat, R. Galvez-Cloutier, R. C. Chaney and K. R. Demars, Eds., ASTM International, West Conshohocken, PA, 2003.

Abstract: This paper describes a new geocomposite overlay, consisting of filter fabric layers surrounding a chemically reactive core, that is being developed to contain and remediate contaminated, subaqueous sediments. This geosynthetic-based reactive material will provide the same isolation as that of traditional soil caps, but will have the added advantages of: providing a remediation layer to adsorb and neutralize target contaminants; block resuspension of fine sediment particles; and serve as a foundation material during remediation. In addition, the geocomposite could be used in a tube configuration to simultaneously store and remediate dredged sediments. The paper describes the results of a two-phase, bench-top experimental program to assess the feasibility of this idea and to help model its scalability for sediment remediation in the field. This testing consisted of two parts: one-dimensional consolidation testing on layered systems of very soft soils and geotextiles, both woven and non-woven; and sorption isotherm testing of lead ions (Pb^{+2}), in solutions of various pH and salt concentration, for both soil and zeolite. Results show the effects of the two geotextile types on the soil-geotextile system during consolidation, including changes in coefficients of consolidation and hydraulic conductivity. The adsorption tests show the effectiveness of the zeolite in binding the lead ions, and the soil's potential for lead adsorption under a variety of pH and salt concentrations.

Keywords: contaminants, soils consolidation, adsorption, geosynthetics, sediment, dredge spoil

---

[1] Associate Professors, Department of Civil and Environmental Engineering, Northeastern University, Boston, MA 02115.

[2] Former undergraduate student, Department of Civil and Environmental Engineering, Northeastern University, Boston, MA 02115.

[3] Research Civil Engineer, U.S. Army Corps of Engineers, Cold Regions Research and Engineering Laboratory, Hanover, NH 03755.

Introduction

Contaminated, subaqueous sediments present one of the most serious environmental challenges on both the national and global levels. In the U.S. alone, the Environmental Protection Agency (EPA) estimates that 1.2 billion cubic meters in the upper 50 mm of subaqueous sediments is contaminated enough to pose health risks to the aquatic food chain (U.S. EPA 1997). The existing state of practice to treat such sediments is either subaqueous capping with some combination of natural soil and/or geosynthetic layers, or removal of the sediment for ex situ treatment and/or storage. However, capping systems are relatively thick layers of material prone to erosion and other deterioration, and these layers isolate the sediment without actively treating it; sediment removal is expensive and can result in significant contaminant resuspension in the overlying water during removal.

In this study, experimental work was performed to investigate a new approach to remediate these sediments using a reactive geocomposite material. Such a material (U.S. Patent Office 2002) will consist of one or more filtering layers surrounding a reactive layer containing chemicals that can react with potential contaminants in the sediment. Figure 1 shows two possible configurations for the reactive geocomposite: a horizontal overlay in large sheets (Fig. 1a) and in smaller strips like wick drains (i.e., drainage strips pressed vertically into the soil commonly used to accelerate consolidation) used in a vertical configuration (Fig. 1b). For the horizontal overlay configuration (Fig. 1a), large sheets would be placed on the surface of a saturated or near-saturated sediment deposit (either subaqueous or terrestrial). A layer of surcharge material (e.g., rip-rap, gravel or sand) would be placed on top of it to consolidate the sediment, producing expulsion of pore fluid that contains target contaminants. As the pore fluid flows through the composite, the middle, reactive layer of the geocomposite will react with the contaminants (e.g., adsorb them), resulting in isolating and concentrating the chemicals within that layer. The middle layer may also retain fine particles on which chemicals are adsorbed. For the wick drain configuration (Fig. 1b), a tube of filter material would surround the reactive or adsorbing layer in a sock-like configuration. An additional configuration that could be used with the reactive geocomposite would be as a tube such as that currently being used for a variety of waterway stabilization projects (e.g., Land and Water 2001).

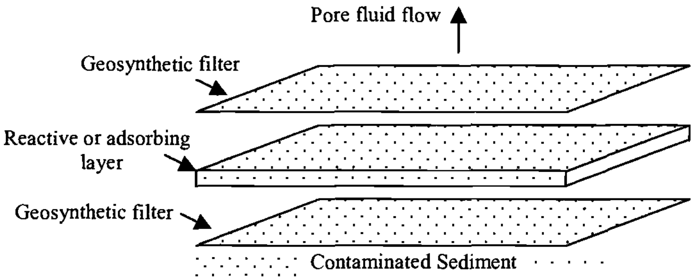

Figure 1a - *Schematic of Layers in Reactive Geocomposite (Horizontal or Overlay Configuration)*

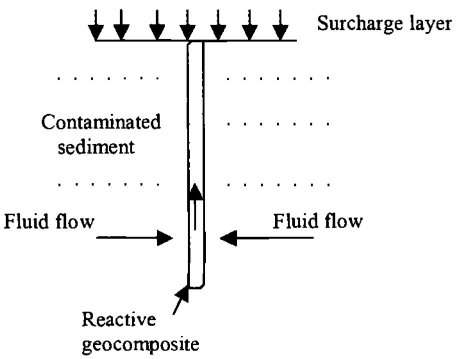

Figure 1b - *Reactive Composite in Vertical or Wick Drain Configuration*

In the overlay configuration, the reactive geocomposite will provide the same isolation as that of traditional soil caps. The additional functions of the overlay include providing a remediation layer that will adsorb and effectively neutralize target contaminants from the underlying sediment; blocking resuspension of fine sediment particles that may be closely bound to contaminants; and serving as a stable, protective foundation material during remediation.

This paper describes the benchtop laboratory testing that has been performed to date to determine the feasibility of this technique and to help model its scalability for sediment remediation in the field. This testing is considered essential prior to necessary pilot testing. One-dimensional consolidation tests were conducted on layered systems of very soft soils and geotextiles, both woven and non-woven. In addition, sorption isotherm tests were performed on lead ions (Pb^{+2}) in solution for both soil and a proposed adsorption agent (zeolite) in the reactive portion of the geocomposite. The adsorption testing also included examining the effects of pH and salt concentration on the sorption isotherms.

Background

Use of Geosynthetics in Subaqueous Sediments

The U.S. EPA program on Assessment and Remediation of Contaminated Sediments (ARCS; U.S. EPA 1996) identifies potential functions of geosynthetics in *in situ* cap designs as 1) providing a bioturbation barrier, 2) stabilizing the cap, 3) reducing contaminant flux, 4) preventing mixing of cap materials with underlying sediments, 5) promoting uniform consolidation, and 6) reducing erosion of the capping materials. ARCS guidelines include a geotextile for separation and stability purposes, i.e., to prevent fines from migrating into the sand layer of the cap and presumably as a bioturbation barrier (both separating functions), and to provide a more stable foundation for the overlying soil layers (reinforcement).

Geomembranes have been used to cap subaqueous sediments but the problem of gas formation and water entrapment under the geomembrane has led to problems with its bulging and/or lifting away from the sediment (e.g., Savage 1986 and Cooke et al. 1993).

Whenever there is flow of water through fine-grained sediments in series with a geotextile, clogging of the geotextile should be considered. Filters in geotechnical structures are required to retain soil particles while allowing water to pass so that excessive water pressure does not build up in the retained (protected) soil. Granular or geosynthetic filters are usually installed in structures where the flow is in one direction only (e.g., pavement edge drains), and the design criteria are well established (Giroud 1996; Holtz et al. 1997).

Henry et al. (1995) described a geocomposite developed and tested for placement on pond bottoms to prevent access of wildlife to contaminated pond sediment. The contaminant was particles of white phosphorous, a neurotoxin that caused thousands of waterfowl deaths annually in Eagle River Flats, Alaska. A laboratory study evaluated whether white phosphorus particles become suspended in the overlying water because of 1) upward water flow through contaminated sediment capped with geotextile, or 2) tapping of the top of the geotextile or sediment and then vigorously stirring the water to simulate waterfowl feeding and swimming. The geotextile formed an excellent cap to the underlying sediment and white phosphorus for both experimental conditions.

Henry and Stark (1997) evaluated the ability of geocomposite that had very large pores interspersed in a geotextile that was overlain by a large-pored drainage net to retain 0.25- and 0.15-mm diameter particles in the presence of turbulent flow and impact loading. The geocomposite was placed in a pond (< 0.5 m deep) and overlain with two different soil covers and without a soil cover. The geosynthetics significantly reduced the amount of fine soil suspended by the stirring and loading compared to the bare pond bottom for all three cases, and they did not float to the surface as did the geotextiles in a previous study.

Koerner and Ko (1982) studied flow through soil-geotextile systems to assess the fabric's long-term flow performance. In flow tests on a variety of these layered systems, they found that the flow rate tended to decline over time and stabilize at a lower flow rate than initially measured. Aydilek et al. (2000) performed consolidation tests on high water content wastewater sludge layered with a woven geotextile, and modeled the results using large strain numerical analysis.

The use of geocomposites for various sediment treatments has developed to the commercial stage. For example, Bishop et al. (1994) describe sand-filled geocomposites for surcharging and stabilizing subaqueous sediments. Zeolite-impregnated geotextiles have been developed for treating liquid and gaseous wastes (GSA Resources, Inc. 2001).

Design of Reactive Filters for Contaminant Remediation

The type of reactive geosynthetic filter will vary depending upon the type of contaminant. The material introduced should provide the necessary reactive conditions for either collection and/or breakdown of the target contaminants. For heavy metal contaminated sediments, the best option is to extract and adsorb the contaminants in a separate phase of the geotextile. Zeolite has a significant negative charge and ion exchange capacity so that it is ideally suited for this reactive purpose.

Zeolites are hydrous aluminosilicates that exist in many natural formations, thus its cost is not prohibitive. Studies have evaluated the potential use of zeolites for soil and water treatment (e.g., Leppert 1990, Misaelides and Godelitsas, 1995, Shanableh and Kharabsheh 1996, Reyes et al. 1997, Sakadevan and Bavor 1998). Others have attempted to modify the sorption potential of zeolites for organic contaminants by treating the zeolites with surfactants (Haggerty and Bowman 1994, Li 1998 and Li et al. 2000). Jacobs and Forstner (1999) discussed the potential of using zeolite as a media for reactive barriers. They evaluated lead sorption on four types of zeolite and demonstrated its capability for immobilizing contaminants.

Sorption rate in any environment is dependent upon the changes in the concentration of the ion in solution. In general, sorption rate is given by

$$\frac{\partial s}{\partial t} = \frac{\partial s}{\partial c}\frac{\partial c}{\partial t} \tag{1}$$

where s is the adsorbed concentration (mg/kg), and c is the concentration in solution (mg/l). The reversible term ds/dt is often used to describe the sorption rate. The equilibrium partitioning between the adsorbed phase and the aqueous phase of the chemical components are commonly measured under controlled temperature and applied pressure, and the resulting correlation of s versus c is often described by several equilibrium models (linear, Freundlich, and Langmuir models). Assuming instantaneous equilibrium in sorption reactions and linear isotherms, the change in concentration of the adsorbed phase of species is linearly related to the change in concentration of the aqueous phase,

$$\frac{\partial s}{\partial c} = K_d \tag{2}$$

where K_d is the distribution coefficient (L/kg). Other methods have also been used to account for sorption because the previous method ignores the effect of pH, ionic strength, redox reactions, competitive adsorption, and the mechanism of adsorption. These methods include isotherm equations, mass action models, and surface complexation models proposed by Langmuir (1987), Kirkner and Reeves (1988), Yeh and Tripathi (1989), Mangold and Tsang (1991), and Selim (1992), among others.

To develop a reactive geocomposite overlay for contaminated sediments, it is necessary to assess the effect of salinity and pH on zeolite performance for collecting lead. In this study the sorption isotherms are evaluated for lead on kaolinite and zeolite using different solutions (deionized water, synthetic sea water and synthetic brackish water) under various pH conditions (3, 5 and 7). The distribution coefficient is calculated for each case to compare sorption characteristics under various conditions. The results will help to understand the potential of lead collection by a zeolite reactive geosynthetic barrier in seawater and brackish water conditions.

Experimental Studies

One-dimensional Consolidation Tests on Soil-Geotextile Systems

To characterize the consolidation behavior of a layered system consisting of a geotextile and a very soft sediment (such as that expected near the surface of a subaqueous sediment), a series of one-dimensional (1-D) consolidation experiments was performed. The primary goal of this set of experiments is to determine how the sediment's consolidation behavior will be affected by the addition of a geotextile filtering layer, including the geotextile's clogging potential during the consolidation process.

A kaolinite powder, produced by U.S. Silica Co., was used as the baseline soil. The powder has a mean particle size of 1 μm, with 95% finer than 10 μm and 65% finer than 2 μm. This powder was mixed at a water content, w = 50%, just above its liquid limit (LL = 41 %), overlain by a piece of geosynthetic, was placed in an incremental loading (IL) consolidation device. Testing was performed in accordance with ASTM Test Method for One-Dimensional Consolidation Properties of Soils (D2435). The consolidation test specimens were allowed to drain only at the top surface, i.e., at the geosynthetic; the bottom surface was kept impermeable to imitate the relatively low hydraulic conductivity of underlying sediments. Two types of geosynthetic, one woven and one non-woven, were selected for use based on the results from the computer program *Geofilter* developed by TC Mirafi, which takes as its primary input the soil type being used under the filter. Table 1 gives the two geotextiles selected and their respective opening sizes and flow characteristics. It is noted that while the apparent opening size is approximately the same for both geotextile types, there is one order of magnitude difference in the three flow characteristics given.

Table 1 – *Properties of Geotextiles Selected for 1-D Consolidation Testing*

Geotextile type	Apparent opening size, mm	Permittivity, sec^{-1}	Permeability, cm/sec	Flow rate, $l/min/m^2$
Non-woven	0.18	1.2	0.21	3866
Woven	0.212	0.28	0.01	733

After mixing the soil at approximately 50% water content (which produced a thick slurry consistency in the soil), it was placed in the consolidation cell confining ring that was already mounted on the impermeable ring base. For the tests in which a geotextile was used, the selected geotextile was cut into a circular piece with approximately the same diameter as the inside diameter of the confining ring holding the soil specimen. This piece was soaked in distilled water, excess moisture removed, and it was placed on the soil surface, after which the top porous stone and the loading platen were placed on the layered system. For tests in which only the kaolinite slurry was tested, a piece of filter paper was moistened and placed directly on the soil, and the stone and platen then placed on the top.

All specimens were incrementally loaded starting at a vertical effective stress, σ'_v = 2.45 kPa, up to σ'_v = 98.1 kPa using a load increment ratio of 1.0. Each load was left on for 24 hours before the next load increment was applied. For each load level, specimen vertical deformation was measured using a displacement transducer and a computer-based data acquisition system. Measurements were taken at 5, 10, 20, 40, 80, 160 and 300 seconds (5 minutes) and then every 5 minutes until the end of the 24-hour period. Each increment was analyzed to determine the deformation at the end of primary consolidation, as well as the coefficient of consolidation (c_v) and the coefficient of hydraulic conductivity (k_v) in the vertical direction (logt method). Comparisons were made between the consolidation behavior of the kaolinite without any geotextile layered on top (i.e., only filter paper between the soil and the top porous stone), and layered systems consisting of kaolinite with either woven or non-woven geotextile. The number of tests for each specimen type are as follows: 8 tests on kaolinite alone (test designation, K); 4 tests on kaolinite with non-woven geotextile (K-NW); and 3 tests on kaolinite with woven geotextile (K-W).

Figure 2 shows the comparison of c_v among the three specimen types, K, K-NW, and K-W, at different σ'_v levels during the consolidation tests. The points plotted represent average values for a particular specimen type at that σ'_v level. There are no data for σ'_v levels less than 25 kPa because the logarithm of time curves did not exhibit a sufficient "break" to apply the graphical construction technique for determining c_v.

These results show that the K and K-W specimens exhibit virtually identical c_v values at the 3 stress levels, and that the K-NW specimens show consistently higher c_v values than the other two specimen types (typically a difference of about 1×10^{-4} cm^2/sec). It is important to note that the c_v values for all the tests increase monotonically and linearly with respect to σ'_v, even at about 100 kPa.

The k_v values are computed using the equation

$$k_v = c_v m_v \gamma_w \tag{3}$$

where m_v is the coefficient of volume change, $\Delta\varepsilon_v/\Delta\sigma'_v$, and γ_w is the unit weight of water. Figure 3 shows the comparison of k_v values (average value at each stress level for a given specimen type, K, K-NW and K-W) for the three specimen types versus σ'_v. For all specimen types, the trend is the same: while the c_v values increase across this stress range (Fig. 2), the stiffening of the soil during consolidation causes a decrease in m_v. The result is an initial drop in k_v, after which the values level off. As with the c_v data, the k_v for the kaolinite with non-woven geotextile shows the highest hydraulic conductivity at all stress levels.

The reason for the different c_v and k_v data between K-NW and K-W is explained by the geotextile properties given in Table 1. The *GeoFilter* program is heavily biased in its geotextile selection for a given application on the grain size distribution input. Thus, referring to Table 1, while the two geotextiles selected have similar apparent opening sizes (0.18 mm for the non-woven and 0.212 for woven), the flow characteristics (permittivity, permeability and flow rate) are all different by about an order of magnitude for the two geotextiles. Since the permeability of the woven geotextile is closer to that of the kaolinite, it has less impact on the layered system's consolidation characteristics. On the other hand, the non-woven represents a layer of relatively high hydraulic conductivity; it is also somewhat thicker than the woven material. This combination produces a layer of much higher flow transmission that aids consolidation of the layered system.

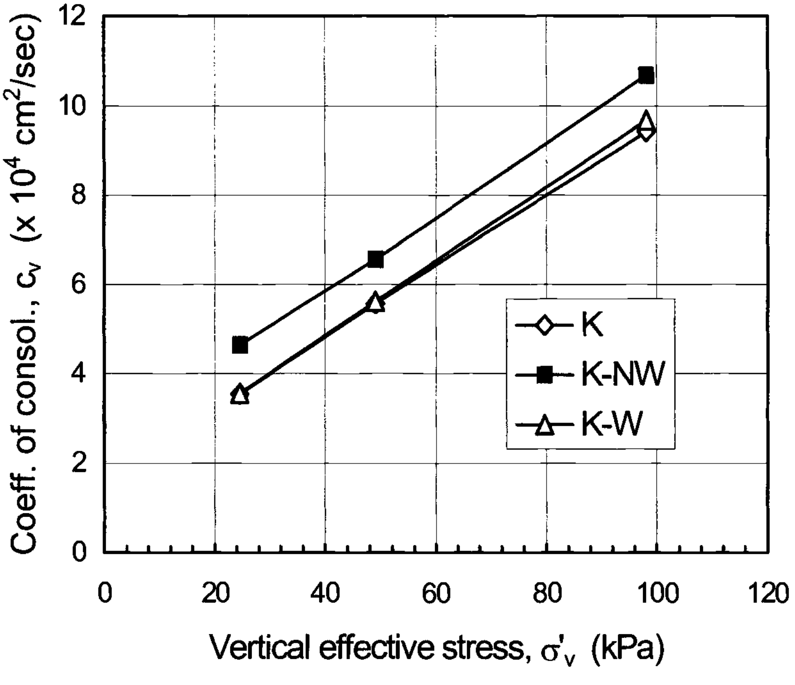

Figure 2 – *Comparison of* c_v *Values During 1-D Consolidation Tests on Kaolinite and Kaolinite-Geotextile Layered Systems*

Lead Sorption Tests on Zeolite and Soil

The lead sorption testing was conducted using a Varian SpectrAA-220 Atomic Absorption (AA) spectrometer, a Fisher Accumet pH meter, and a Fisher Accumet 30 conductivity meter. Materials used include kaolinite, zeolite, synthetic sea water (product CRC007 from Aqua Solutions Inc.), 50 ml centrifuge tubes, lead nitrate, and nitric acid.The kaolinite was the same as that used for the consolidation tests, and was selected for its "average" properties in terms of its cation exchange capacity and ability to adsorb ions. In other words, it lies between silt and montmorillonite in terms of its potential adsorption behavior. Kaolinite has a specific surface area of 10 to 20 m^2/g, and a cation exchange capacity of 3 to 15 meq/100 g (Mitchell 1993). The zeolite used (product ZS500H from GSA Resources Inc.) had a specific surface area of 531 m^2/g and a cation exchange capacity of 250 meq/100g. Zeolite was selected as the adsorption medium due to its high ion exchange and adsorption capacity, and for its ability to immobilize heavy metal ions. Brackish water was prepared by mixing sea water and deionized water at 1:1 ratio.

The sorption capacities were determined by evaluating the partitioning of lead between lead nitrate solution and the soil. A stock of 0.001 M lead nitrate solution was prepared by mixing 331.2 mg of lead nitrate powder with deionized water to make 1 liter of solution. In addition to the 0.001 M stock solution, five diluted solutions ($5x10^{-4}$ M, $3x10^{-4}$M, $1x10^{-4}$M, $5x10^{-5}$M, and $2.5x10^{-5}$ M) were prepared by mixing specific volume of deionized water with 500 ml of the stock solution.

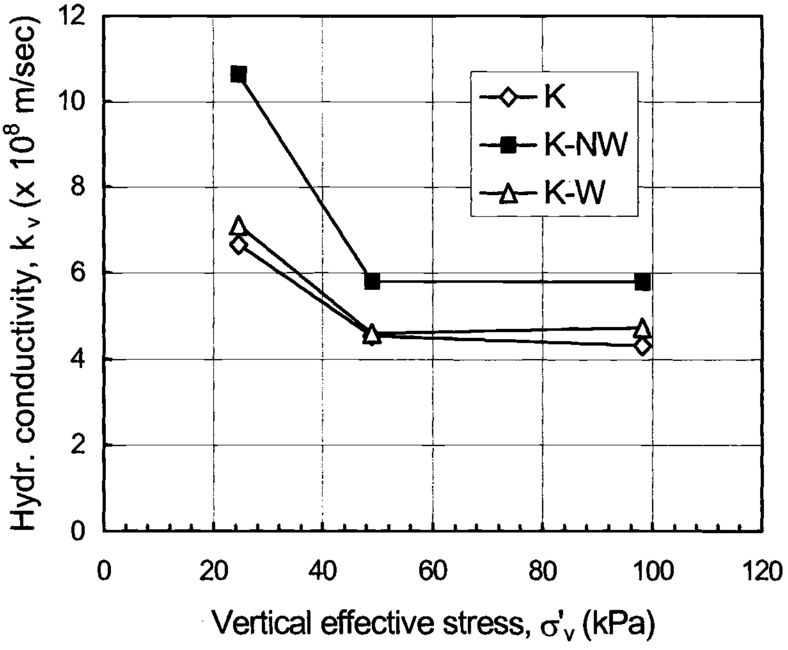

Figure 3 – *Comparison of k_v Values During 1-D Consolidation Tests on Kaolinite and Kaolinite-Geotextile Layered Systems*

The adsorption tests were conducted by mixing 3 grams of the material (kaolinite or zeolite) with 30 ml of lead nitrate solution. A few drops of concentrated nitric acid solution were added to adjust the pH to three specific values (3, 5 and 7). The mixed samples in the centrifuge tubes were stored for at least 24 hours with frequent shaking by hand (in accordance with EPA procedures). The solid and solution were then separated by placing the specimens in a centrifuge. AA analysis was conducted on the solutions to evaluate lead concentration using Varian SpectrAA-220 Atomic Absorption spectrometer. The pH and electric conductivity of each specimen were measured.

Since lead nitrate is a toxic substance that can be absorbed through the skin, care was taken for safe handling of the chemical and to minimize the potential for cross-contamination. All glassware and plastic centrifuge tubes used for the preparation and storage of standard solutions are soaked in an acid bath of 10% nitric acid for approximately 24 hours. Furthermore, the glassware and tubes are rinsed in deionized water three times and allowed to dry before use.

The results of sorption isotherms are displayed in Figure 4 for zeolite and kaolinite. A summary of the distribution coefficient for these cases is also provided in Table 2.

Table 2 - *Distribution Coefficients for Lead on Kaolinite and Zeolite (L/kg)*

Solution	Material	pH=7	pH=5	pH=3
Deionized Water	Kaolinite		600	333
	Zeolite		3333	5333
Synthetic Brackish Water	Kaolinite	60	60	24
	Zeolite	520	866	639
Synthetic Sea Water	Kaolinite	11	27	19
	Zeolite	244	333	300

The significance of zeolite sorption capacity is clear in the case of deionized water. The solution concentration was less than 1 mg/l even though the total adsorbed lead exceeded 2000 mg/kg. The results showed that K_d=5333 L/kg at pH=3 and K_d=3333 L/kg at pH=5. Such values are significantly high; however, it is noted that, at a pH of 3, lead sorption was higher than that at a pH of 5. Although kaolinite sorption is less than zeolite, it also showed significant sorption capacity. The distribution coefficient was 600 L/kg at pH=5 and 333 L/kg at pH=3. As expected, the sorption potential was higher at a pH=5 than at a pH=3. The results show that lead sorption is one order of magnitude higher on zeolite than kaolinite when deionized water is used. The distribution coefficient was highest at pH=5 (higher than at pH=3 or 7).

The impact of brackish water was to reduce the sorption potential for both zeolite and kaolinite. For kaolinite, the distribution coefficient decreased to less than 10% of that in deionized water. This shows the effect of ionic content of the solution on limiting the sorption of lead via ion exchange at the clay surface. Although reduced, lead sorption is still high for the case of zeolite in brackish water. Lead concentration in the solution was less than 2 mg/l, while the sorbed concentration was up to 800 mg/kg. Distribution factors greater than 500 L/kg were measured, and the highest is 866 L/kg at pH=5.

Synthetic sea water provides extreme conditions that can restrict ion exchange and lead sorption on zeolite and other ion exchange materials. This is obvious in the results for kaolinite and zeolite displayed in Figure 4 and Table 2. Kaolinite sorption capacity was limited and K_d decreased to 11 L/kg at pH=7. Zeolite capacity was reduced by one order of magnitude compared to the deionized water case. The highest distribution coefficient is 333 L/kg measured at pH=5.

A summary of the results clearly demonstrates the significance of using zeolite as a sorption media to collect lead from contaminated sediments. Brackish and sea water will contain significant concentration of ions that will compete with lead for sorption sites on

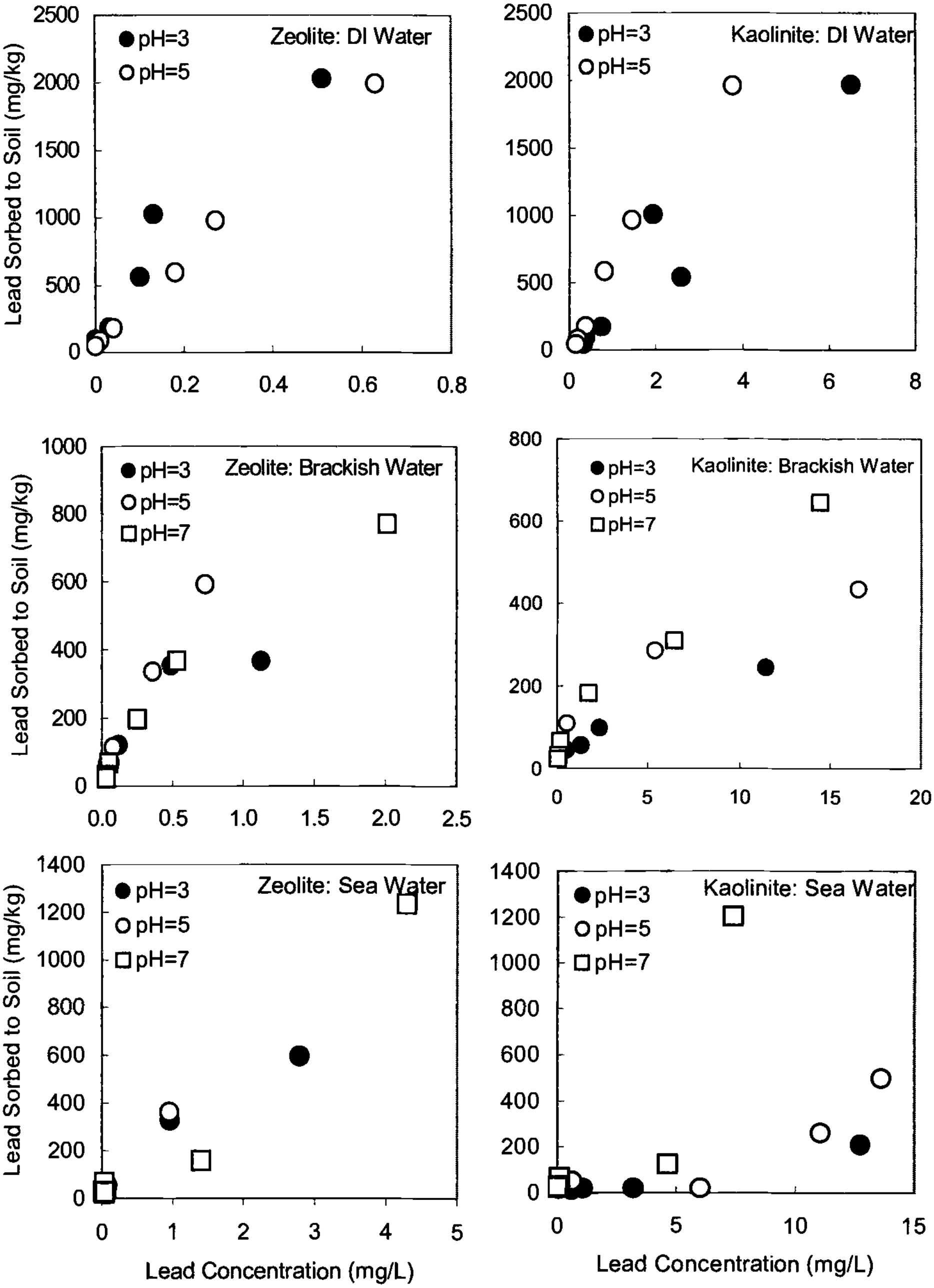

Figure 4 - *Lead Sorption Isotherms on Kaolinite and Zeolite Under Various Conditions*

zeolite. However, the results showed zeolite sorption capacity is still significant (although reduced) at such conditions. Acidification did not seem to negatively impact the lead sorption on zeolite. The highest capacity was obtained at a pH=5.

Conclusions

The consolidation tests showed that the non-woven geotextile can be an effective filter that has minimal clogging potential and promotes consolidation of the underlying sediment layer. Further testing is needed to assess the long-term clogging potential of the layered systems.

A summary of the adsorption test results clearly demonstrates the significance of using zeolite as a sorption medium to collect lead from contaminated sediments. Brackish water and sea water will contain significant concentrations of ions that will compete with lead for sorption sites on zeolite. However, the results showed zeolite sorption capacity is still significant (although reduced) under such conditions. While acidification did not negatively impact the lead sorption on zeolite, the highest capacity was obtained at pH = 5.

The next steps in this research include additional benchtop testing using an illitic clay, and a field test using a prototype reactive geocomposite.

Acknowledgments

The research described in the paper was supported primarily by a grant from the National Science Foundation, CMS-0086733, awarded under the New Technologies for the Environment program. Direct and in-kind support was also provided by Ten Cate Nicolon and its Construction Products Division, which produces Mirafi geosynthetics. The authors appreciate the support provided. Consolidation testing was performed by Mr. Ming Zhang, former graduate student at Northeastern University.

References

Aydilek, A. H., Edil, T. B., and Fox, P. J., 2000, "Consolidation Characteristics of Wastewater Sludge," *Geotechnics of High Water Content Materials, ASTM STP 1374*, T. B. Edil and P. J. Fox, Eds., American Society for Testing and Materials, West Conshohocken, PA, pp. 309-323.

Bishop, D., Johannssen, K., and Kohlhase, S., 1994, "Recent Applications of Modern Geosynthetics for Coastal, Canal and River Works," *Proceedings, 5th Intl. Conf. on Geotextiles, Geomembranes and Related Products*, Singapore, pp. 545-548.

Cooke, D., Welch, E. B., Peterson, S. A., and Newroth, P., 1993, *Restoration and Management of Lakes and Reservoirs*, Lewis Publishers, Tokyo.

Giroud, J. P., 1996, "Granular Filters and Geotextile Filters," *Proceedings, Geofilters '96*, J. Lafleur and A. L. Rollin, Eds., Bitech Publications, Richmond BC, Canada, pp. 565-680.

GSA Resources, Inc. (2001). Personal Communication.

Haggerty, G. M. and Bowman, R. S., 1994, "Sorption of Inorganic Anions by Organo-zeolites," *Environmental Science and Technology*, Vol. 28, pp. 452-458.

Henry, K. S., Collins, C. M., and Racine, C. H., 1995, "Use of Geosynthetics to Prevent White Phosphorus Poisoning of Waterfowl in Eagle River Flats, Alaska," *Proceedings, Geosynthetics '95*, Nashville, TN, Vol. 2, pp. 483-496.

Henry, K. S. and Stark, J. A., 1997, "Geosynthetic Barriers to Prevent Poisoning of Waterfowl," *Proceedings, 14th Intl. Conf. on Soil Mechanics and Foundation Engineering*, Hamburg, A.A. Balkema, pp.1819-1922.

Holtz, R. D, Christopher, B. R., and Berg, R. R., 1997, *Geosynthetic Engineering*, BiTech Publishers, Ltd., Richmond, BC, Canada, 452 pp.

Jacobs, P. H. and Forstner, U., 1999, "Concept of Subaqueous capping of Contaminated Sediments with Active Barrier Systems (ABS) Using Natural and Modified Zeolites," *Water Research*, Vol. 33, No. 9, pp. 2083-2087.

Kirkner, D. J. and Reeves, M., 1988, "Multicomponent Mass Transport with Homogeneous and Heterogeneous Chemical Reactions: Effect of the Chemistry on the Choice of Numerical Algorithm, 1: Theory," *Water Resources Research*, Vol. 24, No. 1, pp. 1719-1729.

Koerner, R. M. and Ko, F. K., 1982, "Laboratory Studies on Long Term Drainage Capability of Geotextiles," *Proceedings, Second International Conference on Geotextiles*, Las Vegas, Nevada, Vol.1, pp. 91-96.

Land and Water, 2001, "The Use of Geotextile Tubes for Spoils Containment," *Land and Water*, Sept./Oct., pp. 41-42.

Langmuir, D., 1987, "Overview of Coupled Processes with Emphasis on Geochemistry," *Coupled Processes Associated with Nuclear Waste Repositories*, Tsang, C. F., Ed., Academic Press, San Diego, Calif.

Leppert, D., 1990, "Heavy Metal Sorption with Clinoptilolite Zeolite: Alternatives for Treating Contaminated Soils and Water, *Journal of Mining Engineering*, Vol. 42, pp. 604-609.

Li, Z., 1998, "Chromate Extraction from Surfactant-Modified Zeolite Surfaces," *Journal of Environmental Quality*, Vol. 27, Nos. 1-2, pp. 240-242.

Li, Z., Burt, T., and Bowman, R. S., 2000, "Sorption of Ionizable Organic Solutes by Surfactant-modified Zeolites," *Environmental Science and Technology*, Vol. 34, pp. 3756-3760.

Mangold, D. C. and Tsang, C., 1991, "A Summary of Subsurface Hydrological and Hydrochemical Models," *Review of Geophysics*, Vol. 29, Feb. 1, pp. 51-79.

Misaelides, P. and Godelitsas, A., 1995, "Removal of Heavy Metals from Aqueous Solutions Using Pretreated Natural Zeolite Material: The Case of Mercury (II)," *Toxicol. Environmental Chemistry*, Vol. 51, pp. 21-30.

Mitchell, J. K., 1993, *Fundamentals of Soil Behavior*, John Wiley and Sons, New York.

Reyes O., Sanchez, E., Pellon, A., Borja, R., Colmenarejo, M. F., Milan, Z., and Cruz, M., 1997, "A Comparative Study of Sand and Natural Zeolite as Filtering Media in Tertiary Treatment of Wastewater from Tourist Areas," *Journal of Environmental Science and Health A*, Vol. 32, Vols. 9-10, pp. 2483-2496.

Savage, C., 1986, "Chicago Area CDF Synthetic Liner and Sand Blanket Experience," in *A Forum to Review Confined Disposal Facilities for Dredged Materials in the Great Lakes*, report of the Dredging Subcommittee to the Great Lakes Water Quality Board, International Joint Commission, Windsor Ontario.

Sakadevan, K. and Bavor, H. J., 1998, "Phosphate Adsorption Characteristics of Soils, Slag and Zeolite to be Used as Substrates in Constructed Wetland Systems," *Water Research*, Vol. 32, No. 2, pp. 393-399.

Selim, H. M., 1992, "Modeling the Transport and Retention of Inorganics in Soils," *Advances in Agronomy*, Vol. 47, pp. 331-384.

Shanableh, A. and Kharabsheh, A., 1996, "Stabilization of Cd, Ni and Pb in Soil using Natural Zeolite," *Journal of Hazardous Materials*, Vol. 45, Nos. 2-3, pp. 207-218.

United States Environmental Protection Agency, 1997, "The Incidence and Severity of Contamination in Surface Waters of the United States," Vol. 1, National Sediment Quality Survey, Rpt. No. EPA 823-R-97-006, Office of Water, URL: http://www.epa.gov/OST/cs/congress.html

United States Environmental Protection Agency, 1996, "Guidance for In-Situ Subaqueous Capping of Contaminated Sediments," Rpt. No. EPA 905-B96-004, Great Lakes National Program Office (GLNPO), URL: http://www.epa.gov/glnpo/sediment/iscmain

United States Patent Office, 2002, "Reactive Geocomposite for Remediating Contaminated Sediments," patent application submitted by U.S. Army Corps of Engineers, pending.

Yeh, G. T. and Tripathi, V. S., 1991, "A Model for Simulating Transport of Reactive Multispecies Components: Model Development and Demonstration," *Water Resources Research*, Vol. 27, No. 12, pp. 3075-3094.

Section III: Monitoring and Performance

Homa J. Lee,[1] Marlene A. Noble,[2] and Jingping Xu[2]

Sediment Transport and Deposition Processes Near Ocean Outfalls in Southern California

Reference: Lee, H. J., Noble, M. A., and Xu, J. P., "**Sediment Transport and Deposition Processes near Ocean Outfalls in Southern California,**" *Contaminated Sediments: Characterization, Evaluation, Mitigation/Restoration, and Management Strategy Performance, ASTM STP 1442,* J. Locat, R. Galvez-Cloutier, R. C. Chaney, and K. R. Demars, Eds., ASTM International, West Conshohocken, PA, 2003.

Abstract: An urbanized coastal ocean that has complex topography and large-scale atmospheric and oceanographic forcing can contain a variety of sediment and pollutant distribution patterns. For example, the central southern California Bight has two large embayments, Santa Monica and San Pedro Bays, that are connected by a short, very narrow shelf off the Palos Verdes peninsula. The complex topography causes quite different oceanographic and sediment distribution patterns in this fairly small region of the coastal ocean. In addition, three sewage outfalls discharge material over the outer shelf. A large suite of sediment cores was obtained and analyzed for contaminants, physical properties, accumulation rates, and grain sizes. Arrays of instrumented moorings that monitor currents, waves, water clarity, water density and collect resuspended materials were deployed. The data and models developed for the Palos Verdes margin suggest that a large reservoir of DDT and its byproducts exists in the coastal ocean sediment and will continue to be exhumed and transported along the shelf for a long time. On the Santa Monica shelf, very large internal waves, or bores, are generated at the shelf break. The near-bottom currents associated with these waves sweep sediment and the associated contaminants from the shelf onto the continental slope. On the San Pedro margin an initial examination of recent data collected in the coastal ocean does not suggest that bacterial contamination on local beaches is primarily caused by transport of material from the adjacent ocean outfall.

Key Words: waste disposal, ocean, sewer outfalls, Southern California, environment, physical oceanography, DDT

---

[1] Civil Engineer, U.S. Geological Survey, 345 Middlefield Road, Menlo Park, CA 94025.
[2] Oceanographer, U.S. Geological Survey, 345 Middlefield Road, Menlo Park, CA 94025.

Introduction

The central Southern California Bight, which is dominated by the Los Angeles metropolis, is a heavily urbanized section of the coastal ocean. More than 12 million people live along the coastal corridor between Point Dume at the northern end of Santa Monica Bay and Newport Beach at the southern end of San Pedro Bay (Fig. 1). The short and very narrow shelf off the Palos Verdes peninsula connects these two large bays. Outfalls that presently discharge treated effluent and other materials into the coastal ocean are located in the middle of Santa Monica Bay, at the eastern end of the Palos Verdes shelf and at the southeastern end of Santa Pedro Bay. Near all three sites, there are disused outfalls that historically discharged sewage and/or effluents with relatively high levels of contamination. Storm-water runoff is discharged into the coastal ocean at numerous sites along this margin. Historically, these several types of discharges have been a source of chemical and biological contaminants into the coastal ocean system.

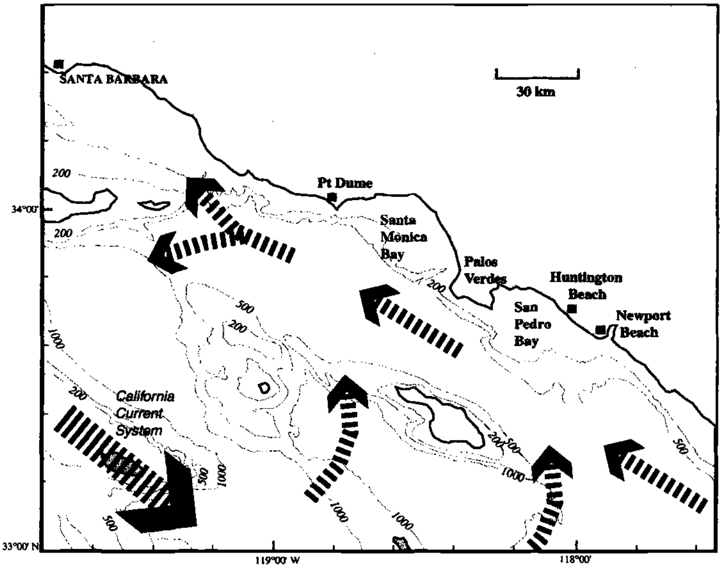

Figure 1 — General circulation patterns in the Southern California Bight (after Hickey 1992).

Once contaminants enter the coastal ocean, they are transported by a variety of processes. Many chemical (e.g. DDT) and some biological contaminants sorb onto fine sediment and are initially deposited near the source. However, this fine sediment and associated contaminants is commonly resuspended by surface waves, internal waves, or coastal currents and transported far from the source regions by currents in the mid to lower portions of the water column. Other effluent material remains suspended in the water column for longer periods of time and is transported by currents near the surface or in the middle of the water column.

Currents over the continental slope and on the eastern margins of the adjacent basins in the bight tend to flow toward the northwest (Fig. 1, Hickey 1992). These northwesterly slope currents are fed by the southeasterly flowing California Current System and by the Undercurrent that flows along the continental slope northwestward from Baja California. Although the transport over the slope is primarily toward the northwest in the Bight, the complex topography in the region is one factor that causes the current, sediment transport and sediment distribution patterns over the adjacent shelf to vary widely. Strong currents transport suspended material primarily to the northwest over the Palos Verdes peninsula. On the Santa Monica Shelf, just 25 km to the northwest, there is no preferred direction for transport in the winter months (Fig. 2). Hence, it is difficult to predict the ultimate fate of contaminates that enter into coastal waters in even this relatively small geographic area.

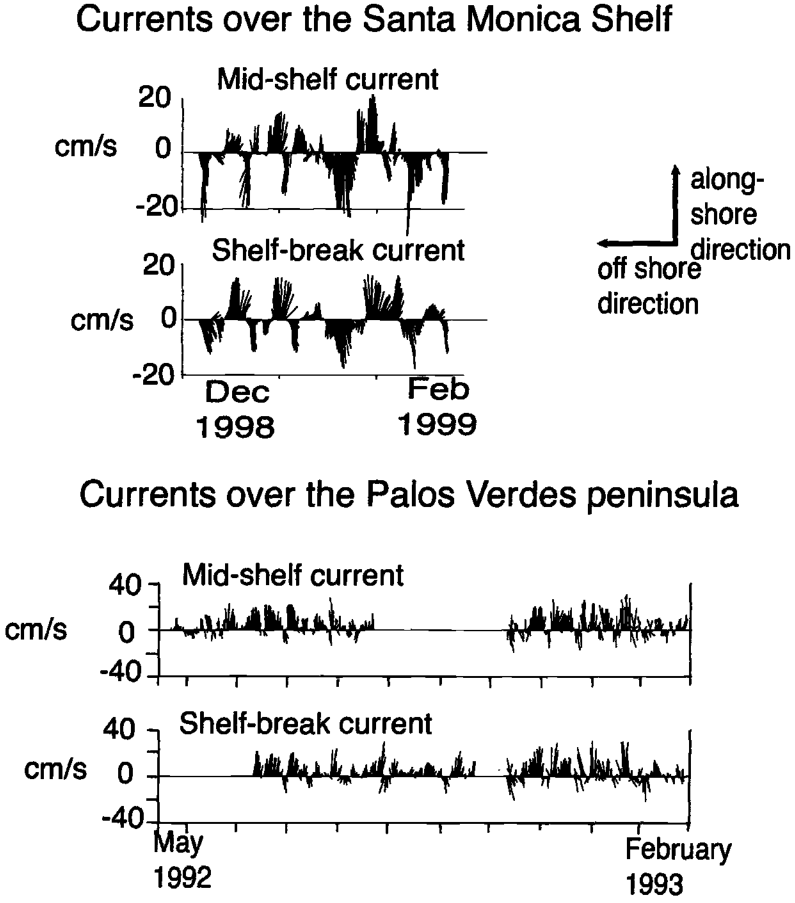

Currents over the Santa Monica Shelf

Currents over the Palos Verdes peninsula

Figure 2 — Mid-water, subtidal currents at two sites in the Southern California Bight.

The U. S. Geological Survey (USGS), together with many allied agencies, began a series of programs in the early 1990s to determine the dominant processes in the Southern California Bight that transport sediment and suspended contaminants. The region of the coast from Santa Monica to San Pedro Bay was selected for initial studies because both the topography and some contaminant distribution patterns, particularly the pattern of DDT distribution, suggested that the transport pathways in these regions were connected (Fig. 3). Three primary studies were located near existing ocean outfalls (Fig. 4). Arrays of instruments measured currents, waves, water clarity, water density, and collected samples of material suspended in the water column. Bottom sediment samples were collected at several hundred sites for physical properties, geochronology, grain size, biological activity and contaminant level analyses. High-resolution seismic and bathymetric surveys (Fig. 5) determined both the seabed morphology and Holocene sediment thickness along much of the margin. Numerical models allowed us to extrapolate the understanding developed locally to larger temporal and spatial regions. These many sources of information have been and are continuing to be jointly analyzed

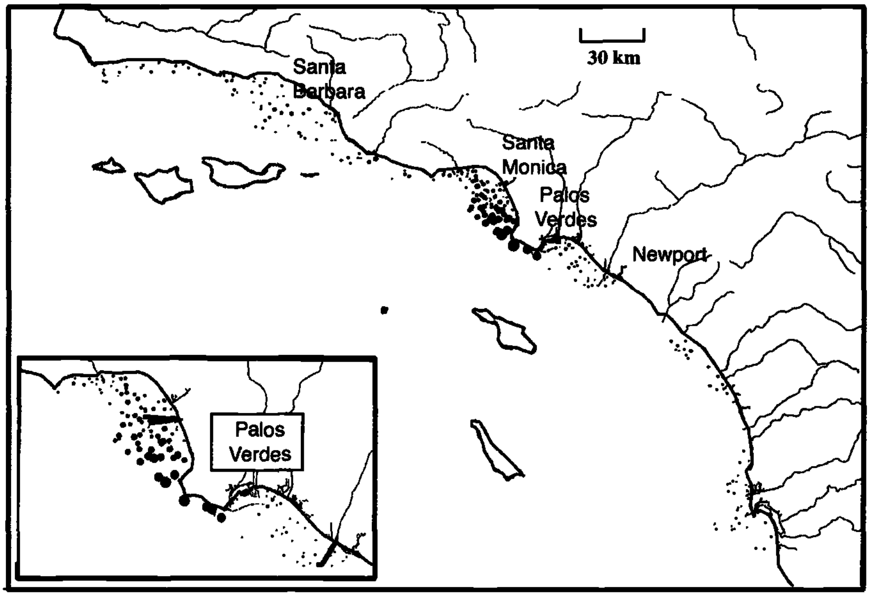

Figure 3 — The distribution of DDT in the sediment of the southern California Bight (modified from Schiff 1998). The major source of DDT in the bight is the ocean outfall off the Palos Verdes Peninsula. This figure shows that sediment from this outfall is being transported far into Santa Monica Bay where it interacts with sediment affected by the City of Los Angeles outfall, which discharges near the center of the bay.

so that a refined understanding of the sediment and contaminant transport and distribution patterns can be developed for this region.

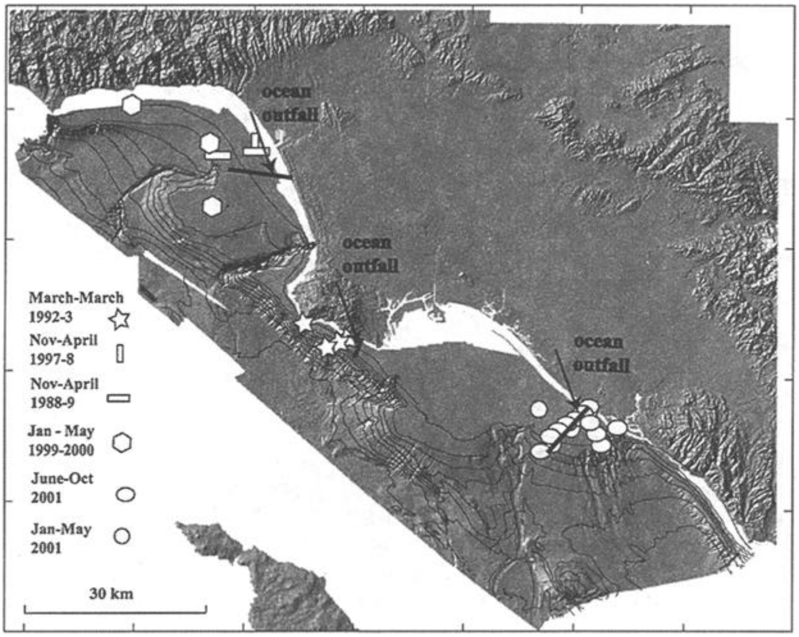

Figure 4 — Locations of major ocean outfalls and USGS moorings, including dates of deployment, in the Southern California Bight. Contour interval for bathymetry is 100 m.

Transport Processes Over the Palos Verdes Margin

In addition to metals and a number of other compounds, DDT and its derivative products, primarily *p,p*'-DDE, are known contaminants in the central southern California Bight (Fig. 3). Much of this DDT entered the coastal waters over the Palos Verdes shelf in effluent from the Whites Point outfall as a result of industrial production at a nearby facility. The contaminant was sorbed onto fine sediment and much of it was deposited near the outfall on the Palos Verdes shelf. Over 9 million cubic meters of effluent-affected sediment lie within a 40 square kilometer area near the outfall (Lee et al. 2002. Fig. 6). This sediment contains over 100 metric tons of *p,p*'-DDE (Lee et al., 2002). DDT is very persistent and accumulates in the marine food chain; at the highest trophic levels it inhibits reproduction in birds that prey on fish and is found at concentrations deemed unsafe for human consumption in white croaker and other endemic fish. Because it sorbs onto fine sediment, normal coastal ocean processes distribute DDT/*p,p*'-DDE over a wide

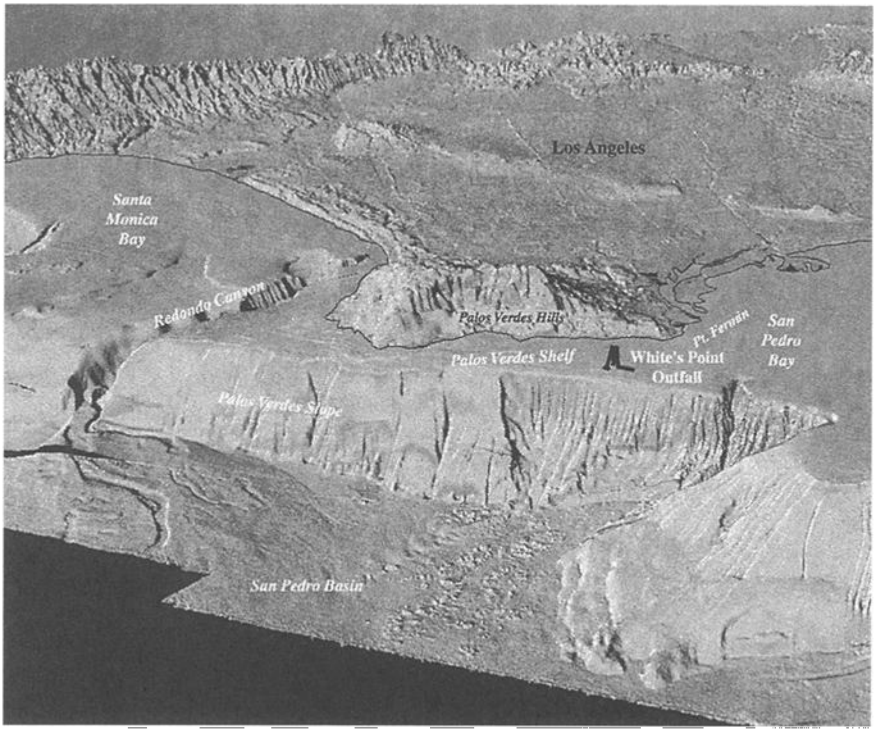

Figure 5 — Oblique view of multibeam bathymetry and a digital elevation model of Santa Monica Bay, the City of Los Angeles, and the Palos Verdes margin (courtesy of J. V. Garner and P. Dartnell, U.S. Geological Survey). Distance across the base of the image is about 40 km.

region. Because the production of DDT in the United States was halted in the early 1970s, sediment deposited since that time has lower levels of contamination than do deeper deposits. Accordingly, the maximum concentrations of DDT/DDE on the Palos Verdes shelf commonly occur 20-30 cm below the seafloor (Fig. 7). However, over many square kilometers, DDT/*p,p'*-DDE is found in significant concentrations (5-10 ppm) near the surface of the seafloor because biological and physical processes transport some of the heavily-contaminated sediment upwards.

The USGS and allied agencies designed a multiyear program in 1992 to determine 1) the amount and distribution of DDT/*p,p'*-DDE on the Palos Verdes margin, 2) the transport processes that move the contaminants, and 3) the fate of the contaminants. Because the highest concentration of DDT/p,p'-DDE is buried, sedimentological studies focused on how animals that live in the sediment transport contaminants upwards. Investigators measured both the physical and biodiffusive rates for contaminant transport. Other investigations focused on how water column processes resuspend and transport contaminants. These results show that contaminants are indeed being mixed to the surface of the seafloor, primarily through biodiffusion. Once they reach the seabed, surface-wave-induced currents resuspend them and subtidal currents transport them.

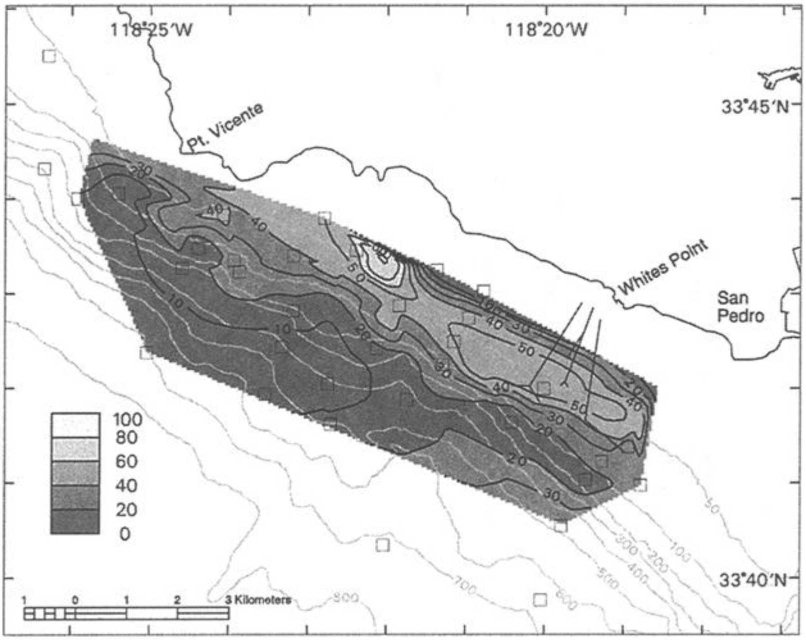

Figure 6 — Thickness (in cm) of effluent-affected sediment on the Palos Verdes margin determined from density logs of core samples. An integration of these data within the context of a GIS yields a total volume of 9 million cubic meters (Lee et al. 2002).

The presence of surface wave currents large enough to resuspend contaminated sediment was not associated with a preferred direction for subtidal currents on the shelf. This is because the currents over the Palos Verdes shelf are not dominated by storms or other wind-driven processes (Noble et al. 2002). The subtidal mid-depth and near-bed currents flow primarily toward the northwest (Fig. 2), so contaminants are preferentially transported toward Santa Monica Bay. In the process, some contaminants move off the shelf, toward the slope, along the northwestern portion of the peninsula. Both the regional DDT distributions (Fig. 3) and the footprint of the contaminated sediment deposit (Fig. 6) on the Palos Verdes margin are consistent with the inferred sediment-transport patterns.

Numerical models that use the sediment properties, the contaminant properties, the sediment-diffusion coefficients, contaminant sorption/desorption coefficients, and measured oceanographic conditions were developed in order to determine the fate of the contaminated deposit over time (Sherwood et al. 2002, Wiberg et al. 2002). These models suggest that shelf sediment is primarily transported toward the northwest. Because transport rates of the fine-grained effluent-affected sediment are greater than transport rates of natural sediment found southeast of the outfalls, erosion is likely to occur on the southeast, or upstream end, of the effluent deposit. Accordingly, highly contaminated sediment is likely to be eroded in that region. Thus, both models and measurements suggest that DDT/*p,p'*-DDE will continue to be exhumed and transported from the Palos Verdes shelf. There is still a large reservoir of DDT/*p,p'*-DDE on the shelf. This reservoir likely will be a potential source of contaminants to the region for a long time, since measurements over the last 18 years suggest that the total amount of DDT/*p,p'*-DDE on the shelf has not decreased substantially (Lee et al. 2002). Hence a quick, natural recovery for the region is unlikely. Studies of remediation methods (e.g. capping) are underway.

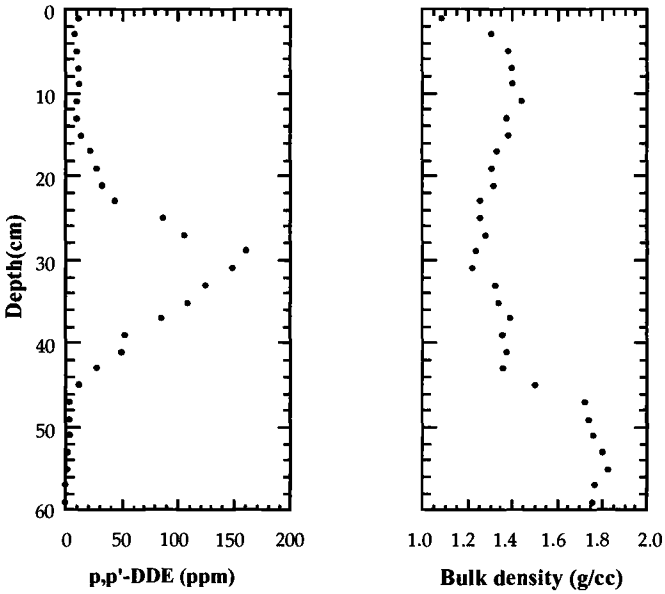

Figure 7 — Profiles of p,p'-DDE concentration and bulk density vs. depth measured on a sediment core obtained at a 60-m-deep site on the Palos Verdes shelf. The profiles show that the most heavily contaminated sediment is buried by several tens of cm although sediment closer to the surface is still contaminated. The density profile shows a low density layer extending to about 45 cm. This layer represents effluent affected sediment deposited afterh the construction of the ocean outfall on the Palos Verdes margin.

Transport Processes Within Santa Monica Bay

The USGS and allied local agencies initiated a multi-year program in 1997 to determine sediment distributions and transport processes in Santa Monica Bay. The sediment-distribution patterns on the Santa Monica shelf are somewhat unusual because sediment grain-size distributions along similar isobaths change markedly over relatively short distances. Fine sediment in the northern part of Santa Monica bay is abundant in the middle and outer shelf regions (40-70 m). The amount of fine sediment at these water depths decreases toward the southeast. In particular, the widest portion of the shelf, which is in the southern part of the bay, has relatively little fine-grained sediment in the 50-70 m depth ranges.

Two sites were occupied in the winter of 1998-1999 at locations just to the northwest of the Los Angeles city sewage outfall in the middle of Santa Monica Bay (Fig. 4). One site was near the shelf break, in 70 m of water; the other site was 2-3 miles inshore of the shelf break, in 35 m. The temporal structure of the subtidal currents in the middle and outer shelf regions was typical of patterns found in other regions of the continental shelf. The currents tended to flow parallel to the isobaths, with a slight tendency for flow toward the southeast (Fig. 2). Hence, one would expect that resuspended material and the associated contaminants would move along the shelf, parallel to the isobaths. However, at sites near the shelf break, resuspended material in the lower portion of the water column is transported offshore because strong currents and large internal depressions of the isotherms are generated over the shelf break during the maximum and falling phases of spring tides. Isotherm deflection amplitudes were 20-40 m in water depths of 70 m. Near-bottom current speeds reached 35-40 cm/s, amplitudes more than sufficient to resuspend and transport fine sediment. The near-bed current direction was exclusively offshore during these events. Hence, any material resuspended and transported by these events leaves the shelf and is deposited on the slope. Bottom stress from these strong shelf-break internal waves was much larger than bottom stress generated by surface waves (Fig. 8). On the mid shelf, bottom stress was caused mainly by surface waves, a situation that is more typical of continental shelf processes (Fig. 8).

The sediment grain-size distribution supports the inference that large internal wave events keep the region swept free of fine material. Photographs from a camera towed across the continental shelf in this area shows that fine material is found over the upper portions of the slope and over the middle region of the shelf. However, cobbles and gravel are the dominant sediment type near the shelf break. The exclusive offshore direction of near-bed transport from these internal oscillations suggests that any contaminants deposited from the nearby outfall will be transported off the shelf and out of the human-impacted coastal system.

Transport processes on the mid-shelf, in 35 m of water, are similar to those found on the Palos Verdes peninsula. The large offshore pulses associated with internal waves are absent. Surface waves primarily resuspend fine materials and any associated contaminants. Presumably, these materials are advected along the shelf by the current field.

Transport Processes Within San Pedro Bay

Coastal contamination issues are highly visible in the southern part of San Pedro Bay. Huntington Beach, which is adjacent to the Orange County Sanitation District ocean outfall, was posted or closed over most the summer of 1999 due to bacterial contamination. Contamination has continued to be a problem in succeeding summers although the source of the contamination was unknown. Several studies examined the likely sources on land, such as broken sewer pipes or discharges from storm-water drains. They also identified a possible new source associated with coastal marshes (Barnett 2000, Grant and Sanders 2000). Another hypothesis is that the beach was contaminated because effluent from the outfall was transported across the shelf by subsurface coastal-ocean transport processes. The primary hypothesis was that strong internal tides could move material from the shelf break to the inner shelf. Once in the nearshore region, the contaminants would then be transported to the beach by cross-shore currents or by entrainment within flows caused by anthropomorphic structures. Other hypotheses were that effluent was transported toward the coast through an adjacent submarine canyon or was mixed to the surface and transported by diurnal wind forcing.

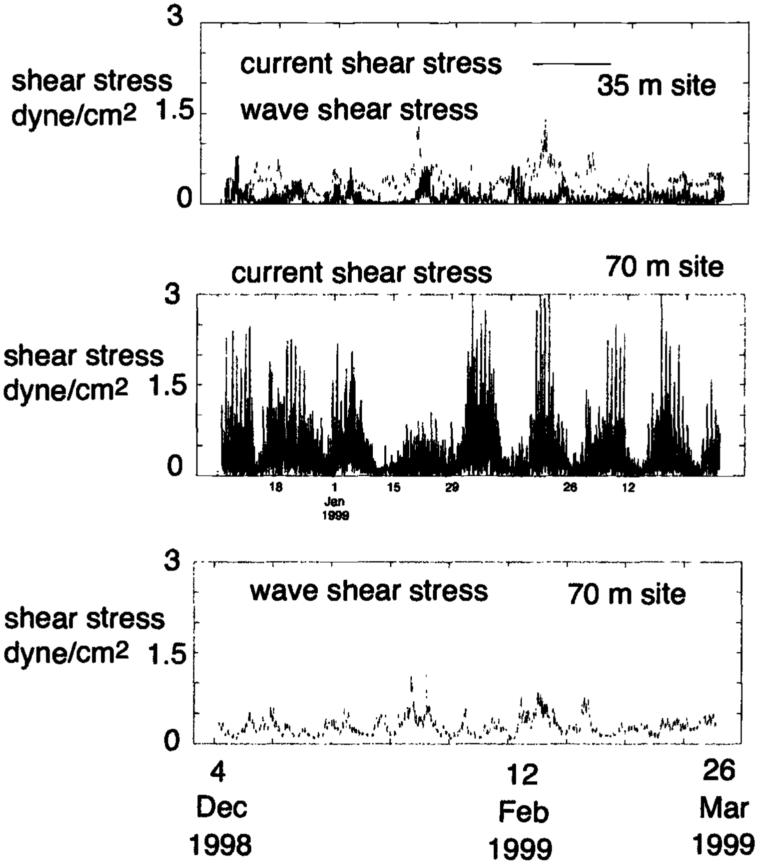

Figure 8 — Bottom stresses generated by surface waves and currents at a mid-shelf (35 m) and a shelf-break (70 m) site. Note that the stresses generated by currents is generally much stronger that stresses generated by surface waves at the shelf-break site.

In the summer of 2001, the USGS and allied agencies deployed arrays of instruments at more than 15 sites on the 5-6 mile wide section of the continental shelf at the southern end of San Pedro Bay. The primary purpose of the arrays was to determine whether there are mid-water cross-shelf transport processes that move contaminants, possibly from the outfall located near the shelf break, onshore to local beaches during stratified summer conditions.

Initial results from this program suggest that although coastal ocean processes can move water and suspended materials 5- 6 km across the shelf, there is no connection between coastal ocean processes and bacterial contamination on the beaches. In particular, internal tides can move water with the same temperature as the effluent plume (12°) toward the inner shelf (Fig. 9). However, no beach pollution events were associated with this process in the entire summer of 2001. Six hydrographic surveys that mapped the plume during the times when the beach was contaminated also showed that there was always a spatial gap between the plume and the contaminated beaches. The plume was seen to enter the submarine canyon with low bacterial levels, but this was not associated with beach contamination events.

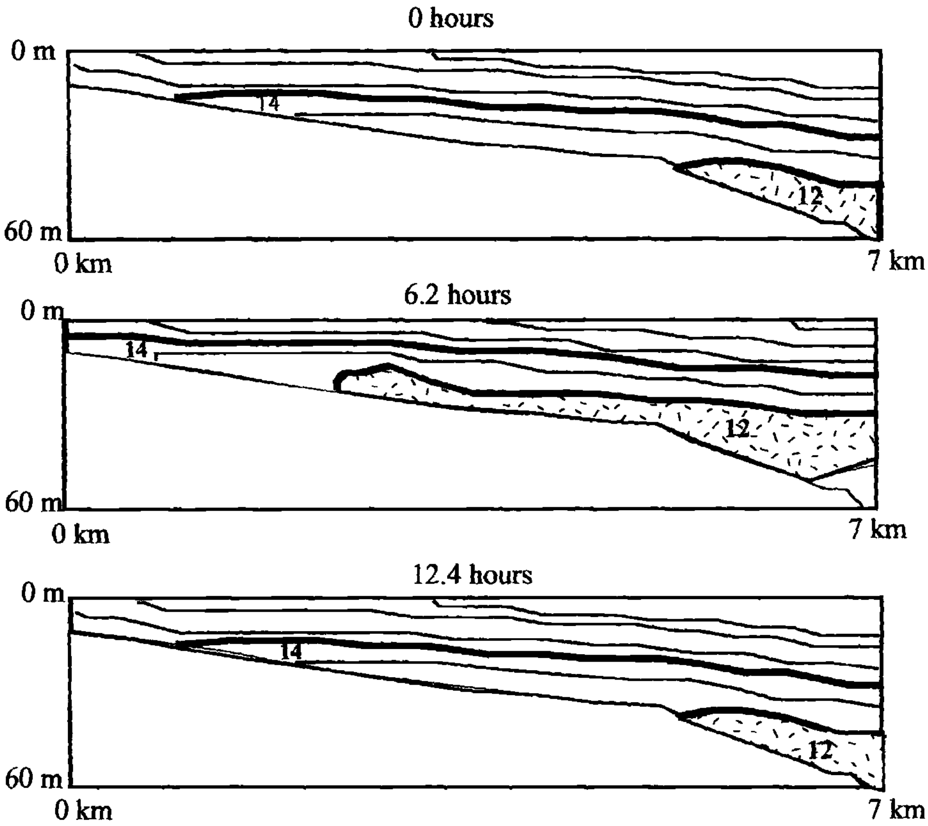
0 hours

6.2 hours

12.4 hours

Figure 9 — Transport of cooler water on and off the shelf due to the internal tides. Water cooler than 12° is the same temperature as the effluent plume.

Conclusions

Clearly, even in this relatively small region of the western U.S. continental margin (alongshore extent is less than 100 km), many processes in the coastal ocean move fine sediment, associated contaminants, and suspended contaminates through the local coastal system. In regions with complex topography, the local processes may change markedly over small spatial scales. Surface waves dominate resuspension events on the Palos Verdes peninsula and in the middle of the Santa Monica shelf. Yet, internal waves are more likely to resuspend material along the shelf break near the middle of Santa Monica Bay. These processes transport material across and off, rather than along the shelf. Preliminary evidence suggests that internal wave resuspension is dominant only over certain regions of the shelf break in Santa Monica and San Pedro Bays. However, if those regions are near a sewage outfall, the presumed direction of transport pathways may change markedly. We would expect that the transport of contaminants and other material that remain suspended in the water column will also be affected by local changes in transport associated with rapid changes in the shelf topography. The large data set collected recently in the southern part of San Pedro Bay does show that there are cross-shelf transport processes that advect suspended material. However, in this region these processes are seldom strong enough to bring contaminants to the local beaches. Developing an understanding of the many coastal ocean processes that transport suspended and resuspended material in the coastal ocean is essential before realistic predictive models can be developed to help manage the coastal ocean ecosystem.

Acknowledgments

Many agencies and institutions participated in portions of the above studies. The authors would like to thank the City and County of Los Angeles, the National Oceanic and Atmospheric Administration, Orange County Sanitation District, the Southern California Coastal Water Research Project, and individuals at the Naval Postgraduate School, University of Delaware, University of Southern California, Skidaway Institute of Oceanography, Scripps Institution of Oceanography and SAIC.

References

Barnett, A. M. , 2000, "Huntington Beach Closure: Relationships between High Counts of Bacteria on Huntington Beachs and Potential Sources." Report prepared for the Orange County Sanitation District.

Grant, S. B., and Sanders, B. F., 2000, "Tidal Transport of Bacteria Between the Talbert Watershed and the Ocean." Interim Report 1 for the UCI Coastal Runoff Study (CRIS). Report prepared for the National Water Research Institute, County of Orange, Cities of Huntington Beach, Fountain Valley, Coast Mesa, Santa Ana, Newport Beach.

Hickey, B. M., 1992, "Circulation Over the Santa Monica-San Pedro Basin and Shelf," *Prog. Oceanogr.* Vol. 30, pp. 37-115.

Lee, H.J., Sherwood, C. R., Drake, D. E., Edwards, B. D., Wong, F., and Hamer, M., 2002, "Spatial and Temporal Distribution of Contaminated, Effluent-Affected

Sediment on the Palos Verdes Margin, Southern California," *Continental Shelf Research*, Vol. 22, Nos. 6-7, pp. 859-880.

Noble, M. A., Ryan, H. F. and Wiberg,, P. L. , 2002, "The Dynamics of Subtidal Poleward Flows over a Narrow Continental Shelf," Palos Verdes CA. *Continental Shelf Research,* Vol. 22, Nos. 6-7, pp. 923-944.

Schiff, K., 1998, "Sediment Chemistry on the Mainland Shelf of the Southern California Bight." Southern California Coastal Water Research Project 1997-98 Annual Report, pp. 76-88.

Sherwood, C. R., Drake, D. E., Wiberg, P. L., Wheatcroft, R. A., 2002, "Prediction of the Fate of *p,p'*-DDE in Sediment on the Palos Verdes Shelf, California, USA," *Continental Shelf Research,* Vol. 22, Nos. 6-7, pp. 1025-1058.

Wiberg, P. L., Drake, D. E. , Harris, C. K., and Noble, M. A. , 2002, "Sediment Transport on the Palos Verdes Shelf over Seasonal to Decadal Time Scales," *Continental Shelf Research,* Vol. 22, Nos. 6-7, pp. 923-944.

Patrick J. Fox[1]

Numerical Model for Contaminant Transport in Consolidating Sediments

Reference: Fox, P. J., "**Numerical Model for Contaminant Transport in Consolidating Sediments,**" *Contaminated Sediments: Characterization, Evaluation, Mitigation/Restoration, and Management Strategy Performance, ASTM STP 1442*, J. Locat, R. Galvez-Cloutier, R. C. Chaney, and K. R. Demars, Eds., ASTM International, West Conshohocken, PA, 2003.

Abstract: A numerical model for coupled, one-dimensional, large strain consolidation and contaminant transport, called CCT1, is presented. The large strain consolidation algorithm includes all the capabilities of a previous code, CS2. The contaminant transport algorithm includes advection, dispersion, and linear equilibrium sorption with a spatially varying distribution coefficient. Advection-dispersion transport is consistent with spatial and temporal variations of porosity and seepage velocity in the consolidating layer. The key to the transport model is the definition of two Lagrangian columns of elements that follow the motions of the fluid and solid phases separately. Verification checks of CCT1 show excellent agreement with analytical solutions for classical transport problems involving advection, diffusion, dispersion, and sorption in rigid porous media. The performance of CCT1 is illustrated for an example problem involving consolidation-induced transport of a dilute contaminant species in a soft sediment layer.

Keywords: consolidation, contaminant transport, large strain, advection, dispersion, sorption, numerical model

Introduction

Classical solutions for contaminant transport through porous media (Ogata 1970, Bear 1972, Freeze and Cherry 1979) are derived strictly for rigid media in which no deformation occurs during the transport process. This assumption is fully acceptable for many cases involving flow through natural groundwater systems and waste containment facilities because applied loads are small to nonexistent or the media has low compressibility. There are, however, cases in which significant volumetric strains may occur during the transport process. Such cases include disposal of contaminated slurry wastes, simultaneous consolidation and mass transport through clay liners, consolidation of contaminated clay deposits, and the consolidation of contaminated sediments due to

---

[1] Associate Professor, Department of Civil and Environmental Engineering and Geodetic Science, The Ohio State University, Columbus, Ohio, USA.

continuing sedimentation or the application of a subaqueous soil capping layer. Although two published works provide theoretical discussion and analyses of the coupled problem (Potter et al. 1994, Smith 2000), a contaminant transport model has yet to be developed for a porous medium that has general constitutive properties and undergoes significant volumetric strain.

This paper presents a numerical model for coupled, one-dimensional, nonlinear, large strain consolidation and contaminant transport called CCT1 (Consolidation and Contaminant Transport 1). CCT1 is based on the piecewise-linear approach (Yong et al. 1983, Fox and Berles 1997, Fox 2000, Fox et al. 2002) in which all variables pertaining to problem geometry, material properties, fluid flow, and effective stress are updated at each time step with respect to a fixed coordinate system. CCT1 was adapted from a previous code, CS2 (Fox and Berles 1997), which simulates vertical consolidation of a soil layer subjected to surcharge loading. The development of CCT1 is first presented, followed by verification checks and an example problem illustrating the performance of the model for contaminant transport within a consolidating sediment layer.

Model Description

Geometry

A saturated soil layer of initial height H_o contains an arbitrary distribution of a single dilute contaminant species. The soil layer is treated as one-dimensional and is represented using two Lagrangian columns of elements—one for the solid skeleton (including voids) and one for the fluid moving through the skeleton. Solid and fluid elements move independently except that they are coupled via values of solid element-to-solid element relative fluid velocity that govern the movement of each system. The Lagrangian analysis framework follows the motion of both fluid and solid phases throughout a simulation.

The initial geometry of the soil layer, prior to the application of a vertical stress increment (time $t < 0$), is shown in Figure 1(a). Vertical position coordinate z and element coordinate j are defined as positive upward from a fixed datum at the bottom of the layer. Initially, both fluid and solid phases are represented as a column of R_j elements. Each j^{th} element has unit cross sectional area, initial height L_o, a central node located at initial elevation $z_{o,j}$, and an initial void ratio $e_{o,j}$. Fluid in the j^{th} element has initial volume $V_{fo,j} = L_o e_{o,j}/(1+e_{o,j})$, initial dissolved contaminant concentration $c_{o,j}$ [mass contaminant/volume fluid], and initial dissolved contaminant mass $C_{fo,j} = c_{o,j}V_{fo,j}$. The initial concentration of sorbed contaminant on the solids of each element is assumed to be in equilibrium with the corresponding fluid concentration. Top and bottom boundaries of the column can be specified as drained or impermeable and, if drained, are assigned individual constant total head values, h_t and h_b, taken with respect to the datum. Constant contaminant concentrations, c_t and c_b, are likewise assigned to the top and bottom boundaries. The distribution of $e_{o,j}$ can be specified by the user or calculated by CCT1 (normally consolidated case only) using an iterative procedure such that it is consistent with the initial overburden effective stress q_o, the compressibility and self-

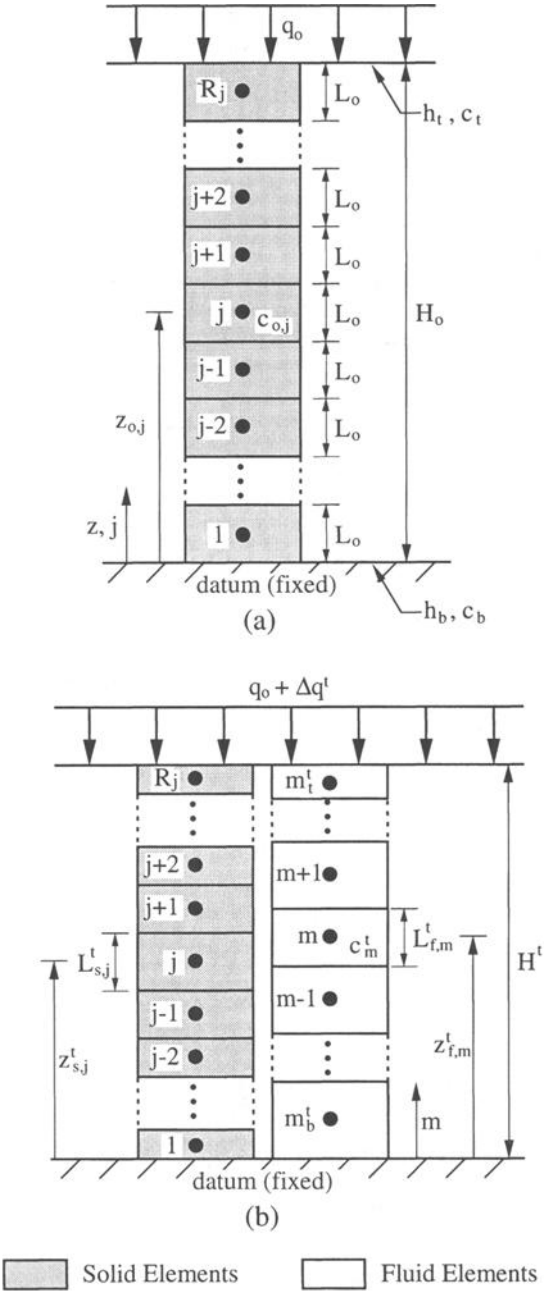

Figure 1 - *Geometry for CCT1: (a) initial configuration ($t < 0$), and (b) after application of vertical stress increment ($t > 0$).*

weight of the soil, and seepage forces due to steady flow across the layer (if $h_t \neq h_b$).

A time-dependent vertical effective stress increment $\Delta q'$ is applied to the column beginning at time $t = 0$ and moves with the upper boundary thereafter. Excess pore pressures created as a result of the stress increment cause fluid flow from the interior of the soil mass to all drainage boundaries. Soil deformation occurs in response to the net fluid outflow from each solid element. Contaminant transport occurs by advection and dispersion in the fluid phase, and sorption onto moving solid elements. The configuration of the system at some later time t is shown in Figure 1(b). Fluid elements have become disconnected from their original solid elements and move in response to the local seepage velocity field. Fluid elements are numbered according to a new coordinate m defined as positive upward from the datum. The height of the layer is H^t, the height of the j^{th} solid element is $L^t_{s,j}$, and the height of the m^{th} fluid element is $L^t_{f,m}$. Solid elements and fluid elements have node elevations $z^t_{s,j}$ and $z^t_{f,m}$, respectively, and are updated at each time step. Fluid elements have concentration c^t_m and dissolved contaminant mass $C^t_{f,m}$. The heights of fluid elements increase as the porosity of the associated solid elements decreases. Fluid elements move through, and possibly out of, the consolidating layer in response to boundary fluid outflow from solids compression and any external hydraulic gradient across the layer (if $h_t \neq h_b$). Thus, unlike the number of solid elements which is always constant at R_j, the number of fluid elements may decrease/increase during the compression/swelling process. The top and bottom fluid elements at any given time are m^t_t and m^t_b, respectively. The volume of solids within each solid element is invariant throughout the consolidation process (Fox and Berles 1997). The volume of fluid within each fluid element $V^t_{f,m}$ is also invariant unless the element is adjacent to a drainage boundary, in which case the element will gain or loose fluid in response to the flow across the boundary. A fluid element is eliminated from the top or bottom of the fluid column when its volume is fully depleted at an outflow drainage boundary. Likewise, a new fluid element is created at an inflow drainage boundary when the existing boundary fluid element is filled to capacity. The capacity of new fluid elements added at the bottom of the fluid column is $V_{fo,1}$ and the capacity of new fluid elements added at the top of the fluid column is $V_{fo,Rj}$.

Constitutive Relationships

Constitutive relationships for the compressible layer, shown in Figure 2, are specified using discrete data points. The compressibility curve (Figure 2a) is defined by $R_s \geq 2$ pairs of corresponding vertical effective stress $\hat{\sigma}'$ and void ratio $\hat{e}$. The hydraulic conductivity relationship (Figure 2b) is defined by $R_t \geq 2$ pairs of corresponding void ratio $\bar{e}$ and vertical hydraulic conductivity $\bar{k}$. A solid element becomes overconsolidated if the vertical effective stress decreases below the preconsolidation stress $\sigma''_{p,j}$ (*i.e.*, maximum past vertical effective stress) for the element. In this case, unloading and reloading follow an identical path defined by $\sigma''_{p,j}$, the corresponding preconsolidation

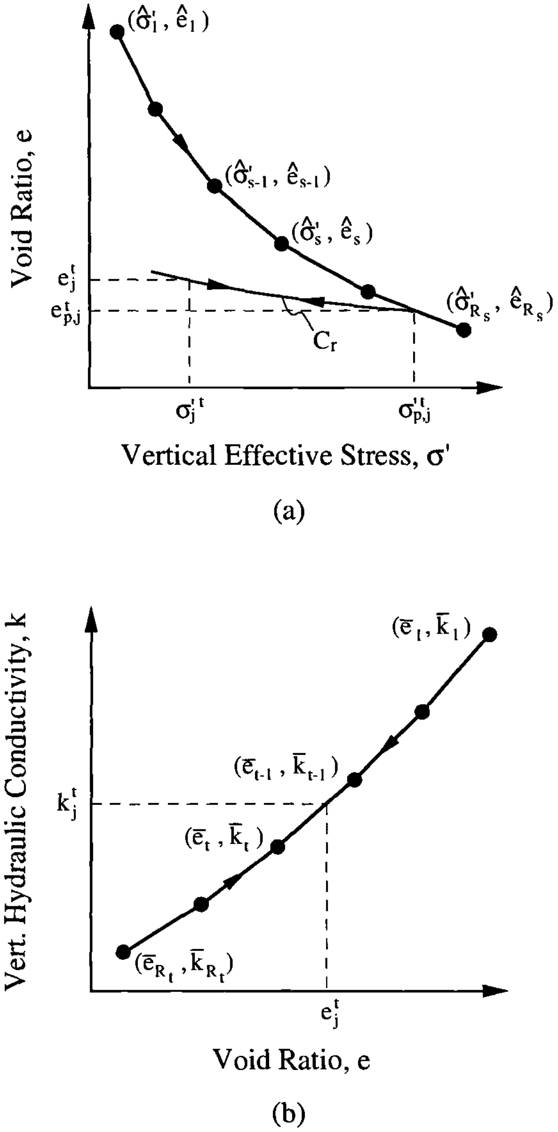

Figure 2 - *Soil constitutive relationships: (a) compressibility, and (b) hydraulic conductivity.*

void ratio $e_{p,j}^t$, and a constant recompression index $C_r = \dfrac{\Delta e}{\Delta \log \sigma'}$. CCT1 uses the same hydraulic conductivity relationship for normally consolidated and overconsolidated conditions, which is consistent with the findings of Al-Tabbaa and Wood (1987) and Nagaraj et al. (1994).

Aside from unload/reload effects, a one-to-one correspondence is assumed for each constitutive relationship in Figure 2. Thus, CCT1 does not account for the effects of strain rate, secondary compression, or aging on the compressibility or hydraulic conductivity of the soil. The constitutive relationships can, however, take essentially any desired form by choosing the appropriate number of data points.

Stress, Pore Pressure, Flow, and Settlement

CCT1 calculates stresses, pore pressure, fluid flow, and settlement in the same fashion as does CS2. Fox and Berles (1997) presented detailed information on these aspects and only a brief review is provided here. The vertical total stress at node j, σ_j^t, is computed from the overburden stress on the layer and the self-weight of overlying elements as,

$$\sigma_j^t = q_o + \Delta q^t + (h_t - H^t)\gamma_w + \frac{L_{s,j}^t \gamma_j^t}{2} + \sum_{i=j+1}^{R_j} L_{s,i}^t \gamma_i^t \qquad j = 1, 2, \ldots, R_j \qquad (1)$$

where γ_j^t is the saturated unit weight of solid element j, e_j^t is the corresponding void ratio, and γ_w is the unit weight of water (constant). The specific gravity of solids G_s is constant for the soil column and e_j^t is taken as constant within each solid element for any given time increment.

Vertical effective stress $\sigma_j'^t$ is computed from void ratio e_j^t by interpolating between data points in Figure 2(a) if $e_j^t \le e_{p,j}^t$ or using the recompression curve if $e_j^t > e_{p,j}^t$. Vertical hydraulic conductivity k_j^t is computed from e_j^t by interpolating between data points in Figure 2(b). The pore pressure u_j^t is the difference between total and effective stresses and the relative discharge velocity (positive upward) $v_{rf,j}^t$ between solid element nodes j and $j+1$ (Figure 3a) is,

$$v_{rf,j}^t = -k_{s,j}^t \frac{h_{j+1}^t - h_j^t}{z_{s,j+1}^t - z_{s,j}^t} \qquad j = 1, 2, \ldots, R_j\text{-}1 \qquad (2)$$

where the total head h_j^t and the equivalent series hydraulic conductivity $k_{s,j}^t$ are,

$$h_j^t = z_{s,j}^t + \frac{u_j^t}{\gamma_w} \qquad j = 1, 2, \ldots, R_j \qquad (3)$$

$$k_{s,j}^t = \frac{k_{j+1}^t k_j^t (L_{s,j+1}^t + L_{s,j}^t)}{L_{s,j+1}^t k_j^t + L_{s,j}^t k_{j+1}^t} \qquad j = 1, 2, \ldots, R_j\text{-}1 \qquad (4)$$

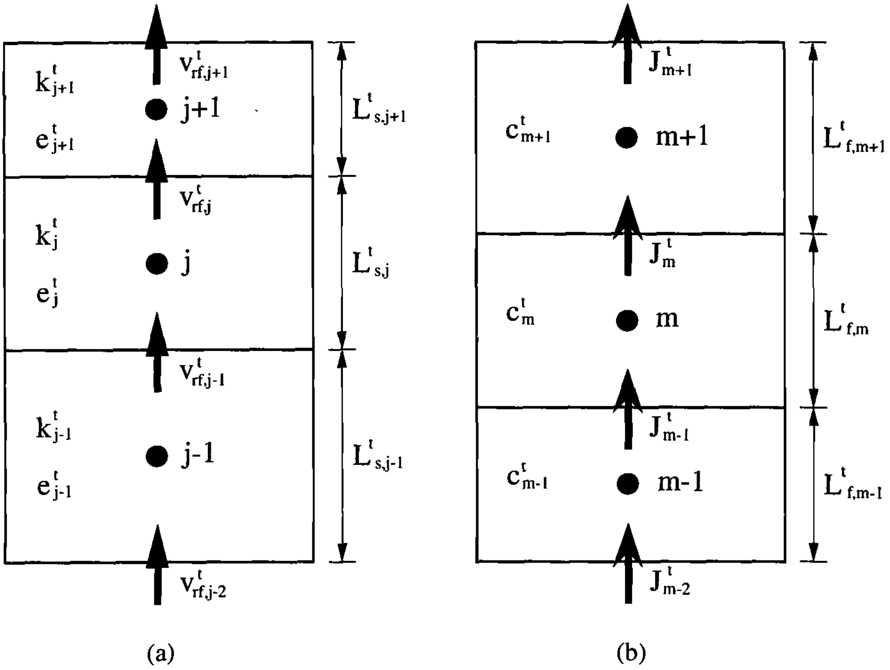

Figure 3 - *(a) Fluid flow between solid elements, and (b) dispersion mass flux between fluid elements.*

Once the relative discharge velocities are known, a new height is computed for each solid element from the net fluid outflow over time increment Δt,

$$L_{s,j}^{t+\Delta t} = L_{s,j}^{t} - (v_{rf,j}^{t} - v_{rf,j-1}^{t})\Delta t \qquad j = 1, 2, \ldots, R_j \tag{5}$$

where Δt is calculated based on numerical stability and accuracy constraints (Fox and Berles 1997). New void ratios, layer height, settlement, and average degree of consolidation are, respectively,

$$e_j^{t+\Delta t} = \frac{L_{s,j}^{t+\Delta t}(1 + e_{o,j})}{L_o} - 1 \qquad j = 1, 2, \ldots, R_j \tag{6}$$

$$H^{t+\Delta t} = \sum_{j=1}^{R_j} L_{s,j}^{t+\Delta t} \tag{7}$$

$$S^{t+\Delta t} = H_o - H^{t+\Delta t} \tag{8}$$

$$U_{avg}^{t+\Delta t} = \frac{S^{t+\Delta t}}{S_t} \tag{9}$$

where S_t is the total settlement at the end of consolidation. Fox and Berles (1997) and Fox (2000) show that numerical solutions obtained using the above method are essentially indistinguishable from analytical and numerical solutions obtained using material coordinates (Gibson et al. 1967, Lee and Sills 1979, Schiffman et al. 1984).

Contaminant Transport

Mass transport of contaminant occurs by advection of fluid elements, dispersion between fluid elements, and sorption onto solid elements that are also moving in response to the consolidation process. The Lagrangian framework of CCT1 automatically accounts for advection transport in the fluid phase and sorption transport in the solid phase. Dispersion transport is calculated between contiguous fluid elements with variable porosity and seepage velocity in the associated solid elements taken into account. The dispersion mass flux between fluid element nodes m and m+1 is (Figure 3b),

$$J_m^t = -D_{Ls,m}^t \frac{c_{m+1}^t - c_m^t}{z_{f,m+1}^t - z_{f,m}^t} \qquad m = m_b^t,\ m_b^t+1, \ldots,\ m_t^t - 1 \tag{10}$$

where the equivalent series longitudinal hydrodynamic dispersion coefficient $D_{Ls,m}^t$ is,

$$D_{Ls,m}^t = \frac{z_{f,m+1}^t - z_{f,m}^t}{N} \qquad m = m_b^t,\ m_b^t+1, \ldots,\ m_t^t - 1 \tag{11}$$

The value of N depends on the relative positions of fluid elements m and m+1 and the associated solid elements. Solid elements that contribute to the value of N satisfy one of the following four possible cases,

Case 1: $z_{s,j}^t + \frac{L_{s,j}^t}{2} \geq z_{f,m+1}^t$ and $z_{s,j}^t - \frac{L_{s,j}^t}{2} \leq z_{f,m}^t$

$$N = \frac{z_{f,m+1}^t - z_{f,m}^t}{n_{eff,j}^t \left(D^* + \alpha_L |v_s|\right)} \tag{12}$$

$$v_s = \frac{v^t_{rf,j-1}}{n^t_{eff,j}} + \frac{v^t_{rf,j} - v^t_{rf,j-1}}{n^t_{eff,j} L^t_{s,j}} \left(\frac{z^t_{f,m+1} + z^t_{f,m}}{2} - z^t_{s,j} + \frac{L^t_{s,j}}{2} \right) \tag{13}$$

Case 2: $z^t_{s,j} + \frac{L^t_{s,j}}{2} < z^t_{f,m+1}$ and $z^t_{s,j} - \frac{L^t_{s,j}}{2} > z^t_{f,m}$

$$N = \sum \frac{L^t_{s,j}}{n^t_{eff,j}\left(D^* + \alpha_L |v_s|\right)} \tag{14}$$

$$v_s = \frac{v^t_{rf,j} + v^t_{rf,j-1}}{2 n^t_{eff,j}} \tag{15}$$

Case 3: $z^t_{s,j} + \frac{L^t_{s,j}}{2} \le z^t_{f,m+1}$ and $z^t_{s,j} + \frac{L^t_{s,j}}{2} \ge z^t_{f,m}$ and $z^t_{s,j} - \frac{L^t_{s,j}}{2} \le z^t_{f,m}$

$$N = \sum \frac{z^t_{s,j} + \frac{L^t_{s,j}}{2} - z^t_{f,m}}{n^t_{eff,j}\left(D^* + \alpha_L |v_s|\right)} \tag{16}$$

$$v_s = \frac{1}{2}\left(\frac{v^t_{rf,j}}{n^t_{eff,j}} + \frac{v^t_{rf,j-1}}{n^t_{eff,j}} + \frac{v^t_{rf,j} - v^t_{rf,j-1}}{n^t_{eff,j} L^t_{s,j}} \left(z^t_{f,m} - z^t_{s,j} + \frac{L^t_{s,j}}{2} \right) \right) \tag{17}$$

Case 4: $z^t_{s,j} + \frac{L^t_{s,j}}{2} \ge z^t_{f,m+1}$ and $z^t_{s,j} - \frac{L^t_{s,j}}{2} \le z^t_{f,m+1}$ and $z^t_{s,j} - \frac{L^t_{s,j}}{2} \ge z^t_{f,m}$

$$N = \sum \frac{z^t_{f,m+1} - z^t_{s,j} + \frac{L^t_{s,j}}{2}}{n^t_{eff,j}\left(D^* + \alpha_L |v_s|\right)} \tag{18}$$

$$v_s = \frac{v^t_{rf,j-1}}{n^t_{eff,j}} + \frac{v^t_{rf,j} - v^t_{rf,j-1}}{2 n^t_{eff,j} L^t_{s,j}} \left(z^t_{f,m+1} - z^t_{s,j} + \frac{L^t_{s,j}}{2} \right) \tag{19}$$

where $n^t_{eff,j}$ $\left(= \zeta \frac{e^t_j}{1 + e^t_j} \right)$ is the effective porosity of the j^{th} solid element, ζ is a constant (≤ 1), D^* ($= \tau D_o$) is the effective diffusion coefficient, τ = apparent tortuosity factor, D_o = free-solution diffusion coefficient, α_L = longitudinal dispersivity of the medium, v_s = equivalent seepage velocity between nodes m and m+1, and the vertical bars signify absolute value. Although ζ, α_L, and D^* may possibly change with media porosity during consolidation, these values are taken as constants in CCT1. The latter assumption is supported by test data of Shackelford and Daniel (1991) for compacted clays.

Mass Balance and Sorption-Desorption

The updated total contaminant mass in the m^{th} fluid element $C^{t+\Delta t}_{f,m}$ is computed as,

$$C^{t+\Delta t}_{f,m} = C^t_{f,m} - (J^t_m + J^t_{m-1})\Delta t \qquad m = m^t_b+1,\ m^t_b+2,\ \ldots,\ m^t_t-1 \tag{20}$$

where the time increment Δt is limited by numerical stability constraints for dispersion (Zhu and Fox 2000). Corresponding mass balance expressions for boundary fluid elements require an additional term to account for advective transport across the boundary. CCT1 accounts for sorption-desorption reactions by defining R_k subcells within each solid element (Figure 4). The elevation of the node for subcell k within solid element j is $z_{sc,jk}^t$. The m^{th} fluid element exchanges contaminant mass with the solids of any subcell jk if the node of the subcell lies within the boundaries of the fluid element (*i.e.*, $z_{sc,jk}^t > z_{f,m}^t - \frac{L_{f,m}^t}{2}$ and $z_{sc,jk}^t \le z_{f,m}^t + \frac{L_{f,m}^t}{2}$). The total mass of sorbed contaminant on the solids associated with the m^{th} fluid element is,

$$C_{s,m}^{t+\Delta t} = \sum_{j=1}^{R_j}\sum_{k=1}^{R_k} \frac{s_{jk}^t \gamma_{d,j}^t L_{s,j}^t}{gR_k} \qquad m = m_b^t,\ m_b^t+1, \ldots, m_t^t \tag{21}$$

where s_{jk}^t is the sorbed contaminant mass per mass of solid for subcell jk, $\gamma_{d,j}^t$ is the dry unit weight of solid element j, and g is the gravitational constant. The total contaminant mass in the fluid and solid phases associated with the m^{th} fluid element $C_m^{t+\Delta t}$ is,

$$C_m^{t+\Delta t} = C_{s,m}^{t+\Delta t} + C_{f,m}^{t+\Delta t} \qquad m = m_b^{t+\Delta t},\ m_b^{t+\Delta t}+1, \ldots, m_t^{t+\Delta t} \tag{22}$$

CCT1 then calculates new fluid element concentrations assuming linear equilibrium sorption between fluid and solid phases,

$$c_m^{t+\Delta t} = \frac{C_m^{t+\Delta t}}{V_{f,m}^{t+\Delta t} + \sum_{j=1}^{R_j}\sum_{k=1}^{R_k} \frac{K_{d,jk}\gamma_{d,j}^{t+\Delta t} L_{s,j}^{t+\Delta t}}{gR_k}} \qquad m = m_b^{t+\Delta t},\ m_b^{t+\Delta t}+1, \ldots, m_t^{t+\Delta t} \tag{23}$$

where $K_{d,jk}$ is the equilibrium distribution coefficient (sorbed concentration/aqueous concentration) for subcell jk. CCT1 treats K_d as a spatially varying parameter to allow for a non-uniform distribution of soil sorption characteristics, such as organic content. The sorbed concentration on the subcells associated with the m^{th} fluid element is then,

$$s_{jk}^{t+\Delta t} = K_{d,jk} c_m^{t+\Delta t} \qquad m = m_b^{t+\Delta t},\ m_b^{t+\Delta t}+1, \ldots, m_t^{t+\Delta t} \tag{24}$$

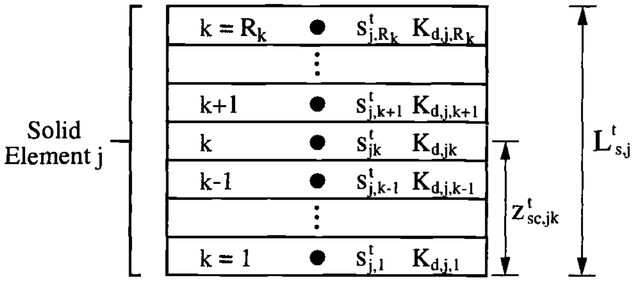

Figure 4 - *Sorption subcells for solid element j.*

CCT1 assumes instantaneous linear reversible sorption for simplicity, although it has been demonstrated for aquifers that, when a system is perturbed by a sudden increase in advection rate, nonequilibrium sorption effects must be taken into account (Rabideau and Miller 1994, Kong and Harmon 1996). Such effects may be important during the early stages of consolidation when the advection rate may be high in comparison to the rate of contaminant sorption/desorption in the system.

Model Performance

CCT1 and CS2 produce identical results for large strain consolidation problems without contaminant transport. The performance of CCT1 was evaluated for several classical transport problems without consolidation ($\Delta q = 0$). Consider an initially uncontaminated stiff soil layer with $H_o = 6$ m, $G_s = 1$, $e = 0.8$, $\zeta = 1$, $k = 2 \times 10^{-8}$ m/s, and drained top and bottom boundaries. At $t = 0$, the concentration of a dilute contaminant at the top boundary is increased to c_t and held constant thereafter. The concentration at the bottom boundary is maintained at zero. Five simulations were performed with CCT1 ($R_j = 100$, $R_k = 4$) corresponding to the following cases: 1) advection, 2) diffusion, 3) advection + diffusion, 4) advection + dispersion, and 5) advection + dispersion + sorption. The transport parameters for these simulations are provided in Table 1. The retardation factor $R_f \left(= 1 + \frac{\gamma_d K_d}{g n_{eff}} \right)$ for the final simulation is 1.625. Each simulation was terminated at $t = 6 \times 10^8$ s. Contaminant concentration ratio (c/c_t) profiles are plotted vs. elevation z along with corresponding analytical solutions for transport in a semi-infinite domain (Domenico and Schwartz 1990) in Figure 5.

The Lagrangian formulation of CCT1 reproduces exactly the simple case of plug flow advection (Simulation 1). CCT1 creates new fluid elements with $c = c_t$ as fluid enters the layer at the top boundary. These elements move downward at the constant seepage velocity and, in the absence of dispersion and sorption, maintain their initial concentration. This produces a step concentration profile, from $c = 0$ to $c = c_t$, at the top of fluid element $m = R_j$. It is worthwhile to note that an earlier version of CCT1 did not utilize the Lagrangian formulation for fluid elements and calculated advection-dispersion transport based on seepage velocities between contiguous solid elements (*i.e.*, treating the fluid in each solid element as well-mixed). This approach produced unacceptable numerical dispersion and was unable to properly simulate plug flow transport.

The remaining plots in Figure 5 show that CCT1 accurately calculates mass transport for diffusion, dispersion, and sorption under steady fluid flow conditions. Errors are small and tend to increase with depth for each simulation, which is likely due to the inconsistent bottom boundary condition for the analytical and numerical solutions. At $c/c_t = 0.5$, the errors in concentration ratio for Simulations 2 through 5 are 0.016%, 0.16%, 0.039%, and 0.40%, respectively. If the simulations are repeated at a higher numerical resolution of $R_j = 200$, these errors decrease to 0.0040%, 0.040%, 0.0075%, and 0.34%.

A final example illustrates the performance of CCT1 for a hypothetical problem involving simultaneous large strain consolidation and mass transport of a nonspecific sorbing contaminant in a soft sediment deposit. The deposit has an initial thickness of 5 m and the contaminant has an initially uniform concentration of 100 μg/L between eleva-

Table 1 - *Transport parameters for five simulations.*

Variable	Simulation 1 Advection	Simulation 2 Diffusion	Simulation 3 Advection + Diffusion	Simulation 4 Advection + Dispersion	Simulation 5 Advection + Dispersion + Sorption
h_t, h_b (m)	6.5, 6.0	6.0, 6.0	6.5, 6.0	6.5, 6.0	6.5, 6.0
v_s (m/s)	$3.75 \times 10^{-9}\downarrow$	0	$3.75 \times 10^{-9}\downarrow$	$3.75 \times 10^{-9}\downarrow$	$3.75 \times 10^{-9}\downarrow$
D^* (m^2/s)	0	5×10^{-10}	5×10^{-10}	5×10^{-10}	5×10^{-10}
α_L (m)	0	0	0	0.2	0.2
K_d (mL/g)	0	0	0	0	0.5
R_f	1	1	1	1	1.625

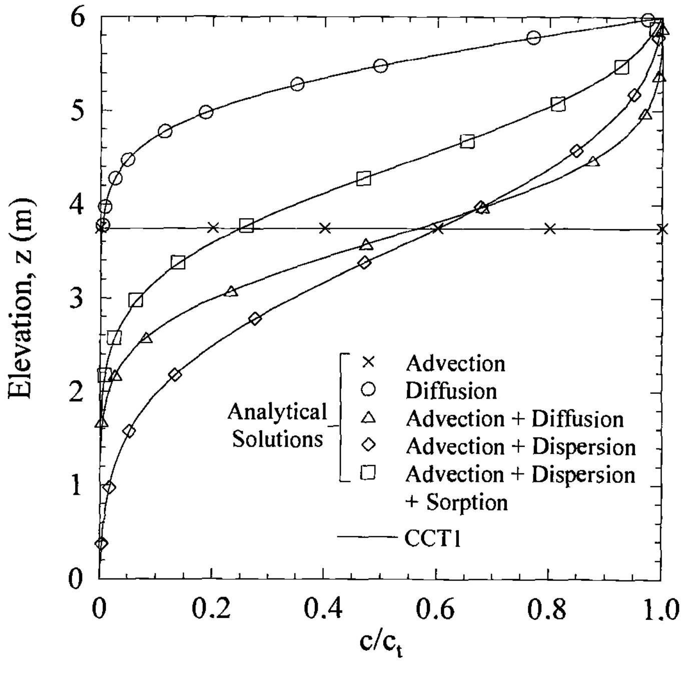

Figure 5 - *Comparison of analytical and numerical solutions for contaminant transport in a rigid porous medium under steady fluid flow conditions.*

tions 3.5 and 4.0 m. The effective diffusion coefficient D^* is 8×10^{-10} m^2/s and the distribution coefficient K_d is 4 mL/g. The normally consolidated sediment has $\alpha_L = 0.5$ m, $G_s = 2.78$, $\zeta = 1$, and the following compressibility and hydraulic conductivity relationships (based on values reported by Fox (1996) for a high plasticity clay slurry),

$$e = 4.3 - 1.0\log\sigma'(kPa) \tag{25}$$

$$\log k(m/s) = -11 + 0.77e \tag{26}$$

Pore pressures are initially hydrostatic and the bottom of the deposit is impermeable. The sediment deposit is to be capped with a granular soil layer having a buoyant unit weight of 11 kN/m^3. Information is needed regarding the possible migration of contaminants into the cap as a result of the capping process.

Simulations were performed ($R_j = 50$, $R_k = 5$, $R_s = R_t = 31$) for cap thicknesses of 1 and 2 m, corresponding to effective stress increments of 11 and 22 kPa (applied instantaneously). The top boundary of the sediment is assumed to maintain zero concentration. Figure 6(a) shows settlement of the sediment and contaminant mass outflow per unit area at the top boundary vs. log time. Total settlements for the 11 and 22 kPa stress increments are 0.494 and 0.713 m, respectively, yielding average final vertical strains of 10% and 14%. At $U_{avg} = 99.9\%$ ($t = 11{,}309$ days), mass outflows of contaminant are 2.78×10^{-2} and 3.84×10^{-2} g/m^2 for $\Delta q = 11$ and 22 kPa, respectively, which amount to 18% and 24% of the initial total contaminant mass within the sludge. Contaminant outflow is greater for the 22 kPa stress increment due to the larger seepage velocities and total fluid outflow from the sediment. Figure 6(b) shows concentration profiles in terms of relative elevation z/H at $U_{avg} = 30\%$, 60%, and 90% for both stress increments. Consistent with Figure 6(a), contaminant concentrations in the sediment decrease with increasing time and stress increment. The location of maximum concentration moves upward with time relative to the solid phase in response to advective flow toward the top boundary. With respect to absolute elevation z, the maximum concentration point moves downward with time due to the large strains occurring in the layer.

Conclusions

CCT1 is a numerical model for analysis of coupled, one-dimensional, nonlinear, large strain consolidation and contaminant transport. The consolidation algorithm of CCT1 accounts for vertical strain, soil self-weight, general constitutive relations, changing hydraulic conductivity and compressibility during consolidation, time-dependent loading, unload/reload effects, and steady flow across the layer due to unequal boundary head conditions. Constitutive relationships for the soil are defined using discrete data points and can take nearly any desired form. The contaminant transport algorithm of CCT1 accounts for advection, dispersion, and linear equilibrium sorption with the distribution coefficient as a spatially varying parameter. Advection-dispersion transport is consistent with spatial and temporal variations of porosity and seepage velocity in the consolidating layer.

Two Lagrangian columns of elements, one for the solid phase and the other for the fluid phase, are defined in CCT1 to properly simulate transport in a consolidating sedi sediment layer. The columns move independently of one another except that they are coupled via values of solid element-to-solid element relative fluid velocity that govern the

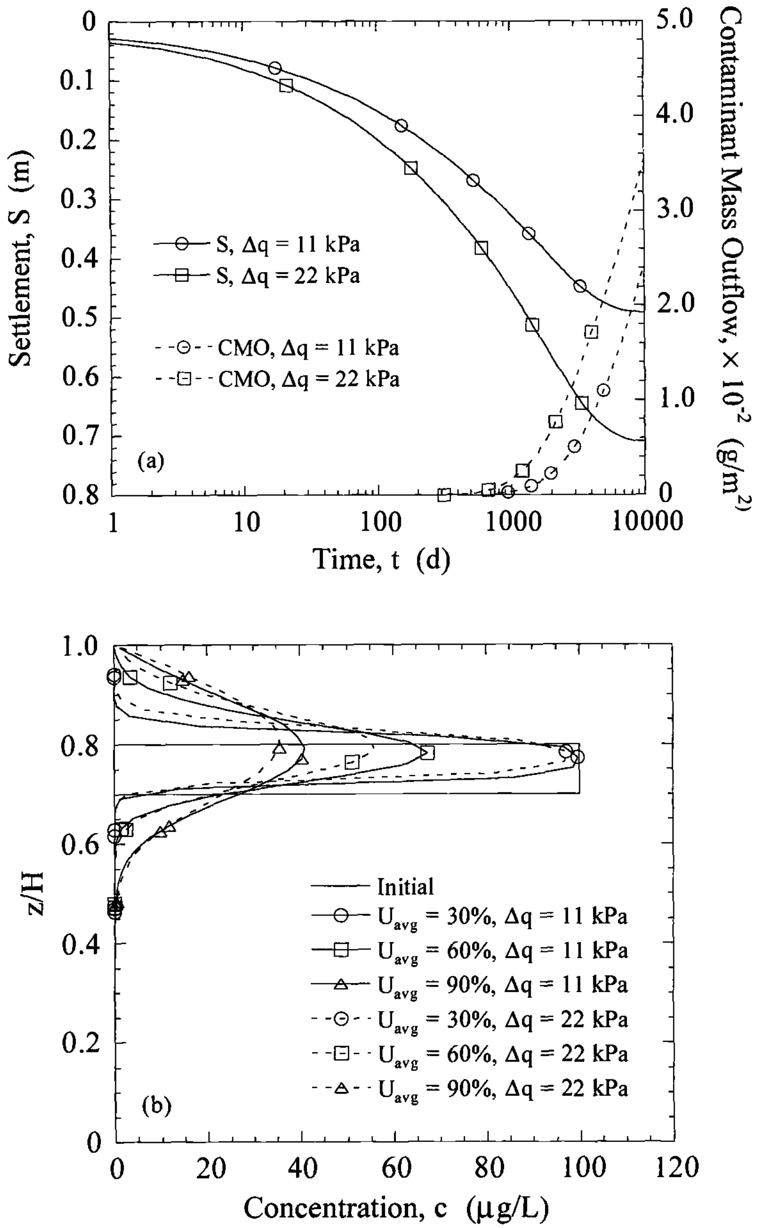

Figure 6 – *Large strain consolidation of a hypothetical contaminated sediment deposit: (a) settlement and contaminant mass outflow, and (b) dissolved contaminant concentration profiles.*

movement of each system. The Lagrangian analysis framework follows the motion of both fluid and solid phases throughout a simulation.

CCT1 provides the following quantities as a function of time: 1) settlement of the consolidating layer, and 2) total mass outflow of contaminant at each boundary. CCT1 provides the following quantities as a function of time and position within the consolidating layer: 1) void ratio, 2) pore pressure, 3) vertical effective stress and preconsolidation stress, and 4) contaminant concentration, including dissolved and sorbed fractions.

The performance of CCT1 for transport in a uniform porous medium (*i.e.*, no consolidation) was evaluated for five simulations involving: 1) advection, 2) diffusion, 3) advection + diffusion, 4) advection + dispersion, and 5) advection + dispersion + sorption. Contaminant concentration profiles for each simulation were in excellent agreement with corresponding analytical solutions for transport in a semi-infinite domain. The performance of CCT1 was then illustrated for an example problem involving consolidation-induced transport of a sorbing contaminant in a soft sediment deposit. Simulations indicate that contaminant mass outflow from the layer increases with increasing applied stress increment.

Acknowledgments

Financial support for this investigation was provided in part by Grant No. CMS-9622644 from the Geomechanical, Geotechnical, Geoenvironmental Systems Program of the U.S. National Science Foundation and is gratefully acknowledged. The author thanks Prof. Thomas C. Harmon of UCLA for several enlightening discussions on mass transport in sorptive porous media.

References

Al-Tabbaa, A. and Wood, D. M., 1987, "Some Measurements of the Permeability of Kaolin," *Geotechnique*, Vol. 37, No. 4, pp. 499-503.

Bear, J., 1972, *Dynamics of Fluids in Porous Media*, Elsevier, New York, 764 pp.

Domenico, P. A. and Schwartz, F. W., 1990, *Physical and Chemical Hydrogeology*, John Wiley & Sons, New York, 824 pp.

Fox, P. J., 1996, "Analysis of Hydraulic Gradient Effects for Laboratory Hydraulic Conductivity Testing," *Geotechnical Testing Journal*, Vol. 19, No. 2, pp. 181-190.

Fox, P. J. and Berles, J. D., 1997, "CS2: A Piecewise-Linear Model for Large Strain Consolidation," *International Journal for Numerical and Analytical Methods in Geomechanics*, Vol. 21, No. 7, pp. 453-475.

Fox, P. J., 2000, "CS4: A Large Strain Consolidation Model for Accreting Soil Layers," *Geotechnics of High Water Content Materials*, Special Technical Publication 1374, T. B. Edil and P. J. Fox, eds., ASTM, pp. 29-47.

Fox, P. J., Di Nicola, M., and Quigley, D. W., 2003, "Piecewise-Linear Model for Large Strain Radial Consolidation," *Journal of Geotechnical and Geoenvironmental Engineering*, in press.

Freeze, R. A. and Cherry, J. A., 1979, *Groundwater*, Prentice-Hall, Englewood Cliffs, New Jersey, 604 pp.

Gibson, R. E., England, G. L., and Hussey, M. J. L., 1967, "The Theory of One-Dimensional Consolidation of Saturated Clays, I. Finite Non-Linear Consolidation of Thin Homogeneous Layers," *Geotechnique*, Vol. 17, No. 3, pp. 261-273.

Kong, D. and Harmon, T. C., 1996, "Using the Mutiple-Cell Balance Method to Solve the Problem of Two-Dimensional Groundwater Flow and Transport with Nonequilibrium Sorption," *Journal of Contaminant Hydrology*, Vol. 23, pp. 285-301.

Lee, K. and Sills, G. C., 1979, "A Moving Boundary Approach to Large Strain Consolidation of a Thin Soil Layer," *Proceedings, 3rd International Conference on Numerical Methods in Geomechanics*, Aachen, Balkema, Vol. 1, pp. 163-173.

Nagaraj, T. S., Pandian, N. S., and Narasimha Raju, P. S. R., 1994, "Stress-State-Permeability Relations for Overconsolidated Clays," *Geotechnique*, Vol. 44, No. 2, pp. 349-352.

Ogata, A., 1970, "Theory of Dispersion in a Granular Medium," *Professional Paper 411-I*, U.S. Geological Survey.

Potter, L. J., Savvidou, C., and Gibson, R. E., 1994, "Consolidation and Pollutant Transport Associated With Slurried Waste Disposal," *Proceedings, 1st International Congress on Environmental Geotechnics*, pp. 525-530.

Rabideau, A. J. and Miller, C. T., 1994, "2-Dimensional Modeling of Aquifer Remediation Influenced by Sorption," *Water Resources Research*, Vol. 30, No. 5, pp. 1457-1470.

Schiffman, R. L., Pane, V., and Gibson, R. E., 1984, "The theory of one-dimensional consolidation of saturated clays. IV. An Overview of Nonlinear Finite Strain Sedimentation and Consolidation," *Proceedings, Symposium on Sedimentation/ Consolidation Models: Prediction and Validation*, R. N. Yong and F. C. Townsend, eds., San Francisco, ASCE, pp. 1-29.

Shackelford, C. D. and Daniel, D. E., 1991, "Diffusion in Saturated Soil. II: Results," *Journal of Geotechnical Engineering*, Vol. 117, No. 3, pp. 485-506.

Smith, D. W., 2000, "One-Dimensional Contaminant Transport Through a Deforming Porous Medium: Theory and a Solution for a Quasi-Steady-State Problem," *International Journal for Numerical and Analytical Methods in Geomechanics*, Vol. 24, No. 8, pp. 693-722.

Yong, R. N., Siu, S. K. H., and Sheeran, D. E., 1983, "On the Stability and Settling of Suspended Solids in Settling Ponds. Part I. Piece-Wise Linear Consolidation Analysis of Sediment Layer," *Canadian Geotechnical Journal*, Vol. 20, No. 4, pp. 817-826.

Zhu, Y. and Fox, P. J., 2000, "Smoothed Particle Hydrodynamics Model for Diffusion Through Porous Media," *Transport in Porous Media*, Vol. 43, No. 3, pp. 441-471.

Antonina Degtiareva,[1] Maria Elektorowicz,[1] and Taghi Ebadi[1]

Assessment of the Lead Release from Cables Buried in Sediments into the Water Column

---

Reference: Degtiareva, A., Elektorowicz, M., and Ebadi, T., **"Assessment of the Lead Release from Cables Buried in Sediments into the Water Column,"** *Contaminated Sediments: Characterization, Evaluation, Mitigation/Restoration, and Management Strategy Performance, ASTM STP 1442*, J. Locat, R. Galvez-Cloutier, R. C. Chaney, and K. R. Demars, Eds., ASTM International, West Conshohocken, PA, 2003.

Abstract: The study investigates the change in the water column quality in a situation where submarine communication cables cross the water bodies. In spite of precautions in technological achievements it is possible that these cables can be subjected to potential corrosion processes. This study was performed for a particular area of the St. Lawrence River. The impact of cables buried in sediments on lead speciation in the water column was shown under different conditions (anaerobic and aerobic, at different partial pressures of CO_2, presence of organic acids). Equilibrium in the water was calculated taking into account gas, water and solid phases. Programs Equilibrium and EPH from FACT were utilized in this study to calculate Eh-pH diagrams and the equilibrium in water. The main form of lead was found to be $PbOH^+$ (3.34×10^{-9} M/kg), the concentration of the free lead ion was two orders of magnitude lower (2.5×10^{-11} M/kg). The calculations, in which solid phases where considered, demonstrated that the water was oversaturated with respect to dolomite and iron(III) hydroxide. It was speculated that under these conditions dolomite could form a protective layer around the cable, which can delay the corrosion. Under anoxic conditions cerussite and lead sulfide precipitated. When P_{CO2} increased, the concentration of the free ion of lead increased.

Keywords: lead, cable, corrosion, speciation, water quality, quality of sediments, Eh-pH diagrams

---

[1] PDF, Associate Professor, and PDF, respectively, Department of Building, Civil, and Environmental Engineering, Concordia University, 1455 Blvd de Maisonneuve W, Montreal, PQ, H3G 1M8, Canada

Introduction

Communication cables often cross water bodies in industrial areas. They consist of copper base, lead and iron protective layers and asphalt covering. These cables could possibly be subjected to the corrosion process. The process of corrosion and the release and fate of corrosion compounds in the water bodies are complex and affected by various factors.

Most metals have a tendency to corrode due to a reaction with the surrounding media, such as water and air. An important way of considering corrosion processes is the thermodynamic one, which shows under which conditions a metal will or won't corrode. If the corrosion in moist environments is considered, redox-potential-pH (Pourbaix) diagrams are necessary to estimate distribution of corroded species in these particular environmental conditions (Wranglen 1985).

This study was conducted to investigate the possibility of corrosion and the possible water quality change due to corrosion of the cable containing lead in the St. Lawrence River. However, this methodology can be applied to other cases. A specific section of the St. Lawrence River (north-shore mix) that represents the area of concern for communication industries was studied. The average values of the concentration of dissolved species present in the river were taken from the State of the Environmental Report on the St. Lawrence River (St. Lawrence Centre 1996a, 1996b).

The construction and use the Eh-pH diagrams help to estimate conditions of possible corrosion. In the present study the program EPH from FACT (Pelton et al. 1998) was used to construct Eh-pH diagrams. To construct a diagram that would closely represent the existing conditions of the St. Lawrence River, the following ions were taken into account: SO_4^{2-}, Cl^- and Ca^{2+}. The activities of the SO_4^{2-}, Cl^- and Ca^{2+} ions introduced into a program were considered equal to the concentrations of these ions in the St. Lawrence River. Concentrations of these ions above average values for the St. Lawrence River were also considered in some cases.

Effects of the different factors such as physico-chemical characteristics of water affecting the speciation and release of corrosion compounds were studied. The equilibrium in water of the St. Lawrence River was calculated using the program Equilibrium from software FACT (Pelton et al. 1998).

Impact of Oxic, Anoxic and Acid-base Conditions on Lead Corrosion

Impact of CO_2 Partial Pressure, Presence of Sulfur, Chloride and Calcium

Corrosion of cables proceeds differently, depending on a number of factors among them the depth of burial. Cables lying on the sediments surface where water can be in the equilibrium with air are subjected to higher concentrations of dissolved oxygen than the cables buried in sediments. If cables are buried in sediments under anaerobic conditions, there is an insufficient amount of oxygen in pore water, values of redox potential are below zero, and corrosion could proceed differently.

The following systems were considered and the Eh-pH diagrams were calculated using the program EPH from FACT to simulate the potential conditions to which communication cables can be subjected:

Case 1 - Water was considered to be in equilibrium with air, therefore a partial pressure was assumed to be $P_{CO2} = 0.0003$ atm. First, the simple system Pb-C-H_2O was considered to better illustrate the influence of changing conditions and different concentrations of ions in water. Figure 1 shows the areas of predominance of ions Pb^{2+} and $PbOH^+$ and the thermodynamic ranges where corrosion occurs (pH varies from 2 to 8.75). In the predominant areas of solid precipitates, $PbCO_3$, PbO_2 and Pb, corrosion is still possible, but precipitated solids may (under suitable conditions) form a partially or fully protective coating that delays corrosion. On the bottom of water bodies, especially in the presence of microorganisms, higher concentrations of CO_2 ($P_{CO2} = 0.01$ atm) may be present.

Increased concentrations of carbon dioxide decrease the possibility of corrosion, which is shown in Figure 2, where an increase of carbon dioxide concentration was considered ($P_{CO2} = 0.01$ atm). The results demonstrate that the predominant area of lead carbonate shifts down to pH = 7.25.

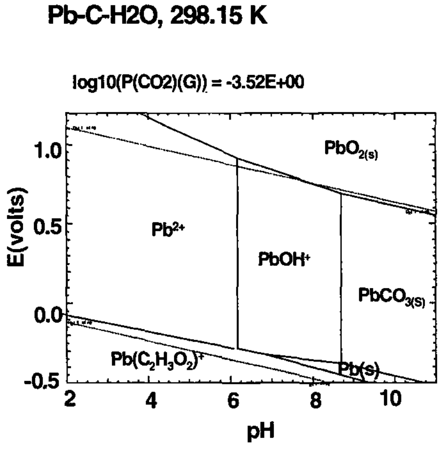
Pb-C-H2O, 298.15 K

log10(P(CO2)(G)) = -3.52E+00

Figure 1 - *Eh-pH diagram (P_{CO2} =0.003 atm). The total dissolved Pb species: 10^{-6} M.*

Case 2 - In this case, an additional element (S) was added to calculations performed by the same program. The activity of the SO_4^{2-} ion was considered equal to the concentration of this ion in the St. Lawrence River. The following system was considered: Pb-C-S-H_2O. The area of the solid lead sulfide appears on the Eh-pH diagram (Fig. 3). As mentioned previously, precipitation of solids may delay the corrosion process. As sulfides are the least soluble species, it could be expected that a low content of soluble lead in the water develops under reduced conditions. A small increase of the sulfate ion concentration does not seem to change the areas of predominance on the diagram, however, if its activity increases up to 0.1 M/kg (mole per kilogram of the water column), solid lead sulfate becomes predominant under low levels of pH (from 2 to 7) and can also form a protective layer as is shown in Figure 4.

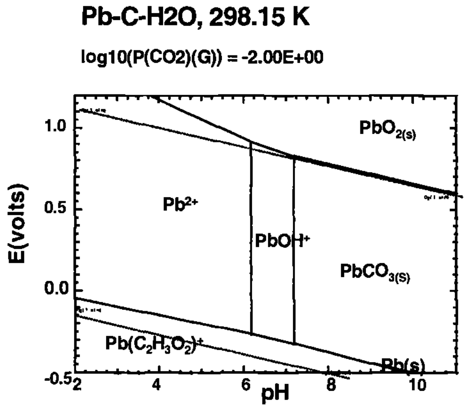

Figure 2 -*Eh-pH diagram* (P_{CO2} *= 0.01 atm). The total dissolved Pb species:* 10^{-6} *M.*

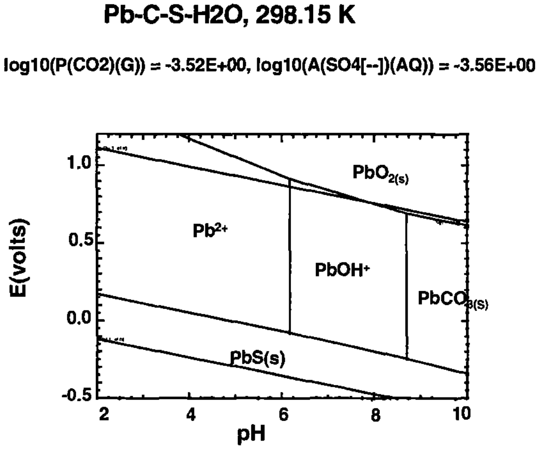

Figure 3 - *Eh-pH diagram for Pb-C-S-*H_2O*. The total dissolved Pb species:* 10^{-6} *M.*

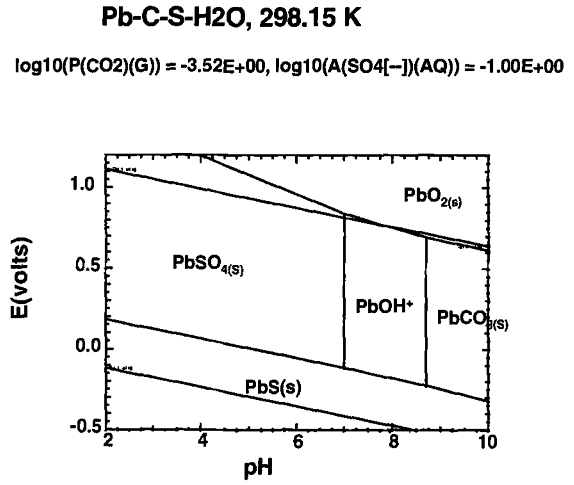

Figure 4 - *Eh-pH diagram for $Pb-C-S-H_2O$ (activity 0.1 M/kg). The total dissolved Pb species: 10^{-6} M.*

Case 3 - In this case, Cl was introduced into calculations. As it was done previously with SO_4 the activity of Cl- was considered equal to its concentration in the St. Lawrence River. The diagram for the following system: $Pb-C-Cl-H_2O$ was calculated. Figure 5 demonstrates that chloride ion at low concentrations does not affect the corrosion; although it can form complexes with lead and subsequently, increase the concentration of the total soluble lead in water.

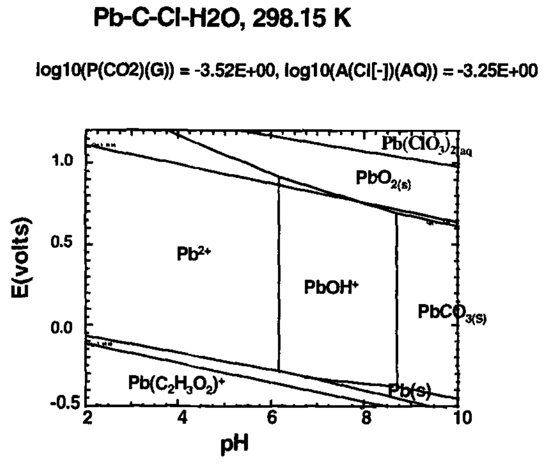

Figure 5 - *Eh-pH diagram for $Pb-C-Cl-H_2O$. The total dissolved Pb species: 10^{-6} M.*

Chloride ions in the absence of strong cations can also decrease pH that would accelerate the corrosion. This fact can be easy illustrated by the following calculations, which were performed using the program Equilibrium from software FACT (Pelton et al. 1998):

Case 3a - The following system was considered: $Pb+1000gH_2O+CO_2+O_2$. The following assumption has been made: P_{CO2} is 0.003 atm (ten times higher than P_{CO2} in water in equilibrium with CO_2 in air) and O_2 is in equilibrium with air (P_{O2}=0.21 atm). In these conditions, pH of this system would be 6.25 and concentrations of predominant lead ions would be as follows:

$Pb^{2+} = 2.33 \times 10^{-5}$ M/kg,
$PbOH^{+} = 2.80 \times 10^{-5}$ M/kg.

Case 3b - Upon addition of chloride to the system 3a (total dissolved chloride was 20 mg/L as in the St. Lawrence River) the value of pH decreased to 5.74 and changed subsequently the lead speciation:

$Pb^{2+} = 2.4 \times 10^{-4}$ M/kg,
$PbOH^{+} = 9.1 \times 10^{-5}$ M/kg,
$PbCl^{+} = 5.5 \times 10^{-7}$ M/kg.

The calculations showed that the concentration of the total dissolved lead increased by an order of magnitude; the concentration of the lead ion increased by one order of magnitude and this ion found to be a predominant species.

When the activity of Cl^- increases up to 0.1 M/kg, the complex $PbCl^+$ becomes the predominant one at low pH. This fact can be illustrated by diagram in Figure 6. To calculate this diagram the activity of Cl- introduced to calculations was assumed to be equal to 0.1M/kg. The diagram shows that the corrosion occurs in these conditions.

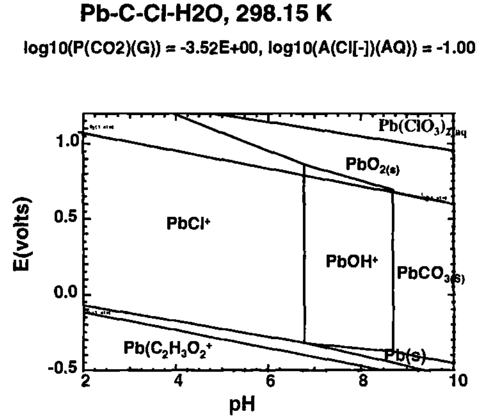

Figure 6 - *Eh-pH diagram for Pb-C-Cl-H_2O system (activity 0.1 M/kg). The total dissolved Pb species: 10^{-6} M.*

Case 4 - In this case, the system including Pb, C, Cl, S, H_2O at P_{CO2} = 0.003 atm was considered. To calculate a diagram that represents conditions similar to those in the St. Lawrence River, activities of SO_4^- and Cl^- were assumed to be 0.000275 M/kg and

0.0005686 M/kg respectively. The applied conditions were close to those observed on the bottom of the St. Lawrence River. In these conditions, PbO_2 precipitating at high Eh, $PbCO_3$ at high pH and PbS at low Eh are the predominant lead forms (Fig. 7). They could form a protective layer and delay the corrosion. If this layer is damaged (for example, due to coarse sediments movement), the corrosion will occur. An increase of concentrations of CO_2 around the cable, which is possible due to the presence of microorganisms, may decrease the corrosion.

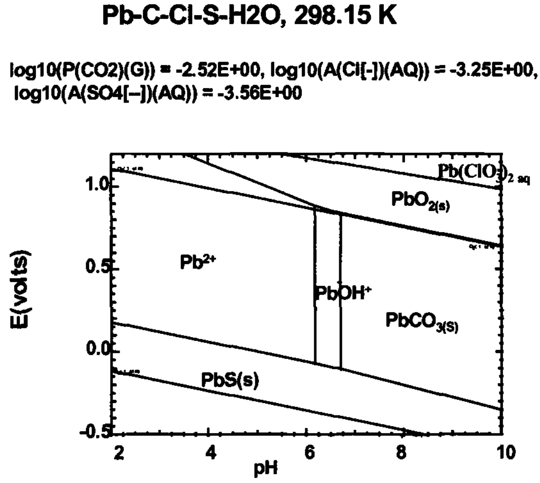

Figure 7 - *Eh-pH diagram for Pb-Cl-S-H_2O. The total dissolved Pb species: 10^{-6} M.*

Case 5 - The following system, which included calcium was considered: Pb-C-Ca-H_2O. The results of calculations (Fig. 8) demonstrate that the presence of calcium does not seem to affect the corrosion at activities close to concentrations of Ca found in the St. Lawrence River (up to 0.1 M/kg).

At the same time, the presence of calcium and calcium carbonates in water may raise pH; therefore, decreasing the content of lead in the solution, which can be demonstrated in the following calculations:

Case 5a - Upon addition of calcium (the total concentration of dissolved Ca = 25 mg/L as in the St. Lawrence River) to the system 3a, pH of the resulting solution becomes 7.56 and the concentrations of predominant lead ions are:

$Pb^{2+} = 5.57 \times 10^{-8}$ M/kg,
$PbOH^{+} = 1.37 \times 10^{-6}$ M/kg.

The results of calculations show that the total concentration of soluble lead is approximately 10 times lower than in the case 3a. The concentration of free lead ion became 3 orders of magnitude lower while lead hydroxide ion becomes highly predominant in the system.

Although Eh-pH diagrams are a valuable tool (Stumm and Morgan 1996) to predict conditions of the possible corrosion, Nordstrom and Munoz (1986) pointed out that they can not be used for quantitative chemical modeling because of the following reasons: a) constant activities of ions are used to construct diagrams; b) noideality corrections are not made; c) the redox potential of a natural water is not a clearly defined. Therefore, in order to investigate the fate of corrosion products and the possibility of lead release into the water column, the water-mineral equilibrium computations were applied in this study.

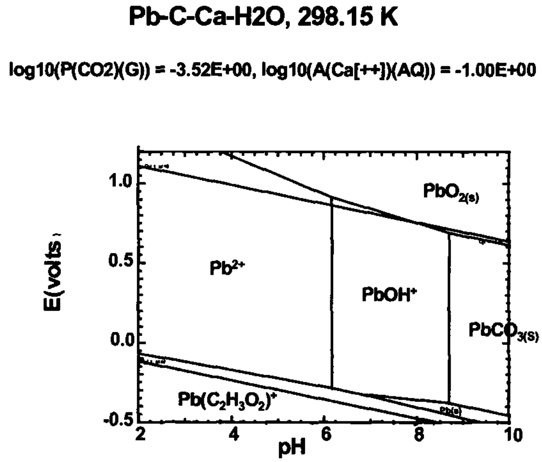

Figure 8 - *Eh-pH diagram Pb-C-Ca-H_2O (activity 0.1 M/kg). The total dissolved Pb species: 10^{-6} M.*

Fate of Corrosion Products Under Oxic and Anoxic Conditions and Their Influence on Water Quality

Fate of Inorganic Corrosion Products

The equilibrium in the water of the St. Lawrence River has been calculated using the program Equilibrium from FACT (Faculty for Analysis of Chemical Thermodynamics). Investigations conducted to study corrosion products showed that in the aquatic environment the main products of corrosion were lead carbonates (cerussite and hydrocerussite) and lead oxides (Nordstrom and Munoz 1986, Pintado and Montero 1992, Al-Khafari and Badawy 1998). Therefore, in the present study the phase that controls the solubility of lead in the water column near the cable was assumed to be cerussite. With increase of P_{CO2} near the bottom of the river and in sediments (close to cables), cerussite apparently is more likely to be formed than oxides. At the same time, being in a more soluble phase, it may control the solubility of lead in the water column near the cable.

In order to investigate the speciation of lead in the water column, the following elements were taken into account: Ca, Mg, Na, K, S, Cl, Pb, Fe and H_2O, CO_2, O_2. Subsequently, the following parameters were considered:

3.38×10^{-9} Pb + $55.5H_2O$ + CO_2 + O_2 + 5.686×10^{-4} Cl + 7.75×10^{-4} Ca + 2.92×10^{-4} Mg + 4.65×10^{-4} Na + 2.75×10^{-4} S + 1.23×10^{-5} Fe

The concentrations of all species are given in moles per kilogram of water (M/kg).
It was assumed that CO_2 and O_2 were in equilibrium with gases in air, where partial pressures $P_{CO2} = 0.0003$ atm and $P_{O2} = 0.21$ atm. No solids were allowed to precipitate.
The calculations showed:
- The ionic strength was 0.0039;
- The calculated values of Eh and pH were: Eh = 713 mV, pH = 8.5

The speciation of lead was calculated and the chemical forms of lead present in water were listed in Table 1.

Table 1 - *Lead speciation in the St. Lawrence River, M/kg*

$PbOH^+$	Pb^{2+}	$PbCl^+$	$HPbO_2^-$	$PbCl_2^0$	$Pb_3(OH)_4^{2-}$
3.37×10^{-9}	1.43×10^{-11}	3.29×10^{-13}	5.09×10^{-14}	2.97×10^{-16}	2.04×10^{-22}

Table 1 shows that the main form of lead was lead monoxide dipositive ion ($PbOH^+$). The concentration of the free lead ion was two orders of magnitude lower, while complexes with chloride ion were also present.

The calculations, in which the solid phases were allowed to precipitate, showed that the water was oversaturated with respect to dolomite and iron(III) hydroxide. Dolomite can form a protective layer around cables, which would delay the process of corrosion. Equilibrium with the above mentioned solid phases were calculated. These calculations showed:
- The ionic strength of the solution was 0.0030.
- The calculated values of Eh and pH were: Eh = 728 mV, pH = 8.3.

The lead speciation is shown in Table 2:

Table 2 - *Lead speciation in the St. Lawrence River, M/kg, where solid phases were allowed to precipitate.*

$PbOH^+$	Pb^{2+}	$PbCl^+$	$HPbO_2^-$	$PbCl_2^0$	$Pb_3(OH)_4^{2-}$
3.34×10^{-9}	2.5×10^{-11}	5.81×10^{-13}	1.6×10^{-14}	5.25×10^{-16}	1.14×10^{-22}

The pH level was lower, than in the previous case (without solids) and this situation influenced the lead speciation. The concentration of the free lead ion was a little higher, and there were the higher concentrations of the lead chloride ion[+] and lead chloride (aq).

To describe the situation where the cable is placed in the water column (on the surface of the sediments), the following parameters were considered:

$3.38\text{x}10^{-9}$ Pb + $55.5H_2O$ + CO_2 + O_2 + $5.686\text{x}10^{-4}$ Cl + $7.75\text{x}10^{-4}$ Ca + $2.92\text{x}10^{-4}$ Mg + $4.65\text{x}10^{-4}$ Na + $2.75\text{x}10^{-4}$ S + $1.23\text{x}10^{-5}$ Fe + Pb,

The calculations showed:
- The ionic strength of the solution became 0.0032.
- The calculated values of Eh and pH were: Eh = 729 mV, pH = 8.3.

The lead speciation changed as shown in Table 3.

Table 3 - *Lead speciation in the water column (St. Lawrence River), M/kg, in the presence of cables*

$PbOH^+$	Pb^{2+}	$PbCl^+$	$HPbO_2^-$	$PbCl_2^0$	$Pb_3(OH)_4^{2-}$
$2.60\text{x}10^{-6}$	$2.01\text{x}10^{-8}$	$4.6\text{x}10^{-10}$	$1.19\text{x}10^{-11}$	$4.16\text{x}10^{-13}$	$5.20\text{x}10^{-14}$

The calculations showed that cerussite ($PbCO_3$) precipitated from the solution. Since cerussite is formed around the cable from dissolution of lead, it may control the solubility of lead in the water column. The total concentration of soluble lead in the water column (0.54 mg/l) became 3 orders of magnitude higher, than that in the St. Lawrence River (0.0007 mg/l). The total concentration of soluble lead in the water column became equivalent to the 90 days LC_{50} = 0.55 mg/L for fish (El-Egamy 1994).

The calculations showed that the relative amount of lead tetrahydroxide dipositive ion also increased.

To find the speciation of lead under anaerobic conditions (cables buried in sediments), the equilibrium was calculated for the same system without oxygen. Due to lack of the data for pore water of the sediments, the concentrations of the major elements were considered the same as in the St. Lawrence River. Subsequently, calculations were performed using the following parameters:

$3.38\text{x}10^{-9}$ Pb + $55.5H_2O$ + CO_2 + $5.686\text{x}10^{-4}$ Cl + $7.75\text{x}10^{-4}$ Ca + $2.92\text{x}10^{-4}$ Mg + $4.65\text{x}10^{-4}$ Na + $2.75\text{x}10^{-4}$ S + $1.23\text{x}10^{-5}$ Fe + Pb

Two cases were considered: 1) P_{CO2} = 0.0003 atm, 2) P_{CO2} = 0.003 atm (ten times higher as an increase of P_{CO2} in pore water and around the cable can be expected; one of the reasons could be an activity of biota).

The calculations showed that in both cases cerussite and lead sulfide precipitated from the solution.

Calculations performed for the first case (lower P_{CO2}) showed:
- The ionic strength: 0.0023.
- The calculated values of Eh and pH such as: Eh = - 343 mV, pH = 8.4.

Lead speciation for the above-mentioned conditions is shown in Table 4. Since lead carbonate was still formed in these conditions, it might control the solubility of the lead. The total concentration of lead in the solution was $1.98x10^{-6}$ M/kg (less than in aerobic conditions). The distribution of chemical forms of lead was almost the same.

Table 4 - *Lead speciation in the water column (St. Lawrence River), M/kg, in the presence of cables, in anaerobic conditions at different values of* P_{CO2}, *atm*

P_{CO2}	$PbOH^+$	Pb^{2+}	$PbCl^+$	$HpbO_2^-$	$PbCl_2^0$	$Pb_3(OH)_4^{2-}$
0.0003	$1.90x10^{-6}$	$1.15x10^{-8}$	$2.64x10^{-10}$	$1.58x10^{-13}$	$2.39x10^{-13}$	$2.98x10^{-14}$
0.003	$1.05x10^{-6}$	$3.29x10^{-8}$	$7.55x10^{-10}$	$2.96x10^{-13}$	$6.82x10^{-13}$	$8.51x10^{-16}$

In the second case, where higher P_{CO2} was considered, the following values were obtained:

- The ionic strength was 0.0036.
- The values of Eh and pH were: Eh = - 285 mV, pH = 7.69, both values were lower than in the first case.

The lead speciation is shown in Table 4. Because of pH increase (by 8%) comparing to the first case, the concentration of free lead was approximately 300% higher. Concentrations of the complexes with chloride ion were also higher. The total concentration of lead in the solution ($1.08x10^{-6}$ M/kg) was lower than in the first case. The increase of P_{CO2} around the cable may decrease the total concentration of the soluble lead in the water column, but in the same time increase the concentration of free ions.

Fate of Organo-metallic Corrosion Products

Pintado and Montero (1992) studied degradation of sheath covers of communication cables and demonstrated that the asphalt cover can release some carboxylic acids. In addition, it is known that organic acids are usually present in the bottom sediments of shallow waters. Due to these facts, it was worthwhile to evaluate the impact of organic acids on the fate of corrosion products.

To investigate the influence of organic acids on lead speciation three organic acids: acetic, formic and oxalic (containing two atoms of carbon) were introduced to the mentioned above system in the presence of cables. Various concentrations of acids were considered in aerobic and anaerobic conditions.

The calculations showed that in aerobic conditions when the partial pressures of CO_2 around the cable were assumed to be 0.0003 and 0.003 atm, acetic, formic and oxalic acids did not influence very much the speciation of lead, redox potential and pH in the water column at the concentrations up to 10^{-1} M/kg ($3.3x10^{-2}$ each).

Table 5 - *Speciation of lead in the presence of organic acids in anaerobic conditions, M/kg*

P_{CO2}, atm	N	Eh	pH	$PbOH^+$	Pb^{2+}	$PbCl^+$	$Pb(C_2H_3O_2)^+$	$PbCl_2^0$	$HPbO_2^-$	$Pb(CHO2)^+$
0.0003	1	-330	8.4	$1.90x10^{-6}$	$1.15x10^{-8}$	$2.64x10^{-10}$	$1.2x10^{-12}$	$2.39x10^{-13}$	$1.6x10^{-11}$	$5.8x10^{-15}$
0.003	2	-321	7.7	$1.05x10^{-6}$	$3.29x10^{-8}$	$7.55x10^{-10}$	$6.7x10^{-12}$	$6.82x10^{-13}$	$2.9x10^{-13}$	$1.7x10^{-14}$
0.003	3	-321	7.7	$1.05x10^{-6}$	$1.05x10^{-6}$	$7.55x10^{-10}$	$8.1x10^{-12}$	$6.82x10^{-13}$	$2.9x10^{-13}$	$1.9x10^{-14}$

1,2 – concentrations of organic acids are $3.3x10^{-7}$ M/kg each (10^{-6} M/kg in sum).
3 - concentrations of organic acids are $3.3x10^{-2}$ M/kg each (10^{-1} M/kg in sum).

Repeated calculations for anaerobic conditions showed that in the presence of the above-mentioned acids in the water column, the values of Eh decreased (Table 5). Even at acid concentrations of 3.3×10^{-7} M/kg, lead formed complexes with acetic and formic acids. The concentration of complexes with oxalic acid was below 10^{-20} M/kg. These values were comparable with the concentrations of other complexes. It was concluded that presence of organic acids could increase the total concentration of soluble lead in water column.

At the same time, according to Poubaix diagram for lead (Fig. 1), in the absence of sulfur in the system at low values of Eh, the complex with acetic acid becomes predominant. Subsequently, in these conditions, acetic acid will increase the possibility of corrosion and a protective layer consisting of solid precipitates might not be formed.

Another study considered volatile compounds present in the environment that can represent sediment in shallow waters. In this case, the calculations showed that part of the organic acids was transformed into methane. One part of methane was dissolved in the water column and the other was in the gaseous phase. It was concluded that in shallow waters under anaerobic conditions, after some time, a part of the organic acids could be transformed into methane, which eventually will lead to decrease in the total soluble lead concentration.

Conclusion

The corrosion of the cable is a very complex process from the thermodynamic point of view and is influenced by many factors. These factors can affect corrosion directly, for example, increasing the concentration of soluble lead by:

- Forming soluble complexes; as it was shown above, chloride and organic acids can form soluble complexes with lead and increase the concentration of soluble lead;
- Forming solids precipitates; carbonates form solid precipitates such as lead carbonates and can decrease the lead concentration in solution.

Other factors can affect corrosion indirectly, for example, by:

- Changing pH of the solution; the addition of Ca (and other strong cations) increases pH.
- In hard waters with high concentrations of calcium and magnesium, their carbonates can form a protective layer around cables.

The above-mentioned factors must be considered together since their impacts are interdependent. To study corrosion of submarine cables buried in sediments, the composition of pore water of these sediments has to be taken into account. In addition, information about the solid phase, which controls the solubility of lead have to be supplied.

The chemical corrosion of the cable containing lead can possibly increase in the total concentration of soluble lead in the water column up to 3 orders of magnitude compared to that existing in the St. Lawrence River (0.54 mg/L). This value is equivalent to 90 days LC_{50} for non-salmonid fish (0.55 mg/L) (Firouseh 1999). Free lead ion Pb^{2+} is predominant below $pH = 6$, so any change in pH towards acidity will lead to increase in the concentration of free lead ion, which is more toxic to biota. Organic acids such as acetic and formic can increase the total concentration of soluble lead in a water column.

The methodology described in this paper can be successfully applied to the assessment of the fate of other metals released from sediments in to the water column.

References

Al-Kharafi, F.M., Badawy, W.A., 1998, Effect of oxygen and oxidizers on the corrosion and passivation of lead in chloride-containing acidic solutions. *Corrosion prevention and control,* vol. 43(3), pp. 75-85.

El-Egamy, S.S., 1994, Corrosion and passivation behavior of lead in aqueous carbonate media. *Bulletin of Electrochemistry,* vol. 11(9), pp. 418-423 .

Firouseh, A.S., 1999, "An investigation about the effects of cable corrosion on water creatures", Internal Report, Concordia University, Montreal, Canada, pp. 21.

Nordstrom, D.K, Munoz, J.L., 1986, *Geochemical thermodynamics.* Blackwell Scientific publications, pp. 477.

Pelton, A.D., Bale, C.W., Tompson, W.T., The FACT system, École Polytechnique, Montreal, Canada, http://www.crct.polymtl.ca, March 1999.

Pintado, J.L., Montero, F., 1992, "Underground biodeterioration of medium tension electric cables". *J. International Biodeterioration and Biodegradation,* vol.29, pp. 357-365.

St. Lawrence Centre, 1996a, "State of the Environment", Report on the St. Lawrence River. Volume 1: The St. Lawrence Ecosystem. Environment Canada-Quebec Region, Environmental Conservation, and Editions MultiMondes. " St. Lawrence UPDATE" series.

St. Lawrence Centre, 1996b, "State of the Environment", Report on the St. Lawrence River. Volume 2: The State of the St. Lawrence. Environment Canada-Quebec Region, Environmental Conservation, and Editions MultiMondes. " St. Lawrence UPDATE" series.

Stumm, W., Morgan, J.J., 1996. *Aquatic chemistry.* Chemical equilibria and rates in natural waters, Third ed., Willey-Interscience publications, New-York, pp.1022.

Wranglen, G., 1985, *An introduction to corrosion and protection of metals.* Chapman and Hall, New York.

Şebnem Elçi,[1] and Paul A.Work[2]

Numerical Modeling of Hydrodynamic Circulation and Cohesive Sediment Transport in Hartwell Lake, South Carolina/Georgia, USA

Reference: Elçi, Ş. and Work, P. A., "**Numerical Modeling of Hydrodynamic Circulation and Cohesive Sediment Transport in Hartwell Lake, South Carolina/Georgia, USA,**" *Contaminated Sediments: Characterization, Evaluation, Mitigation/Restoration, and Management Strategy Performance, ASTM STP 1442*, J. Locat, R. Galvez-Cloutier, R. C. Chaney, and K. R. Demars, Eds., ASTM International, West Conshohocken, PA, 2003.

Abstract: This paper describes numerical modeling of hydrodynamic circulation and cohesive sediment transport in Hartwell Lake, South Carolina/Georgia, a U.S. Army Corps of Engineers (USACE) hydropower and flood control reservoir. A U.S. Environmental Protection Agency (EPA) "Superfund" site is located on a tributary to the lake because of high concentrations of polychlorinated biphenyls (PCBs) in the lake sediments. The primary objective of this study involves prediction of depositional zones for sediments transported within the reservoir.

The EFDC (Environmental Fluid Dynamics Code) model developed by Hamrick (1996) is used to describe lake hydrodynamics and sediment fate. Historical records of wind and flow were used to determine frequencies of occurrence and representative conditions for prediction of long-term deposition zones for sediment transported by the flow.

Sensitivity of hydrodynamic processes to model parameters were investigated and wind was found to be the major force driving the circulation. Model results for cases with realistic long-term forcing indicated likely zones of sediment deposition, useful for mitigation of pollution problems as well as predictions of reservoir lifetime and development of maintenance schemes.

Keywords: Hartwell Lake, EFDC, deposition, sedimentation

---

[1] Graduate Research Assistant, School of Civil and Environmental Engineering, Georgia Tech Regional Engineering Program, Savannah, GA 31405.

[2] Associate Professor, School of Civil and Environmental Engineering, Georgia Tech Regional Engineering Program, Savannah, GA 31405.

Introduction

Hartwell Lake, a U.S. Army Corps of Engineers reservoir, is located on the Savannah River, between Anderson, South Carolina, and Hartwell, Georgia, USA (Figure 1). The reservoir was built between 1955 and 1963, with joint goals of flood control, power production, water supply, and recreation. It covers 227 km^2, has a shoreline length of 1548 km with an average depth of 20 meters. The terrain consists primarily of gentle rolling hills and pine forest near the southern terminus of the Appalachian mountain chain. Sediments contain high fractions of silt and clay.

High concentrations of polychlorinated biphenyls (PCBs) are found in the lake and in Twelve-Mile Creek, a tributary, resulting from the operation of a capacitor manufacturing facility in the Twelve Mile Creek Watershed between 1955-1976. PCBs are known to cause cancer in animals and can cause non-cancer health problems, such as reduced ability to fight infections, and low birth weights in humans (Clearwater 1997). PCBs are hydrophobic, and typically bond to sediments. They also exhibit an affinity for fine-grained sediments, such as silts and clays (EPA 1991). The U.S. EPA performed and sponsored research on PCBs in Hartwell Lake (Elzerman et al. 1994), and EPA's selected remedy was to rely on burial by natural sedimentation processes. Over time, incoming "clean" sediments should bury the contaminated sediments, providing a clean sediment cap on top and gradually reducing the health risks. Numerical modeling of sediment transport in Twelve-Mile Creek has also been performed to support this conclusion, focusing on non-cohesive sediments (EPA 1991). However, the degree of contamination of the main pool of the lake, due to transport of (primarily) cohesive sediments from Twelve-Mile Creek, has not been studied previously and is addressed in this paper.

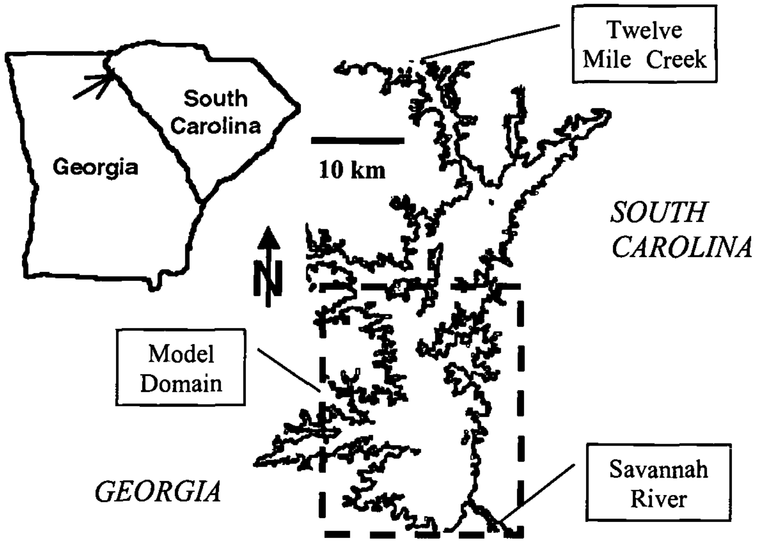

Figure 1 – *Map of Study Site. Model Domain Shows the Main Pool of the Lake Modeled to Describe the Circulation and Sediment Deposition Patterns.*

The primary objectives of this study are thus to describe hydrodynamic circulation and sedimentation in the main pool of Hartwell Lake. The cohesive sediments are of primary interest because of their potential to travel greater distances and to transport PCBs.

The hydrodynamic model of Hartwell Lake is developed using the Environmental Fluid Dynamics code (EFDC), developed by Hamrick (1996). EFDC was developed to simulate flows and transport processes in surface water systems, including rivers, lakes, estuaries, wetlands and coastal areas. The structure of the EFDC model includes four major modules: (1) a hydrodynamic model, (2) a water quality model, (3) a sediment transport model, and (4) a toxics model. EFDC is capable of simulating both cohesive and noncohesive sediment transport, near-field and far-field discharge dilution from multiple sources, eutrophication processes, and the transport and fate of toxic contaminants in the water and sediment phases. For a detailed description of EFDC, the reader is referred to Hamrick and Wu (1997).

The model has been applied to several water systems. Applications of the model include a study of tidal intrusion and its impact on larval dispersion in the James River estuary (Shen et al. 1999a), modeling an estuarine front and its associated eddy (Shen and Kuo 1999b), investigation of bottom shear stress in estuaries (Kuo et al. 1996), hydrodynamic and sediment transport modeling in the middle Atlantic Bight (Kim et al. 1997). Simulation of Lake Okeechobee hydrodynamic and thermal processes (Jin et al. 2000, 2001, 2002), hydrodynamic and water quality modeling in Peconic Bay (Tetra Tech 1999), and simulation of wetting and drying processes of hydrodynamic and sediment transport in Morro Bay (Ji et al. 2000, 2001a) are among other applications.

Hydrodynamic Model Setup

Hydrodynamic circulation patterns in the main pool of Hartwell Lake are mainly controlled by wind, inflows and outflows. Daily inflow and outflow data for Hartwell Lake were obtained from the U.S. Army Corps of Engineers. USACE derives inflow values from volume balance of the reservoir and calculates outflows by converting the power measured at the power plant into discharge. Thus the published inflow values include the changes in the reservoir including rainfall, evaporation, and infiltration. Wind data were obtained from the National Oceanic and Atmospheric Administration for Greenville-Spartanburg Airport, SC, located 65 kilometers northeast of the lake. Available data include average and peak hourly wind speed and corresponding direction, and cover the period 1962 to the present.

EFDC has been applied to Hartwell Lake to simulate lake response to wind forcing and inflows/outflows and to simulate long-term sediment deposition patterns. For this purpose a careful examination of available data is necessary since it is not practical to simulate and obtain results for every single wind forcing and flow condition. To determine which forcing combinations should be simulated to represent long-term deposition patterns, a statistical analysis of daily mean values of inflow, outflow and wind data for ten years (1990-1999) was performed. Figure 2 is a histogram based on 10 years of flow data, and shows that 20% of the time no water was released at the dam, and about 40% of the time outflows were in the range of 75-150 m^3/s. Whereas about 30% of the time inflows in the range of 25-75 m^3/s were observed. Mean outflow and inflow values were the same: 120 m^3/s.

Histogram of daily mean wind speeds is shown in Figure 3, indicating that 46% of the time observed wind speeds were in the range of 2-3.5 m/s. Two dominant wind directions were observed in the study area, northeast and southwest. 36% of the time winds were blowing to northeast with a mean speed of 1.7 m/s and 35% of the time winds were blowing to southwest with a mean speed of 2.6 m/s.

The computational mesh was constructed using Digital Elevation Model data and is shown in Figure 4. The computational grid had 51×94 horizontal cells and five vertically stretched layers, each with a fractional thickness of 20% of the water depth. Horizontal discretization was 150 m on a side. Bathymetry of the lake is shown in Figure 5.

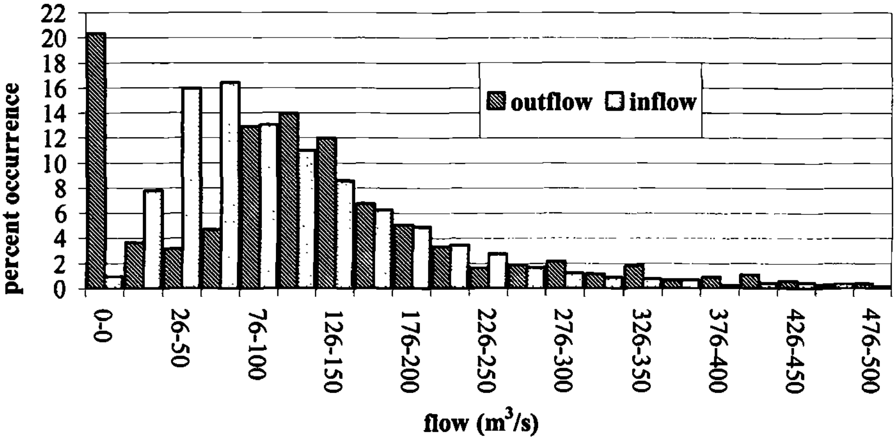

Figure 2 – *Histogram of Daily Mean Flows for Ten Years (1990-1999).*

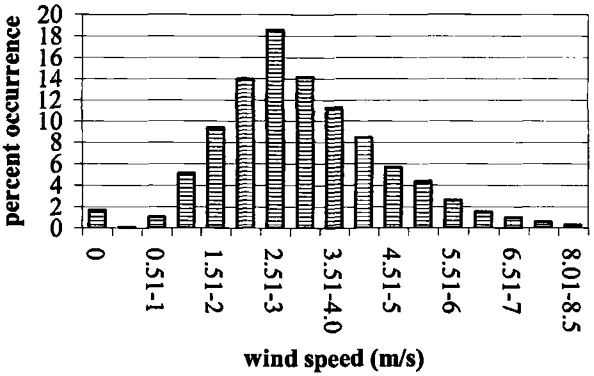

Figure 3 – *Histogram of Daily Mean Wind Speed Measured at 10 m Height for Greenville-Spartanburg Airport, SC, for Ten Years (1990-1999).*

The river inflows and controlled outflow at the dam were simulated as sources and sinks in the model system. At upstream boundaries, the river inflow rates were uniformly distributed according to the depth of each computational cell in horizontal and according to thickness of vertical layers in vertical. The controlled outflow at the dam was specified at one cell at the downstream boundary.

Sensitivity Analysis

Several variables including lake water level, grid size, number and thickness of vertical layers, wind direction and inflow and outflow magnitudes were systematically altered as part of a sensitivity analysis. The analysis of daily water level data from 1964-2001 (Figure 6) showed that minimum and maximum water levels in Hartwell Lake have varied by up to six meters. When the same analysis was conducted for 1990-1999, minimum and maximum water levels have varied by three meters. In order to investigate the sensitivity of the model results to seasonal changes in lake level, the model was run using two water levels where depth was changed by five meters. During the simulation, zero initial velocity was considered in a closed basin.

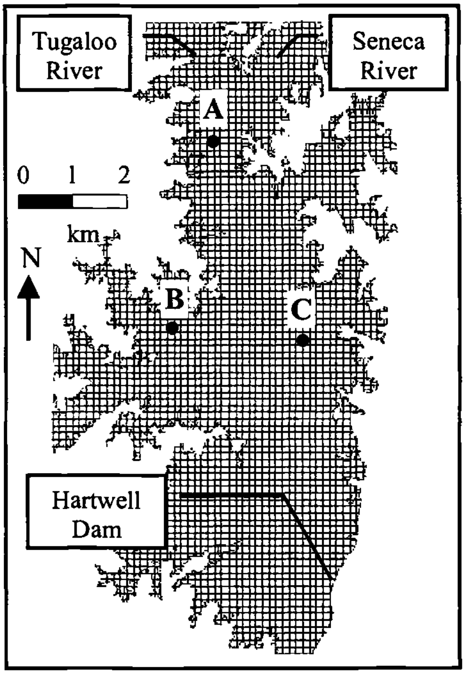

Figure 4 – *Finite Difference Computational Mesh for Hartwell Lake. Computational Cells are 150 m × 150 m. A, B, and C Represent Arbitrarily Selected Locations for Comparison of Model Results.*

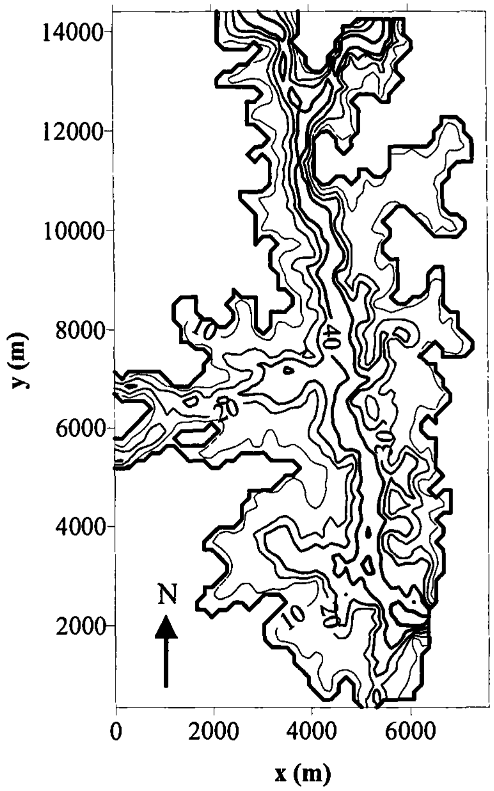

Figure 5 – *Bathymetry of Hartwell Lake Used in Simulations. Depth Ranges between 0 to 50 Meters. Contour Interval is 10 Meters.*

In shallow parts of the lake, significant differences in surface layer velocities were observed because of drying of cells that were wet in the initial run. The root-mean-square (RMS) value was used to evaluate the differences in simulation results and calculated by equation (1).

$$H_{RMS} = \sqrt{\frac{\sum_{i=1}^{N} (H_1 - H_2)^2}{N}} \tag{1}$$

where

H_1, H_2 = the value of same variable obtained from first and second simulations
N = the number of different data locations being compared

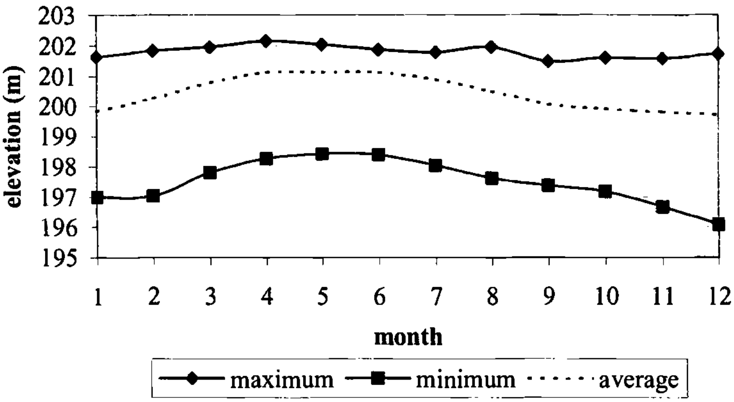

Figure 6 – *Variation in Maximum, Minimum and Average Monthly Water Levels throughout the Year on Hartwell Lake for the Years 1964-2001.*

The RMS of change in flow speed magnitude was 0.02 cm/s (about 0.1% of maximum velocity observed) when the cells initially shallower than 5 m were excluded (*N* = 2405). Whereas the RMS change increased to 2.5 cm/s when all cells were included in the calculation (*N* = 2468). In the analyses velocity components were compared separately. Based on the results above it has been concluded that for deeper parts of the lake (>5 meters), which in fact are of interest for purposes of this study, the simulation results are not sensitive to seasonal changes in water levels.

Sensitivity of model results to grid cell size was investigated using two different grid configurations as given in Table 1. In the main pool calculated velocities were almost the same with an RMS change of 0.01 cm/s, whereas in the shallower parts of the lake (<5 meters) the results changed significantly with a RMS change of 1.52 cm/s. It is concluded that Hartwell Lake can be simulated using 51 × 94 grid configuration.

Table 1 – *Computational Grids Used in Calculations*

Cases	Grid configuration	Cell width (m)	No. of vertical cells
1	51 × 94	150	5
2	103 × 188	75	5

Selection of vertical layers was found to be important for Hartwell Lake. When three vertical layers were simulated and velocities were compared to simulation results with ten vertical layers, RMS change of velocities increased to 6 cm/s, whereas RMS change obtained from comparison of five layer and ten layer simulations was 0.8 cm/s. Therefore in all runs five or more vertical layers were selected. Another purpose of the sensitivity analyses was to evaluate the sensitivity of bottom layer (10% of depth in each case) velocities, which is important for sediment transport studies, to the total number of vertical layers. The results showed that when the same relative thickness was selected for the bottom layer, bottom layer velocities were not sensitive to the number of layers.

Lakewide circulation patterns are very sensitive to wind direction and magnitude, inflow and outflow magnitudes. Wind is typically the major force driving the circulation. Surface currents followed the dominant wind direction in each case. When wind speed was reduced from 6.8 to 2.8 m/s and the flows were kept constant, we observed an average difference of 3.5 cm/s in surface velocities. RMS change was calculated as 4 cm/s.

Sensitivity of model results to inflows was investigated by comparing three different inflow magnitudes. In all simulations wind was kept at zero. The second and the third tests of sensitivity to inflow included two times and five times the initial inflow in magnitude. Increase of inflow by two times resulted in an increase of two times, while an increase of inflow by five times resulted in an increase of six times the average of surface layer velocity in the model domain.

Long-term deposition patterns for the sediments were investigated for representative wind and flow conditions. Joint histograms of the inflow, outflow and wind speed data were investigated. The most frequently observed conditions were determined and used for numerical simulations of hydrodynamic processes in Hartwell Lake. The selected cases discussed in this paper are listed in Table 2. The values in case 1 are the most frequently observed values when individual histograms are considered, values in cases 2, 3 and 4 are selected based on results of joint histograms.

Table 2 – *Values of Parameters Used in Model Simulations.*

Cases	Inflow (m^3/s)	Outflow (m^3/s)	Wind Speed (m/s)	Wind Direction (°)
1) Average inflow, no outflow, dominant northeast wind with average speed	68	0	2.8	55
2) High inflow, high outflow, dominant northeast wind with high speed	465	447	6.8	55
3) High inflow, high outflow, dominant southwest wind with high speed	465	447	6.8	235
4) Moderate inflow, moderate outflow, dominant northeast wind with moderate speed	96	30	3.6	55

Discussion of Results

The top and the bottom layer velocity distributions within Hartwell Lake after five days of simulation with forcing conditions specified as case 3 in Table 2 are given in Figures 7 (a) and 7 (b). At least five days of simulation was required because it takes four days for sediments to settle 50 meters with the specified settling velocity. A 90 day simulation with measured time series of input was conducted and it was observed that velocity distribution and sedimentation patterns were similar to the five day simulation with average values of wind and flows as input data. Figure 7(a) shows that surface flow velocities closely match the wind direction except where the vortices were present. Maximum surface velocities (approximately 5 cm/s) were about 1% of wind speed. The bottom layer velocities shown at Figure 7(b) are much lower in magnitude than the surface velocities and formed a return flow.

Sediment deposition within Hartwell Lake with the conditions corresponding to case 3 in Table 2 is shown in Figure 8, indicating that sediments have mostly deposited in the deeper parts of the lake closer to the dam. When extrapolated, 3.6 m of deposition in 40 years (0.09 m per year) is estimated. Two bathymetric surveys of the lake were conducted by USACE; one in 1959 before completion of the reservoir, and one in 1973. Although the 1959 survey includes several cross sections within the main pool, surveys from both years were mostly available for the upstream region of the model domain. Results of these surveys suggested deposition rates of 0.29 m per year in shallow regions, and 0.05 m per year in deeper regions of both the Seneca and the Tugaloo Rivers. A surveyed

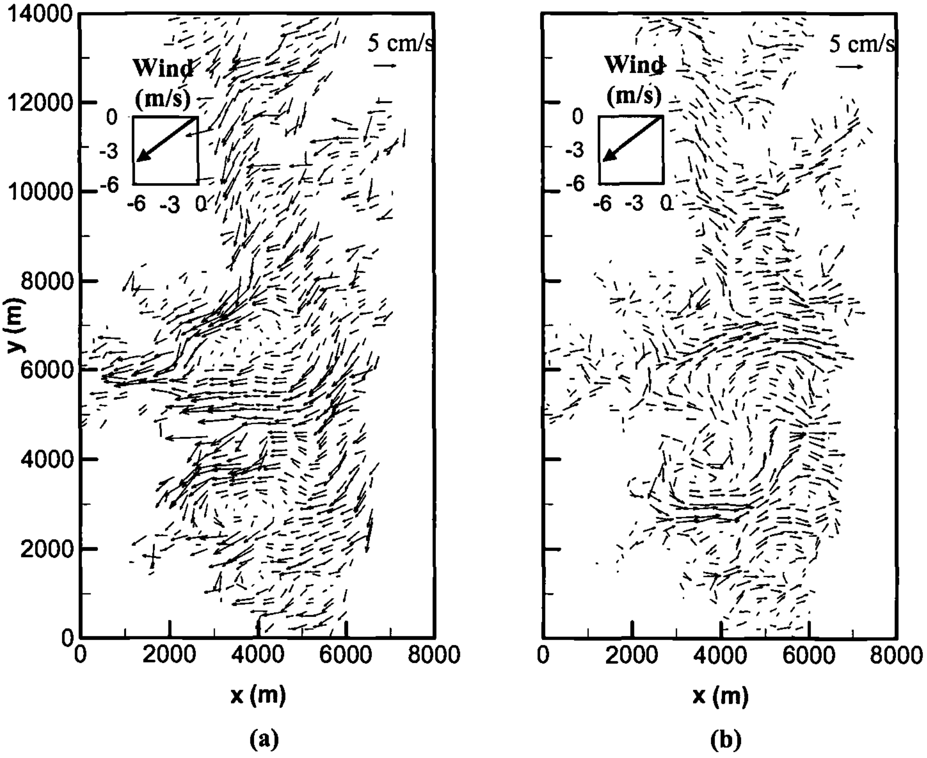

Figure 7 – *Simulated (a) Top Layer and (b) Bottom Layer Cell Velocity Distribution for Case 3 in Table 2 (Inflow = 465 m^3/s, Outflow = 447 m^3/s, Wind Speed = 6.8 m/s).*

section within the model domain boundaries shown by the dotted line in Figure 8 indicated a deposition rate of 0.1 m per year that agrees well with the estimated deposition rate of 0.09 m per year. An ongoing field study conducted by the authors will reveal the deposition rates after 40 years of operation of reservoir.

When results for cases with lower wind speeds were generated, it was observed that sediments followed the thalweg and were deposited in the deeper parts of the lake regardless of the magnitudes of inflows and outflows. Local effects of inflows and outflows were observed. When the inflow magnitude was increased for instance, higher sediment deposition was observed in the uppermost part of lake, the throat, although the deposition patterns remained the same elsewhere, indicating that higher inflow affected the bottom layer velocity distribution, thus the deposition pattern there.

Simulated velocity profiles at 3 different locations represented by points A, B, and C in Figure 4 are shown in Figures 9 and 10 for east-west and north-south components respectively. Corresponding water depths at these locations are 34 m, 31 m, and 24 m. In all cases the velocity profiles showed variability in directions at surface and bottom layers indicating reverse flow. This was expected, since, the shear force developed by the wind at the surface would be balanced by the hydrostatic force of reverse flow. These results agree well with bottom layer velocity vector distributions.

Summary and Conclusions

In this study, application of a numerical model for simulation of hydrodynamic circulation and sediment transport in a lake with respect to wind forcing and inflows/outflows is described. The motivation is related to a PCB contamination problem in the upper reaches of the lake. Remediation of the pollution problem requires knowledge of the level of sedimentation in the lake, its rate of change, and the fate of contaminated sediments.

This study also describes a sensitivity analysis conducted to assess the response of the lake hydrodynamics to different variables. The model assessment was quantified in terms of RMS values. Several variables, including lake levels, grid size, number and thickness of vertical layers, wind direction and inflow/outflow magnitudes, were investigated through a sensitivity analysis. The results of the sensitivity analysis indicated that the calculated velocities in the main pool were not sensitive to lake levels and grid size. Selection of the number and thickness of the vertical layers, on the other hand, were found to be critical, and selection of at least 5 vertical layers was suggested. Although not investigated in this paper, thermal stratification can be used as a reference for selection of vertical layer boundaries. Lakewide circulation patterns were very sensitive to wind direction and magnitude, inflow and outflow magnitudes. Wind was found to be the major force driving the circulation.

The zones where contaminated sediments are likely to deposit and the deposition rates were presented for one set of forcing conditions. We observed that sediments have mostly deposited in the deeper parts of the lake closer to the dam. It can be stated that, wind direction and magnitude primarily control the bottom layer velocity distribution, which

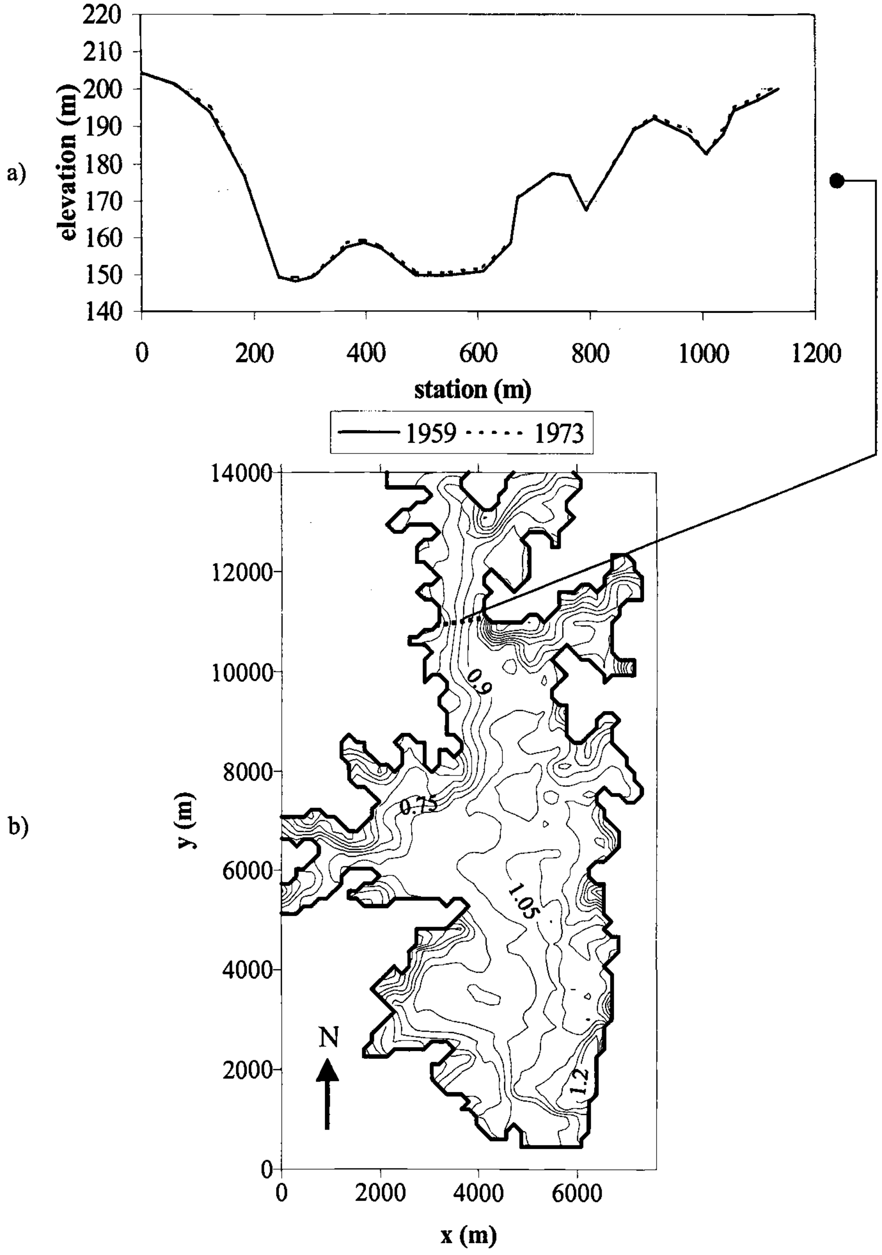

Figure 8 – *Sediment Deposition in Millimeters within Hartwell Lake after 5 Days of Simulation for Case 3 in Table 2 (Inflow = 465 m*^{3}*/s, Outflow = 447 m*^{3}*/s, Wind Speed = 6.8 m/s). Dashed Line in Part b) Shows the Cross-Section Surveyed by USACE in 1959 and 1973.*

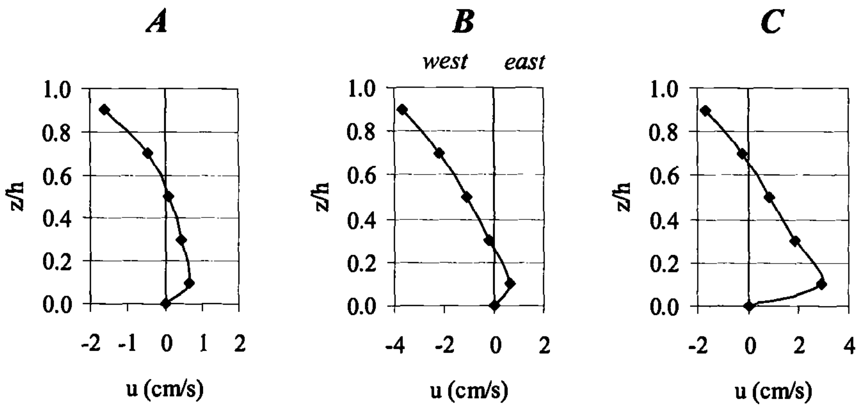

Figure 9 – *Velocity Profiles for East-West Component of Velocity Computed by the Model at Three Locations (A, B, C Shown in Figure 4) for Case 3 in Table 2 (Inflow = 465 m³/s, Outflow = 447 m³/s, Wind Speed = 6.8 m/s).*

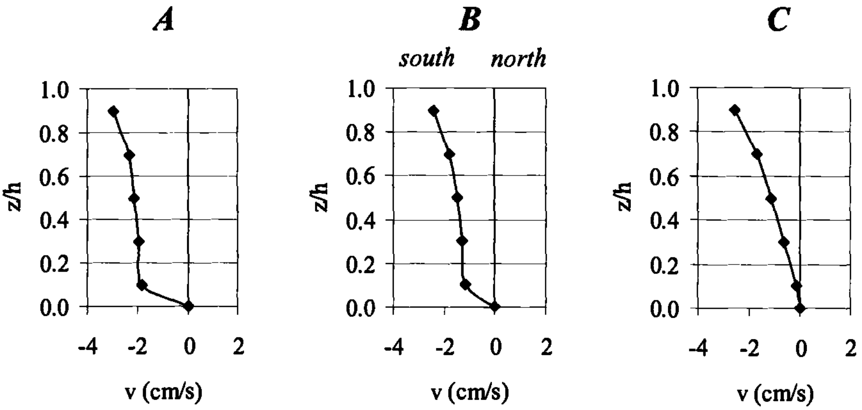

Figure 10 – *Velocity Profiles for North-South Component of Velocity Computed by the Model at Three Locations (A, B, C Shown in Figure 4) for Case 3 in Table 2 (Inflow = 465 m³/s, Outflow = 447 m³/s, Wind Speed = 6.8 m/s).*

directly controls the depositional patterns. For high wind speeds, deposition zones were shifted away from the thalweg according to dominant wind direction. For low wind speeds, sediments simply followed the thalweg and were deposited in deeper parts of the lake. Inflows and outflows had local effects at bottom velocity vectors. Increased inflow rate coming from the tributaries introduced vortices in the upstream regions of the model domain, resulting in higher deposition rates.

Maximum deposition rate was estimated as 0.09 m per year for a selected forcing combination representing commonly observed winds, inflows and outflows. This deposition rate was compared to available surveys conducted in 1959 and 1973 by USACE. Two surveys indicated a maximum deposition rate of 0.1 m per year that agreed well with the estimated deposition rate of 0.09 m per year by the numerical model. An ongoing field study conducted by the authors will reveal the deposition rates after 40 years of operation of the reservoir.

Acknowledgements

The work summarized in the present paper was supported by the South Carolina Water Resources Center (SCWRC), the Georgia Water Research Institute (GWRI), and the U.S. Geological Survey (USGS).

References

Clearwater, 1997, *PCB Contamination Of The Hudson:* addressed at http://www.clearwater.org/news/hazard.html.

Elzerman, A. W., Farley, K. J., Dunnivant, F. M., and Cooper, C., 1994, "Predicting the Future Fate of PCBs in Lake Hartwell," *Technical Completion Report, G1588-03,* submitted to U.S. Department of the Interior, U.S. Geological Survey Reston, VA.

EPA, 1991, *Sangamo-Weston Inc./Twelve-Mile Creek/Lake Hartwell PCB Contamination*: addressed at http://www.epa.gov/oerrpage/superfund/sites/npl/nar486.htm

Hamrick, J. M., 1996, "User's Manual for the Environmental Fluid Dynamics Computer Code," *Special Report No. 331*, The College of William and Mary, Gloucester Point, VA.

Hamrick, J. M., and Wu, T. S., 1997, "Computational Design and Optimization of the EFDC/HEM3D Surface Water Hydrodynamic and Eutrophication Models," *Next Generation Environmental Model and Computational Methods*, G. Delich and M. F. Wheeler, eds., Society of Industrial and Applied Mathematics, Philadelphia, pp. 143–161.

Ji, Z. G., Morton, M. R., and Hamrick, J. M., 2000, ''Modeling Hydrodynamic and Sediment Processes in Morro Bay,'' *Estuarine and Coastal Modeling: Proceedings, 6th International Conference*, M. L. Spaulding and H. L. Butler, eds., ASCE, New York, pp. 1035–1054.

Ji, Z. G., Morton, M. R., and Hamrick, J. M., 2001a, ''Wetting and Drying Simulation of Estuarine Processes,'' *Estuarine, Coastal Shelf Science*, 53, pp. 683-700.

Jin, K. R., Hamrick, J. H., and Tisdale, T., 2000, ''Application of a Three-Dimensional Hydrodynamic Model for Lake Okeechobee,'' *Journal of Hydraulic Engineering*, 126 (10), pp. 758–771.

Jin, K. R., and Ji, Z. G., 2001, ''Calibration and Verification of a Spectral Wind-Wave Model for Lake Okeechobee,'' *Journal of Ocean Engineering*, 28, pp. 571–584.

Jin, K. R., Ji, Z. G., and Hamrick, J. M., 2002, ''Modeling Winter Circulation in Lake Okeechobee, Florida,'' *Journal of Waterway, Port, Coastal, and Ocean Engineering*, ASCE, 128 (3), pp. 114-125.

Kim, S., Wright, D. L., Maa, J., and Shen, J., 1997, ''Morphodynamic Responses to Extratropical Meteorological Forcing on the Inner Shelf of the Middle Atlantic Bight: Wind Wave, Currents and Suspended Sediment Transport,'' *Estuarine and Coastal Modeling: Proceedings, 5th International Conference*, M. L. Spaulding and H. L. Butler, eds., ASCE, New York, pp. 456–466.

Kuo, A.Y., Shen, J., and Hamrick, J. M., 1996, "The Effect of Acceleration on Bottom Shear Stress in Tidal Estuaries," *Journal of Waterway, Port, Coastal, and Ocean Engineering*, ASCE, 122 (2) pp. 75–83.

Shen, J., Boon, J., and Kuo, A. Y., 1999a, ''A Numerical Study of a Tidal Intrusion Front and Its Impact on Larval Dispersion in the James River Estuary, Virginia,'' *Estuaries*, 22 (3), pp. 681–692.

Shen, J., and Kuo, A. Y., 1999b, ''Numerical Investigation of an Estuarine Front and Its Associated Eddy,'' *Journal of Waterway, Port, Coastal, and Ocean Engineering*, ASCE, 125 (3), pp. 127–135.

Tetra Tech, 1999, ''Theoretical and Computational Aspects of Sediment Transport in the EFDC Model,'' *Technical Report Prepared for U.S. Environmental Protection Agency*, Tetra Tech, Inc., Fairfax, Va.

Rosa Galvez-Cloutier,[1] Myriam Muris,[2] Jacques Locat,[3] and Cyril Bourg[2]

Retention of Heavy Metals in the Post '96 Flood Sediment Layer Deposited in the Saguenay River, Quebec, Canada

Reference: Galvez-Cloutier, R., Muris, M., Locat, J., and Bourg, C. **"Retention of Heavy Metals in the Post '96 Flood Sediment Layer Deposited in the Saguenay River, Quebec, Canada,"** *Contaminated Sediments: Characterization, Evaluation, Mitigation/Restoration, and Management Strategy Performance, ASTM STP 1442*, J. Locat, R. Galvez-Cloutier, R. C. Chaney, and K. R. Demars, Eds., ASTM International, West Conshohocken, PA 2003.

Abstract: In July 1996 during a 50 year event flood, a new layer of sediments composed of debris, gravel and fine materials was transported and deposited over an ancient, one meter contaminated layer of sediments in the Saguenay River Fjord and Ha! Ha! Bay floors. During the Industrial Revolution years, various metallurgic, plastic, aluminum and pulp and paper production industries discharged their wastes on these waters, resulting in the high contamination of both water and sediments. This contamination limited the exploitation of fish and seafood. Given that the new layer is composed essentially of cleaner material, the zone is presenting important changes in the direction of a healthier environment. The Canadian Government and some of the surrounding industries aim to assess the new potential of the zone and its environmental safety. At present, it represents over a million-dollar study.

This part of the Saguenay project aimed to recognize and evaluate the capacity of the new layer to contain and retain the contaminants left at the bottom layer. Particular interest is given to mercury and to heavy metals such as Pb, Zn, Cd, and Ni and to their geochemical distribution among natural adsorbing materials such as clays, oxides, carbonates and organic matter.

The paper presents the recognition and sampling mission on the Alcide Horth Ship, the contamination profiles given in two dimensions (length and depth), the geochemical distribution of heavy metals on the contaminated layer, transition layer and new layer as well as the evolution of their retention and transfer. Discussion and relations with common sediment characteristics such as grain size, cation exchange capacity and surface area are also given. Sequential selective extraction has been used jointly with scanning electron microscopy (SEM) to study heavy metal species.

Keywords: heavy metals, sediments, speciation, retention

---

[1] Associate Professor, Department of Civil Engineering, Laval University, Quebec, Canada, G1K 7P4.

[2] Graduate students, Ecole Nationale de Travaux Public de l'État, Lyon, France.

[3] Professor, Department of Geology, Laval University, Quebec, Canada, G1K 7P4.

Introduction

On July 1996, the Saguenay region north of Quebec City in Canada was affected by a 50-year diluvial rain that caused the flood of the Saguenay River. During 3 days, 200 mm of precipitation caused the erosion and transport of six million tonnes of sediments composed of debris, gravel and fine materials that were deposited over an ancient, about one meter contaminated layer of bottom sediments in the Saguenay River Fjord and the Ha! Ha! Bay. During the Industrial Revolution years, various metallurgic, plastic, aluminium and pulp and paper production industries discharged their wastes in to these waters, resulting in the high contamination of water and sediments. Mercury and heavy metals such as Pb, Zn, Cd, Ni, Hg and PAH (Poly Aromatic Hydrocarbons) and MAH (Mono Aromatic Hydrocarbons) have been detected in the Saguenay zone during earlier studies before the flood (Gagnon et al., 1993; Fortin and Pelletier 1995). This contamination limited the exploitation of fish and seafood. Given that the new layer is composed essentially of cleaner material, the zone is presenting important changes in the direction of a healthier environment. The Canadian government and some of the surrounding industries are aiming to assess the new potential of the zone and its environmental safety. At present, it represents over a million-dollar study.

Sediments are an important and integral component of aquatic ecosystems because they provide a substrate and habitat for a wide variety of organisms as well as species that are important in the food chain (Galvez-Cloutier et al., 1995). Sediments are also recognized contaminant reservoirs and constitute, under certain conditions, a source for contaminant release. Upon release into the interstitial water, they may diffuse to the overlying water, affecting benthic and higher organisms. The aim of this project was 1) to diagnose the quality of the bottom and upper layer sediments, and 2) to assess the potential for retention or transfer of contaminants into the interstitial water.

Site Characteristics and Sampling Strategy

The Saguenay Fjord is located 200 km north east of Quebec (see Figure 1) and it expands linearly from Chicoutimi to Tadoussac. The Saguenay River takes its sources at the Saint-Jean Lake and flows at 1000 m^3/s. The Saguenay fjord is a narrow corridor, 1 to 3 km large, perpendicular to the Saint-Lawrence River Estuary. It is approximately, 70 km long and 280 m deep. At the East end of the fjord, the river splits in two portions forming the Ha! Ha! Bay and the "northern branch". The sedimentation rate varies from 0.1 cm/year in the bay to 7 cm/year in the northern branch (Smith and Walton, 1980). For this study, 3 sampling locations were chosen: the SAG5 in the northern branch, the B04 in the Ha! Ha! Bay and the B08 where the bay and river melt its waters. Respectively, these locations were representative of high erosion-high advection, low erosion-low currents and average conditions.

During a recognition and sampling mission on the Alcide Horth Ship during the summer of 2000, core and box sediment samples were taken at the three locations described above. Core samples were extracted using a Lehigh core equipment that allowed the extraction of about 2 m long, 10 cm diameter cores.

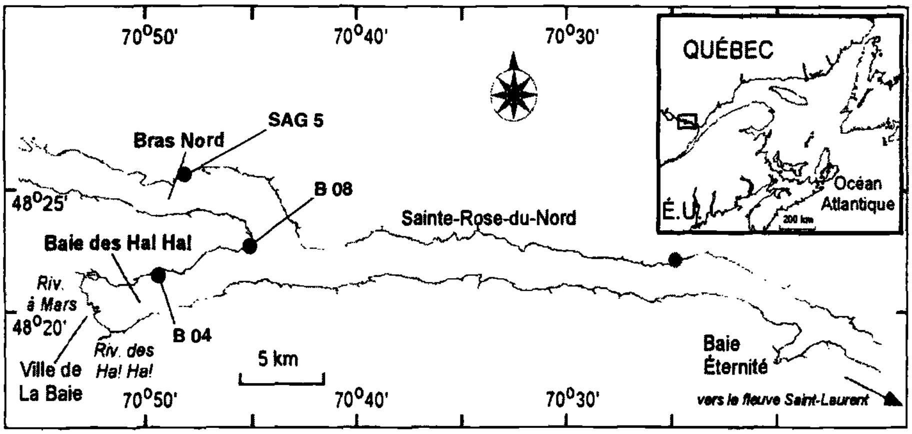

Figure 1 — *Sampling Sites at the Saguenay Fjord*

Physico-chemical, mineralogical and contaminant characterization were run on core samples. Boxes of 50 cm x 50 cm x 60 cm were used to obtain smaller core samples that were placed on Plexiglas columns to run the diffusion tests.

General Geochemical Characterization of Sediments

General characteristics included the measurement of water content according to ASTM standard D-2216, alkaline metals and mineralogy by X-ray diffraction according to procedures described in ASA, (1986), carbonate content by acid titration (AFN, 1982), organic matter by combustion (BNQ 1993), buffering capacity by acid/base titration (Yong, 1990), Cation and Anion Exchange Capacities (CEC & AEC) according to Duquette and Hendershot (1993) and Specific Surface Area (SSA) according to the blue methyl method (BNQ, 1993).

Based on the characteristics measured in the core samples, the Saguenay and Ha! Ha! Bay floor may be schematized as presented in Figure 2. Depending on the location (Bay, Northern branch or Melting sector) the thickness profile of the cores varied. The interface layer was located at 60 cm deep on the northern branch but only 21 cm deep on the Bay and 25 cm on the Melting sector. A typical profile indicating these limits can be viewed from the water content profile shown in Figure 3.

For samples taken at depths before the flood, titration results showed that all locations presented important buffering capacities. Higher values were found in upper layers that were richer in carbonates. CEC determinations yield 15 to 20 meq/100g for all locations showing higher values to locations with higher pH. SSA values fall between 12 and 30m^2/g that are characteristics of soils with poor clay materials. In this case, kaolinite and illite were found at trace levels.

All metals (alkaline, heavy metal and transition metals) were measured by AAS following the procedure described by CSL (1993). As can be seen in Figure 4, for elements such as Mg, Na, Fe, Mn and K, the trace of the flood resulted in a decrease of concentration. Opposite to this, Ca presented a peak that corresponded to the '96 layer that is associated with higher carbonate concentrations (i.e. for the Ha! Ha! Bay: 0.70 in the ancient layer and 3.5 in the '96 layer) (Ize, 2000) and to the higher buffering capacity discussed previously.

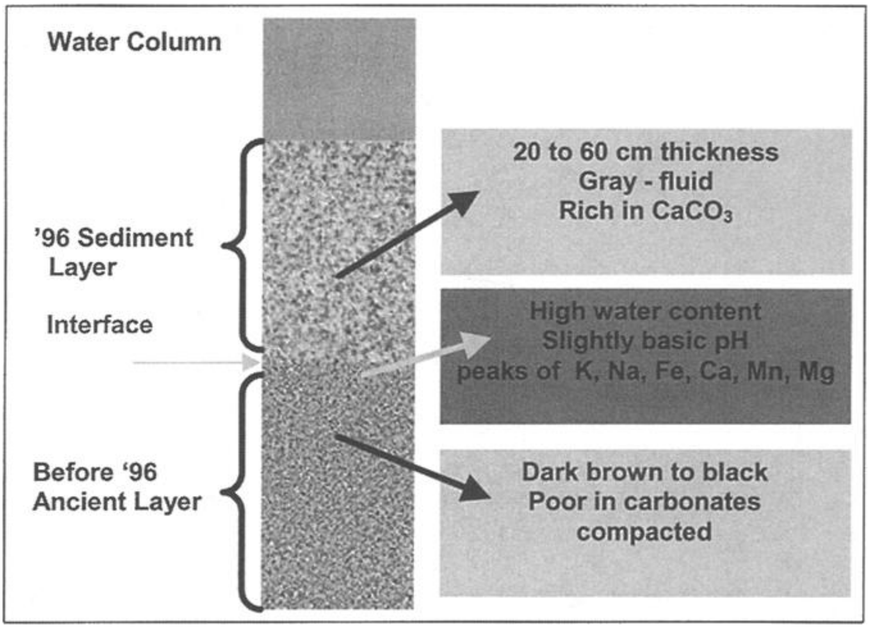

Figure 2 —*Typical Sediment Profiles after the '96 Flood*

Evaluation of Retention

Various studies (Yong and Phadungchewit 1993; Galvez-Cloutier et al. 1995) have shown the importance of metal partition and distribution in the determination of metal availability for transfer and transport. Changes in the physico-chemical conditions of the immediate surrounding environment have to be considered in the evaluation of the final fate of contaminants. As shown in Figure 5, the mechanisms of retention of cations are adsorption at the surface of clay minerals, oxides and hydroxides, organic matter, the (co)precipitation and with secondary minerals, complexation and coagulation with organic matter, and the penetration of metals in the crystalline structure of primary minerals (Galvez-Cloutier, 1995). Heavy metal retention by the solid components of the sediments results from the heterogeneous equilibrium set among water, sediments components and contaminants. Reactions such as oxidation-reduction, precipitation and changes in pH or Eh may modify the geochemical form and bioavailability of heavy metals.

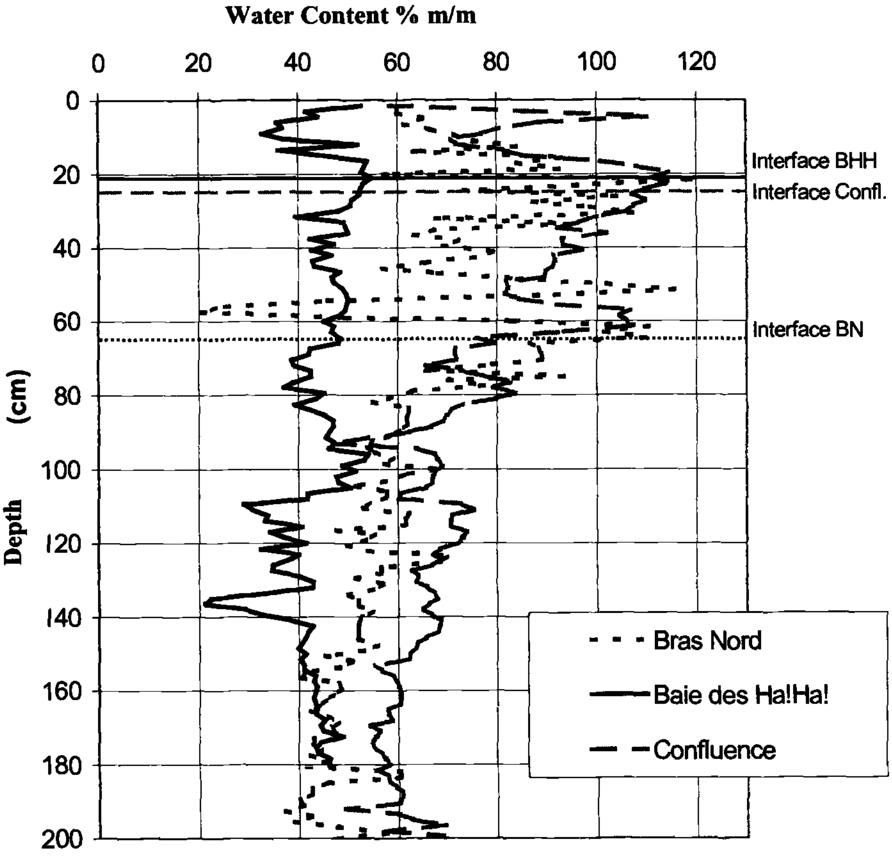

Figure 3 — *Water Content Profiles*

During this study, heavy metal retention was evaluated using a sequential selective extraction (SSE) method. SSE relies on the concept that by using appropriate chemical reagents the different metal fractions can be released once the binding phase is destroyed. The extracting reagents in most of the cases are taken from routine individual soil analysis. According to the method used in Yong et al. (1993) a maximum of five metal fractions can be separated by sequential extractions associated to: (1) exchangeable, (2) to carbonates, (3) to metal oxides, (4) to organic matter and (5) to residual mineral crystals.

A metal mass balance was obtained by comparing total metal concentrations to SSE results. Total concentrations were obtained by acid digestion using nitric acid, hydrogen peroxide and Aqua-Regia reagent (Centre Saint Laurent, 1993) and were dosed using a 3110 Model Perkin-Elmer AAS instrument. Mercury was transformed to hydride before its detection by cold vapour in AAS.

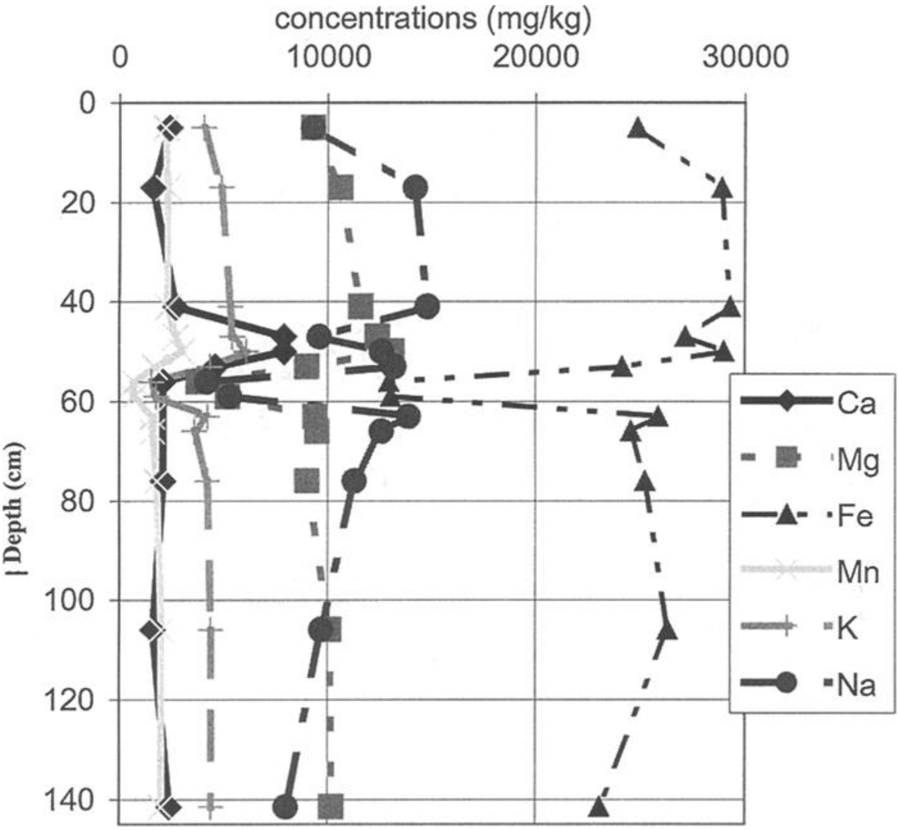

Figure 4 — *Typical Metal Profiles, Case of the Northern Branch*

As shown in Figure 6, the 3 sites showed high concentrations of mercury exceeding the SEM (Minimal Effect Level) value for all samples within the first 60 cm with a peak at the interface layer. It also presented higher values than those reported by Barbeau et al. 1981. Concentrations decreased with depth except for a deeper peak that was found about 1.35 cm depth below the melting zone that exceeded the SET (Toxic) level. This may have corresponded to a more ancient deluge most probably that one at St-Vianney (Quebec) that had similar effects to the '96 flood.

Figure 7 shows the concentration profiles for Cr, Cu, Pb and Zn for the 3 sampling sites (Figs. 7a, 7b and 7c respectively). As it can be seen, concentrations were higher within the interface layer, which is mostly a mixture of the most superficial portion of the ancient layer.

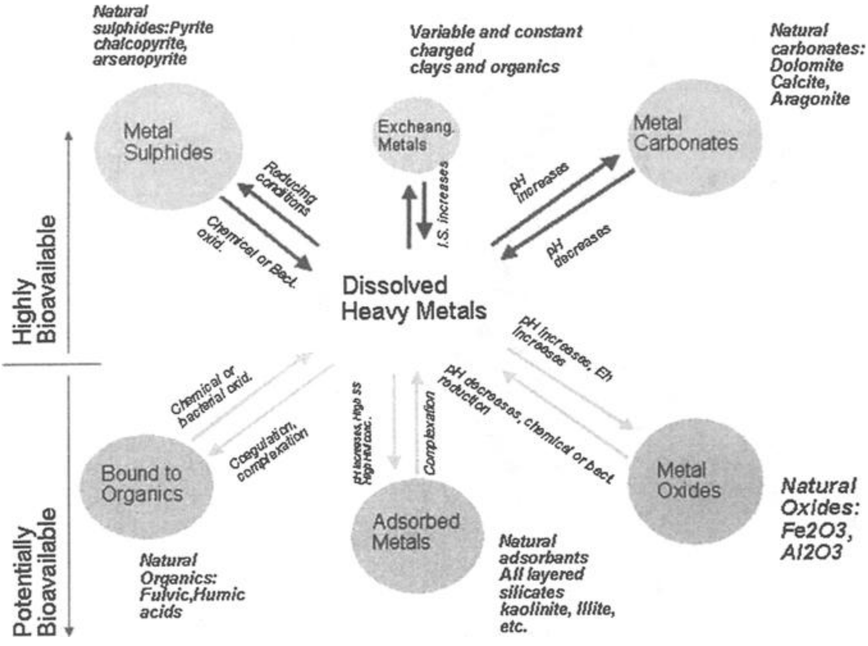

Figure 5 — *Heavy Metal Partition. Source: Galvez-Cloutier (1995)*

Indeed, when the new layer was transported it caused an abrasive front that scavenged the ancient layer forming an "interface layer" that presented various depths ranging from almost zero to 50 cm.

Lower concentrations were found in the Northern branch followed by the Bay and finally the melting zone. In general, the order of decreasing concentrations was Zn>Pb>Cr>Cu for the 3 sites. All metals concentrations exceeded the SEM values of the MEO (1990) and MEC (1992) guidelines at the interface layer and decreased with depth.

The Figure 8 presents the distribution of Cu, Zn and Pb found at the interface zone for the sites at the Ha! Ha! Bay and at the Northern branch (which were the most contaminated). Each sample was analyzed for ESS in triplicate following the procedure described in Yong et al, 1993. From Figure 8 it can be seen that only 4 of the six phases analyzed were present in significant manner. Also, it can be seen that the distribution was similar for both sites.

At the northern branch Cu and Zn presented, in decreasing order of importance, associations to: organic matter > residual > oxides and hydroxides > carbonates > exchangeable. For Pb the order was: oxides and hydroxides > residual > organic matter > carbonates > exchangeable. At the Bay, the pattern was similar for Pb and Cu but slightly different for Zn in which the fraction associated to OM was lower.

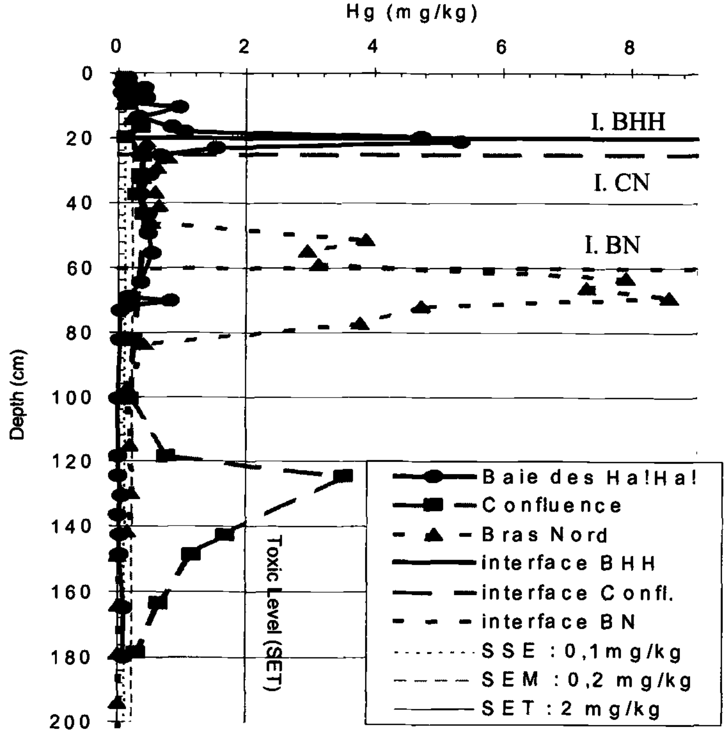

Figure 6 — *Mercury Profiles at the 3 Sites*

Since Cu and Zn are essential elements to living organisms, their affinity to organic matter is confirmed. Pb can form easily Pb carbonate or oxide and Zn can form easily ZnO and thus, these associations were confirmed by the EES results. Despite the abundance of carbonate, Pb or even Zn did not associate largely with carbonates. This is explained by the fact that sediments were slightly anoxic and that a relatively large portion of these elements was associated to the residual fraction. Indeed, from Figure 6 it can be seen that there is an important background concentration (visible at about 1m depth and deeper) for Zn > Pb > Cr but almost absent for Cu.

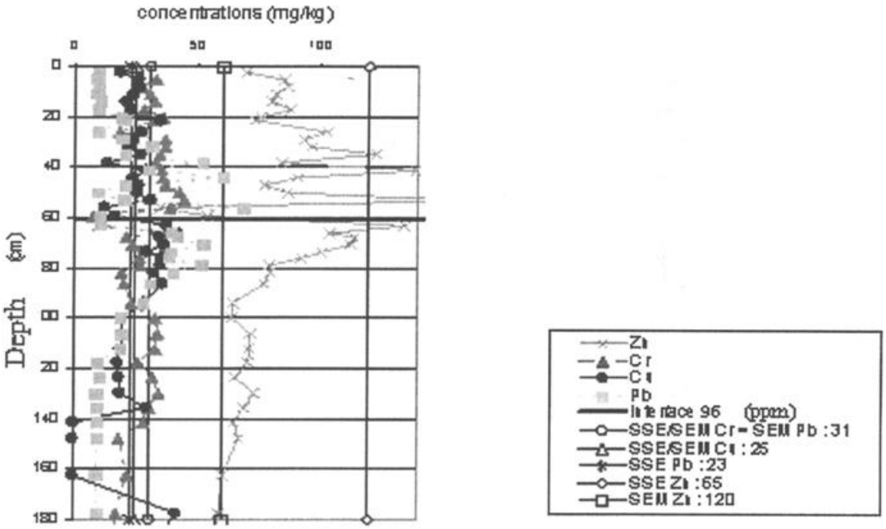

a) Norther Branch

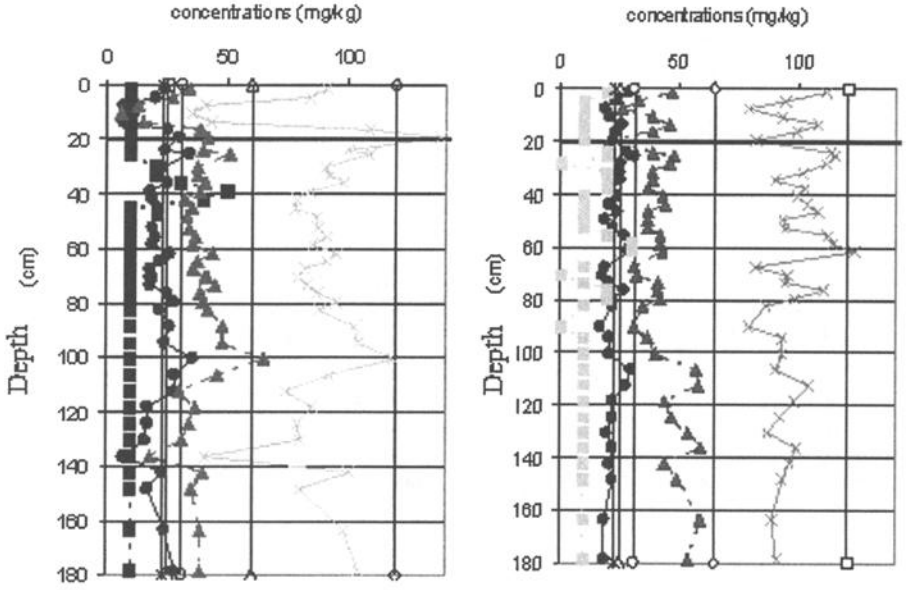

b) Ha!Ha! Bay

c) Melting sector

Figure 7a -7c— *Heavy Metal Contamination Profiles at the 3 Sites*

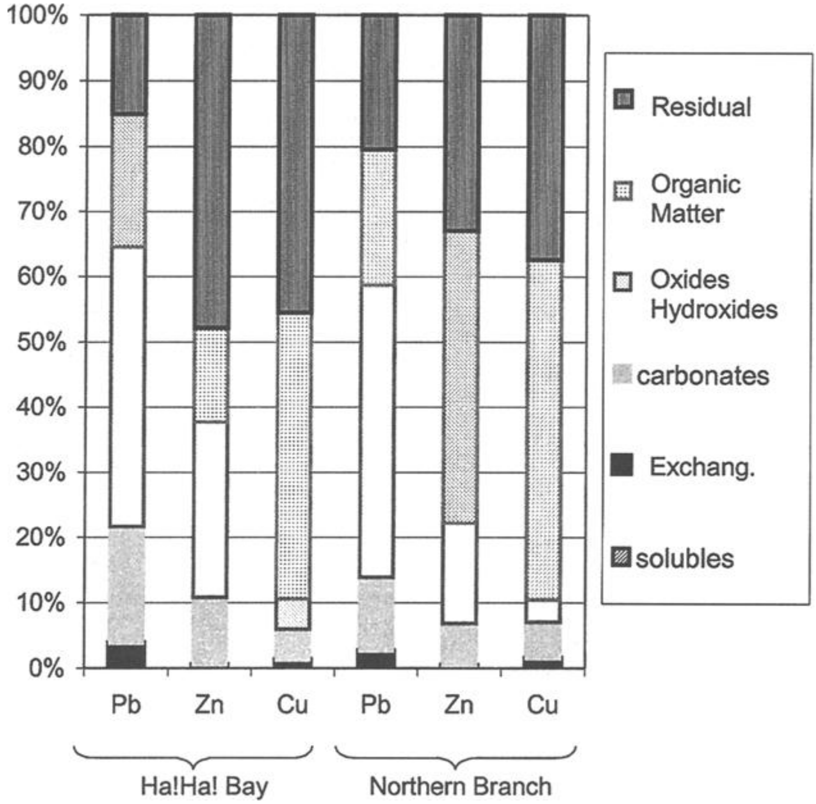

Figure 8 —*Heavy Metal Mass Distribution Patterns for the Northern Branch and Ha! Ha! Bay*

As presented earlier in Figure 5 and in Yong (1995), these fractions do not present equal potentials for release. Exchangeable, the most easily releasable metals, due to the fact that alkaline ions (Na, K, Ca, Mg) in enough concentrations can exchange with heavy metals, are not present in great amounts. Carbonates, the second more easily extractable fraction is important for Pb but in a small proportion compared to other retention mechanisms. The strongest association is with the residual fraction, which for Zn and Cu counts for almost 50% of the total concentration in the Bay and 35% for the northern branch. Given the poor oxic (over 50 m depth) and saline conditions of the Saguenay fjord the forms with higher potential for release would be Cu and Zn. However these fractions do not represent more than 30 to 40% of the total metal concentration, which will always fall under the SSE (no effect) level. Included in the residual phase, sulphur minerals such as pyrite can be included. If conditions change to more oxygenated status, AVS (acid volatile sulphides) and their associated metals can be released, this may increase metal bioavailability.

Conclusion

Before the '96 flood, heavy metals were present in various concentrations higher than the background value but lower than the minimal effect level. On the contrary, Hg has exceeded the toxic level in each interface layer. This is more critical for the bay, where the interface layer is close to the surface (20 cm deep). The Northern Branch has its interface located at 60 cm deep.

This study allowed the comparison between the ancient layer (old state of contamination) and the new layer plus interface (new state of contamination) after 4 years of the flood. According to our results and analysis, heavy metals are trapped within the ancient and interface layer and are not in direct contact with the recent layer or upper water column. If the physical conditions do not change, the adsorbing materials present in the sediments should retain heavy metals. It would seem that its retaining capacity has not been exceeded. Carbonates and oxides are present in abundance and offer precipitation and complexation sites for further retention of heavy metals.

This study did not evaluate other forms of transport mechanisms such as bioturbation, which gave new health to the zone and should develop greatly in the near future. Other parts of the Saguenay project focused on this issue.

References

American Society of Agronomy (ASA), 1986, "Methods of soil analysis", C.A. Black Editor.

ASTM International, 1998, *Special Procedure for Testing Soil and Rock for Engineering Purposes*, West Conshohocken, PA, pp.101–103.

Association Française de Normalisation (AFN), 1982, Evaluation des carbonates. norme expérimentale X31-105.

Barbeau, A., Bougie, R., and Côté, J., 1981, "Temporal and Spatial Variations of Mercury, Lead, Zinc and Copper in Sediments of the Saguenay Fjord" *Canadian Journal of Earth Sciences*, 18, pp. 1065-1074.

Bureau de Normalisation du Québec, 1993, Granulats-essai au bleu de méthylène. BNQ 2560-255.

Centre Saint Laurent, 1993, "Methods Manual for Sediment Characterization" Plan d'action Saint- Laurent.

Duquette, M. and Hendershott,W., 1993, Soil Surface Evaluation by Back titration. *Soil Science Society of America Journal*, 57, pp. 1222-1228.

Fortin G.R and M. Pelletier, 1995, "Synthèses des connaissances sur les aspects physiques et chimiques de l'eau et des sédiments du Saguenay" Rapport technique, Zones d'intervention prioritaires 22 et 23, Centre Saint-Laurent, Environnement Canada

Gagnon C., Pelletier, E. and Maheux S., 1993, "Distribution of Trace Metals and Some Major Constituents in Sediments of the Saguenay Fjord, Canada" Marine Pollution Bulletin, Vol. 26, N°2, pp.107-110.

Galvez-Cloutier, R., Yong, R., Chan, J., and Bahout, E., 1995, "Critical analysis of Sediment Quality Criteria and Hazard/Risk Assessment Tools." *ASTM STP1293*. Proc.

of the 1995 Int. Symposium on Dredging, Remediation and Containment of Contaminated Sediments, pp. 306-316.

Galvez-Cloutier, R., 1995, "Study of Heavy Metal Accumulation Mechanisms in the Lachine Canal Sediments". PhD Thesis, Department of Civil Eng. McGill University, Montreal. 195 pages.

Ize, S., 2000, Rapport de stage : Résultats sur la caractérisation physico-chimique des sédiments du Saguenay, ENTPE, France.

Ministry of Environment Canada (MEC), 1992, "Review and Recommendations for Canadian Interim Environmental Quality Criteria for Contaminated Sites" Inland Water Directorate, Water Quality Branch, Scientific Series No 197.

Ministry of Environment Ontario (MEO), 1990, "Provincial Sediment Quality Guidelines," p. 21.

Smith, J. and Walton, A., 1980, "Sedimentation Accumulation Rates and Geochronologies Measured in the Saguenay Fjord using the Pb-210 dating method" *Geochimica et Cosmochimica Acta*, 44, pp. 225-240.

Yong, R., Galvez-Cloutier, R., and Phadungchewit, Y., 1993, Selective Sequential Extraction Analysis of Heavy Metal Retention in Soil. *Canadian Geotechnical Journal*, 30, pp. 834-847.

Yong, R. and Phadungchewit, Y., 1993, pH Influence on Selectivity and Retention of Heavy Metals in Some Clay Soils. *Canadian Geotechnical Journal*, 30, pp. 821-833.

Yong, R.,1990, Buffer Capacity and Lead Retention in Some Clay Materials. *Water, Air and Soil Pollution J.*, 53, pp. 53-67.

Yong, R.,1995, The fate of Toxic Pollutants in Contaminated Sediments. *ASTM STP 1293* Proceedings of the 1995 Int. Symposium on Dredging, Remediation and Containment of Contaminated Sediments, pp. 13-19.

Author Index

Subject Index